THE UNIVERSITY
of EDINBURGH

THE QUANTIFICATION OF STRUCTURAL REDUNDANCY AND ROBUSTNESS

COLIN BRETT

DOCTOR OF PHILOSOPHY

THE UNIVERSITY OF EDINBURGH

2014

DECLARATION

I declare that this thesis and the work herein have been composed entirely by the author, Colin Brett, under the supervision of Professor Yong Lu, at the University of Edinburgh. All work is my own, except where clearly indicated. The work has not been submitted for any other degree or professional qualification.

Signed: _____

Date: _____

PUBLICATIONS

Brett, C. and Lu, Y., (2013). Assessment of robustness of structures: Current state of research. *Frontiers of Structural and Civil Engineering*, 7 (4), 356–368.

Brett, C. and Lu, Y., (2012). Developing a Quantitative Approach for Assessment of Structural Robustness Against Collapse. *In*: M.C. Forde, ed. *Structural Faults & Repair*. Edinburgh: Engineering Technics Press, 10.

ABSTRACT

Historical collapse events are testament to the inherent dangers of non-robust structures. Designing robust structures is vital to ensure that localised damage events, such as the failure of a single structural element, do not lead to catastrophic disproportionate collapse. While the advent of robustness research can be dated to the collapse of the Ronan Point building in 1968, the quantification of robustness remains an active and important research field.

The importance of developing effective robustness assessment methods is emphasized by a number of factors. One issue is the growing problem of inspecting, maintaining and ensuring the safety of ageing infrastructure. Older structures are more likely to be non-redundant and are more susceptible to structural defects. Another factor is the pursuit of greater efficiency and design optimisation, which has eliminated traditional design conservatism and many undocumented factors of safety. As a result, modern buildings may be more vulnerable to unforeseen conditions during their service life.

The objective of quantifying robustness highlights the need for a new system-oriented perspective on structural performance to complement traditional component-based design. There is, as of yet, no single framework that incorporates all the essential aspects in an explicit, transparent and quantitative manner leading to a comprehensive outcome in terms of quantification of the structural robustness.

This thesis focuses primarily on the quantification of redundancy and robustness, with the view that the capacity of a structure to withstand a damage event is an inherent property of the structure, which can be considered complementary to other commonly discussed structural properties, such as strength and ductility. Hence, a comprehensive unified

framework for redundancy quantification is proposed, which builds upon existing strength-based measures.

The role of structural uncertainties in the quantification of robustness is investigated, with a focus on the importance of the sequence of events which precede the collapse of a structure. Directly incorporating structural uncertainties into robustness quantification typically requires computationally expensive methods such as Monte Carlo simulations. Moreover, such collapse analyses are susceptible to numerical instabilities, further complicating the simulation of multiple collapse scenarios. To address these issues, a novel incremental elastic analysis method is proposed in this thesis, which analyses the full load-displacement relationship of a structure and additionally, has an inbuilt capacity to incorporate structural variability and thus output a spectrum of possible response outcomes.

LAY SUMMARY

Designing structures which can continue to function safely after the occurrence of localised damage is vital for structural safety. This research area was initiated by the partial collapse of the Ronan Point apartment building in 1968, in which a large portion of the building collapsed following an explosion which destroyed walls in a single apartment. This type of event highlights the need to consider the performance of structures from the system perspective rather than just the individual components. The capacity of a structure to withstand a damage event, such as the one which occurred in the Ronan Point building, is generally referred to as structural robustness.

Many redundancy and robustness quantification methods have been proposed. The wide variety of quantification methods reflects differing views on the scope of robustness quantification and the aspects of structural performance which should be included in the quantification process. A critical evaluation of three representative methods is presented in Chapter 3 in order to provide a 'road map' to the research area. The key strengths and weaknesses of each are identified.

One common approach by which redundancy may be evaluated is to use the ultimate strength of a structure. Comparing the ultimate strength of an intact structure and the ultimate strength of a damaged structure facilitates an evaluation of the capacity of the structure to withstand a damage event. However, methods which employ strength to evaluate capacity, only consider part of the structural performance. Other properties such as the ductility of a structure and its stiffness are also measures of the structural capacity. Therefore, a unified method is proposed which can incorporate these additional properties, thereby providing a more comprehensive evaluation.

The performance of a structure is subject to many sources of variation, such as variations in the strength of the members, variations in the loads applied to the structure and so on. Naturally, these variations are also relevant to the quantification of robustness. Incorporating these variations into an analysis can be achieved using a Monte Carlo simulation, which involves many simulations, in which parameters such as the strength are varied. The main drawback of a Monte Carlo simulation is that the simulation of large numbers of alternative structures imposes significant time and computation demands. Thus, an incremental elastic analysis is proposed. This method can alleviate the computational difficulties associated with using Monte Carlo simulations to quantify robustness.

ACKNOWLEDGEMENTS

Firstly, I would like to thank my supervisor, Professor Yong Lu, for his excellent supervision, encouragement and constant support throughout my PhD. His guidance has been invaluable.

Financial support from the EPSRC made my PhD possible. For this I am very grateful.

Life in the King's Buildings is enriched by the many great people who work there. I count myself lucky to have had so many great friends and colleagues.

My partner, Ana, who was first down the research rabbit hole, has provided unending support and patience. Thank you! It hasn't gone unnoticed.

My flatmates at Lauriston Place, Simon and Eithne, were with me for most of the PhD journey. Living with great people makes everything easier.

And last, but certainly not least, I would like to thank my parents for all their support throughout my PhD and the many years of education leading to this point. It has been a long, interesting and fruitful journey.

TABLE OF CONTENTS

LIST OF FIGURES

LIST OF TABLES

NOMENCLATURE

A	Area
C_i	Consequence index
$C_{k,i}$	Stiffness consequence index
$C_{s,i}$	Serviceability consequence index
$C_{u,d,i}$	Displacement consequence index
$C_{u,f,i}$	Ultimate strength consequence index
$C_{u,i}$	Ultimate consequence index
$C_{y,i}$	Yield strength consequence index
D	Damage
d	Displacement
D_r	Damage demand
e	Failure path event
E	Young's Modulus
F	Global applied load
$F_{u,i}$	Residual ultimate strength
$F_{u,o}$	Intact ultimate strength
f_y	Yield strength
$F_{y,o}$	Intact structure yield load
H	Hazard
K	Global stiffness
k	Member stiffness
L	Length
p	Failed member axial force
P_f	Probability of failure

R	Redundancy
w	Index weight
W_f	Work of failure
α	Scaling factor
γ	Separateness
Δ	Incremental parameter
δ	Nodal displacement
ε	Strain
σ	Stress
ΣU^i	Total global energy
φ	Vulnerability

1 INTRODUCTION

1.1 BACKGROUND

The capacity of a structure to withstand a localised damage event is vital for structural safety. The recognition of this imperative may be traced back to the 1968 partial collapse of Ronan Point building in Newham, East London. This collapse was caused by a gas explosion which blew out a number of load bearing walls in a 19th floor apartment. Subsequent to the gas explosion, the entire corner of the building collapsed, killing four people. The disproportionate consequences of this relatively minor and localised event highlighted a serious deficit in the collapse resistance of the structure. The significance of this collapse event was reflected by the introduction of design guidelines against disproportionate collapse in The Building (Fifth Amendment) Regulations 1970. These guidelines have remained largely unchanged since (Arup 2011). In the intervening years, more high profile collapse events such as the Alfred P. Murrah Federal Building, World Trade Towers and the I-35W Bridge over the Mississippi have served as reminders of the necessity to develop rational and practical methods to quantify structural robustness.

While robustness design code provisions have remained relatively unchanged since their inception, the design of structures has continued to evolve. This has been partly driven by the use of more advanced materials and the advancement of computer aided design, which has facilitated a much greater degree of structural optimisation. One consequence of greater optimisation is that structures, through lack of conservatism, may possess a diminished capacity to survive localised damage events.

The growing problem of ageing infrastructure further highlights the need to consider system properties such as redundancy and robustness. Older structures, such as bridges, are more likely to be susceptible to fatigue cracks, corrosion and traffic loads which exceed the original design specifications (Connor *et al.* 2005). Such defects may render a structure more susceptible to member failure events, which may be catastrophic in non-redundant structures. In the USA for example, 11% of steel bridges have fracture critical members; tension members whose failure is expected to cause collapse of the structure (Connor *et al.* 2005).

The fundamental characteristics of a structure such as stiffness, strength, ductility, as well as stability can generally be controlled through codified design procedures in adherence to specific requirements. Additionally, modern structures are much less susceptible to issues such as fatigue and corrosion due to better detailing, improved materials and so on. However, during its long service life, a structure may be exposed to some exceptional events which are outside the coverage of a normal design process such as impact, blast loading or terrorist attack. These events are typically unpredictable and the cause is difficult to control; therefore it is not feasible, nor practical, and clearly not economical, to include such hazards directly into design considerations. A more rational approach is to ensure that the structure can withstand such an exposure without disproportionate damage or collapse.

1.2 PROBLEM STATEMENT

From a qualitative point of view, there is evidence of convergence regarding the basic concept of robustness in terms of consequences which are disproportionate to an initial damage event. However, with respect to the quantification of robustness, the research field exhibits less harmony. The discord can be attributed to a number of factors.

One such issue is the differing perspectives on the scope of robustness assessment; whether robustness should be considered solely as an inherent structural system property or alternatively include the relationship between a structure and its environment. Another complicating issue is the fact that robustness, due to its systemic nature, is dependent on many other structural properties such as strength, ductility, continuity, redundancy, structural form, type of damage and so on. These different facets are reflected in the various quantification approaches.

The multi-layered nature of robustness has inspired a diverse range of quantification methods; approaches may be response-based or a function of the static stiffness, time variant or invariant, solely in terms of structural consequences or additionally in terms of the initial damage event, deterministic or probabilistic, strength based or energy based and so on.

Ultimately, it can be concluded that, despite the longstanding recognition of the importance of collapse resistance system properties such as robustness, there is currently no generally accepted quantification approach which is practical, generally applicable and fully expressive of robustness as an inherent structural system property.

1.3 OBJECTIVES AND SCOPE OF THE RESEARCH

It is the view in this thesis that properties such as redundancy and robustness are inherent properties of a structural system which can be considered as complementary to the more conventionally evaluated properties such as stiffness, strength and ductility. This perspective informs both the connection to the general robustness literature and the direction of the research herein.

Other branches of the research literature, such as those which focus on prescriptive rules to ensure a minimum level of robustness are briefly discussed in the literature review. Such methods include the direct design Eurocode provisions which specify prescriptive rules regarding acceptable collapse areas following the failure of a structural element.

Damage events are defined as the failure of a single member. The research focuses on robustness in terms of catastrophic collapse of a structure. Therefore analyses are implemented with respect to the ultimate capacity of a structure. Given an initial damage event, robustness is quantified primarily in terms of the capacity of a residual structure with respect to an intact structural state.

As noted, the research field is characterised by a broad range of quantification methods which reflect alternative views of the nature and scope of robustness. Accordingly, a comprehensive literature review is presented with the aim of providing some clarity regarding the various aspects of the research field. Additionally, three contrasting methods, which focus on different sides of the robustness problem, are investigated in detail.

This thesis focuses on two key research issues; the quantification of robustness in terms of the structural deterioration which is caused by an initial damage event and the role of structural uncertainties in robustness assessment. The main research objectives are as follows:

- Develop a comprehensive framework for quantifying robustness using an assessment of the capacity of a residual structure with respect to the intact structural state. This should include a unified metric which encompasses all aspects of the structural robustness, and an overall system index which may be used for a comparative robustness rating.

- Explore the role of structural uncertainties in the quantification of robustness, with a focus on the sequence of events which precede the collapse of a structure. This will be achieved using Monte Carlo simulations.

- Develop an efficient means to:

    - Determine the full load-displacement relationship of a structure in order to facilitate a quantification of robustness

    - Incorporate structural uncertainties into the assessment process without the need for computationally intensive Monte Carlo simulations

1.4 THESIS OUTLINE

Chapter 1 introduces the background to this research project and the objectives of the work.

Chapter 2 reviews the key literature concerning structural robustness. The core concepts which are relevant to the discussion are presented. Various approaches for the assessment of collapse resistance in structures are discussed.

Chapter 3 investigates three alternative quantification methods in detail. These methods focus on different aspects of the general structural collapse resistance such as vulnerability to damage and structural robustness.

Chapter 4 presents a new comprehensive quantification of the deterioration of a post damage residual structure with respect to the intact state. Four measurement criteria (elastic stiffness, yield strength, ultimate strength and ductility) are combined into a single index. A

probabilistic weighting is proposed as a means to generate an overall system index, where the index weights are defined as the probability of failure of the initial damage event.

Chapter 5 investigates the impact of structural uncertainty on the quantification of robustness. Monte Carlo simulations are used to illustrate how variations in member strength may affect the quantification of robustness. Two different levels of uncertainty are considered. It is shown that minor variations in strength may cause significant variations in ductility, due to deviations in the sequence of events leading to failure.

Chapter 6 proposes a novel incremental elastic analysis. This method uses series of incremental elastic analyses to determine the force-displacement relationship of a structure. Additionally, it has the capacity to incorporate structural uncertainties by considering a range of possible events at each stage of the analysis.

Chapter 7 demonstrates the application of the incremental elastic analysis in a variety of structural settings, using a series of examples. The use of the method to incorporate structural uncertainties is also demonstrated by using the method to efficiently quantify the structural robustness.

Chapter 8 presents the thesis conclusions, the limitations of the project and ideas for future work.

2 LITERATURE REVIEW

2.1 INTRODUCTION

Structural robustness is a general term that may be used to refer to a variety of desirable structural behaviours which are not explicitly considered in a standard code-required design procedure. In the context of this study, the definition is confined to the ability of a structure in withstanding an abnormal event involving a localised failure with limited levels of consequences, or simply structural damages.

A large body of studies exist in the literature, which fall within the general theme of collapse resistance. This following review is aimed at providing a comprehensive account with regard to the current state of research in this subject area. The review will focus primarily on studies which consider robustness as an integral structural property. Recognising the fact that progressive collapse, although related, has developed into a dedicated area of robustness, and as such has become a specialised subject, the topic of resistance to progressive collapse will be discussed in Section 2.4.

2.2 BASIC CONCEPTS AND TERMINOLOGY

Structural robustness is generally concerned with the ability of a system to withstand abnormal circumstances without disproportionate failure. The abnormal circumstances could arise from extreme events such as explosions, impact, fire, or the consequences of human errors and structural deterioration (EN 1991-1-7:2006 2010). Structural robustness has been

recognised as an intrinsic requirement which is fundamentally inherent to the structural system organisation and is associated with the vigorous strength and toughness (GSA 2003). A range of variants in the more detailed definitions exist. Slotine and Li (1991) define structural robustness as the degree to which a system is insensitive to effects outside the design considerations. Beeby (1999) regards robustness as a specified energy absorption capacity of a structure.

Although there is a lack of generally accepted methods for the direct quantification of structural robustness, various proposals on the definitions of some closely associated characteristics exist. Lind (1995) proposed the definition of vulnerability as the ratio of failure probability of the damaged system to that of the undamaged system, and such a definition of vulnerability may be easily converted to a measure of robustness. Augusti *et al.* (2001) use the concept of sensitivity (in damage terms) of the facility to a given event. Hendawi and Frangopol (1994) looked into the reliability of redundant systems using a failure path approach that requires all failure probabilities to be enumerated. Ellingwood and Leyendecker (1978) were among the first to advocate the alternative path analysis which involves removing a member to determine if the "damaged" structure can tolerate the redistribution of loads. Agarwal *et al.* (2003) developed a so-called "rings & rounds" approach to evaluate the vulnerability of structural systems.

Ultimately, a systematic quantification of system robustness needs to be assessed in the context of three fundamental elements, 1) type of abnormal exposure (abnormal "hazard"), 2) the structural consequence of such exposure, and 3) the broader consequence or risk including fatalities and economic loss. While defining the exposure and assessing the broader consequence will involve a number of other factors (see a comprehensive list in Baker *et al.* (2008), the structural consequence under a given exposure lies at the centre of the whole

framework and generally is the most controllable aspect as far as structural engineers are concerned. The review shall focus on robustness in relation to the structural consequence under a given exposure in the form of local failure or severe damage causing a serious disruption to the structural system.

Closely related to the above-outlined concept of structural robustness is the broader-sense structural redundancy which forms the basis for the system to adapt to the structural change, and the ductility which determines whether the system can sustain the usually large deformations without progressive loss of strength in the course towards the establishment of a new equilibrium state. With this in mind, it is useful to clarify several concepts that may be involved in the different approaches of assessing the robustness of a structure.

2.2.1 Robustness

There is no absolute universally accepted definition of robustness. However, while the wording may vary, the underlying theme or concept is relatively consistent, and several common keywords can be extracted from the various definitions such as damage, vulnerability, disproportion, consequences, insensitivity, unforeseen loading, risk and so on. While robustness itself may be considered to be a property inherent to a particular structure, it is a function of other structural properties. Knoll and Vogel (2009) discuss some of the many elements of robustness including strength, structural integrity, multiple load path redundancy, ductility, progressive failure versus zipper stopper, stiffness considerations, physical system limits and so on.

Given the wide variety of definitions and quantification approaches, it is useful to have some criteria by which robustness measures may be evaluated and compared. For this purpose,

Starossek and Haberland (2011) propose some common objective targets for robustness measures:

- Expressiveness – Robustness measures should clearly and distinctly quantify all aspects of robustness and collapse resistance
- Objectivity – Each measure should be user independent
- Simplicity – Measures should be simple
- Calculability – All inputs should be readily quantifiable
- Generality – Measures should be applicable to arbitrary structures.

2.2.2 Hazards

JCSS (2008) defines exposures or hazards acting on a system as all possible endogenous or exogenous effects which have the potential to cause consequences. The nature of exposures can vary both in type and temporally. Some exposures will occur instantly while other exposures might occur slowly such as a fire. In the context of bridge structures, some exposures might include corrosion, overloading, fatigue, collision, terrorist attack and so on. Due to the difficulty of predicting and quantifying unforeseen hazards, and the general appreciation of robustness as a property which is a function of the inherent system properties, robustness analyses are generally hazard independent.

2.2.3 Structural Consequences

Structural consequences are the potential outcomes of events. These can be considered in terms of loss of life, economic costs and damage to the environment (JCSS 2008). As far as

structural robustness is concerned, it is the indirect consequences, or the subsequent additional damage following the direct consequence of an exposure, that is of interest. For example, in the event that a structure is exposed to a collision leading to the failure of a column (direct consequence), if the column failure causes the progressive collapse of the structure, then collapse would be categorised as an indirect consequence.

The type or extent of consequences may also be used to determine the scope of a robustness quantification analysis. To this end, EN 1991-1-7:2006 (2010) identifies three consequence classes for buildings. For buildings in consequence class 1, which includes buildings such as single occupancy houses not more than 4 storeys, no specific action is required. However, for consequence class 3, which includes residential buildings in excess of 14 storeys, a full risk assessment for foreseeable and unforeseeable hazards is required in addition to the provision of sufficient tie forces and analysis with notional element removal.

2.2.4 Damage Events

A common damage definition in the context of evaluating redundancy or robustness is the complete removal of one, or sometimes a few members from a structure. The most common approach is to define damage as the failure of a single member. This approach is used in both robustness assessment (GSA 2003, IStructE 2010), and also in the direct design alterative path procedure used for progressive collapse analyses. This simplified definition represents the ultimate direct consequence in many abnormal exposure scenarios, and therefore allows the analysis to focus on the indirect consequence regardless the cause. An alternative to removing an entire member is to introduce damage to a member which is a proportion of the cross-section area. Such damage can represent section loss due to corrosion (Hendawi and Frangopol 1994).

2.2.5 Damage Effort

As discussed previously, structural robustness is concerned with disproportion between an instance of damage and the consequences of damage. Solely considering the consequences is not sufficient to quantify the disproportion magnitude. The probabilistic approach detailed above is one method to evaluate disproportion. Another method explored in the literature is to incorporate damage effort into the analysis. There are a number of methods which have been proposed for this purpose. Lu *et al.* (1999) and the other papers from this group suggest that the damage effort is proportional to the loss of principal stiffness due to a damage event. Smith (2003) uses the energy required to cause failure of a member to quantify damage effort.

2.2.6 Redundancy

Redundancy is a concept which is closely related to robustness. In the extreme, a system is completely non-redundant when the failure of a component causes the failure of the entire system (Bertero and Bertero 1999). To quote Ghosn and Moses (1998), "redundancy is defined as the capability of the structure to continue to carry loads after the failure of one main member". The implied capacity certainly requires adequate static redundancy but involves a number of other contributors, particularly in terms of deformability and ductility. Different types of redundancy may also be considered such as internal redundancy (member redundancy), structural redundancy and load path redundancy (Connor *et al.* 2005). Bertero and Bertero (1999) note that redundancy may be active or standby. Active redundancy describes the case in which all members are sharing loads, and standby redundancy refers to the situation where some components are inactive and only become active when other active members fail.

2.2.7 Static Determinacy

While redundancy is related to static indeterminacy, it has been demonstrated that the two should not be considered to be equivalent (Frangopol and Curley 1987). Lind (1995) notes that redundancy is related to static determinacy, although only superficially. Additionally, higher levels of static indeterminacy can even reduce the collapse loads of trusses and frames by giving rise to unfavourable states of prestress due due to lack of fit; which may be exacerbated by differential settlement of the supports or differential temperature changes (Sebastian 2004).

2.2.8 Vulnerability

JCSS (2008) differentiates between vulnerability and robustness based on their relationship to consequences; vulnerability is regarded as being related to the direct consequences of damage whereas robustness is related to the indirect consequences of damage.

When vulnerability is confined to being a measure related to the tolerance of a structural system to an initiation exposure, it becomes generally a term reciprocal to robustness. Lind (1995) discusses vulnerability in tandem with damage tolerance. They are considered to be complementary concepts as a system which is vulnerable is not damage tolerant (and hence not robust) and vice versa. Agarwal *et al.* (2001) adopted a similar approach. A structure is considered to be vulnerable if damage from any exposure results in consequences which are disproportionate to the original damage event. It is proposed that system vulnerability is related to the form of the structure. Disproportionate consequences arise from a structure with poor structural form and connectivity which renders it susceptible to progressive collapse.

2.2.9 Reliability

Reliability in the context of structural robustness brings aspects of uncertainty into the framework. The reliability is classically evaluated by reliability indices, which can be determined for individual members or the overall system; however a member-oriented approach could lead to the design of non-robust systems (Ghosn *et al.* 2010). Schafer and Bajpai (2005) note that current design methods provide estimates of the failure probability (P_f) for each component; however no direct estimate of the system P_f is used. Furthermore, knowledge of the sensitivity of P_f of a damaged building is believed to be a key quantity regarding decision making for catastrophic unforeseen events.

With respect to robustness and progressive collapse the probability of failure is commonly considered in terms of conditional probabilities as follows (Ellingwood and Dusenberry 2005a, JCSS 2008):

$$P(F) = P(F \mid DH_i)\,P(D \mid H_i)\,P(H_i) \qquad \textbf{2.1}$$

where F = event of structural collapse, $P(H_i)$ = probability of hazard H_i, $P(D|H_i)$ = probability of local damage, D, given that H_i occurs, and $P(F|DH_i)$ = probability of collapse, given that the hazard and local damage both occur. The relationship is illustrated in Figure 2-1.

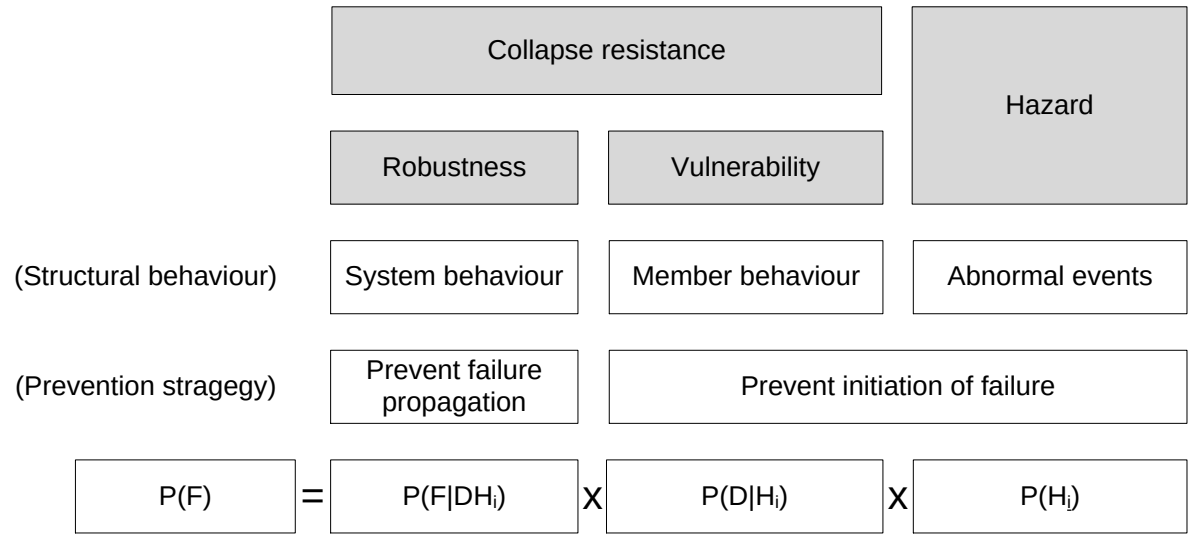

Figure 2-1: Probabilistic framework (adapted from Starossek and Haberland 2012)

While $P(F|DH_i)$ is concerned with system behaviour, $P(D|H_i)$ is related to individual member behaviour. Therefore, in contrast with $P(H_i)$, they are both within the remit of the structural engineering design (Starossek and Haberland 2008). Typically, methods proposed to assess redundancy or robustness focus on $P(F|DH_i)$ by assuming a specific level of damage such as the failure of a member. This facilitates an evaluation of the system response.

2.2.10 Risk

The risk, R, associated with a particular event is equal to the probability, P, of the event occurring, multiplied by the consequence, C, of the event (JCSS 2008). Therefore, using the equation for $P(F)$ in Equation 2.2, the risk can be evaluated as follows;

$$R = P\left(F \mid DH_i\right) P\left(D \mid H_i\right) P\left(H_i\right) \times C_i \qquad \textbf{2.2}$$

where C_i is the consequence of event i. Given that preventing damage in the event of a hazard may be unfeasible, the above equation is sometimes simplified as follows (Deco and Frangopol 2011):

$$R = P\left(F \mid DH_i\right) P\left(H_i\right) \times C_i \qquad \textbf{2.3}$$

While the above risk and probabilistic approaches are useful in terms of clarifying the relationship between the constituent terms, the practical applicability of this framework remains limited.

Alexander (2004) discusses some of the hazards which may be considered as part of a risk assessment such as construction errors, design errors, vehicle impact, explosions and so on. While the consequences of such events may be severe, the probability of occurrence is small. Therefore they can be classed as low-risk high-consequence events. The author notes that frequency of such events is so small, that a probabilistic risk assessment is almost impossible and therefore meaningless. Therefore it is proposed that risks should be covered by applying a small number of standard events such as an explosion, an impact and a roof overload.

2.3 GENERAL METHODOLOGIES

2.3.1 Static Stiffness-based Methods

Static stiffness-based methods, by which the damage resilience of a structure may be evaluated, have been proposed by a number of research papers in one form or another. In general stiffness matrices can be used to assess the stability of a structure following a damage event.

Nafday (2008) provides an informative and concise discussion regarding system safety performance metrics for skeletal structures which are based on properties of stiffness matrices. Two indices are proposed to evaluate the stability of a structure. The first index, which is based on the stiffness matrix condition number, is a measure of the distance of a structural stiffness matrix from a set of noninvertible matrices, which represent unstable structural states. The second index uses the determinant of the static stiffness matrix to assess the stability of a structural system. The determinant provides a measure of the linear dependence of column vectors in the stiffness matrix with increasing linear dependence tending towards instability. An unstable system will have a zero determinant. The index is simply the normalised determinant of the elastic stiffness matrix;

$$\Delta s = | K_n |, \quad 0 \leq \Delta s \leq 1 \qquad \textbf{2.4}$$

While both of these indices are useful from the point of view of structural system stability, they do not directly evaluate robustness. However, another index is also presented which compares the normalised determinant of the intact structure with the normalised determinant of a damaged state;

$$I = | K_n | / | K_n^* | \qquad \textbf{2.5}$$

where $| K_n |$ and $| K_n^* |$ are the determinants of the normalised stiffness matrix of the intact and damaged structures respectively. More critical members will have a higher importance factor, *I*. This index can be considered to have more in common with the objectives of robustness assessment as it provides an evaluation of how the structure withstands a damage event.

Similarly, Starossek and Haberland (2009) consider the static stiffness matrix in order to define a stiffness-based robustness index;

$$R_s = \min\left(\frac{\det K_i}{\det K_o}\right) \qquad \textbf{2.6}$$

where det(K_i) and det(K_o) are the determinants of the stiffness matrices for the damaged and intact structures respectively.

Several other papers from Bristol University (e.g. Lu *et al.* 1999) propose a methodology to determine a vulnerability index, which relates to the form of the structure. A detailed investigation of this methodology is provided in Section 3.3. Disproportionate consequences arise from a structure which has poor form and connectivity which renders it susceptible to progressive collapse. Vulnerability, which essentially is a system sensitivity measure, is quantified as follows (Pinto *et al.* 2002):

$$\varphi = \frac{\gamma}{D_r} \qquad \textbf{2.7}$$

where the vulnerability φ is the ratio of the separateness (damage consequences), γ, to the damage effort, D_r. Critical members or sequences have a high vulnerability due to the disproportion between the damage consequences and the damage effort.

Methods such as those outlined above, purely evaluate the form and stability of a structural system. Therefore they are independent of both loading and boundary conditions. One potential advantage of this approach is that the susceptibility to any arbitrary damage event may be considered without the normal constraints which would govern a response-based analysis. Furthermore, they are easy to implement as they do not require computationally

intensive structural response analyses. However, as noted by Starossek and Haberland (2011), there may be little correlation between a stiffness robustness analysis and a traditional strength-based analysis. Therefore, while there may be some complementary benefit, methods which only consider the form and stability of a structure cannot feasibly replace traditional response-based analysis.

2.3.2 Vulnerability Methods

Vulnerability may be quantified as expressed in Equation 2.8. Vulnerability is therefore a quantitative measure of the disproportion of a damage event. φ generally varies from zero to infinity. Lind (1995) considers the vulnerability as the reciprocal of damage tolerance and is defined as follows:

$$v = v(r_d, S) = \frac{P(r_d, S)}{P(r_o, S)} \qquad \textbf{2.8}$$

where v is vulnerability, r_d and r_o represent the damaged and intact states respectively and S is the prospective loading. So, $P(r_d,S)$ is the probability of failure of the damaged condition given the prospective loading S. V varies in a range of 1.0 to infinity.

It is interesting to note that JCSS (2008) defines vulnerability the other way round, as

$$I_V = \frac{R_D}{V_A} \qquad \textbf{2.9}$$

where the vulnerability Iv is equal to the ratio of the direct risk R_D, to the parameter which is used to measure the value of the indirect risk. The value might be expressed in terms of lost lives, monetary value or another suitable measure. The implication from this equation is that when a minimum direct risk results in a maximum indirect risk, the vulnerability is the

smallest, which tends to contradict the general understanding in the context of structural robustness under abnormal conditions.

The vulnerability analyses proposed by Lu *et al.* (1999) and Smith (2003b) are both primarily concerned with the assessment of structural vulnerability. Each of these approaches is evaluated in detail in Chapter 3.

2.3.3 Energy-based Methods

The principles of energy absorption and energy balance are commonly discussed with respect to the evaluation of progressive collapse and robustness. The use of energy as a quantitative measure in the assessment reflects the importance of ductility, both at the local level in terms of joint and member ductility and also at the global level in terms of general system ductility.

Fang and Li (2009) consider the use of energy as a quantitative measure in robustness assessment. Two objectives are considered important: improving the energy absorption capacity of structures and reducing the energy released during damage propagation. A number of strategies are proposed to achieve the objectives: improving element performance, developing dissipative properties such as damping and friction, ensuring good structural form through alternative load paths, providing effective horizontal and vertical ties and implementing additional energy absorption devices such as dampers.

Beeby (1999) considers the safety of structures given the prevalence of structural mistakes, which could occur during the design or construction of a structure. It is argued that safety factors cannot be used to reduce the risk arising from mistakes and errors. Therefore robustness is vital to reduce the risk associated with these events. Robustness is interpreted as the capacity of a structure to absorb damage due to unforeseen events without collapse. In

this context, similarly to (Smith 2003b), unforeseen events or accidents can be considered as unforeseen energy inputs. It is proposed, more specifically, that a structure or member, should be able to absorb an amount of energy equal to the volume of the material multiplied by a limiting energy, e_c;

$$E_u = e_c \times V \qquad \textbf{2.10}$$

where E_u is the energy to cause failure, e_c is the allowable energy per unit volume and V is the volume of the member. A method for determining e_c is not proposed; it is suggested that values would be defined by appropriate Code drafting bodies. Beeby notes that, given the close relationship between failure energy and ductility, the provision of ductility is an effective measure to reduce the risk due to unforeseen structural errors or accidents and increase safety.

Starossek and Haberland (2011) propose an energy-based robustness index. It is noted that energy-based measures, such as Equation 2.11, may fulfil the objectives of expressiveness and calculability. The proposed index is based on a comparison between the energy released by the initial failure and the energy required for a collapse progression:

$$\mathrm{R_e} = 1 - \max_j \frac{E_{r,\mathrm{j}}}{E_{s,k}} \qquad \textbf{2.11}$$

where R_e = energy-based robustness measure; $E_{r,j}$ = energy released by the initial failure of a structural element j and available for the damage of the next structural element k; $E_{s,k}$ = energy required for the failure of the next structural element k. R_e establishes the possibility of total collapse; negative values of R_e indicate that progressive will propagate.

The concept of energy balance and energy flow has been explored by a number of research papers. If a structure can develop sufficient strain energy to dissipate the kinetic energy released by member failure, collapse may be averted. Otherwise, the initial failure event will lead to progressive damage and potential collapse. Szyniszewski and Krauthammer (2012) consider the capacity of a multi-storey building to arrest progressive collapse by the dissipation of kinetic energy produced by a failure event. Similarly, Dusenberry and Hamburger (2006) present two simplified approaches; one method is a push-down method using commonly available linear elastic software and the second method is based on a flexural/catenary energy absorption analysis.

Smith (2003a) uses the effort (in terms of strain energy) required to cause failure in a structure to identify critical sequences of member failure. This approach is analysed in more detail in Section 3.4.

2.3.4 Reserve Factor / Redundancy Methods

Various forms of strength-based redundancy indices have been proposed. A selection of these indices is discussed below.

2.3.4.1 Residual strength factor

The residual strength factor (R_1) quantifies the consequences of damage by determining the ultimate load of a damage state and normalising it with the ultimate load of the intact structure (Feng and Moses 1986, Frangopol and Curley 1987, Maes *et al.* 2006).

$$R_1 = \frac{f_{u,i}}{f_{u,o}} \qquad \textbf{2.12}$$

where $f_{u,i}$ is the ultimate strength of damaged state *i*, and $f_{u,o}$ is the ultimate strength of the intact structure.

This index provides a quantification of the strength capacity of damaged structure with respect to the intact structure. A value of one indicates that the damage event does not produce any deterioration in strength and a value of zero, indicates that damage caused complete failure of the residual structure.

2.3.4.2 Redundancy factor

Similarly to the residual strength factor, the redundancy factor quantifies the margin between the ultimate strength of intact structure and a particular damage state (Frangopol and Curley 1987, Frangopol and Klisinski 1989). In this case the indices will range from 1, indicating that the damaged structure has no strength, to infinity, indicating that the ultimate capacities are equal and damage has no consequence with respect to the ultimate strength.

$$R_2 = \frac{f_{u,o}}{f_{u,o} - f_{u,i}} \qquad \textbf{2.13}$$

The redundancy factor can be related to R_1 as follows:

$$R_2 = \frac{f_{u,o}}{f_{u,o} - f_{u,i}} = 1 - \frac{f_{u,o}}{f_{u,i}} = 1 - \frac{1}{R_1} \qquad \textbf{2.14}$$

This definition of redundancy may be interpreted as the reciprocal of the sensitivity of the structure to a specified damage, with the sensitivity being measured as the normalised change

in strength of the damaged structure compared to the intact structure. Thus when the sensitivity approaches zero, i.e., the system strength is not changed with the given damage, the structure is said to have infinite redundancy with respect to the given damage, and vice versa.

The capacity of the strength redundancy factor (R_2) to provide a measure of structural safety and the influence of the damage of different members is demonstrated using a set of examples subjected to different types of damage. The results indicate the importance of the combination of damaged members in a multiple damage scenario and also the influence on the failure type (ductile or brittle) on the system strength.

The generality of the above formulation of redundancy quantification (which herein has been interpreted to connect to the robustness) permits optimisation to be sought in terms of the system redundancy. Frangopol and Klisinski (1989) investigated the effect of optimisation on the redundancy on a three-dimensional space truss. Optimisation is considered in terms of minimising the weight of the truss subject to a number of constraints. Three strength-based redundancy measures are considered: the reserve strength factor, the residual strength factor, and the redundancy factor. These measures are considered to be good indicators of the strength and redundancy as they are directly related to system strength for both the damaged and undamaged structure. When optimisation is introduced in the form of weight minimisation, the material volumes of the truss are significantly reduced. This results in an increase in the number of fully stressed members at failure. The paper demonstrates a conflict between optimisation and the requirement for sufficient redundancy.

2.3.4.3 First member yield index

The yield strength of the intact structure may also be used to normalise the strength of the residual structure (Ghosn & Moses, 1998). The first member yield index is defined as follows:

$$R_3 = \frac{f_{u,i}}{f_{y,o}} \qquad \textbf{2.15}$$

where $f_{y,o}$ is the yield strength of the intact structure. The index ranges from 0, where the residual structure has no strength to value greater than 1 if the residual strength exceeds the intact yield strength. Any values less than one indicate that the residual structure will be able to sustain less load than that required to cause first yield in the intact structure.

2.3.4.4 Reserve strength factor

The reserve strength factor is simply a factor which quantifies the margin between the ultimate capacity of an intact structure and some reference such as a design or nominal load (Feng and Moses 1986, Frangopol and Curley 1987, Yuansheng 1988).

$$R_4 = \frac{f_{u,o}}{f_n} \qquad \textbf{2.16}$$

This index does not consider a damaged structure and therefore cannot be considered to be a quantification of redundancy or robustness. However, if the numerator is replaced with $f_{u,i}$, then the index is more useful from a redundancy analysis perspective.

2.3.4.5 Redundancy strength index

Husain & Tsopelas (2004) define a redundancy index which is similar to R_4, however in this case the index relates the ultimate strength of the intact structure to the first yield.

$$R_5 = \frac{f_{u,o}}{f_{y,o}} \qquad \textbf{2.17}$$

This index quantifies the reserve strength which exists in a structure after the first yield. If the structure has no redundancy, the index will equal 1, as the structure fails immediately upon the first yield. The index will exceed 1 if a structure possesses some redundancy. Similarly to R_4, this index does not reference a damaged structure, however the index does have more in common with general objective of redundancy analysis as it quantifies the capacity of a structure to sustain load after a member has yielded.

2.3.4.6 Design-oriented redundancy analysis

Ghosn and Moses (1998) present a general design-oriented procedure for robustness quantification based on load-capacity under multiple limit states; functionality, ultimate and damaged condition. This procedure has also been implemented by Wisniewski *et al.* (2006) in order to evaluate railway bridges. The methodology is discussed in detail in Section 3.5.

2.3.5 Probabilistic and Risk Methods

2.3.5.1 Probabilistic Factors

The same framework of evaluating the redundancy indices factors has also been extended to incorporate probabilistic redundancy measures (Frangopol and Curley 1987, Frangopol and

Nakib 1991). In this case the load and strength of the members are assumed to be random variables. A reliability index is determined for each member in a structure according to the different damage levels:

$$\text{Reliability index: } \beta_1 = \frac{\bar{M}_i}{\sigma(M_i)}, \text{ where } M_i = S_i - Q_i \qquad \textbf{2.18}$$

where $\bar{M}_i$ and M_i are the mean and nominal performance function of element *i* respectively; S_i is the random strength of element *i* and Q_i = random load effect on member *i*.

Additionally the influence of the failure type (brittle or ductile) is demonstrated by plotting the reliability index against the mean applied load for each damage level. The probabilistic redundancy in systems is expressed as:

$$\beta_2 = \frac{\beta_{intact}}{\beta_{intact} - \beta_{damaged}} \qquad \textbf{2.19}$$

We can also re-write Equation 2.19 to yield:

$$\beta_2 = \frac{1}{1 - (\beta_{damaged} / \beta_{intact})} \qquad \textbf{2.20}$$

which is analogous to the deterministic Equation 2.14, albeit using reliability indices.

Additional measures of the redundancy in terms of the reliability indices of the intact and damaged structures may also be constructed (Frangopol *et al.* 1992).

2.3.5.2 A Generalised Risk Approach

Baker *et al.* (2008) propose a conceptual model that relates robustness to both direct and indirect risks. This approach divides consequences into i) Direct consequences associated

with element damage (which could be considered as proportional damage), and ii) Indirect consequences assimilated with subsequent structural failure (which could be considered disproportionate damage).

An index is formed by comparing the risk associated with direct and indirect consequences. The index of robustness I_{ROB} is defined as:

$$I_{ROB} = \frac{R_{Dir}}{R_{Dir} + R_{Ind}} \quad \textbf{2.21}$$

where R_{Dir} is the direct risk and R_{Ind} is the indirect risk.

The risks are defined as illustrated in Figure 2-2. First, an exposure occurs which has the potential of damaging structural elements in a system; this is named the exposure before damage, or EX_{BD}. If no damage occurs ($\overline{D}$), then the analysis is finished. If damage does occur, a number of damage (D) states can follow. For each of these damage states, there is a probability that system failure (F) occurs. Consequences are assimilated with each of the possible damage and failure scenarios, and are specified as direct (C_{dir}) or indirect (C_{ind}).

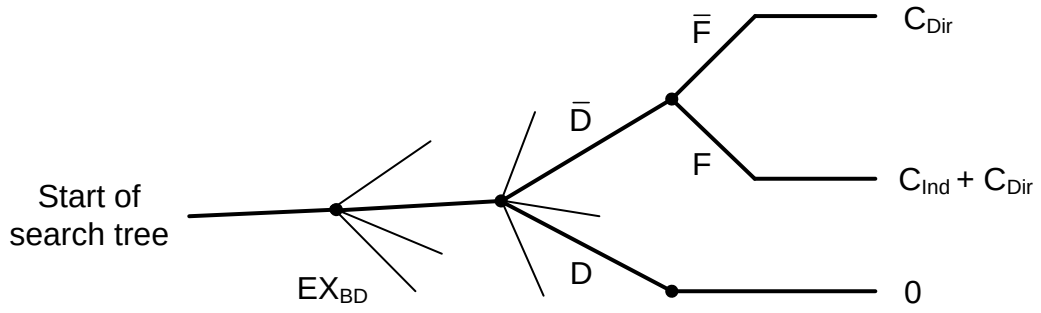

Figure 2-2: An event tree for robustness quantification (adapted from Baker *et al.* 2008)

Provided that the required direct and indirect risks (consequences) are available, I_{Rob} can be evaluated and it takes values between zero and one, with robust systems having an index value approaching one. In principle, such a definition could potentially account for the effect of repair strategies, inspection and maintenance as well as the system's ability to accommodate accidental events, since such actions can alter failure consequences and this risk.

2.4 PROGRESSIVE COLLAPSE

The partial collapse of Ronan Point in 1968 was widely regarded as a starting point for the structural engineering community to become aware of the need for robustness against disproportionate structural failure, which is often of a progressive collapse scenario. This incident prompted the introduction of regulations for designing against disproportionate collapse in the 5th Amendment to the Building Regulations in 1970 in the UK, and numerous research studies followed. A new wave of attention to this subject was brought about following the 1995 bombing of the Alfred P. Murrah Federal Building, the 1998 bombing of the US embassy buildings in Tanzania and Kenya, and the collapse of the World Trade Centre Towers in New York on September 11, 2001.

A progressive collapse is a catastrophic partial or total structural failure that ensues from an event that causes local structural damage that cannot be absorbed by the inherent continuity and ductility of the structural system (Ellingwood and Dusenberry 2005a). Progressive collapse is the spread of damage through a chain reaction, for example through neighbouring members or storey by storey. There are a number of different types of progressive collapse; pancake-type collapse, zipper-type collapse, domino-type collapse, section-type collapse, instability-type collapse and mixed-type collapse (Starossek 2007). Such characterisation of collapse is useful from the point of view of identifying links between collapse types and structural configuration, which may provide a more informed platform from which to consider appropriate collapse prevention mechanisms.

Progressive collapse is thus closely associated with both redundancy and robustness. However, the concept of structural robustness in the context of resisting progressive collapse has been expressed in the form of specific limiting requirements, rather than a quantifiable property of the structure that may be measured and compared. In this respect, research studies on the structural robustness against progressive collapse have been focused on two areas of the subject, namely the "indirect design" and the "direct" design approaches.

The so-called "indirect design" approach resorts to specifying minimum levels of robustness through prescriptive measures of tie forces, continuity and ductility to develop resistance to disproportionate failure. The provision of ties increases the structural continuity, resulting in inbuilt redundancy to redistribute loads in case a part of the structure is removed accidentally. The tie force methodology is event independent and is intended to provide a minimum level of accidental damage tolerance (BS 5950-1:2000 2008). In practice the ties are usually provided by one or a combination of the following; i) the steel members including the connections that must be capable of transferring the horizontal tying forces, ii) the steel bar

reinforcement - provided that it is anchored to the steel frame and embedded in concrete, and iii) the steel mesh reinforcement in a composite slab with profiled steel sheeting.

The "direct design", on the other hand, involves specific analysis and design procedures to ensure a structure's ability to absorb local damage and resist disproportionate failure. There are generally two possible means to achieve this: i) alternative path method, which emphasises the behaviour of the structure after damage has occurred, regardless of the action causing damage. It relies on the ductility and continuity of the structure to redistribute forces. In this approach, it is typically assumed that part of the structure is lost, and design is carried out to enable the remaining structure to redistribute the loads to the undamaged areas. BS 5950-1:2000 (2008) recommends that the structure should be designed to bridge over a loss of an un-tied member and that the area of collapse should be limited and localised. This is usually achieved by removing each untied element, one at a time, and checking that on its removal the area of structural risk of collapse is within a specified limit. ii) Local resistance or key element method: this approach is recommended especially for situations where the loss of an element cannot be tolerated or when tying or bridging over of a member is not possible.

Stemming from the The Building Regulations (1970), more detailed requirements and design provisions have been gradually incorporated in various design codes and guides, e.g. The Building Regulations (1985), EN 1991-1-7:2006 (2010), GSA (2003), UFC 4-023-03 (2005, 2009), and ASCE 7-05 (2005).

A comprehensive review of the evolution of the design provisions as well as the development of relevant analysis methods against disproportionate collapse can be found in a report by Arup (2011).

2.5 RELIABILITY BACKGROUND

The analysis of structural reliability is a means by which the probability of a failure of a structure may be determined. The probably of failure is determined with respect to a limit state, such as the ultimate limit state for example. In the standard case, with two variables, a limit state (performance) function may be defined for a structural component as follows:

$$g_i = R_i - S_i \qquad \textbf{2.22}$$

where R is the component resistance and S is the component force. A function is considered safe if $g \geq 0$ (or $R \geq S$). Conversely failure is deemed to have occurred if $g < 0$.

Thus the probability of failure is the probability that the limit state function is less than zero:

$$P_f = P\left[g_i < 0\right] \qquad \textbf{2.23}$$

where P_f is the probability of failure.

The reliability index is a measure of the distance between the mean and the limit state function (see Figure 2-3). If R and S are independent and normally distributed the reliability index is determined as follows:

$$\beta = \frac{\mu_r - \mu_s}{\sqrt{\sigma_r^2 + \sigma_s^2}} \qquad \textbf{2.24}$$

where μ_r, μ_s, σ_r^2 and σ_s^2 are the mean and standard deviation of the resistance and loading. If, on the other hand, the variables are correlated, the reliability index may be similarly determined by including a correlation coefficient, ρ;

$$\beta = \frac{\mu_r - \mu_s}{\sqrt{\sigma_r^2 + \sigma_s^2 - 2\rho\sigma_r\sigma_s}} \qquad \textbf{2.25}$$

The probability of failure may be determined from the reliability index:

$$P_f = 1 - \Phi(\beta) \qquad \textbf{2.26}$$

where Φ is the cumulative normal distribution function. The probability of failure is illustrated in Figure 2-3. The probability of failure is equal to the area under the probability density function of g which is defined by the limit state $g<0$.

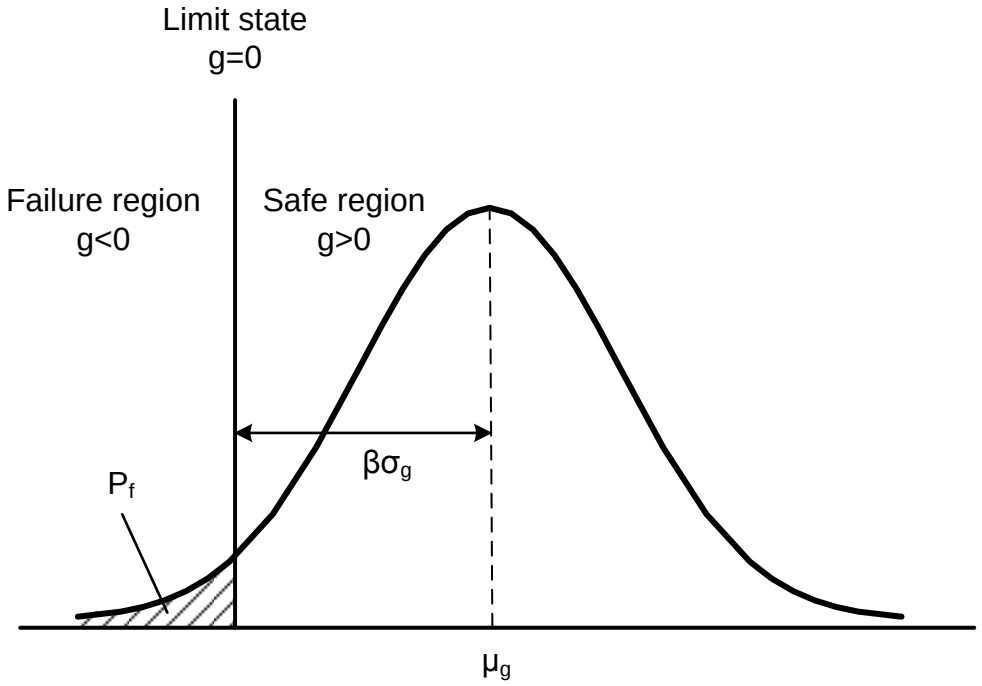

Figure 2-3: Joint probability distribution function (adapted from Choi *et al.* 2007)

The fundamental *R-S* may be extended by introducing additional variables. For example, the following limit state function may be used in the case of truss members (Park *et al.* 2004):

$$g_i = A_i\sigma_y - \sum_{j=1}^{NL} e_{ij} S_j \qquad \textbf{2.27}$$

where S_j is the applied j-th load on the structure, e_{ij} is the influence coefficient (the member force) for member *i* caused by the j-th applied load, A_i is the area of member *i*, σ_y is the yield stress and NL is the number of applied loads.

2.5.1 First Order Second Moment Method (FOSM)

In general, such as the limit state function defined in Equation 2.27, the limit state function *g* is non-linear. However, various methods exist in order to linearise the limit state function. If all of the random variables (σ_y, A_i and S_j) are normally distributed and, a reliability index may be determined for the limit state using the first order second moment method (FOSM). In the FOSM the limit state function is represented by a Taylor series expansion about the mean value (Choi *et al.* 2007);

$$\mu \approx g(\mu_{x_1}, \mu_{x_1}, ...\mu_{x_n}) \qquad \textbf{2.28}$$

$$\sigma^2 \approx \left(\sum_{i=1}^{n} \left(\frac{\partial G}{\partial X_i} \right)\Bigg|_{\mu_{x_i}} \sigma_{x_i}^2 \right)^{0.5} \qquad \textbf{2.29}$$

As before, the reliability index is defined as $\beta = \mu/\sigma^2$, and the probability of failure $P_f = \Phi(-\beta)$, where Φ is the cumulative normal distribution function.

2.5.2 Hasofer-Lind Reliability Index

However the FOSM suffers from two significant drawbacks; it is not accurate for highly non-linear failure surfaces and secondly it may not be invariant with respect to the functions

which are the same, albeit formulated differently. In order to circumvent these weaknesses, the Hasofer-Lind reliability index may be used. The Hasofer-Lind index involves a transformation of the variables into standard normal variables with a mean of zero and a standard deviation of one.

$$U_i = \frac{X_i - \mu_{X_i}}{\sigma_{X_i}}, \qquad i = 1, 2....., n \tag{2.30}$$

where μ_{X_i} and σ_{X_i} are the mean and standard deviation of X_i respectively. In contrast to the FOSM method, the Taylor series expansion takes place about the most probable point. The Hasofer-Lind reliability index is equal to the smallest distance from the origin to the failure surface in normalised space (Thoft-Christensen and Murotsu 1986). This geometrical representation is depicted in Figure 2-4.

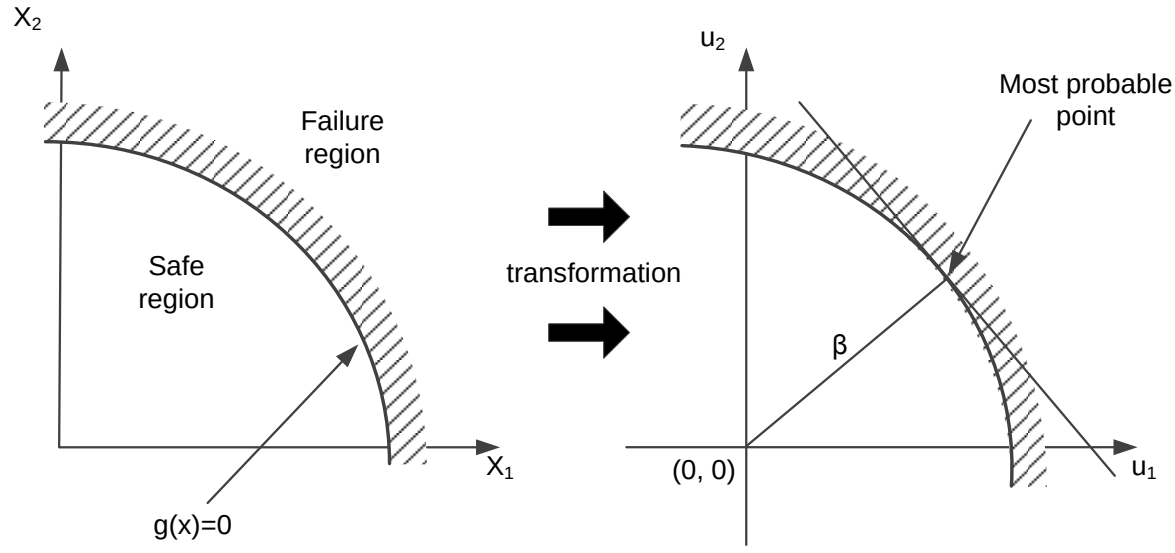

Figure 2-4: Hasofer-Lind reliability index (adapted from Choi *et al.* 2007)

The Hasofer-Lind method assumes normally distributed variables. JCSS (2001) notes that strength is typically modelled using a lognormal distribution and that variable loads are

typically modelled using an extreme value distribution such as the Gumbel distribution. In the event that variable are non-normally distributed, the modified Hasofer Lind - Rackwitz Fiessler may be used.

2.5.3 Hasofer Lind - Rackwitz Fiessler Method

The Hasofer Lind-Rackwitz Method determining equivalent normal variables for each non-normal random variable prior to using the Hasofer-Lind method (Nowak and Collins 2012). Additionally correlated variables may also be incorporated using a method to transform them into uncorrelated variables. The steps required for the method are as follows (Choi *et al.* 2007, Nowak and Collins 2012):

1. Formulate the limit state function and determine the probability distributions for all variables.

2. Assume an initial design point, such as the mean value, for all variables.

3. For each of the non-normal variables; determine the equivalent normal mean and standard deviation as follows;

$$\sigma_{P'} = \frac{\phi\left(\Phi^{-1}\left[F_p\left(P_1\right)\right]\right)}{f_p(P_1)} \qquad \textbf{2.31}$$

$$\mu_{P'} = P_1 - \Phi^{-1}\left[F_p\left(P_1\right)\right]\sigma_{P'} \qquad \textbf{2.32}$$

For the Gumbel distribution the probability density function and cumulative density function are as follows:

$$f_p(P_1) = a \exp\left\{-(P_1 - \delta)a - \exp\left[-(P_1 - \delta)a\right]\right\} \quad \textbf{2.33}$$

$$Fp(P_1) = \exp\left\{-\exp\left[-(P_1 - \delta)a\right]\right\} \quad \textbf{2.34}$$

4. Determine the gradients of the limit state function at the design point

5. Calculate an initial value for β using the mean-value method:

$$\beta = \frac{g(x) - \sum_{i=1}^{n} \frac{\partial g(U)}{\partial x_i} \sigma_{xi} u_i^*}{\sqrt{\sum_{i=1}^{n} \left(\frac{\partial g(U)}{\partial x_i} \sigma_{xi} \right)^2}} \quad \textbf{2.35}$$

For the first iteration, the numerator is equal to *g(x)*.

6. Calculate the direction cosines for each variable:

$$\alpha_i = \frac{\frac{\partial g(U)}{\partial x_i} \sigma_{xi}}{\sqrt{\sum_{i=1}^{n} \left(\frac{\partial g(U)}{\partial x_i} \sigma_{xi} \right)^2}} \quad \textbf{2.36}$$

7. Determine the coordinates of the new design point

$$x_i^* = \mu_{xi} + \beta \sigma_{xi} \cos\theta_{xi} \quad \textbf{2.37}$$

$$u_i^* = \frac{x_i^* - \mu_{xi}}{\sigma_{xi}} \quad \textbf{2.38}$$

8. Repeat the above steps until the value of β converges

2.5.4 Monte Carlo Simulations

Monte Carlo Simulation (MCS) methods may be used to determine system reliability when it is not possible or feasible to determine system reliability using methods such as FORM. The MCS is a random sampling method. The basic or 'crude' MCS method involves a number of basic steps (Choi *et al.* 2007):

1. Select a distribution for each random variable
2. Generate a sample set from the distribution
3. Use the sample set to conduct simulations

The probability of failure for a system may be estimated as follows:

$$P_F = \frac{N_f}{N} \qquad \textbf{2.39}$$

where N_f is the number of simulations where $g<0$ and N is the total number of simulations. The standard error for a MCS is determined as follows:

$$s = \sqrt{\frac{P_F(1-P_f)}{N}} \qquad \textbf{2.40}$$

where s is the standard error. As Equation 2.40 indicates, the error is inversely proportional to the number of simulations. This highlights the fact that a very large number of simulations may be required to achieve an acceptable error value. The required number of simulations is particularly large if the probability of failure for a system is small. Due to the inefficiency of random sampling and thus the prohibitive computational demands, variance reduction techniques may be useful in cases where the probability of failure is low. Various methods

including importance sampling or Latin hypercube sampling (LHS) may be used to reduce the estimate variance.

2.6 CONCLUSIONS

Robustness of structures in withstanding abnormal exposures involving local failure is an important consideration in the design and management of civil engineering structures. Robustness can be viewed a key component of the broader collapse resistance of a structure which encompasses related properties such as the vulnerability of a structure to initial damage and the interaction of a structure and its environment. Notwithstanding the broader context, robustness is fundamentally a property of structural systems which effectively constitutes a new dimension of the fundamental structural capacities such as strength and ductility.

Research on the subject of structural robustness, particularly in terms of generalised characterisation and quantification, is still limited; however, conceptual methods and specific measures have been proposed from a varied range of evaluation perspectives. In this thesis, these approaches are classified into five groups, namely i) static stiffness-based methods, ii) vulnerability methods, iii) energy-based methods, iv) reserve factor/ redundancy methods and v) probabilistic methods.

In the context of general robustness as presented in this thesis, structural robustness concerning resistance to progressive or disproportionate collapse, especially those induced by removal of a vertical load carrying member, is a specialised theme. With this in mind, readers are directed to the progressive collapse literature regarding the evolution of the robustness-

oriented design guides and corresponding structural analysis techniques under progressive collapse scenarios.

3 CRITICAL EVALUATION OF ROBUSTNESS ASSESSMENT METHODOLOGIES

3.1 INTRODUCTION

Chapter 2 presented a subset of the general collapse resistance literature which is consistent with the view of robustness as an inherent system property. This chapter will evaluate three contrasting assessment methods. These methods were selected for further examination on the basis of a number of criteria.

Most importantly, each method is closely related to the research presented in this thesis. The redundancy assessment method proposed by Ghosn and Moses (1998) is related to the comprehensive index which is presented in Chapter 4. The other two methods differ in the sense that one is based on the static stiffness of a structure whereas the other quantifies damage resilience in terms of energy absorption. Nevertheless, they are both concerned with the identification of critical failure sequences, which is the focus of Chapter 5 and 7.

Finally, each method addresses several of the requirements which are proposed by Starossek and Haberland (2011) as a means to assess the usefulness of robustness measures. Most importantly for the present investigation, each of the methods is calculable; the inputs required for the quantification may be readily determined and the methods yield a clear output. Furthermore, each of the methods is objective in terms of the user input and they are generalizable in terms of the structures to which they may be applied.

3.2 BENCHMARK STRUCTURE

A benchmark truss structure is selected for the illustrative analysis. The use of a truss structure enables a convenient handling of the static redundancies whilst enabling a clear identification of the structural contribution of each member. At the same time, the capacity of a truss-based analysis to demonstrate the essential concepts and procedures associated with the assessment of the general redundancy and robustness is largely retained.

The same structural configuration is used for each analysis in order to facilitate a clear comparison of the methods. Each assessment method is demonstrated using an analysis of a two-dimensional 21-member truss, as illustrated in Figure 3-1. All joints are pinned; therefore there is no rotational resistance and members are only subjected to axial forces. The structure was designed using SAP 2000 in accordance with BS EN 1993-1-1:2005. The total loads are simplified as three equal concentrated loads of 726 kN applied at the bottom joints.

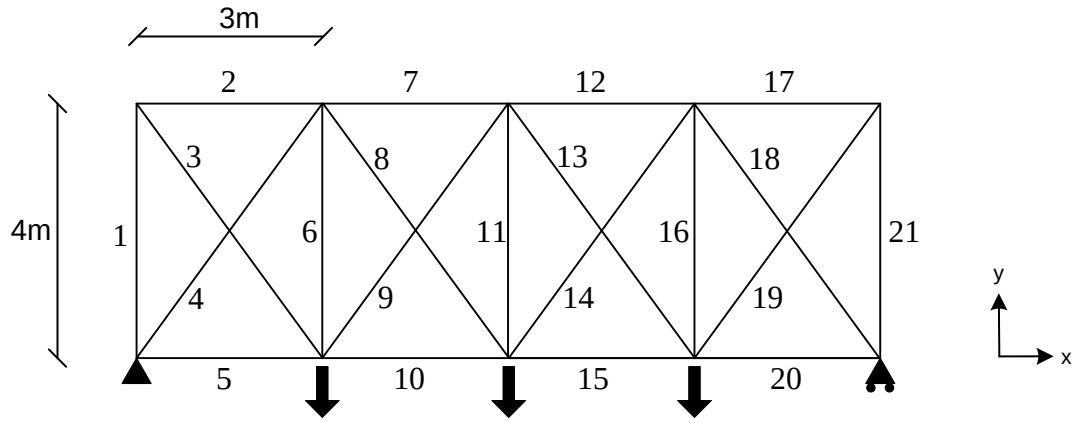

Figure 3-1: Benchmark truss structure

The left-hand support is pinned, restraining translation in the x and y directions. The roller at the right-hand support allows translation in the x direction. The area of each member is listed in Table 3-1. The truss is symmetrical in terms of the topology and the member sizes.

Table 3-1: Member cross-section area and length

Member	L (m)	Area (m^2)
1, 21	4	0.00726
2, 17	3	0.00472
3, 19	5	0.00472
4, 18	5	0.01440
5, 20	3	0.00548
6, 16	4	0.00203
7, 12	3	0.01170
8, 14	5	0.00320
9, 13	5	0.00320
10, 15	3	0.00726
11	4	0.00165

3.2.1 Material Properties and Member Failure

All members are steel and have identical material properties. A Young's Modulus of 200 GPa, a yield stress of 250 MPa and an ultimate stress of 450 MPa are assumed. This is consistent with S275 grade steel. The stress-strain relationship is simplified using a piecewise-linear stress-strain relationship, as illustrated in Figure 3-2. For common steel grades, such as S275, the ultimate strain typically ranges from 20% to 25% (Kuhlmann *et al.* 2009). However, Knoll and Vogel (2009) note that truss connections are generally less resistant than the members which they connect. This is due to the presence of bolt holes or welds which can cause localised concentrations of plasticity; rendering the connection susceptible to tensile rupture. Ghosn and Moses (1998) propose a strain limit of 2%. It is believed that strain levels in excess of 2% will cause connection failure and member unloading. As illustrated in Figure 3-2, a 2% strain limit is assumed for the subsequent analyses.

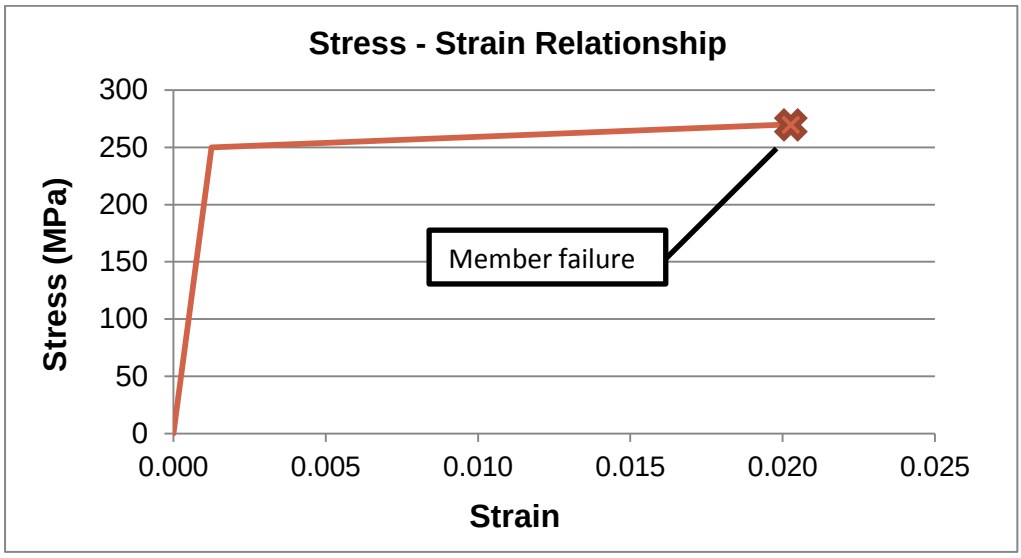

Figure 3-2: Stress-strain relationship

3.3 STIFFNESS-BASED VULNERABILITY ASSESSMENT

3.3.1 Introduction

As discussed in Section 2.3.2, various properties of stiffness matrices may be used to assess the stability of a structure. The structural vulnerability analysis methodology outlined by Pinto et al. (2002) and several other papers from Bristol University, proposes to quantify the vulnerability of a structure to disproportionate collapse. One of the most notable features of this approach is that it quantifies the susceptibility of a structure to any arbitrary damage event without the normal constraints which would govern a response-based analysis, such as a specific load pattern. This is achieved by determining a vulnerability index which evaluates the degree of disproportion between the effort required to cause a damage event and the subsequent consequences in terms of structural deterioration. This definition of vulnerability is effectively the reciprocal of the conventional robustness definition; vulnerable structures are non-robust and vice versa.

The methodology consists of two main steps. The first step involves forming a structure hierarchy based on how the members are connected together. The quantitative measure of how well the structure is connected together is referred to as the well-formedness. The hierarchy generation, which involves clustering the members into substructures, is based on graph theory. The second step involves searching the hierarchy in order to identify vulnerable scenarios in which the damage consequences are disproportionate to the effort required to cause the damage.

3.3.2 Vulnerability Theory

The two core components of the analysis are the effort required to cause a damage event and the consequences of the damage event. For any individual damage event, each of these parameters may be easily determined, thus yielding a quantification of the vulnerability for a specific damage event. However, in addition to individual damage events, the method also proposes to analyse a range of damage scenarios including the total failure scenario, which is the collapse scenario with the highest vulnerability index, and the maximum failure scenario, which is the failure scenario with the highest vulnerability index irrespective of whether or not collapse occurs. These damage scenarios may involve sequences of several members. The following description is a summary of the work which may be found in (Lu *et al.* 1999, Pinto *et al.* 2002, Agarwal *et al.* 2003), and other papers from this group.

3.3.2.1 Damage Demand

The damage demand is the effort required for a damage event to occur. A damage event is defined as the loss of a degree of freedom (DOF). For example a fixed joint can be reduced to a pin joint by releasing the rotational DOF. This is a single damage event. For this scenario

the degree of effort is assumed to be equal to the rotational stiffness coefficient in the fixed joint prior to damage. This consideration of the damage effort is based on assumption that the stiffness coefficient represents the capacity of the joint to resist forces in a principal direction.

The damage demand quantification method, described in Lu *et al.* (1999), relies on the stiffness of the individual members and the joints which connect them. It is assumed that the damage demand is proportional to the loss of stiffness which occurs due to the damage event. If for example, the damage event is the loss of rotational stiffness at a joint, the damage demand is equated to the rotational stiffness of the joint prior to damage.

The relative damage demand is created by normalising the damage demand for each event by dividing the damage demand for an event by the maximum possible damage demand, as shown in Equation 3.1.

$$D_r = \frac{D}{D_{\max}} \qquad \textbf{3.1}$$

The denominator, which is the maximum possible damage demand, is derived from the scenario in which all members in the structure are damaged. If the type of damage considered is putting a pin in the centre of a member, then the relative damage demand is the sum of the damage demand of a pin in every member of the structure.

3.3.2.2 Well-formedness

The well-formedness is the measure used to quantify how well the structure is connected together and also the consequences of a damage event. The well-formedness of a joint q_i is the determinant of the stiffness submatrix associated with joint *i*.

$$q_i = \det\left(K_{ii}\right) \quad \textbf{3.2}$$

K_{ii} is the sum of the stiffness submatrices of all members meeting at joint *i*. The determinant of the stiffness submatrix is equal to the product of the eigenvalues. In the case of a pin joint:

$$\det\left(K_{ii}\right) = \lambda_1 \times \lambda_2 \quad \textbf{3.3}$$

where λ_1 and λ_2 are the principal translational stiffness coefficients.

A structure is considered in terms of individual substructures called structural rings, or clusters which are simply one or more rings joined together. The ring is the basic structural unit which is, in the case of a truss, comprised of three members and three joints. Structural rings for a truss and frame are illustrated in Figure 3-3. The well-formedness of a structural ring, Q, is the average of the well-formedness of all joints in the ring:

$$Q = \Sigma q_i / N \quad \textbf{3.4}$$

where *N* is the total number of joints in the ring.

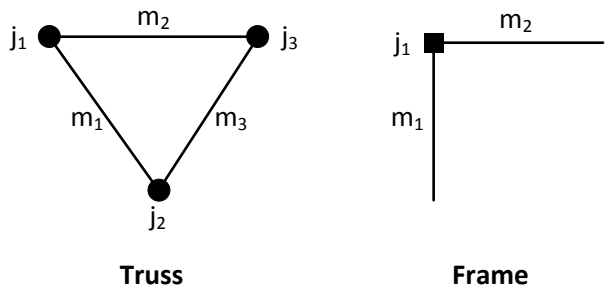

Figure 3-3: Structural ring

The failure consequences of a damage event are evaluated in terms of the well-formedness of the structure. In order to calculate the failure consequences, the change in well-formedness

following the damage event is divided by the well-formedness of the intact structure. For a given structure, the well-formedness of the intact structure is a constant. The consequences are referred to as the degree of separateness. The equation is as follows:

$$\gamma = \frac{Q(S) - Q(S')}{Q(S)} \qquad \textbf{3.5}$$

where γ is the separateness, Q(S) is the well-formedness of the intact structure and Q(S') is the well-formedness of the damaged structure.

A structure is deemed to have collapsed when it can no longer form a stable structural unit with the ground. This occurs if there are no clusters which can form a ring with the ground. Therefore Q(S') can be understood as the well-formedness of clusters which are still connected to the ground. In the case of collapse Q(S') is equal to zero and the separateness is equal to one. However, if local failure occurs but some clusters remain structurally connected to the reference, then the separateness will range between zero and one. If no damage occurs then the separateness is equal to zero.

3.3.2.3 Structural Hierarchy

In order to facilitate the identification of critical scenarios, the structure is assembled into a hierarchy comprised of rings and larger substructures. The hierarchy is a 'map' which describes how a structure is connected together. While the creation of the hierarchy encompasses the form and connectivity of the structure, the subsequent searching of the hierarchy provides a method to identify critical sequences. Similarly to the searching algorithm employed by Smith (2003a), the hierarchy is intended to facilitate a more efficient solution to the identification of critical sequences.

The formation of the structural hierarchy begins with a single ring and ends when the entire structure is represented by a single cluster. An algorithm is proposed to identify the selected members and rings at each stage. The well-formedness is the primary selection criterion; ensuring that at each level the well-formedness is maximised. Other criteria such as the damage effort are also considered. An algorithm is also proposed to search the hierarchy for critical damage scenarios which have a high vulnerability index.

3.3.2.4 Vulnerability Index

The vulnerability index for a particular scenario is determined by dividing the consequences of damage by the relative damage demand:

$$\varphi = \frac{\gamma}{D_r} \qquad \textbf{3.6}$$

where the vulnerability φ, is the ratio of the separateness (damage consequences), γ, to the relative damage demand, D_r. This formula establishes the degree of disproportion between the damage effort and the damage consequences.

3.3.3 Analysis

The subsequent analysis uses the 2D truss structure outlined in Section 3.2. The hierarchy is determined using the algorithm described in Pinto et al. (2002). Each stage of the procedure is illustrated in Figure 3-4. Firstly, each ring in the structure is analysed and the ring with the highest well-formedness is used to start the hierarchy. There are two options; the ring formed by Members 1, 2 and 4, or the ring formed by Members 17, 18 and 21. Each ring is identical in terms of all selection criteria. Therefore, ring 1, 2, and 4 is arbitrarily selected to start the hierarchy. Successive members are added at each stage until Cluster 26 is formed. At this

point, the addition of more members to Cluster 26 will decrease the well-formedness. Therefore, a new branch of the hierarchy is started by creating Cluster 28 using Members 17, 18 and 21. Likewise, members are successively added to this branch of the hierarchy until Cluster 32 is formed. Cluster 32 and Cluster 27 are combined to form Cluster 33, thereby uniting both sides of the structure into a single Cluster. Finally, the ground is added to form Cluster 34.

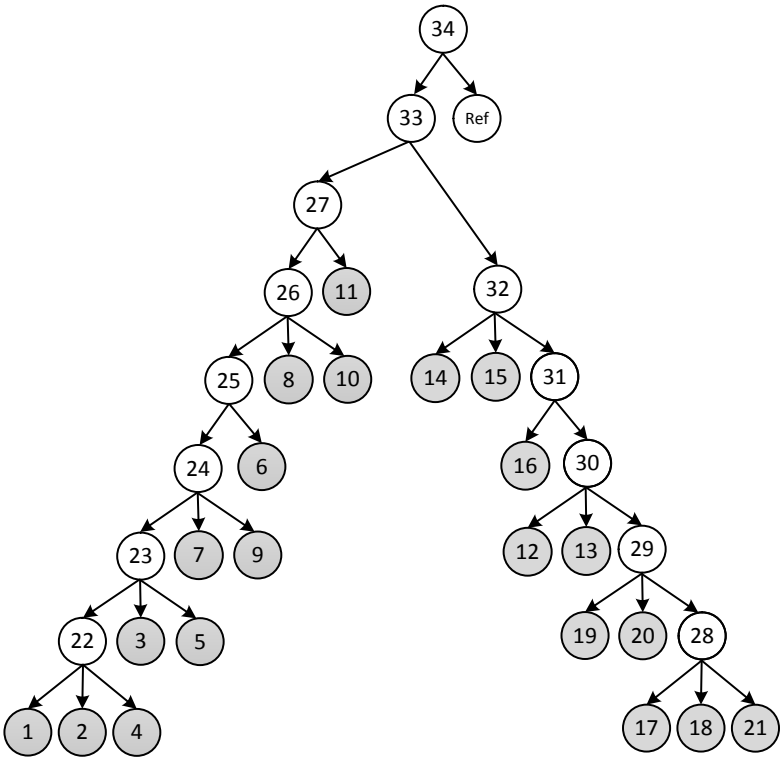

Figure 3-4: Structure hierarchy

This hierarchy formation procedure is also illustrated in Figure 3-5 with the aid of structure diagrams. At each stage, the cluster which is created is identified by the outlined text and the members which are added to the structure are identified by the non-outlined text.

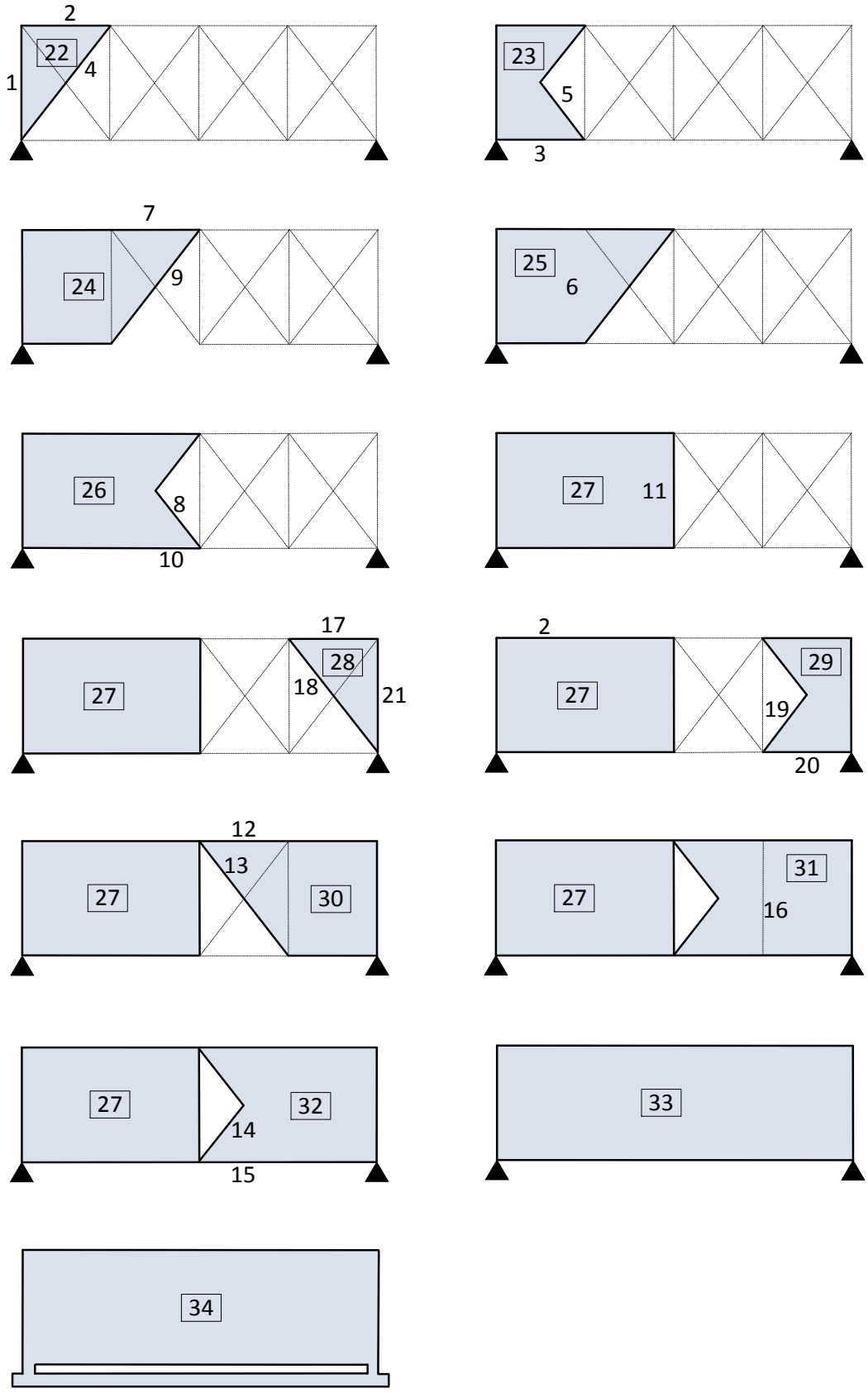

Figure 3-5: Hierarchy formation

The next step is to search the hierarchy using the proposed algorithm. The search begins from the top, Cluster 34, and continues downwards using the searching algorithm which is described in Pinto et al. (2002). The path of the searching algorithm is illustrated by the highlighted path in Figure 3-6. The first event to be identified is the failure of Member 20. Member 20 is therefore removed from the structure and the structure is re-clustered to form a new hierarchy without Member 20. The new hierarchy and the path identified by the searching algorithm are illustrated in Figure 3-7. Similarly, the search begins at the top of the hierarchy. Member 21 is identified as the next member in the sequence and it is removed from the structure. Following the removal of Member 21, the structure can no longer be re-clustered to form a stable ring with the ground. Therefore, the structure has collapsed and the well-formedness is equal to zero.

Searching may also be initiated from lower levels in the hierarchy, yielding different damage events. From each level the search continues until the root cluster has failed. For example, if the searching procedure begins from Cluster 26, the sequence identified is the failure of Member 8 followed by the failure of Member 10. Non-collapse sequences may also be identified. For example, if Cluster 22 is searched, the failure of Member 2 is the only damage event, as it is sufficient to fail the cluster. However, although this event does not cause collapse of the structure, it may have a high vulnerability index if the total damage demand for the sequence is relatively low.

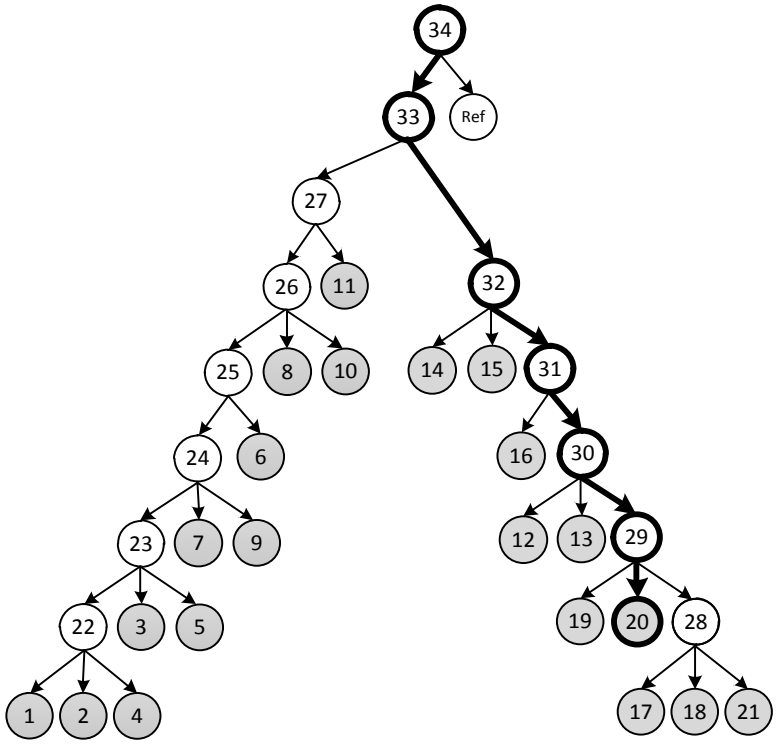

Figure 3-6: Hierarchy search

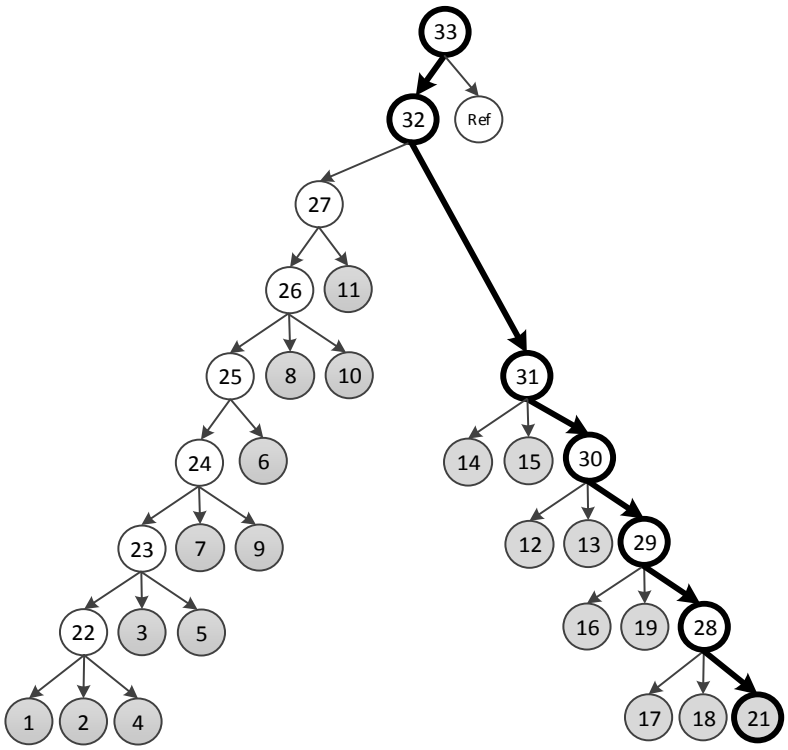

Figure 3-7: Re-clustered hierarchy

In addition to the events identified by the searching algorithm, the vulnerability of all two member sequences in the structure was determined. Table 3-2 shows the twenty most critical sequences and the associated separateness, relative damage demand and vulnerability. Due the fact that all results are function of the stiffness properties of the structure, the order of the sequences is irrelevant. For example, sequence 2 – 6 is the same as sequence 6 – 2. Repeat sequences are not reported. The notation '2 – 6' indicates that the first member in the sequence is Member 2 and the second member in the sequence is Member 6.

In the present analysis, the most critical events are those with the highest vulnerability index. Therefore the results are ranked according to vulnerability. The most critical sequence (the sequence with the highest vulnerability index) is sequence 8 – 9. All sequences which are ranked from 1 to 13 are collapse sequences. This is indicated by the separateness value of 1. The most vulnerable single member sequence is Member 11. Member 11 is also the easiest member to damage as it has the lowest relative damage demand.

Table 3-2: Two member sequences

Rank	Sequence	Separateness	Relative Damage Demand	Vulnerability
1	8 - 9	1.000	0.037	27.114
2	5 - 3	1.000	0.080	12.526
3	10 - 9	1.000	0.088	11.342
4	10 - 8	1.000	0.088	11.342
5	2 - 5	1.000	0.098	10.208
6	5 - 1	1.000	0.105	9.530
7	4 - 3	1.000	0.110	9.076
8	4 - 2	1.000	0.128	7.793
9	7 - 9	1.000	0.131	7.644
10	8 - 7	1.000	0.131	7.644
11	4 - 1	1.000	0.135	7.392
12	4 - 5	1.000	0.136	7.374
13	7 - 10	1.000	0.182	5.491
14	11	0.064	0.012	5.415
15	6 - 11	0.132	0.027	4.973
16	11 - 16	0.132	0.027	4.973
17	6	0.067	0.015	4.615
18	16	0.067	0.015	4.615
19	6 - 16	0.135	0.029	4.615
20	9 - 11	0.122	0.030	4.038

3.3.4 Discussion

Although the most critical sequence is 8 – 9, this sequence is not identified by the searching algorithm irrespective of which level of the hierarchy the searching procedure begins. This indicates that the searching algorithm is not a completely effective method of identifying critical sequences. If using the algorithm is not sufficient to identify the most critical

sequences, this may make the justification for using the hierarchy and algorithm less compelling.

The consequences of damage, or separateness, are quantified in terms of the loss of well-formedness. In order to provide some context by which this approach can be assessed, the consequences of damage events are also quantified in terms of the reduction in ultimate strength with the commonly used residual strength index:

$$R_i = \frac{F_{u,i}}{F_{u,o}} \qquad \textbf{3.7}$$

Firstly, the ultimate strength of the intact structure is determined by increasing the load until the ultimate strength is reached. Next, each member is removed one at a time and the ultimate strength is similarly determined for each residual structure. Table 3-3 compares the indices determined using the separateness index and the ultimate strength index. In the case of the well-formedness indices, the most critical member is Member 4. This is principally due to the fact the Member 4 has the largest axial stiffness and thus its removal causes the greatest reduction in well-formedness. Member 3 is the least critical member. As can be expected, there are significant discrepancies between the results obtained using the stiffness-based measure and the results obtained using the strength-based measure. The most critical members in terms of a reduction in ultimate strength are Members 7 and 10. This simple comparison highlights the drawbacks associated with using a stiffness-based approach.

Table 3-3: Comparison of well-formedness and ultimate strength indices

Stiffness Indices		Strength Indices	
Member removed	**Separateness**	**Member removed**	R_i
4	0.182	7	0.768
7	0.179	10	0.768
5	0.109	4	0.539
1	0.100	5	0.539
2	0.094	1	0.449
10	0.077	2	0.449
6	0.067	3	0.449
11	0.064	8	0.305
9	0.059	6	0.227
8	0.051	11	0.064
3	0.050	9	0.062

However, the definition of the separateness index as a means to assess the consequence of a damage sequence represents an improvement over similar indices which have been discussed by Starossek & Haberland (2011) and Nafday (2008). For example, Starossek & Haberland (2011) propose the following robustness index:

$$R_s = \min_j \frac{\det K_j}{\det K_o} \qquad \textbf{3.8}$$

where $\det K_j$ and $\det K_o$ are the determinants of the intact and damaged structural stiffness matrices respectively. If any eigenvalue of a structural stiffness matrix is zero, the corresponding stiffness matrix determinant will also be equal to zero. For example, in the analysed truss structure, if Members 1 and 2 fail, the stiffness matrix determinant will be equal to zero despite the capacity of the structure to continue carrying load. In contrast, the stiffness-based method proposed by Pinto et al. (2002) uses the determinant of the stiffness

matrices at each joint in the structure. This facilitates better analysis resolution and a more specific collapse definition. Collapse is defined as disconnection from reference. Therefore, if Members 1 and 2 fail, the structure is not considered to have collapsed, as the rest of the structure may still form a stable connection to the ground. This definition is more reasonable if collapse is defined as the loss of load carrying capacity.

3.4 ENERGY-BASED VULNERABILITY ASSESSMENT

3.4.1 Introduction

Smith (2003a) proposes an energy-based structural vulnerability assessment. The primary aim of this method is to evaluate critical sequences of damage events which lead to the collapse of a structure. The most critical sequences are those with the lowest total energy requirement. The most critical sequence is effectively the easiest way to cause collapse of the structure. Both the energy required to cause the failure of a member, referred as the work of failure, and the subsequent consequences of member failure are expressed in terms of strain energy. The work of failure is comparable to the damage demand discussed in Section 3.3.

"The underlying principle is similar to the conditions leading to fast fracture in linear elastic fracture mechanics. When a member is damaged, energy is released and is available to cause overstress of other members. Loss of a single member may not be sufficient to cause overall failure and therefore the aim is to find the sequence of damaged members that requires the least amount of effort to cause collapse" (Smith 2003b).

Each damage event is defined as the failure of a single member. Members are removed one at a time until total collapse of the structure occurs. The total energy requirement is the sum of

the work of failure for each event in the sequence. Smith proposes to use an energy ratio which can make the identification of critical sequences more efficient. This approach is similar to Dijkstra's shortest route algorithm which can be used to find the shortest distance through a network, such as traffic network (Dijkstra 1959). In the case of this methodology, the objective function to be minimised is not distance but energy.

3.4.2 General Methodology

3.4.2.1 Work of Failure

In order to determine the total work of failure for a sequence, the net work failure for each event is used. When loads are applied to a structure, strain energy develops in each member. Therefore, the net work of failure for a member is equal to the work of failure minus the strain energy in the member under loading. The net work of failure is, in effect, the energy reserve in a member and represents the additional energy required to cause member failure. The net work of failure is defined as follows (Smith 2003a):

$$\Delta W_{f,i} = W_{f,i} - U_i \qquad \textbf{3.9}$$

where $W_{f,i}$ is the work of failure for a Member *i* and U_i is the strain energy in the member. The total effort required for a failure sequence is equal to the sum of the net work of failure of all *n* members in the failure sequence (Smith 2003a):

$$Total\ work\ of\ failure\ = \sum_{i=1}^{n}\left(\Delta W_{f,i}\right) \qquad \textbf{3.10}$$

Damage is simulated by removing elements one at a time until the structure fails. In theory, this could be conducted by a simple trial and error procedure until all possible collapse

sequences have been evaluated. Although this approach would be sufficient to identify the sequences with the lowest energy requirement, a searching algorithm is proposed to make the identification of critical sequences more efficient.

3.4.2.2 Searching Algorithm

An energy ratio is proposed to identify the next member in each sequence. The energy ratio is defined as follows (Smith 2003a):

$$f(U) = \frac{\Delta W_{fi}}{\Sigma U^{i}} \qquad \textbf{3.11}$$

where $\Delta W_{f,i}$ is the net work of failure for Member *i*, and ΣU^{i} is the consequence of removing Member *i*. ΣU^{i} is defined as the total strain energy in the structure after the failure of Member *i*. The numerator is the net effort required to fail a member. If at any stage the strain energy in a member exceeds the work of failure, then the member is considered to have failed and is removed from the structure. This scenario is indicative of progressive collapse behaviour. The denominator is a measure of the consequences after a member has been removed from the structure. It is equal to the total strain energy in the structure, which is the integral of the force displacement relationship up to the prescribed point of failure. The energy ratio is minimised according to equation 3.12 (Smith 2003a):

$$f(U)_{y} = \min\left[f(U)_{x} + \Delta f(U)_{x,y} \right] \qquad \textbf{3.12}$$

where $f(U)_{y}$ is the value of the function from the root to a candidate node *y*, $f(U)_{x}$ is the value of the function from the root to a node *x* which is already in the tree, and $\Delta f(U)_{x,y}$ is the change in value from the solved node to the candidate node.

All candidate members are evaluated by trial and error. Firstly, a member is removed from the structure and the energy ratio is evaluated. The member is then replaced and the next member is removed from the structure. Similarly, the energy ratio is calculated. This process is carried out for all candidate members and the member which minimises the energy ratio is selected for removal. Members are removed consecutively until collapse occurs.

The procedure is illustrated in Figure 3-8. Each node represents a removed member and the extending branches are candidate members which are evaluated using energy ratio and searching algorithm. Some branches of the tree may remain incomplete due to repetition of existing sequences or because they are no longer optimal.

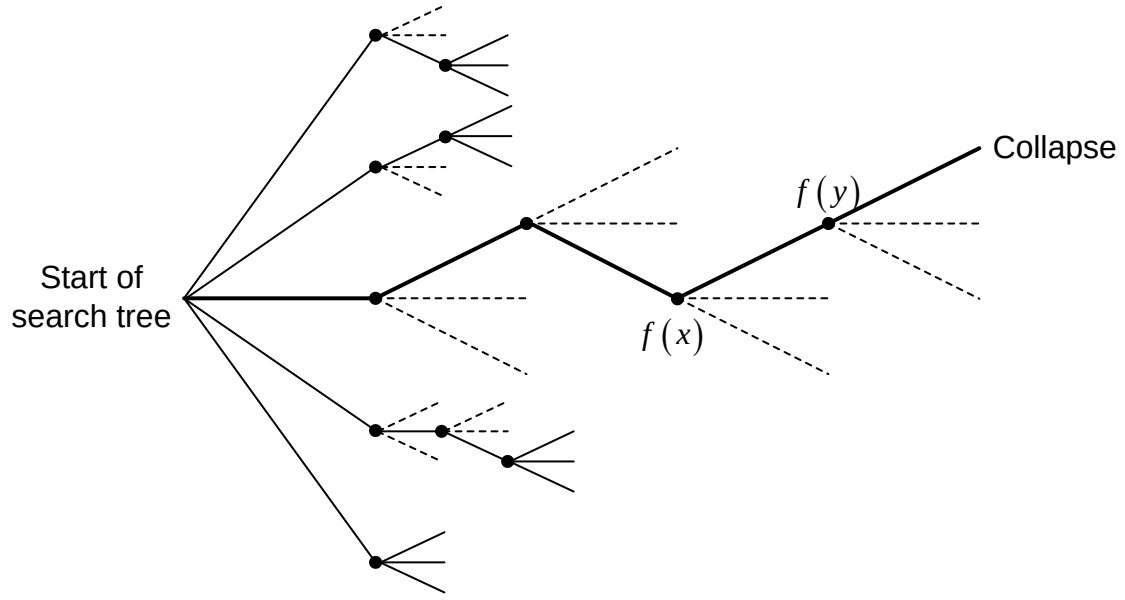

Figure 3-8: Search path (adapted from Smith 2003b)

3.4.3 Analysis

The first step of the analysis is to determine the work of failure for each member in the structure. The 21 member truss, presented in Figure 3-1, is used for the analysis. The

calculation of the work of failure is a relatively open ended procedure which may be determined to suit the specific application. Similarly to Smith (2003b), the work of failure is defined as the elastic strain energy. The tensile work of failure at member yield was determined using the following formula:

$$U_y = \frac{\sigma_y{}^2 AL}{2E} \qquad \textbf{3.13}$$

where U_y is the strain energy at yield, L is the length, E is the Young's modulus, A is the area and σ_y is the yield stress.

Smith (2003a) uses the Perry Robertson formula to determine the critical buckling stress in compression members. The Perry-Robertson formula assumes that a member will fail if the maximum compressive stress at the extreme fibre of the member cross-section reaches its yield stress (Paik and Thayamballi 2003). However, as noted by Dwight (1975), this assumption may be overly conservative as strain hardening is ignored. Despite these limitations, the approach suggested by Smith (2003a) is used for the following analyses.

The Perry-Robertson formula is used to determine the critical buckling stress given a specified bow imperfection. The maximum value of the bow imperfection was determined as member length/ 250 using Table 5.1 of EN 1993-1-1:2005 (2010). Given an initial imperfection, the critical load is determined using the Perry-Robertson formula below.

$$\sigma_{cr} = \frac{\sigma_y + \sigma_E(1+\eta)}{2} - \left[\left(\frac{\sigma_y + \sigma_E(1+\eta)}{2}\right)^2 - \sigma_y\sigma_E\right]^{0.5}, \quad \text{where } \eta = \frac{ac}{r^2} \qquad \textbf{3.14}$$

σ_y is the yield stress, σ_E is the Euler buckling stress, α is the initial displacement, c is the distance from the centroid to the most stressed fibre and r is the radius of gyration.

The work of failure for each member in the structure is detailed in Table 3-4. The work of failure for both tension and compression members is similar due to the assumption that the members exhibit brittle failure.

Table 3-4: Work of failure

Member	Section (mm)	Tension (N/m)	Compression (N/m)
1	356x171x57	4538	3539
2	305x127x37	2213	1757
3	305x127x37	3688	2521
4	610x229x113	11250	9274
5	254x146x43	2569	2000
6	152x89x16	1269	720
7	533x210x92	5484	4807
8	254x102x25	2500	1584
9	254x102x25	2500	1584
10	356x171x57	3403	2821
11	127x76x13	1031	522
12	533x210x92	5484	4807
13	254x102x25	2500	1584
14	254x102x25	2500	1584
15	356x171x57	3403	2821
16	152x89x16	1269	720
17	305x127x37	2213	1757
18	610x229x113	11250	9274
19	305x127x37	3688	2521
20	254x146x43	2569	2000
21	356x171x57	4538	3539

The structure is analysed using the algorithm described in Smith (2003a) and Smith (2003b). Firstly, the intact structure under service load is analysed. The strain energy in each member of the structure is determined. Next, each member is removed from the structure one at a time

and the total strain energy in the residual structural state is determined. This allows the energy ratio (Equation 3.11) to be determined for each member in the structure.

Table 3-5 presents the ranked energy ratios, which have been determined using Equation 3.11. The two most critical members are Member 7 and Member 10. The removal of each of these members causes progressive collapse of the structure. Therefore, there is only one event for each of these sequences.

Table 3-5: Energy ratios for the members of the intact structure

Member	Energy Ratio
10	0.181
7	0.183
6	0.211
11	0.225
2	0.293
5	0.345
9	0.349
8	0.383
3	0.578
1	0.598
4	1.293

Member 6 is the third most critical member. Therefore, Member 6 is removed from the structure; creating a new branch. Similarly the energy ratio is determined for each member in residual state 6. Members are removed sequentially until collapse occurs.

The 15 most critical damage sequences are presented in Table 3-6. They are ranked according to the total net work of failure. Two types of collapse are observed; progressive collapse and the occurrence of a mechanism. Progressive collapse occurs when the failure of one member

releases strain energy which then causes another member to fail. This process continues until collapse occurs. A mechanism occurs when the failure of a member causes structural instability.

As illustrated by the results in Table 3-6, the criticality of a failure sequence is independent of the number of events which are in the sequence. Although the failure of Members 7 and 10 causes progressive collapse of the structure, and thus only require one damage event, these sequences are not the most critical. The most critical failure sequence is the failure of Member 2 followed by the failure of Member 6.

Table 3-6: Most critical damage sequences

Rank	Member Sequence	Total net work of failure (N/m)	Collapse Type
1	2 - 6	1948	Progressive
2	2 - 11 - 6	2434	Progressive
3	6 - 2	2631	Progressive
4	11 - 2 - 6	2941	Progressive
5	10	3061	Progressive
6	6 - 11 - 2	3145	Progressive
7	2 - 8	3619	Progressive
8	6 - 16 - 2	3646	Progressive
9	5 - 2	3662	Mechanism
10	9 - 8	3699	Mechanism
11	5 - 3	3746	Mechanism
12	2 - 5	3808	Mechanism
13	6 - 3	3909	Progressive
14	6 - 15	4097	Progressive
15	11 - 10	4100	Progressive

Smith (2003a) notes that there is very little difference between the total effort required to cause collapse in sequences which are the same, albeit in a different order. However, as the results in Table 3-6 demonstrate, in some cases there is a substantial difference between collapse sequences with the same events but in a different order. For example, the total net work of failure for sequence 2 – 6 is 1948 N/m, whereas the total net work of failure for sequences 6 – 2 is 2631 N/m. This is primarily due to the fact that the consequence of removing Member 2 from the structure is greater than the consequence of removing Member 6.

3.4.4 Discussion

Given that the objective is to minimise the net work of failure, it may initially seem prudent to use the minimum net work of failure to select the next member in each sequence rather than an energy ratio which incorporates the work of failure and the failure consequences.

However, using the minimum work of failure to guide the identification of damage events is not an optimal searching strategy. Members with the lowest net work of failure are the easiest to damage. However, such members generally play a less important structural role and therefore their removal from the structure causes less damage to the rest of the structure than, for example, a member selected using the energy ratio. This means that if members are selected using the minimum net work of failure, more events are required to cause structural collapse. As a result the total net work of failure for the sequence will be higher than the total net work of failure of a sequence selected using the energy ratio.

An example to illustrate the difference between sequences determined using the net work of failure and energy ratio is presented in Table 3-7. Member 11 is selected first as it has the minimum net work of failure. Similarly Member 6 has the minimum net work of failure in residual state 11. The sequence ends when the removal of Member 2 causes the progressive collapse of the structure. Although the net work of failure for each event is low, four events are required to cause collapse of the structure. The total net work of failure for the sequence is equal to 4646 N/m, which is considerably higher than the total net work of failure for sequences determined using the energy ratio.

Table 3-7: Sequence determined using the net work of failure

Member	Net work of failure (N/m)
11	1025
6	1074
16	1014
2	1533
Total net work of failure for sequence = 4646 N/m	

Similarly to the stiffness-based evaluation method discussed in the Section 3.3, the energy assessment methodology is principally a way to evaluate the vulnerability of a structure; i.e. how susceptible a structure is to collapse. It is therefore different to most redundancy analyses which typically analyse the consequence of an assumed damage event. By confining the scope of the approach to collapse sequences, the consequences of all collapse sequences can be considered equivalent and in effect neglected. Therefore, sequences may reasonably be evaluated in terms of the total damage effort. On the other hand, if individual events are considered, as for example in Ghosn & Moses (1998), the net work of failure is not a useful quantitative measure in the context of robustness. This is principally due to the fact that the net work of failure for a single member is a member property and thus does not reflect how a system responds to damage.

In order to illustrate this discrepancy, Table 3-8 shows the evaluation of Members 1 to 11 using both the net work of failure and the residual strength index (Frangopol and Curley 1987). Each set of results is ranked according to the most critical; members with a low work of failure are the most critical, while damaged states with a high residual strength index are critical. Clearly, there is very little agreement between the two sets of results. In terms of

energy, Member 11 is the most critical. However, in terms of residual strength, Member 11 is the second least critical.

Table 3-8: Comparison of net work of failure and damage consequences

Ranked Net W_f		**Ranked Strength Indices**	
Member	**Net W_f (N/m)**	**Damaged state**	**Residual Strength Index**
11	1025	7	0.768
6	1053	10	0.768
9	1583	4	0.539
2	1672	5	0.539
8	2168	1	0.449
5	2417	2	0.449
10	3061	3	0.449
3	3296	8	0.305
1	3409	6	0.227
7	4459	11	0.064
4	9009	9	0.062

One feature of conventional response-based redundancy or robustness analyses is that the sequence of events leading to collapse is a ‘natural’ failure path which is governed by the properties of the structural system. The term natural here means that, for example, the member which fails first in intact structure is the member with the highest strain. Similarly, the member which fails next is the member which reaches its ultimate strain and so on.

The most critical collapse sequences in terms of the total net work of failure are examined to ascertain the degree to which they are the natural failure sequences or on the other hand arbitrary failure sequences. The primary issue with regard to arbitrary failure sequences is that they will have a higher probability of failure.

The probability of failure is determined using the first order second moment method as described in Section 2.5.1 and the statistical data presented in Table 3-9.

Table 3-9: Statistical data

	Applied Load	**Yield Stress**
Mean	500 kN	250 MPa
COV	0.25	0.11

Table 3-10 presents the probability of failure for each member of the intact structure. The member with the highest probability of failure is Member 6. The probability of failure of Members 4, 9 and 11 is effectively zero as these members are lightly stressed in the intact structure.

Table 3-10: Probability of failure for members of the intact structure

Rank	**Member**	**Pf**
1	6	2.84E-06
2	8	1.42E-07
3	3	8.09E-09
4	10	3.94E-09
5	7	1.22E-11
6	5	4.55E-12
7	2	3.36E-14
8	1	1.78E-15
9	4	0.00E+00
10	9	0.00E+00
11	11	0.00E+00

Next, the probability of failure of the collapse sequences is determined. Table 3-11 ranks the 15 most critical collapse sequences in order of probability of failure. Collapse sequences 1

and 5 only have one member, as the removal of Members 7 and 10 causes collapse. The collapse sequence with the highest probability of failure is Member 10. The ranked probability of failure shows that there is a clear discrepancy between the most critical sequences in terms of the net work of failure (Table 3-6) and the most probable failure sequences. This discrepancy arises due to the arbitrary nature of the failure sequences.

Table 3-11: Ranked probability of failure for collapse sequences

Rank	Member 1	Member 2	Probability of Failure
1	10		3.94E-09
2	3	6	2.31E-09
3	6	3	1.99E-10
4	6	8	1.70E-10
5	7		1.22E-11
6	5	3	6.22E-13
7	3	8	4.51E-13
8	3	5	2.12E-14
9	6	15	2.06E-14
10	2	6	9.63E-15
11	6	10	1.02E-15
12	6	2	7.44E-16
13	1	6	5.08E-16
14	5	2	3.45E-16
15	6	7	1.82E-16

For example, the most critical failure sequence in terms of the net work of failure is sequence 2 - 6. However, the probability of failure of Member 2 in the intact structure is relatively low. Similarly, in the case of collapse sequence 6 – 2, the probability of failure of Member 2 given that Member 6 has failed is also low relative to the other members in the damaged state.

Both, the energy-based assessment and the stiffness-based vulnerability assessment proposed by Lu et al. (1999) incorporate the effort required to cause a failure event. The energy-based net work of failure is a significant improvement over the purely stiffness-based approach proposed by Lu et al. (1999). The main improvement is derived from the use of the net work of failure rather than a quantitative measure of effort which is constant irrespective of the level of damage in the structure. Using the net work of failure means that as damage accumulates in the structure, the effort required for members to fail decreases as they accumulate strain energy. On the other hand, if the stiffness is used to determine the damage effort, the damage effort for a member is invariant with respect to the state of the structure.

3.5 LOAD FACTOR BASED ASSESSMENT OF REDUNDANCY

3.5.1 Introduction

The following redundancy assessment, proposed by Ghosn and Moses (1998), aims to bridge the gap between the traditional single component perspective of structural design and more general system properties such as structural redundancy. Redundancy is defined here as the capacity of a structure to continue to carry loads after the failure of one of its members. A practical application of the method may be found in Wisniewski *et al.* (2006). The following description is a summary of the method which may be found in Ghosn and Moses (1998)

Two alternative redundancy assessment approaches are proposed. The first simply involves using system factor tables corresponding to particular structures. However, for structures which do not correspond to the system tables, a direct redundancy check using an incremental

structural analysis is proposed. The direct redundancy check is discussed in the following text.

Four limit states are considered in order to ascertain the capacity of a structure to function after an instance of damage. The member failure limit state is defined as the load factor at which first yield occurs in the intact structure. The load factor is a general factor which may be adapted to a particular analysis. It is defined here as two side by side AASHTO HS-20 trucks (AASHTO 2002). The ultimate limit state is defined as the load factor which causes structural collapse such as in the case of a collapse mechanism. The functionality limit state is defined as the load factor corresponding to the maximum acceptable displacement which is defined here as span/100. The damaged condition limit state is defined as the ultimate capacity of the damaged structure.

A system reserve ratio is defined for the ultimate, serviceability and damage condition limit states. Each reserve ratio establishes the reserve capacity between first member yield of the intact structure and its respective limit state.

$$R_f = \frac{LF_f}{LF_1}, \quad R_u = \frac{LF_u}{LF_1}, \quad R_d = \frac{LF_d}{LF_1} \qquad \textbf{3.15}$$

Each reserve ratio provides a deterministic evaluation of different aspects of the reserve capacity with respect to the intact structure, and thus these indices may be used to determine whether a structure has sufficient redundancy. In order to provide a more robust assessment of the target values, while maintaining relative ease of implementation for the end user, target values for each of the reserve ratios are determined using a reliability analysis of redundant bridge structures.

A large number of redundant bridges were analysed including pre-stressed concrete, I-beam, box-girder bridges and so on. Assuming a lognormal distribution, each load factor is related to its respective relative reliability index as follows;

$$\Delta\beta_u = \beta_u - \beta_{member} = \frac{\ln R_u}{\sqrt{V_{LF}^2 + V_{LL}^2}} \qquad \textbf{3.16}$$

where V_{LF} and V_{LL} are the COV of the member load factor and the maximum expected live load respectively. Firstly, a target reliability index is determined for each limit state. Next, the above equation (similarly for each limit state) is used to determine the target reserve ratio. These target values are as follows; $R_{u,req} = 1.30$, $R_{f,req} = 1.10$ and $R_{d,req} = 0.50$ (Ghosn and Moses 1998). The target reserve ratios are used to determine the redundancy ratio for each limit state as follows.

$$r_f = \frac{R_f}{1.10}, \quad \mathrm{r}_u = \frac{R_u}{1.30}, \quad \mathrm{r}_d = \frac{R_d}{0.50} \qquad \textbf{3.17}$$

If each of these target values is satisfied, a structure is deemed to have sufficient redundancy.

It is also noted that, while bridges may not have sufficient redundancy with respect to the target values, they may still provide a high level of safety. Therefore, it is proposed to also perform a member safety check in accordance with some design criteria. A required member load factor is determined and used to calculate a member reserve ratio, which is the member load factor divided by the required member load factor.

$$r_1 = \frac{LF_1}{LF_{req}}, \text{ where } \quad LF_{req} = \frac{R_{req} - D}{L_{HS-20}} \qquad \textbf{3.18}$$

The system redundancy may be determined as follows, taking into account the reserve capacity:

$$\phi_{red} = \min\left(r_1 r_u, r_1 r_f, r_1 r_d\right) \qquad \textbf{3.19}$$

where ϕ_{red} is the system redundancy factor. If the minimum value is greater than one, the structure is considered to have sufficient redundancy. If, on the other hand, the redundancy of the structure is less than one, the structure should be modified to provide additional redundancy or alternatively increased member strength.

3.5.2 Analysis

The truss structure, as depicted in Figure 3-1, is used herein for an analysis using the above methodology to facilitate an evaluation of the approach. Similarly to Section 3.4, elastic-perfectly plastic material properties are assumed.

Firstly, the intact structural state is analysed in order to determine the member limit state, the functionality limit state and the ultimate limit state. Ghosn & Moses (1998) use load factors which are multiple of HS-20 truck loads to quantify each limit state. Similarly, Wisniewski et al. (2006) use code specified train load to define the load factor. The present analysis is general evaluation and not intended to accord with any particular code specifications. Therefore, rather than a load factor, the applied load in kN is used.

In order to determine the member load factor, LF_l, the load is increased until the first member yields. This occurs at a total applied load of 4025 kN. Next, the load is increased further in

order to determine LF_f. With respect to railway bridges, Wisniewski et al. (2006) suggest a deflection limit state of span/500 in order not to cause discomfort to train users. On the other hand, Ghosn & Moses (1998) propose a deflection limit state of span/100 as the maximum visible displacement that will be acceptable to bridge users or observers. For the present analysis, the more conservative limit of span/500 is used. Therefore, the applied load is increased until the deflection limit state of span/500 is reached. This occurs at applied load of 4196 kN. Finally, the load is further increased until collapse occurs. Collapse is defined here as the failure of the first member. The ultimate load is 4439 kN.

The next stage is to evaluate the damaged condition of the structure. Each member is removed from the structure, one at a time, and the ultimate strength of the damaged structure is determined. The damaged state with the lowest ultimate strength is used to determine the damaged condition reserve ratio. Table 3-12 presents the ultimate strength of each residual state. The most critical member is Member 7; the residual state has an ultimate strength of 1028 kN.

Table 3-12: Ultimate strength of each damage state

Member Removed	Ultimate Strength (kN)
1	2445
2	2445
3	2445
4	2045
5	2045
6	3431
7	1028
8	3087
9	4164
10	1029
11	4155

The reserve ratios are now determined for the functionality, ultimate and damaged condition limit states using Equation 3.15. The reserve ratios for each limit state are presented in Table 3-13.

Table 3-13: Reserve ratios

Limit State	Reserve Ratios
Ultimate	1.10
Functionality	1.04
Damaged Condition	0.26

Redundancy ratios are determined using the reserve ratios and the target redundancy values (see Equation 3.17). Table 3-14 shows the target redundancy values and the redundancy ratios for each limit state. If any of the three redundancy ratios is less than one, the structure is deemed to have insufficient redundancy. The results therefore indicate that the truss structure has insufficient redundancy with respect to all three limit states.

Table 3-14: Redundancy ratios

Limit State	Target Value	Redundancy Ratio
Ultimate limit state	1.3	0.85
Functionality limit state	1.1	0.95
Damage condition limit state	0.5	0.51

Although the redundancy ratios imply that the structure has insufficient redundancy, a conservatively designed structure may still provide adequate safety levels if the most critical member has a sufficient reserve capacity. The member capacity check can be carried out with respect to the relevant design codes. For example, a simple evaluation of the reserve capacity of the most critical member (Member 6) is carried out. The member axial capacity is determined (LF) as A x f_y = 507.5 kN. The required member capacity, LF_{req}, is simply determined as the axial force in the member under service load; 304.5kN. The member reserve ratio, r_1, is equal to 507.5/ 304.5=1.67. Thus, minimum system redundancy is calculated;

$$\begin{aligned}\phi_{red} &= \min\left(r_1 r_u, r_1 r_f, r_1 r_d\right) \\ &= \min(0.85\times 1.67,\ 0.95\times 1.67,\ 0.51\times 1.67) \\ &= 0.85\end{aligned} \qquad \textbf{3.20}$$

Therefore, despite considering the member reserve ratio, the structure is deemed to have insufficient redundancy, principally due to the performance of the damaged structure. It is suggested by the Ghosn & Moses (1998) that this result would necessitate remedial action such as altering the topology of the structure or increasing the strength of members in order to ensure that the redundancy targets are satisfied.

3.5.3 Discussion

The redundancy assessment methodology is a useful approach which can provide a broad assessment of the safety of a structure in addition to the structural redundancy. The member reserve ratio establishes the individual member reserve capacity. The reserve ratios for the functionality and ultimate limit states determine the reserve capacity of the intact structure after yielding of the first member. Similarly to the ultimate limit state reserve ratio, the damaged condition ratio calculates the reserve capacity of the damaged condition with respect to first yield in the intact structure. A key aspect of the method is that it is designed to be easily applied by the end user. Therefore, while a reliability analysis of redundant structures underpins the target redundancy values, the method can be applied using relatively simple deterministic load factors.

The target reliability ratios, presented in Ghosn and Moses (1998) were calibrated by analysing many redundant bridge structures. It is unclear, however, to what extent these target values can be reliably applied to other structures such as the truss structure which is analysed herein. Connor et al. (2005) observe that the method relies upon measures of statistical variation which are commonly not available. However, even in the absence of target reliability ratios the deterministic reserve ratios provide a useful and objective analysis of structural redundancy.

Although the ultimate capacity of the damaged condition is determined, there is no explicit consideration of the distribution which exists among the different damaged states; the most critical value is used to calculate the damaged condition reserve ratio. Therefore, the most critical value may be an outlier in terms of the structural response to each damage event or alternatively it may signify a more general susceptibility to the failure of a member. Also, the

only quantitative measure for the damaged condition capacity is the ultimate strength. Thus, there is no evaluation of other important measures of the structural performance such as the yield strength or ductility of the damaged structure.

3.6 CONCLUSIONS

Three contrasting quantitative approaches have been examined in detail; a static stiffness vulnerability assessment, an energy-based vulnerability assessment and general redundancy analysis.

The defining characteristic of the stiffness-based vulnerability assessment is that it is not a response-based analysis; in contrast with more conventional response-based analyses, it does not directly consider loads or boundary conditions. In common with the perspective of robustness as an inherent system property, this approach assesses the quality of the structural form and its capacity to resist disproportionate collapse. Its arbitrariness may be considered as an advantage in some circumstances and additionally the computational demands are negligible. However, it cannot be overlooked that the structural loads and the physical interaction of a structure with its environment are generally well defined. Moreover, it is difficult to envisage a circumstance where a static stiffness-based analysis would be sufficient to quantify the vulnerability or robustness of a structure with resort to an additional response-based analysis. In terms of the requirement of a robustness measures, as proposed by Starossek and Haberland (2011), the primary weakness of this approach is that it lacks expressiveness as it does not quantify all relevant aspects of the structural collapse resistance.

The energy-based vulnerability assessment has more in common with conventional collapse resistance analyses, as it is response based. Similarly to the stiffness-based method, critical

sequences of member failure events are identified, however strain energy is used as the quantitative measure. Critical sequences are those which require relatively little energy to cause structural collapse. However, as indicated by the investigation herein, identifying the 'easiest' way to cause collapse of a structure may lead to arbitrary sequences. This raises the question of how the energy input required to cause member failure arises, in particular for sequences involving multiple member failure events.

The redundancy assessment approach proposed by Ghosn and Moses (1998) is one of the most complete and applicable methods. Although the target redundancy values are calibrated using a reliability assessment, the method may be implemented using a nonlinear deterministic FE analysis. This feature greatly adds to the simplicity and calculability of the proposal. However, the suitability of the target ratios for structures other than those in the original calibration study is unclear. Additionally there are no provisions for considering the distribution in collapse resistance arising from the analysis multiple damage events.

4 A COMPREHENSIVE ROBUSTNESS ASSESSMENT FRAMEWORK AND ASSOCIATED DAMAGE INDEX

4.1 INTRODUCTION

As discussed in Chapter 2, redundancy and robustess are both properties which goven the collapse resistance of a structure. Each is a function of many other more properties such as the structural form, energy absorption capacity, stiffness and so on. Among the wide variety of quantitative assessment methods, several authors have proposed strength-based indices (Frangopol and Nakib 1991, Ghosn and Moses 1998, Husain *et al.* 2004). In the more narrowly defined scope of redundancy analysis, proposed methods typically focus on strength.

For a given a set of performance measures, a reference state or some design-oriented criteria by which the performance of a damaged structure must be determined. For example, alternate path based progressive collapse analyses compare the area of floor which collapses following the removal of a column to a prescribed limit in order assess the performance (IStructE 2010). Other analyses may use a particular resistance level such as a design load to assess performance (Frangopol and Curley 1987). The approach taken here, which accords with many deterministic and probabilistic redundancy analyses (Hendawi and Frangopol 1994, Ghosn and Moses 1998, Husain *et al.* 2004), is to use the intact structure. Using the intact structure as the reference state to assess performance ensures that all aspects of the analysis are a function of the inherent properties of the structure.

The primary focus is an assessment of the structural deterioration caused by a localised damage event with respect the intact state. A failure event is defined as the complete and sudden failure of a member. Focussing on any one structural property is not sufficient to fully quantify the post damage structural deterioration. Therefore, a comprehensive unified index is proposed herein which provides an enhanced evaluation of the consequences arising from a damage event by incorporating additional structural properties; the yield strength, the elastic stiffness and the ductility. The proposed indices will expand on existing strength-based measures such as the residual strength factor. It is not the intention of the present study to determine a suitable target value for a combined index. This is a secondary issue which may be addressed by future work.

Analyses are implemented with respect to the ultimate capacity. This is equivalent to the damaged condition limit state used by Ghosn & Moses (1998). The capacity of each structural state will be determined by pushing the structure until complete collapse occurs. Despite the focus on catastrophic collapse, the proposed methodology is not restricted to any particular limit state.

4.1 Structural Performance in Context of Robustness

The focus of the present work is the performance of a damaged structure with respect to the intact state. In this context, the focus of the analysis is a quantification of the change or deterioration relative to the intact state. If a structure has perfect redundancy with respect to a specific damage event, then the performance of the damaged state will be the same as the intact state. Conversely, if a structure collapses immediately following a damage event, the

structure can be considered to have no redundancy. Each of the four measures, which will be used to quantify the change, is discussed in the following sections.

4.1.1 Ultimate Strength

The first performance indicator to be considered is the ultimate strength. Naturally, the ultimate strength of a damaged structure is an integral part of a post damage structural assessment. Consequently, as discussed in Section 2.3.4, several authors have proposed a variety of strength-based redundancy indices.

4.1.2 Ductility

Ductility is commonly recognised as a structural property which contributes to the redundancy and robustness of a structure. The relationship between ductility and robustness assessment has been discussed by several authors. Generally it is widely accepted that ductility is an essential component of robustness and a means by which disproportionate collapse can be avoided (Dusenberry *et al.* 2002, Ellingwood and Dusenberry 2005b, England and Agarwal 2008, Knoll and Vogel 2009). Bertero & Bertero (1999) emphasise that indices which are based solely on strength reduction are incomplete descriptions of the brittleness of a system, as displacement is not considered.

IStructE (2010) notes that it is generally accepted that the more ductile a structural system is, the more robust it is, as ductility desensitises both the members and the overall system from uncertainties which may arise during the service life of a structure. Structures which do not have inherent ductility are vulnerable to brittle failure and disproportionate collapse. At the individual member level, the provision of ductility is dependent on good detailing, while at the system level, ductility is related to the energy absorption capacity and the nature of failure

sequences. Beeby (1999) considers that the ability to absorb damage from unseen events is one possible definition of robustness.

Ductility is also a key consideration concerning the economic design of robust structures by extending the design envelope from a traditional strength limit state to a ductility limit state (Izzuddin 2010). This economic benefit is also reflected in the relationship between ductility and reliability as a linear increase in ductility produces a much steeper increase in reliability, thus providing substantial reliability increases for a relatively small ductility increase (Kirkegaard and Sørensen 2009).

4.1.3 Elastic Stiffness and Yield Strength

Performance indicators such as strength and ductility are key considerations regarding the ultimate collapse resistance of a structure. However, damage events may result in a deterioration of structural performance which does not lead to collapse or a significant loss of strength or ductility. Given the assessment of structural deterioration relative to the intact structure, it is therefore necessary to consider additional performance criteria such as the elastic stiffness and yield strength. Clearly these criteria are related to the elastic behaviour of the structure in contrast with the nonlinear behaviour in the case of strength and ductility. Biondini & Restelli (2008) note that serviceability performance indicators such as the elastic stiffness and first yielding are particularly important in life cycle robustness analysis and ageing structures, as ageing structures may exhibit a deterioration of structural performance without structural collapse.

4.1.4 A Unified Approach

Given the objective of comprehensively quantifying structural deterioration with respect to an intact structural state, it is not sufficient to use any of the four performance indicators in isolation. Each indicator quantifies only one aspect of the structural performance. Therefore, each of the performance indicators will be combined in order to create a single unified measure.

4.2 REDUNDANCY / CONSEQUENCE INDICES

Four performance measures have been outlined. In order to maintain consistency and clarity, a single index is used to quantify the performance of the damaged structure in terms of each performance indicator. The primary purpose of the indices is to quantify the capacity of the damaged structure compared to the intact structure. Therefore, the consequences of a damage event are expressed in terms of change or deterioration with respect to the intact structure.

Each index will vary from zero to one. If the performance of the damaged structure is the same as the intact structure, then the damage event has produced no consequences in terms of the measured performance, and the consequence index will equal to zero, thus indicating that the structure is redundant with respect to the damage event. Alternatively, if damage results in complete deterioration with respect to the intact structure, in other words collapse of the structure, the value of the consequence index will equal to one and the redundancy index will equal to zero. Thus, the relationship between redundancy and consequences is as follows;

$$C_i = 1 - R_i \quad \textbf{4.1}$$

where C_i is the consequence index for damage event *i* and R_i is the redundancy index for damage event *i*.

Figure 4-1 is used to illustrate each index. The diagram illustrates a notional load displacement relationship for an intact structure and one corresponding damage state.

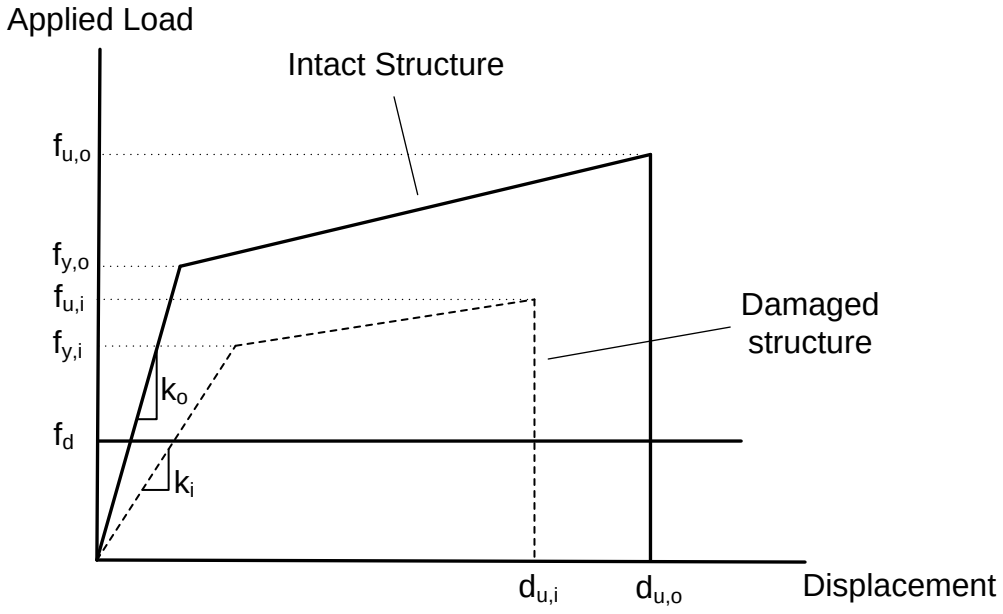

Figure 4-1: Indices illustration

The first consideration is the elastic stiffness of the structure. In Figure 4-1, this is the change from k_o to k_i, where k_o is the stiffness of the intact structure and k_i is the stiffness of the damaged structure. This stiffness change will govern the deflection increase following damage to the structure, when it is in an elastic state. A stiffness consequence index is defined as follows:

$$C_{k,i} = 1 - \frac{k_i}{k_o} \quad \textbf{4.2}$$

where $C_{k,i}$ is the stiffness consequence index. The index may also be formulated in terms of redundancy rather than damage consequences. The corresponding redundancy index is simply as follows:

$$R_{k,i} = 1 - C_{k,i} = \frac{k_i}{k_o} \quad \textbf{4.3}$$

where $R_{k,i}$ is the redundancy index in terms of elastic stiffness.

If the stiffness of the damaged structure is equal to the stiffness of the intact state, then k_i will be equal to k_o, and the consequence index will be equal to zero. If damage results in immediate failure and the damaged state has zero stiffness then damage will be complete and $C_{k,i}$ will equal one.

The index for yield strength is similarly formulated. Considering Figure 4-1 above; this is the reduction in yield strength from $f_{y,o}$ to $f_{y,i}$. The yield strength consequence index is as follows:

$$C_{y,i} = 1 - R_{y,i} = 1 - \frac{f_{y,i}}{f_{y,o}} \quad \textbf{4.4}$$

As before, if there is no reduction in yield strength, then the index will equal zero.

Similarly to residual strength factor, the ultimate strength will also be incorporated. This will evaluate any changes in ultimate strength.

$$C_{u,f,i} = 1 - R_{u,f,i} = 1 - \frac{f_{u,i}}{f_{u,o}} \quad \textbf{4.5}$$

The final consideration is the ductility of the structure. The index will be as follows:

$$C_{u,d,i} = 1 - R_{u,d,i} = 1 - \frac{d_{u,i}}{d_{u,o}} \quad \textbf{4.6}$$

D. Frangopol & Nakib (1991) note that in some cases of brittle behaviour, a damaged structure may have a higher ultimate strength than the intact structure (i.e., $f_{u,i} > f_{u,o}$). It is also conceivable that a damage state may exhibit greater ductility that an intact structure due to a more favourable failure path. The focus of this work is the deterioration in performance resulting from a localised damage event. Therefore, if the residual strength, ductility or other measures are greater than the corresponding intact performance, this behaviour will be interpreted as no deterioration with respect to the intact state and the index will be equated to zero. This also serves the purpose of maintaining indices which range between zero and one.

In order to determine the ductility of each structural state, the concept of maximum useful displacement is introduced. Knoll & Vogel (2009) define maximum displacement as the maximum displacement which the structure can tolerate while maintaining a useful resistance. For the purpose of this analysis, useful resistance will be defined as the design resistance; however any suitable resistance may be used. The following diagram presents an illustrative example. Two alternative structural states are presented.

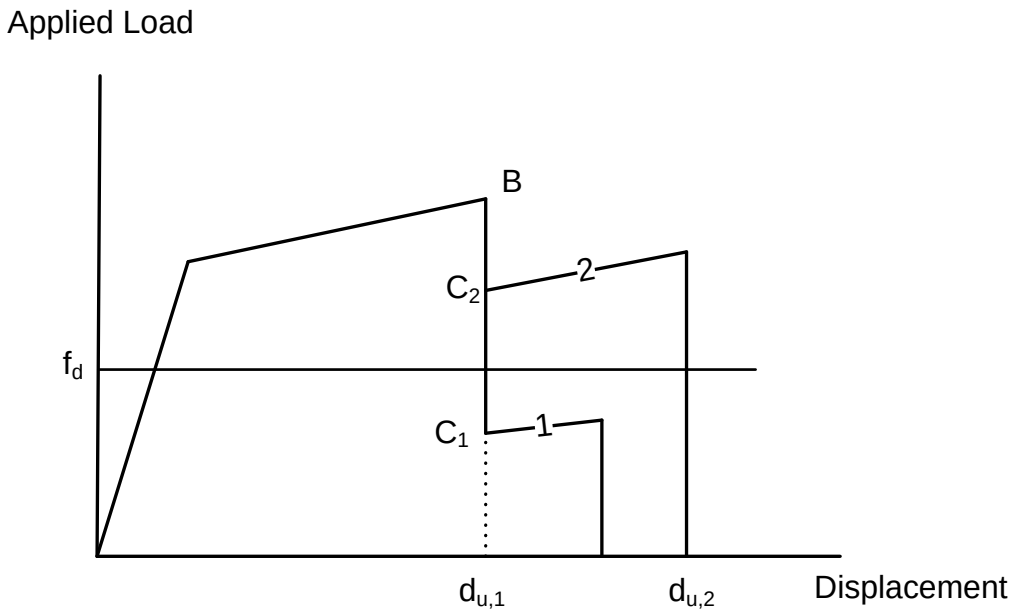

Figure 4-2: Maximum acceptable displacement

Each state experiences a drop in load carrying capacity without complete collapse following a member failure event (point B). Subsequently each state reaches a new equilibrium state in which additional displacement is possible until complete collapse is precipitated by failure of additional member. In structural state 2, the resistance when the new equilibrium state (C_2) is reached is greater than the design load. Therefore, the ductility of state 2 is $d_{u,2}$. However in structural state 1, the resistance (C_1) following the failure event is less than the design load. Consequently the additional displacement is not considered useful and the displacement for damage state 1 is $d_{u,1}$.

4.2.1 Indices Combination

The first stage is to determine an index corresponding to each performance indicator for a particular damage state. The next stage in the process is to combine the individual indices for

each performance indicator in order to create one single system. This index will quantify the overall performance of a damage state with respect to the intact structure.

A number of requirements must be fulfilled with respect to the combined index. Firstly, similarly to each individual index, the final combined index should range between zero and one. In the case of the consequence index, a value of one will indicate complete deterioration and collapse of the structure, whereas a value of zero will indicate that damage has not resulted in any measured deterioration. Furthermore, a value of one for any individual consequence index implies that the overall index should also equal one. This simply reflects the fact that if any consequence index such as the ultimate strength is equal to one, complete failure has occurred. Therefore the combined index must also equal to one. This behaviour could occur when a damage event produces structural instability and subsequent collapse.

The indices will be combined as illustrated in Figure 4-3. The order in which the indices are combined will not change the value of C_i. However, it is proposed to combine the indices as illustrated below in order to provide a logical formulation from the point of view of the different types of analysis which are required (linear in the case of stiffness and yield strength, and non-linear in the case of ultimate strength and ductility). Also, as noted by Biondini & Restelli (2008), the elastic stiffness and yield strength are more closely related to the serviceability of the structure ($C_{s,i}$), while ultimate strength and ductility are related to the ultimate limit state ($C_{u,i}$). Using this combination will also facilitate separation of the indices if, due to the requirements of a particular redundancy analysis, consideration of individual parts of the performance is required.

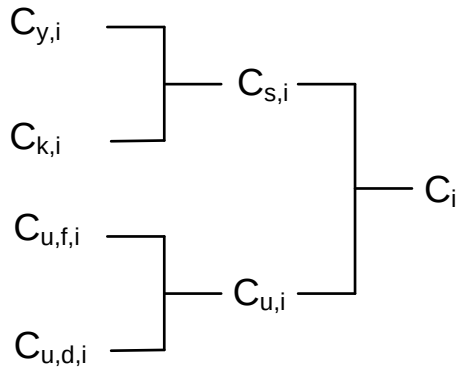

Figure 4-3: Indices combination

Initially four consequence indices are determined; $C_{K,i}$, $C_{Y,i}$, $C_{u,f,i}$ and $C_{u,d,i}$. The index combination, as illustrated in Figure 4-3, effectively assigns an equal weight to each of the individual consequence indices. Therefore, in terms of the overall index C_i, a 20% reduction in elastic stiffness is equivalent to a 20% reduction in ultimate strength. Depending on the nature of a particular analysis, it may be desirable to attribute greater importance to a particular performance indicator such as the strength. Therefore it is proposed to assign a weighting factor to each index. This will ensure the process has maximum flexibility, thereby allowing it to be adjusted to suit specific structures or analysis requirements. Determining suitable values for a weighting factor remains a topic for future work, however in general, a weighting factor, α, for each performance indictor may be defined as follows:

Weighted stiffness index: $\bar{C}_{k,i} = \alpha_{k,i} C_{k,i}$ **4.7**

Weighted ultimate strength index: $\bar{C}_{u,f,i} = \alpha_{u.f,i} C_{u,f,i}$ **4.8**

Weighted yield strength index: $\bar{C}_{y,i} = \alpha_{y,i} C_{y,i}$ **4.9**

Weighted ductility index: $\bar{C}_{u,d,i} = \alpha_{u.d,i} C_{u,d,i}$ **4.10**

where $\bar{C}_{k,i}$ is the weighted stiffness consequence index, $\alpha_{k,i}$ is the weighting factor for the stiffness index and so on. If α is equal to one, the maximum weight is assigned to the consequence index. If a value of one is assigned to each consequence index, then each consequence index will have equal importance in the overall index C_i.

Firstly, the consequence indices for stiffness, $\bar{C}_{k,i}$ is combined with the consequence index for yield strength, $\bar{C}_{y,i}$. This will generate a new index, $C_{s,i}$. $C_{s,i}$ can be determined using a simple linear analysis. As discussed above, the indices must be combined in such a way that the range of zero to one is preserved. Therefore, it is proposed to combine the indices as follows:

$$C_{s,i} = \bar{C}_{k,i} + \bar{C}_{y,i} - \bar{C}_{k,i} \times \bar{C}_{y,i} \quad \textbf{4.11}$$

If either index is equal to one, the combined index $C_{s,i}$ is equal to one. For example:

$$C_{s,i} = 1 + 0.5 - 1 \times 0.5 = 1$$

If one index, $\bar{C}_{k,i}$ for example is equal to zero, indicating that stiffness is unchanged, then the combined index $C_{s,i} = \bar{C}_{y,i}$.

$$C_{s,i} = 0.8 + 0 - 0.8 \times 0 = 0.8 = \bar{C}_{y,i}$$

This is logical, as a value of zero indicates that there has been no reduction in elastic stiffness. Therefore, the combined index is purely a function of the yield strength. If for example both indices are equal to 0.5, then the combined index will be as follows:

$$C_{s,i} = 0.5 + 0.5 - 0.5 \times 0.5 = 0.75$$

In this case the combined index reflects the contributions of each performance indicator.

The consequence indices for ductility and ultimate strength will also be combined using the same approach. The combined index $C_{u,i}$ provides a measure of the damage resilience with respect to the ultimate collapse of a structure.

$$C_{u,i} = \bar{C}_{u,f,i} + \bar{C}_{u,d,i} - \bar{C}_{u,f,i} \times \bar{C}_{u,d,i} \qquad \textbf{4.12}$$

The last stage is to combine $C_{u,i}$ and $C_{s,i}$ to determine the index C_i, which will represent the overall structural consequence due to the damage event for damage state *i*.

$$C_i = C_{s,i} + C_{u,i} - C_{s,i} \times C_{u,i} \qquad \textbf{4.13}$$

Therefore, the combined final index is a function of each performance indicator. Similarly to $C_{u,i}$ and $C_{s,i}$, C_i will range from zero to one, with one indicating complete collapse and a value of zero indicating the performance of damage state *i* has not deteriorated relative to the intact structure.

Each index may also be expressed in terms of redundancy rather than consequence. In this case, the indices will be as follows: $R_{k,i}$, $R_{y,i}$, $R_{u,f,i}$, $R_{u,d,i}$, $R_{u,i}$, $R_{s,i}$ and R_i. The final index R_i can be determined as follows:

$$R_i = (1 - C_i) = R_{s,i} \times R_{u,i} = R_{k,i} \times R_{y,i} \times R_{u,f,i} \times R_{u,d,i} \quad \textbf{4.14}$$

4.3 FINITE ELEMENT ANALYSIS

FE analyses of three alternative structures are used to illustrate the proposed indices. A nonlinear FE analysis facilitates the identification of the force-displacement relationship of a structure and thus each of the required parameters; the elastic stiffness, the yield strength, the ultimate strength and the ductility. The ultimate strength and ductility are determined with respect to the ultimate capacity of a structure. Therefore a FE analysis is used to push the structure to a collapse state.

4.3.1 Analysis Control

Displacement control is used in order to obtain the full load displacement curve. Therefore, given nonlinear system behaviour, such as that depicted in Figure 4-2, in which the structure experiences decreasing load capacity, the analysis can continue until system collapse occurs. This enables the displacement at failure to be determined and also the total strain energy in the structure, if necessary.

Marjanishvili *et al.* (2006) note that load controlled analyses may require time intensive adjustment of key parameters such as the time step in order to achieve a stable solution. Conversely, displacement controlled analyses circumvent many of the difficulties associated

with load control, in particular convergence of the solution, and are generally less onerous (Kim and Kim 2009).

While a displacement controlled analysis is used here for expediency, the implementation of the proposed indices is not limited to displacement controlled analyses. Irrespective of whether an analysis is load controlled or displacement controlled, the response of a structure to a local damage event may be assessed in terms of the four key properties.

In order to implement a displacement controlled analysis, the displacement corresponding to the applied loads is incrementally increased and the vertical reaction force at each node is equal to the applied load. This reaction force is the equivalent of the applied load in a load controlled analysis and thus can be used to indicate the loss in load carrying capacity of the structure.

The loading and boundary conditions are applied in a static general step. During the analysis the displacement is increased until the collapse occurs. Geometric nonlinearity is used to provide a more accurate representation of the large displacement effects. The use of nonlinear geometry means that elements are formulated in their current configuration using current nodal positions rather than the original state. Therefore elements can distort from their original state as displacement increases.

4.3.2 Material Properties and Member Failure

In order to model the full load-displacement relationship for a structure, member failure events must be incorporated in the modelling process. It is assumed that all members are braced and thus buckling does not occur. Therefore, both compression and tension members exhibit ductile failure when the ultimate strain is reached.

Member failure may be simulated by gradually or instantaneously removing the member from the model; allowing the force present in the member prior to failure to be redistributed to the remaining members in the structure. However, given that the present analysis is an implicit static analysis, the sudden complete removal of a member from a structure gives rise to convergence problems. Furthermore, ABAQUS does not offer any direct methods by which member failure can be modelled in a static analysis. Therefore, an approximate method is proposed here in order to simulate a member failure event. This is accomplished by defining material properties such that, when the ultimate strain is reached, the stress reduces to approximately zero. The reduction of the stress is analogous to member unloading. Consequently, the forces present in the member are redistributed to the remaining members in the structure.

In order to generate a good approximation of member failure, it is desirable to reduce the post failure stress as close to zero as possible without causing convergence problems. Trial and error was used to determine the minimum possible stress value. This was found to be 0.001 MPa. A multistep approach, in which member removal is modelled as a separate step, is also possible. However, for the current analysis it was found that modifying the material properties was the most suitable solution.

All members are steel. The general material properties are as described in Section 3.2.1. However, when the ultimate strain (2%) in a member is reached, the stress decreases to approximately zero (0.001 MPa). The objective is to approximate member failure as closely as possible by reducing the post failure stress to approximately zero. This relationship is illustrated in Figure 4-4. The material yields at 250 MPa. The stress increases to 270 MPa when ductile failure occurs. Subsequent to failure, the stress reduces to 0.001 MPa.

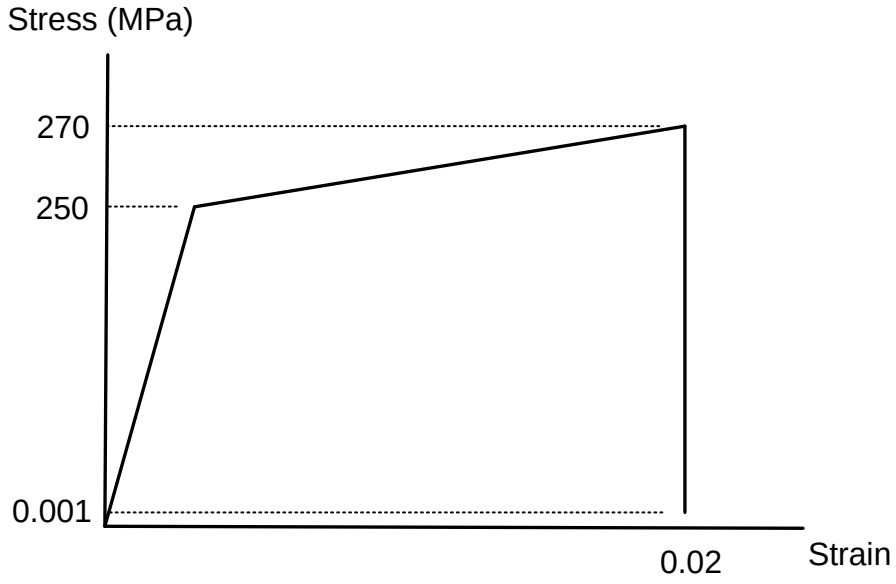

Figure 4-4: Steel stress-strain relationship

4.3.3 Example 1

4.3.3.1 Finite Element Model

Firstly, the proposed methodology will be demonstrated using a two-dimensional truss model. The truss, its dimensions and boundary conditions are illustrated in Figure 4-5.

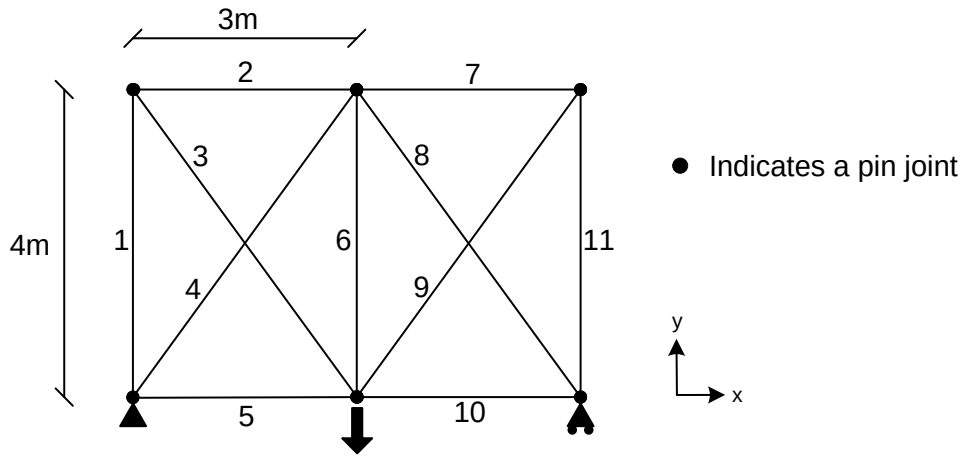

Figure 4-5: Truss model

The truss is 4m high and 6m long. All joints are pin joints. Consequently, the members only transmit axial forces and the internal static indeterminacy is equal to two. The left-hand support is pinned, restraining translation in the x and y directions. The roller at the right-hand support allows translation in the x-direction. The analysis is initially implemented with identical sections for each member. The area of the sections is $0.004m^2$.

4.3.3.2 Analysis

A displacement controlled analysis is carried for the intact structure and each damage state using ABAQUS 9.10. The load-displacement relationship and the key events in the failure sequence of the intact structure are presented in Figure 4-6. The structure is initially elastic. Member 6 is the first member to yield. Members 3 and 9 yield next; they yield simultaneously due to the symmetric configuration of the structure. The first failure event is the failure of Member 6. The forces present in Member 6 prior to failure are distributed to the remaining members of the structure. A new equilibrium is reached and the displacement increases until Members 3 and 9 fail. The failure of Members 3 and 9 causes a complete loss of resistance. Therefore, the FE analysis is complete.

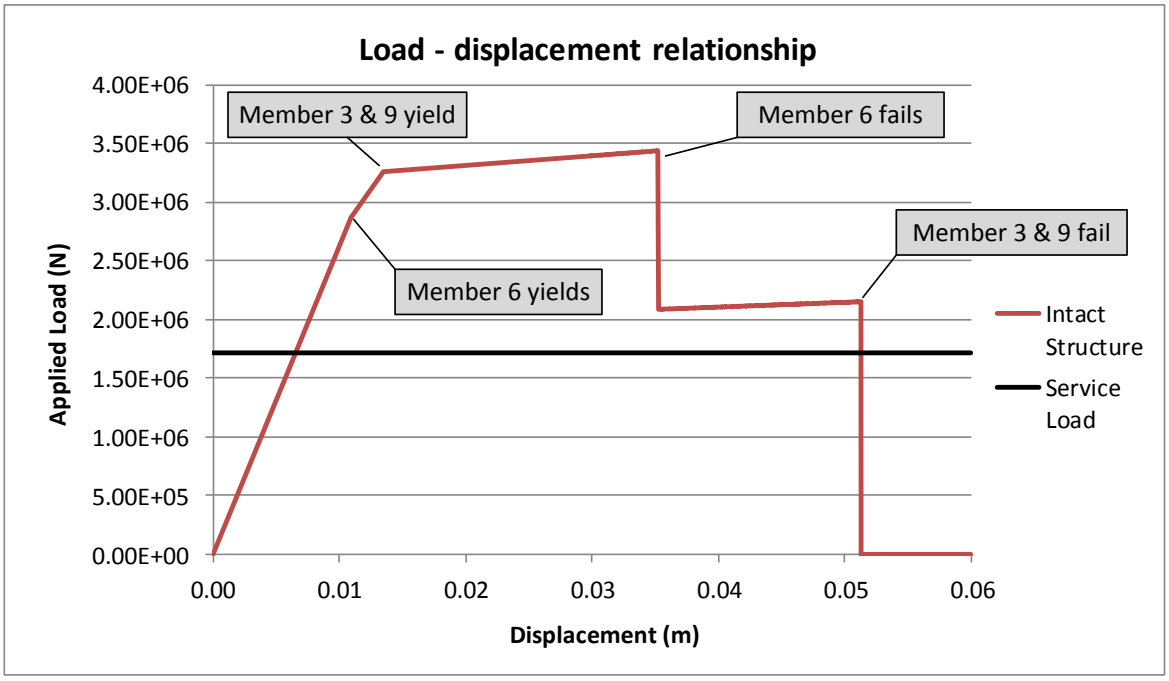

Figure 4-6: Intact Structure

Each damage state is also analysed. Due to the symmetrical nature of the structure, only the damage states corresponding to Members 1 to 6 are analysed.

Following the structural analysis, the reference values (elastic stiffness, yield strength, ultimate strength and ductility) for the calculation of the consequence indices are determined for the intact structure and each damage state. Table 4-1 lists the performance measures for each structure state. Structural state 1 corresponds to the structure with Member 1 removed and so on.

Table 4-1: Performance measures

Structural State	Elastic Stiffness (N/m^2)	Yield Strength (N)	Ultimate Strength (N)	Ductility (m)
Intact	2.62E+08	2.87E+06	3.44E+06	0.051
1	1.69E+08	1.85E+06	2.20E+06	0.035
2	1.69E+08	1.85E+06	2.20E+06	0.035
3	1.69E+08	1.85E+06	2.20E+06	0.035
4	1.98E+08	1.99E+06	2.13E+06	0.029
5	1.98E+08	1.98E+06	2.13E+06	0.029
6	1.48E+08	2.00E+06	2.15E+06	0.051

The next step is to calculate the indices for each damage state using the consequence indices outlined in Section 4.2 (Equation 4.2, to Equation 4.6). Figure 4-7 presents the consequence indices for each structural state. The results demonstrate a varied response; in particular for damages states 4 to 6. For example, state 4 experiences the greatest reduction in elastic stiffness and the greatest reduction in ductility.

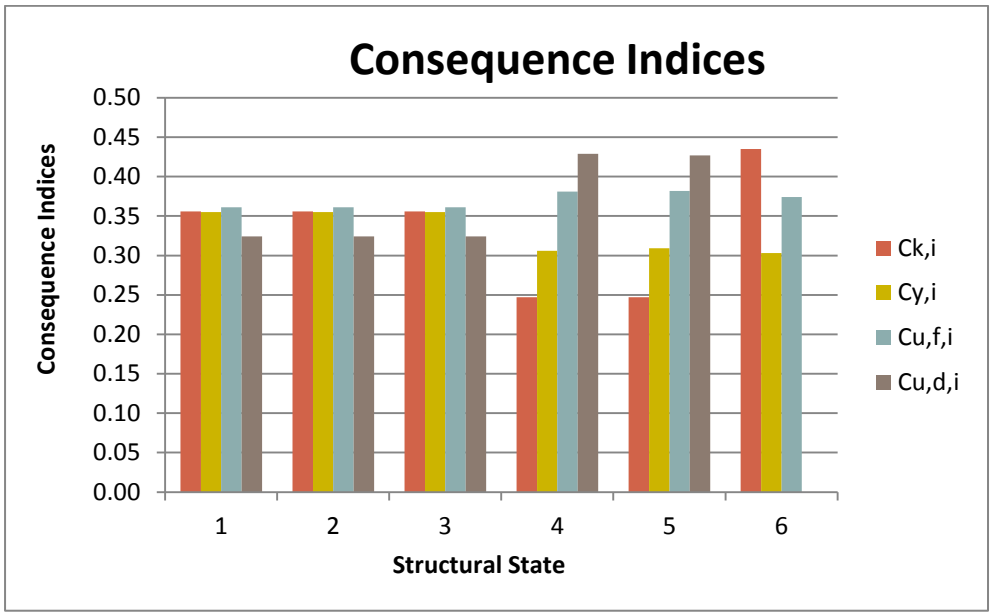

Figure 4-7: Consequence indices

The final step is to combine the individual indices in order to determine the overall consequence index for each damage state (see Equation 4.11 to Equation 4.13). The intermediate combined indices $C_{s,i}$ and $C_{u,i}$ are displayed in Figure 4-8 and the overall combined indices are presented in Figure 4-9.

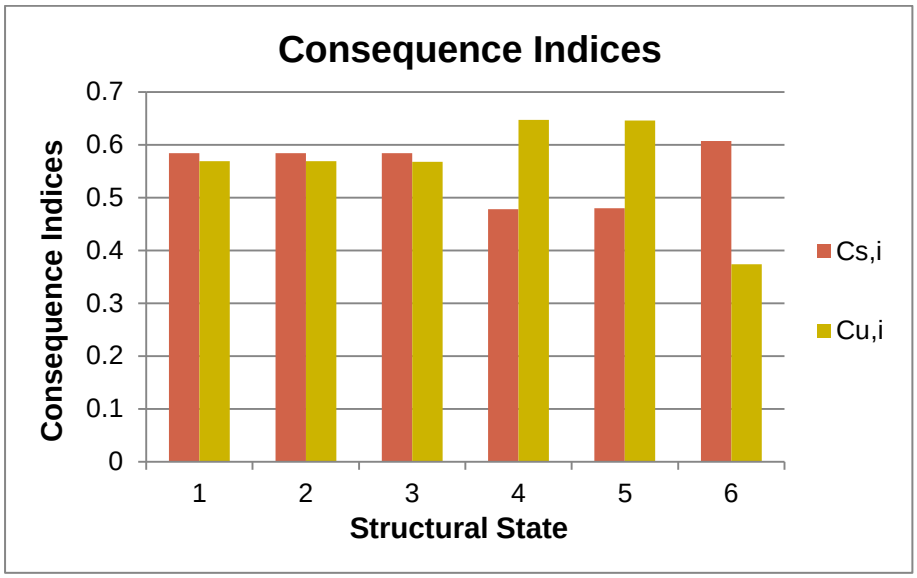

Figure 4-8: $C_{s,i}$ and $C_{u,i}$

The most critical members are Members 1, 2 and 3 as their removal produces the highest consequence indices. The least critical member is Member 6. However, there is relatively little variation among the unified indices for each damaged state.

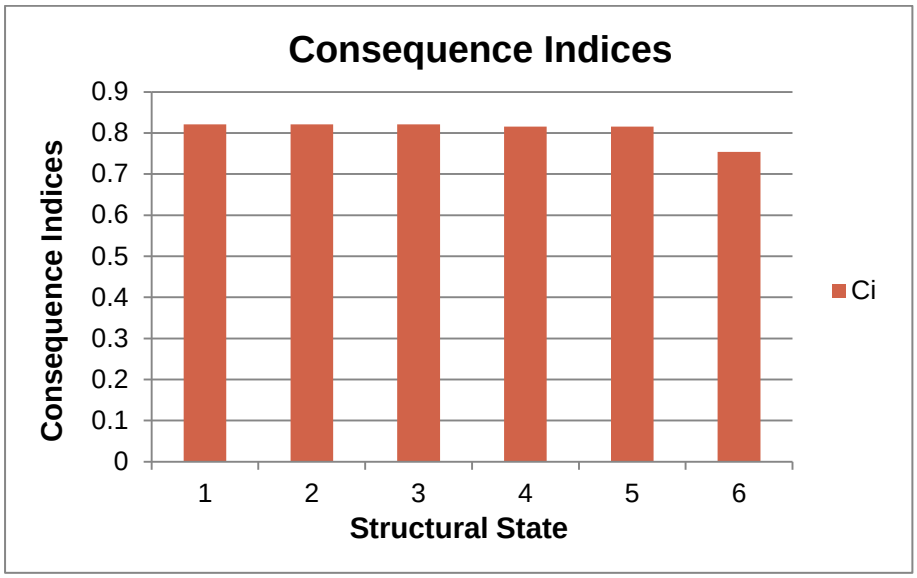

Figure 4-9: Overall combined indices (C_i)

Table 4-2 presents the ranking for the combined index, C_i, and the strength index $C_{u,f,i}$ ($C_{u,f,i}$ is the same as the residual strength index, discussed in 2.3.4.1). If strength alone is considered, it is apparent that the most critical member is Member 5. However, if the unified indices are considered, Member 5 is the second least important index. One of the primary objectives of redundancy analyses is an identification of the most critical members and a relative importance ranking of the members. This example highlights that using strength as the sole measure of performance does not fully capture the overall structural deterioration.

Table 4-2: Ranked indices

Structural State	$C_{u,f,i}$	Structural State	C_i
5	0.382	1	0.821
4	0.381	2	0.821
6	0.374	3	0.821
1	0.361	4	0.816
2	0.361	5	0.816
3	0.361	6	0.754

4.3.4 Example 2

4.3.4.1 Finite Element Model

The second example uses the truss structure described in Section 3.2. The structure is illustrated in Figure 4-10.

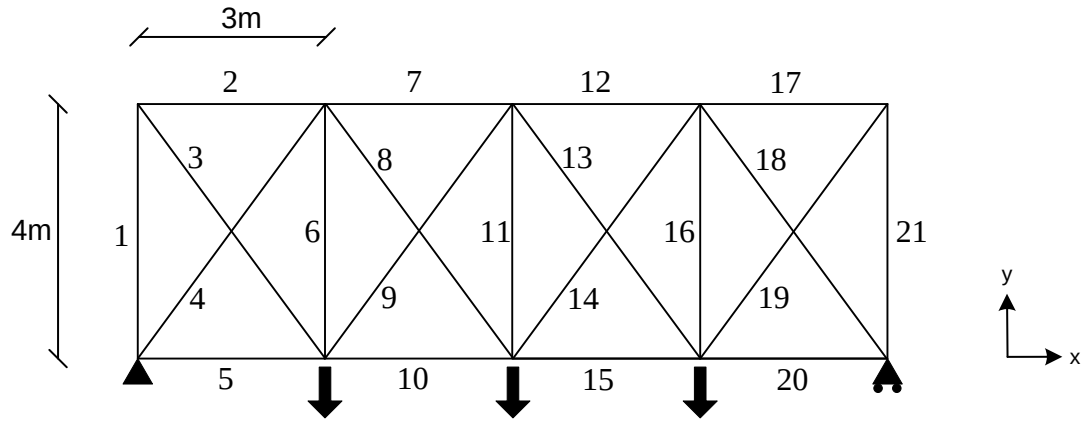

Figure 4-10: 21 Member truss

Similarly to Example 1, a displacement controlled analysis is used to push the structure to collapse. In this example however, there are three loading positions. Therefore, in order to

conduct a displacement controlled analysis with three equal loads, a system of linear springs is used. The spring stiffness is calibrated such that reaction force (corresponding to the applied loads) at each location is approximately equal; the percentage difference between the three reaction forces is less than 1%. A spring stiffness of $1x10^4$ is used.

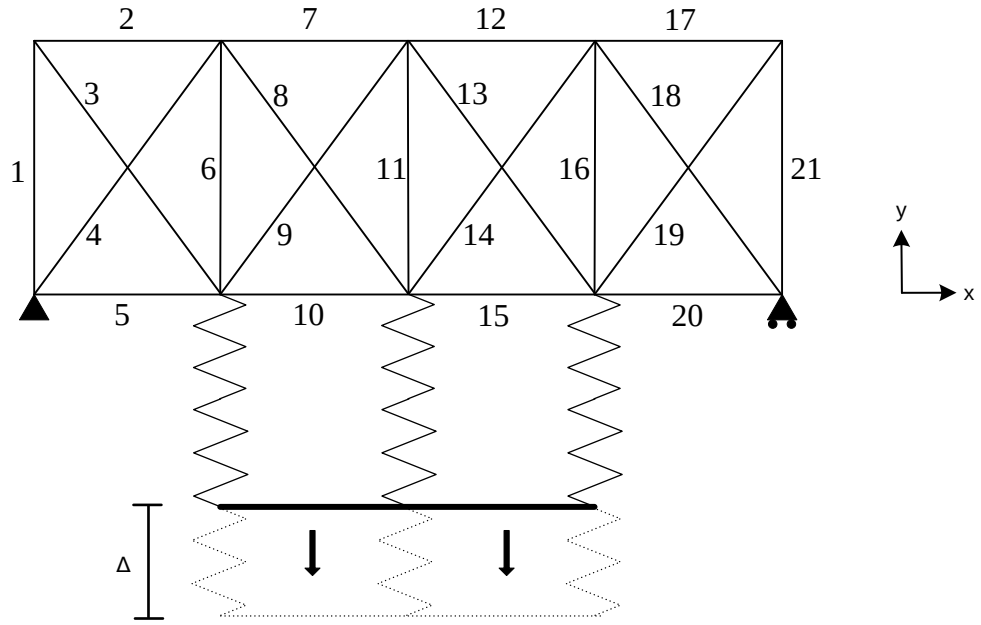

Figure 4-11: Displacement control using linear springs

Similarly to the material properties described in Section 4.3.2, it is assumed that the members exhibit ductile failure when the ultimate strain of 2% is reached. However, in this case, failed elements are removed using the model change function in ABAQUS. During an element removal step, the forces present in the failed member(s) are ramped down gradually such that, at the end of the step, the element has been removed from the model. The forces released by the failed element are redistributed to the rest of the structure and the overall resistance of the structure decreases.

The analysis is carried out in a series of steps. In the first step, the displacement Δ is increased until the first member(s) fail. In the second step, the failed member(s) is removed from the model. In the subsequent step the displacement is increased further until the next member(s) fail. This process is continued until total collapse of the structure has occurred. While this approach is an effective method to determine load-displacement relationship for each structural state, it requires significant user input in order to manually select the failed elements to be removed from the model.

4.3.4.2 Analysis

The intact structure and the residual states corresponding to the removal of Members 1 to 11 are evaluated using the proposed indices. Table 4-3 presents the nominal values for each performance measure.

Table 4-3: Performance measures

Structural State	Stiffness (MPa)	Yield Strength (kN)	Ultimate Strength (kN)	Ductility (m)
Intact	213.00	4030.00	4500.00	0.126
1	188.00	1700.00	2440.00	0.047
2	188.00	1700.00	2440.00	0.047
3	188.00	1700.00	2440.00	0.047
4	134.00	1890.00	2040.00	0.073
5	134.00	1890.00	2040.00	0.073
6	213.00	3160.00	3430.00	0.074
7	35.10	825.00	1040.00	0.148
8	141.00	2130.00	3080.00	0.058
9	211.00	3620.00	4160.00	0.079
10	55.90	960.00	1040.00	0.132
11	206.00	3840.00	4150.00	0.137

Figure 4-12 presents the indices for each damage state. In contrast with Example 1, there is much greater variation among the values for each index. For example, the indices for States 1, 2 and 3 vary from 0.118 to 0.626. Additionally, while damage state 6 does not experience a reduction in elastic stiffness, it experiences a significant reduction in ductility. On the other hand, damage state 9 exhibits small reduction in ultimate strength and relatively larger reduction in ductility. The variable nature of the structural deterioration produced by the damage events highlights the potential pitfalls associated with using a single structural property to quantify the overall structural response.

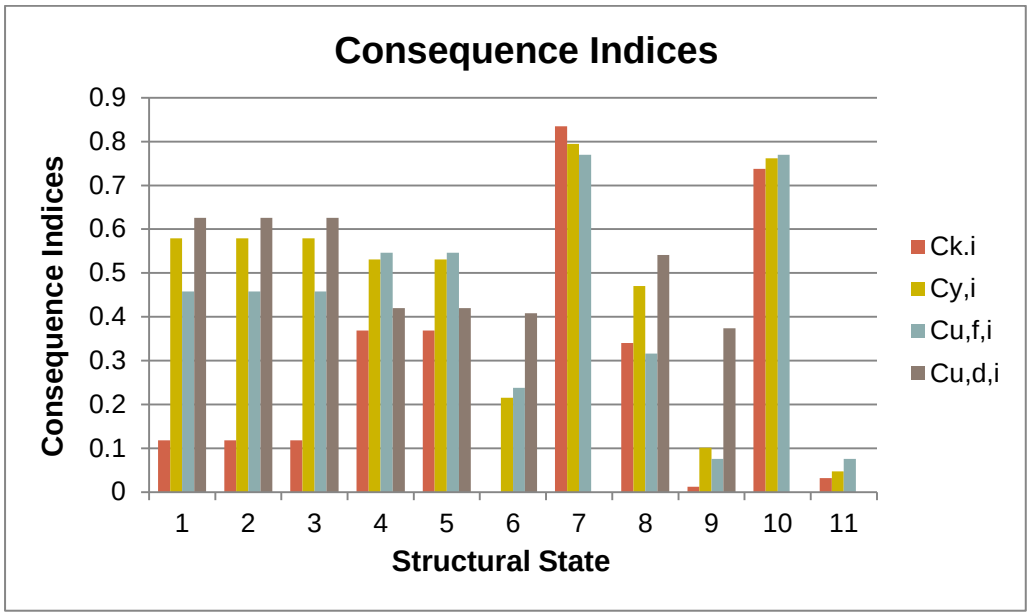

Figure 4-12: Consequence Indices

The combined indices for each damage state are reported in Figure 4-13 and Figure 4-14.

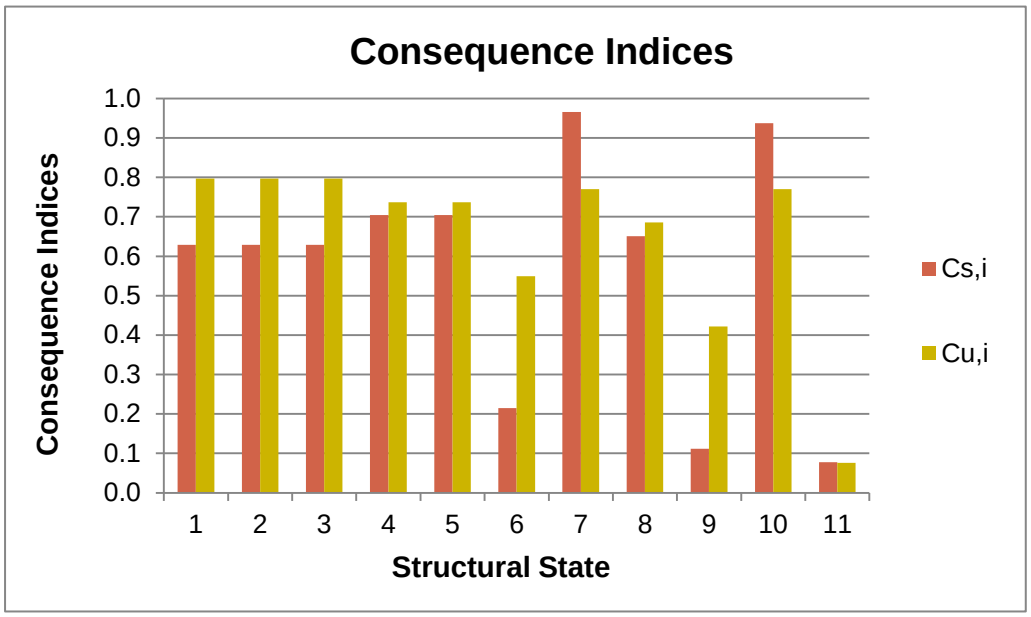

Figure 4-13: $C_{s,i}$ and $C_{u,i}$

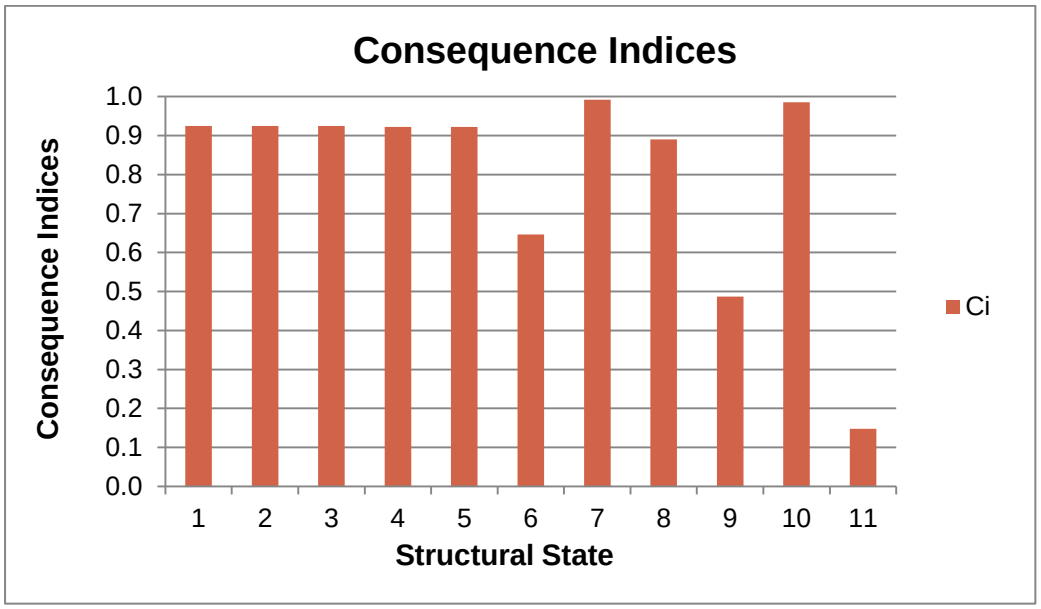

Figure 4-14: Overall combined index (C_i)

The ranked consequence indices are shown in Table 4-4. The most critical member is Member 7 due to the fact that State 7 exhibits a significant reduction in elastic stiffness, ultimate strength and yield strength.

Table 4-4: Ranked unified indices

Structural State	C_i
7	0.992
10	0.986
1	0.925
2	0.925
3	0.925
4	0.922
5	0.922
8	0.890
6	0.646
9	0.487
11	0.148

The ranking obtained using the residual strength index is displayed in Table 4-5. The relative member importance ranking is similar to that determined using the unified indices. The main exception is that, when using the unified indices, Members 1, 2 and 3 are more critical than Members 4 and 5.

Table 4-5: Ranked residual strength indices

Structural State	Residual strength index
7	0.770
10	0.770
4	0.546
5	0.546
1	0.458
2	0.458
3	0.458
8	0.316
6	0.238
11	0.076
9	0.076

4.3.5 Example 3

Example 3 is simply a repeat of example 2, albeit with optimised members, in order to minimise the total volume of material used in the truss design. A simple optimisation scheme is formulated. Under service load, the area of each member is minimised subject to the following constraints:

- Minimum area – $0.001m^2$
- Maximum stress – 150 MPa

The analysis is first carried out using the original configuration. The stress in each member of the structure was determined and the area was updated using the following ratio:

$$\text{area adjustment ratio: } \frac{\sigma_i}{\sigma_{\max}} \qquad \textbf{4.15}$$

where σ_{max} is the maximum stress (150 MPa) and σ_i is the stress in Member *i*. After a number of iterations the total material volume was reduced by approximately 47%. The updated member sizes are presented in Table 4-6 for Members 1 to 11.

Table 4-6: Optimised member areas

Member	Length (m)	Area (m^2)
1	4	0.0027
2	3	0.0027
3	5	0.0020
4	5	0.0020
5	3	0.0033
6	4	0.0033
7	3	0.0052
8	5	0.0052
9	5	0.0031
10	3	0.0031
11	4	0.0019

The analysis is carried out using the optimised members. Figure 4-15 reports the consequence indices for each damage state. There is clearly a substantial variation in the distribution of the indices for any particular damage state, underlining the need to quantify the structural change from a holistic perspective. For example, in damage state 1 the indices vary from 0.114 to 0.963, with the ductility index as the most critical. The most critical index in damage state 7 is the strength index, whereas in damage state 8 the yield strength index is the most critical, while the ductility index is the least critical.

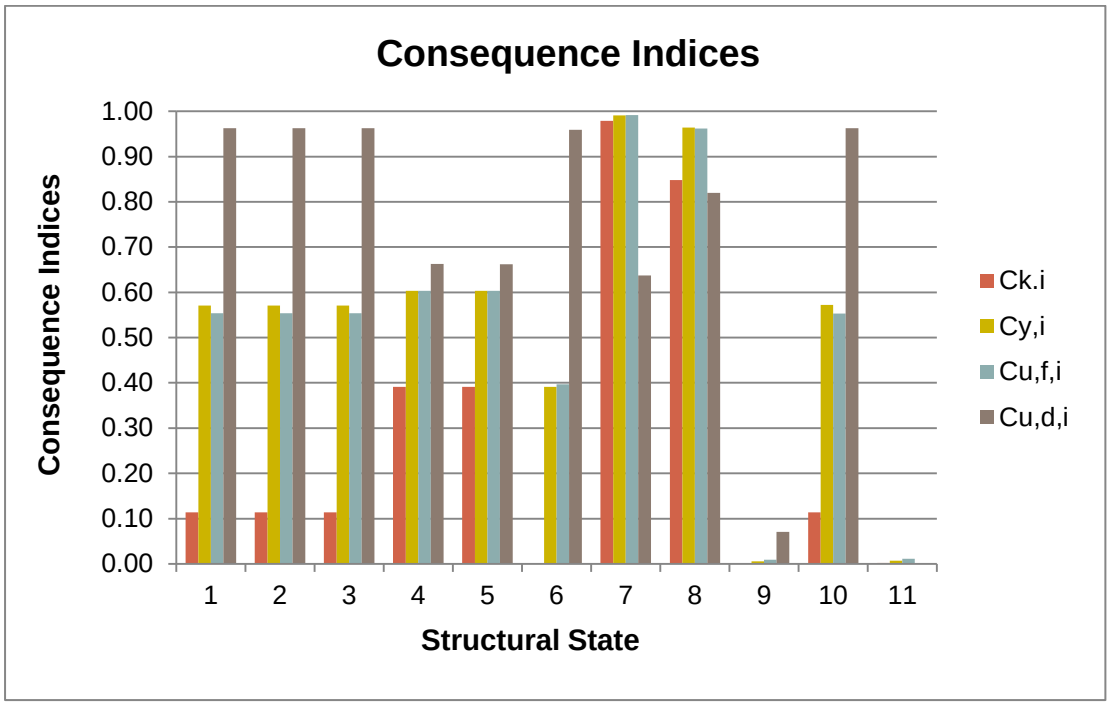

Figure 4-15: Consequence Indices

The ranked unified indices are presented in Table 4-7. A cursory comparison of the indices with the non-optimised structure indicates that the optimised structures have higher consequence indices. The mean unified index for the non-optimised structure is equal to 0.777, whereas the mean index for the optimised structure is 0.818. Evidently, the optimised structure is less robust. This finding accords with that of Frangopol and Klisinski (1989), who identified a conflict between the objectives of redundancy and more efficient structures.

Table 4-7: Ranked unified indices

Structural State	C_i
7	1.000
8	1.000
1	0.994
2	0.994
3	0.994
10	0.994
6	0.985
4	0.968
5	0.968
9	0.086
11	0.020

The comparison of the optimised and non-optimised structures also highlights the need to generate a measure of the overall system robustness in addition to measures which can quantify the importance of each member.

4.4 GENERATING A SYSTEM INDEX

There a number of different approaches by which a system index may be determined. As discussed in Section 3.5, Ghosn & Moses (1998) analyse the redundancy of structure according to a number of limit states, including the damaged condition, after failure of a member. This generates a distribution of ultimate strengths representing the capacity of each damaged state. In order to quantify the performance of the structure with respect to the damaged condition limit state, the most critical value is used. However, the objective of that

analysis is to ensure that a structure has a minimum level of redundancy rather than providing a comprehensive account of the structure's capacity to resist damage.

A simple example is presented to illustrate. Two notional structures are considered; structure A and structure B. Three alternative damage states are proposed for each structure and a combined consequence index is determined for each damage state. If the most critical consequence index is used to evaluate the overall structure, then it is apparent that each structure has the same capacity to withstand damage. However, if the other consequence indices are considered, and the mean consequence index is evaluated, it is evident that structure B possesses greater overall redundancy.

Table 4-8: Consequence indices

Structural State	**Consequence Indices (C_i)**	
	Structure A	**Structure B**
Member 1	0.10	0.80
Member 2	0.20	0.80
Member 3	0.90	0.90
Mean	0.40	0.83

Another issue, which limits the descriptive power of using the most critical member, is the probability of the initial damage event occurring. Although a damage event may result in a significant loss in strength, the probability of occurrence may be low. Conversely, damage events with low consequences may have a high probability of occurrence.

One way of addressing the distribution and the probability of occurrence is to use a weighted mean index in which the weights are defined as the probability of failure. A general weighted mean is defined as follows:

$$\bar{C}_i = \frac{\sum_{i=1}^{n} w_i C_i}{\sum_{i=1}^{n} w_i} \qquad \textbf{4.16}$$

where $\bar{C}_i$ is the weighted mean consequence index and w_i is the weight assigned to the consequence index for Member *i*. From a general point of view, a weighted index presents a flexible solution to the creation of a system index, such that the results may be adjusted in order to create a system index which provides a good estimate of the overall distributed system redundancy. However, it is proposed herein to use a probabilistic weighting where the weight w_i is equal to the probability of failure associated with event *i* ($P_{f,i}$) such as follows:

$$w_i = P_{f,i} \qquad i = 1,...,n \qquad \textbf{4.17}$$

where $P_{f,i}$ is the probability of failure of Member *i*.

4.4.1 Probabilistic Weighting

The choice of weighting can be related to the damage event, which is defined in this work as the complete failure of a member. It is assumed that the initial damage event occurs due to an event such as the overloading of a member, section loss due to corrosion (which will increase member stress) or an event related to the stress level, such as failure due to the development of fatigue cracks. Therefore, the weight w_i may be defined as the probability of failure of the initial member to be removed. As outlined in Section 2.5, the probability of failure is a function of the margin between member force and member resistance. Members which are highly stressed will have a high probability of failure and vice versa for members which are not highly stressed. This probability of failure is equivalent to the probability of failure given the occurrence of a hazard, $P(D|H_i)$, which was discussed Section 2.2.9

The probability of damage given the occurrence of a hazard is commonly used to describe the vulnerability of a structure and is commonly referred to as a direct consequence (see Section 2.2.3). JCSS (2008) outlines the physical characteristics of this type of risk including yielding, corrosion, fatigue, cracking and so on. One method, by which the probability of damage given a hazard may be quantified, is to use the stress level under service load in the member to be removed in order to determine a probability of failure. The stress level under service load can be linked to the possible development of fatigue cracks and member yielding.

Using a probabilistic weighting factor, as defined in Equation 4.17, ensures that events which have a high probability of occurrence will have a proportionately greater contribution to the mean system index. Conversely, events which have a high consequence index but a low probability of failure will be of lesser importance. If all indices have the same probability, then the weighted mean index will equal the mean index.

The probability of failure of a member is primarily a function of the member behaviour rather than the system behaviour. Therefore, incorporating a probabilistic weighted mean index expands the scope of the analysis, from one which is concerned purely with the system response to damage, to a broader analysis which also includes vulnerability to failure. Nevertheless, despite the broader scope, the proposed approach still falls within the general remit of collapse resistance as described by Starossek and Haberland (2012).

While the above definition of index weighting is useful from the point of view of pre-failure load-capacity margin of a member, it does not account for the fact that member failure may also occur due to some arbitrary cause such as collision. Therefore, the above definition may

need future amendment to enhance to the probabilistic weight by incorporating other potential sources of member failure.

Two examples are presented to illustrate. The weight w_i, is defined as the probability of failure of Member *i*. The first example shows the case in which each damage event has the same probability of failure. Therefore, the weighted mean index is equal to the mean index. Although the weighting does not affect the system index, the system index will benefit the use of the mean which ensures that the distribution of consequence indices is reflected.

Table 4-9: Weighted consequence indices

Members	$\mathbf{C_i}$	$\mathbf{W_i}$	$\mathbf{W_i \times C_i}$
1	0.40	0.01	0.004
2	0.50	0.01	0.005
3	0.70	0.01	0.007
Mean	0.53		0.53

In the second example, Member 1 has a lower probability of failure (0.001). Consequently the weighted mean system index has increased from 0.53 to 0.59. This example illustrates how the weighted system index may reflect both the probability of failure and the distribution of the consequence indices.

Table 4-10: Weighted consequence indices

Members	C_i	W_i	W_i x C_i
1	0.40	0.001	0.0004
2	0.50	0.010	0.0050
3	0.70	0.010	0.0070
Mean	0.53		0.590

4.4.2 Examples

Each of the three examples presented in Sections 4.3.3 to 4.3.5 is re-examined using the proposed probabilistic weighting. Table 4-11 presents the data for the analysis. The coefficients of variations have been taken from Ellingwood and Galambos (1982). In the case of the applied load, the coefficient of variation is the value for the 50-year maximum live load. In the case of the resistance, 0.11 is the coefficient for yielding a tensile structural steel member. The coefficient of variation for the member areas is taken from Naess *et al.* (2009) in which a component reliability analysis was carried out for a 10-bar truss. It is assumed that compression members have the same coefficient of variation.

Table 4-11: Statistical data

	Mean	Coefficient of Variation	Probability Distribution
Applied Load (kN)	1720	0.25	Gumbel
Yield strength (MPa)	250	0.11	Normal
Area	Varies	0.05	Normal

The Hasofer Lind-Rackwitz Fiessler method is used to determine the probability for each member. This is an iterative procedure which involves an expansion about the most probable

point. The non-normal applied load variables are first transformed to normal variables. The procedure is carried out as described in Section 2.25.

4.4.2.1 Example 1

A table outlining the iterations is presented in Appendix A. The iterations are continued until the error is less than an acceptable value. The maximum error of 0.001 is the same as that used by Choi *et al.* (2007). In total, 9 iterations were carried out for Member 1, yielding a reliability index, β, of 3.286. The reliability index is similarly determined for each member in the structure. The probability of failure is determined as outlined in Section 2.5. The reliability index and probability of failure are reported for each member in Table 4-12. The member with the highest probability of failure is Member 6, principally due to the fact that it is the most highly stressed member in the intact structure under service load.

Table 4-12: Reliability index and probability of failure for each member

Member	β	P_f
1	3.289	5.0E-04
2	4.255	1.0E-05
3	2.552	5.3E-03
4	3.407	3.3E-04
5	5.145	0.0E+00
6	1.861	3.1E-02
7	4.255	1.0E-05
8	3.407	3.3E-04
9	2.552	5.3E-03
10	5.145	0.0E+00
11	3.289	5.0E-04

Table 4-13 shows the calculation of the weighed system index. The consequence indices exhibit very little variability. Therefore, the weighted mean index is similar to the mean index. The fact that the weighted mean index of 0.773 is lower than the mean index of 0.821 can be attributed to the high probability of failure of Member 6.

Table 4-13: Weighted system index

Member	C_i	W_i	W_i x C_i
1	0.821	5.0E-04	0.0004
2	0.821	1.0E-05	0.0000
3	0.821	5.3E-03	0.0044
4	0.816	3.3E-04	0.0003
5	0.816	0.0E+00	0.0000
6	0.754	3.1E-02	0.0236
7	0.821	1.0E-05	0.0000
8	0.816	3.3E-04	0.0003
9	0.821	5.3E-03	0.0044
10	0.816	0.0E+00	0.0000
11	0.821	5.0E-04	0.0004
Mean	0.813		0.773

4.4.2.2 Example 3

The probabilistic weighting is also applied to example 3. Table 4-14 lists the reliability and probability of failure associated with each event. Due to the optimisation, all members have a similar probability of failure, with the exceptions of Member 9 and Member 11.

Table 4-14: Reliability index and probability of failure for each member

Member	β	Pf
1	1.974	0.0242
2	1.971	0.0244
3	1.969	0.0245
4	2.044	0.0205
5	1.960	0.0250
6	2.007	0.0223
7	2.164	0.0152
8	1.919	0.0275
9	6.624	0.0000
10	2.057	0.0198
11	5.241	0.0000

Table 4-15 presents the weighted system index for example 3. The weighted index is significantly higher than the mean index. The value of the mean index is lowered considerably by Member 9 and Member 11 as each of these members has a low consequence index. However, as both members have a low probability of failure, they contribute little to the weighted index. Thus, the weighted system index is significantly higher than the mean value. This outcome is logical as due to the fact that the probability of failure for Member 9 and 11 is low relative to the other members.

Table 4-15: Weighted system index

Member	C_i	W_i	W_i x C_i
1	0.994	0.024	0.024
2	0.994	0.024	0.024
3	0.994	0.024	0.024
4	0.968	0.020	0.020
5	0.968	0.025	0.024
6	0.985	0.022	0.022
7	1.000	0.015	0.015
8	1.000	0.027	0.027
9	0.086	0.000	0.000
10	0.994	0.020	0.020
11	0.020	0.000	0.000
Mean	0.818		0.988

4.5 CONCLUSIONS

A general framework by which additional performance measures may be incorporated into a unified robustness assessment has been proposed. The proposed indices build upon existing indices such as the residual strength factor and more general redundancy assessment methodologies, such as that proposed by Ghosn and Moses (1998). The primary focus of the indices is a quantification of the change in structural performance, with respect to the intact structural state, caused by a damage event. The proposed method is simple in its application, easily calculable in terms of the inputs, and objective in terms of the outputs. This formulation of the indices therefore addresses many of the general robustness assessment requirements discussed by Starossek & Haberland (2011).

Four performance measures have been incorporated in order to facilitate a comprehensive quantification of the change in structural performance; elastic stiffness, yield strength, ultimate strength and ductility. Each indicator quantifies an important aspect of the structural behaviour. The analyses presented show that using any individual performance measures such as the strength or ductility is not sufficient to provide a complete quantification of the structural change. Additionally, the final unified index can be easily degenerated if, given the requirements of a specific analysis, it is desirable to focus on a single property.

A system index has also been proposed. The index addresses two important issues; firstly, the distribution in structural response which arises when multiple damage states are simulated, and secondly, the probability of failure of the initial damage event. If the probability of each damage event is equivalent, the system index will approximately equal a simple mean index. On the other hand, any important differences in the probability of occurrence will also be reflected by the weighted system index.

The probability of failure is analogous to the work of failure as defined by Smith (2003a) and Pinto *et al.* (2002). In terms of the consequences (Section 2.2.3) discussed in Baker *et al.* (2008) and JCSS (2008), the probability of failure of the initial event may be considered as the direct consequence, whereas the consequences of the event are the indirect consequences. The probabilistic weighted index thus expands the scope of the analysis and provides a more holistic quantification of the structural collapse resilience.

5 ALTERNATIVE FAILURE PATHS

5.1 INTRODUCTION

The quantification of structural capacity is a fundamental part of robustness assessment. As presented in Chapter 3, different aspects of structural capacity may be quantified as part of a structural robustness assessment, such as the stiffness, yield strength, ultimate strength or ductility. Commonly, the assessment of structural robustness relies on deterministic FE analyses, with an assumed set of damage events (Frangopol and Curley 1987, Ghosn and Moses 1998, Pinto *et al.* 2002, Smith 2003b). Such analyses generate a unique structural response, comprising of a series of events, such as yielding and failure of members, leading to the collapse of a structure.

However, there are many sources of structural uncertainty, such as variations in the resistance of members and the load applied on a structure. Furthermore, structures are subject to time varying loads such as traffic and wind. Structural uncertainties may impact on key contributing properties such the strength or ductility; thus affecting the robustness of a structure. This phenomenon may be particularly important in the post damage residual structure, in which the structural integrity has already been compromised due to an initial damage event.

While the general subject of structural uncertainties in relation to the reliability of a structure is well established, the influence of pertinent uncertainties on the assessment of the structural performance in the context of structural robustness is less understood. As a matter of fact, the degree to which the behavioural characteristics of a structure are sensitive to uncertainties is

an important consideration in robustness assessment. If a structure is sensitive to uncertainties, small variations may result in significant changes to the overall structural performance and thus the assessment of the structural robustness. Structural uncertainty is thus relevant to the robust design of structures. Doltsinis (2004) notes the increasing importance of designing robust structures, in which the structural performance is insensitive to the natural variability of the parameters. In this context, the structural robustness may be assessed in terms of the performance variability about the mean; using, for example, the standard deviation or coefficient of variation.

The prevalence of structural uncertainties is also particularly relevant to assessment of robustness in ageing structures. Older structures may have additional inherent uncertainties due to the less advanced design, materials and construction methods. The degree of uncertainty is further compounded by the ageing process which increases the likelihood of defects such as corrosion or fatigue, thus widening the margin of variance. Consequently, it is of great importance to incorporate structural uncertainties into the robustness quantification of ageing structures.

Pinto *et al.* (2002) and Smith (2003a) both investigate critical sequences of events which lead to the collapse of a structure using deterministic structural analyses. Inherent structural uncertainties may however lead to deviations in collapse sequence, which may affect the robustness of a structure. This chapter will investigate the degree to which structural robustness is sensitive to structural uncertainties with a focus on the importance of variations in the sequence of events leading to failure.

The importance of structural uncertainties will be investigated using FE analyses in conjunction with a Monte Carlo simulation (MCS). Two levels of uncertainty will be

investigated; an assumed normal distribution and a uniform distribution with a prescribed upper and lower bound.

5.2 OVERVIEW OF STRUCTURAL UNCERTAINTIES

In general, structural uncertainty may be classified into three categories: aleatoric uncertainty, epistemic uncertainty and ontological uncertainty (Elms 2004). Aleatoric uncertainty arises from the inherent variability in a structural system. The variability can be described by probability distribution and known parameter. However, given that this type of uncertainty is associated with inherent randomness, it cannot be reduced by additional testing.

On the other hand, epistemic uncertainty arises from the use of imperfect models which are based on simplifications and assumptions. The primary reason for differentiating between these two types of uncertainty, is to clarify how each type of uncertainty may be reduced; from a decision making perspective, the differentiation is unimportant (JCSS 2008). Frangopol *et al.* (2008) note that aleatoric uncertainty gives rise to a calculated risk, whereas epistemic uncertainty relates to the uncertainty associated with the calculated risk. Both types are considered to be equally important and require the same probabilistic and statistical tools.

Elms (2004) also discusses ontological uncertainty. Ontological uncertainty arises from factors which are unknown and unexpected. It is noted that structural failures often arise from unknown and unexpected causes. Ontological uncertainty is related to the difference between an engineer's assumptions and reality (Brown *et al.* 2008). While probabilistic methods may be used to address both aleatory and epistemic uncertainty, the approach cannot address ontological uncertainly. Events which fall into the category might be simple mistakes or malicious acts.

In addition to the above categorisation, uncertainties may also be considered from the perspective of the different stages in the lifecycle of a structure; the structural design, manufacturing and construction, service life and also the ageing process (Doltsinis 2004).

The uncertainty which is pertinent to the present analyses is aleatory uncertainty; such as variation in the material properties of members, member sizes, structural loads and so on. As noted in the introduction, the robustness of assessment of ageing structures is of great importance. The analysis of ageing structures is subject to both greater epistemic and aleatoric uncertainty which are compounded by gradual structural ageing and deterioration. For example, Connor *et al.* (2005) note that many older steel bridges, which were built before the development of modern fatigue provisions, may possess poor fatigue details. Other factors which might make older bridges susceptible to fracture are also considered;

- Insufficient steel fracture toughness
- A lower standard of detailing, fabrication quality and shop inspection
- Severe corrosion problems
- Traffic volume which exceed the original design specifications.

5.3 FAILURE PATHS

Smith (2003) and Pinto *et al.* (2002) both quantify the vulnerability of a structure to critical failure sequences from different perspectives; stiffness and energy. In each case, a FE-based deterministic analysis is used to identify the most critical failure sequences, where failure sequences are comprised of individual member failure events. The present study will also

investigate failure sequences; however the focus here is the sensitivity of residual structural capacities to uncertainties, in particular those which result in significant changes in failure sequences.

Figure 5-1 depicts a tree diagram which may be used to illustrate the alternative failure paths which may exist in a structure. The tree begins with the intact structure. Firstly, an event such as member yielding or failure is assumed. A notional nominal path is identified in red. Damage event *i* is denoted by e_i^o, which refers to event *i* in the intact structural state. Next, the structure is pushed until it reaches a collapse state. The path to failure will involve a number of events such as member yielding and failure. The second event in the nominal path is e_2^i; event 2 given that event *i* has already occurred. This failure path continues until overall collapse of the structure occurs.

Alternatively, at each stage, other events of similar probability may exist. For example, when event e_2^i occurs, there may be another event, e_3^i, which, given the various structural uncertainties, may be equally probable. If, event 3 occurs instead of event 2, a new divergent branching failure path is created.

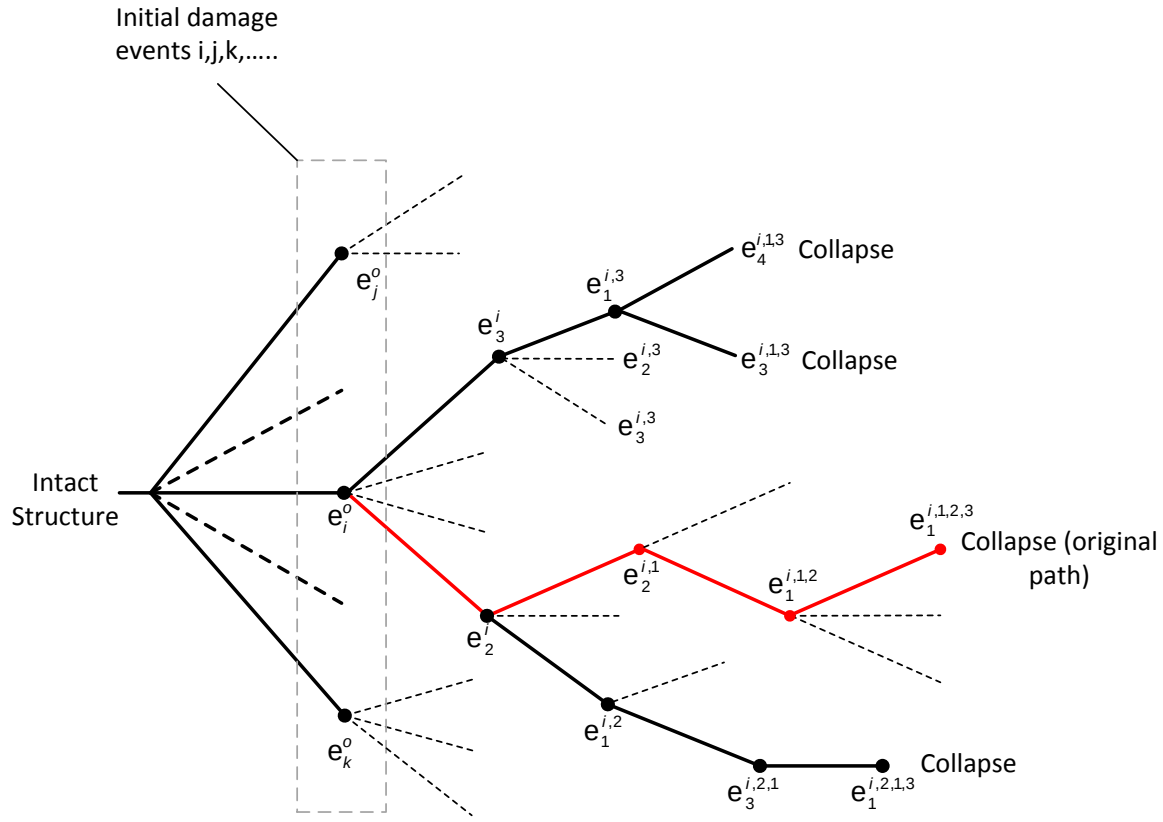

Figure 5-1: Alternative failure paths

For any given structure, many different failure paths may exist. The number of alternative failure paths is structure dependent and will be influenced by a number of factors. One key factor is the degree of optimisation. If a structure is optimised in order to minimise the volume of material used, so that the stress level in each member of the structure is equivalent, there may exist many potential failure paths. This is a common problem associated with modern computer designed structures and high performance materials which have reduced safety margins (Janssens and Dwyer 2001), and in the present context of structural robustness the influence could be even greater.

A second factor is the assumed degree of uncertainty. Greater uncertainty will increase the number of alternative failure paths which may arise. Conversely, with decreasing uncertainty the number of paths will converge with a deterministic analysis.

5.4 PROBABILISTIC MODEL

It is proposed to consider the general uncertainties which may affect structural robustness rather than any specific variable. Table 5-1 lists some typical COV and probability distributions taken from a variety of sources in the literature. Two values are presented for the yield strength; the first is for the yield strength of rolled steel and the second is for the yield strength of a tensile member considering all sources of uncertainty which would affect the strength.

Table 5-1: Statistical data

Parameter	COV	Distribution	Literature Source
Yield Strength	0.07	Lognormal	(JCSS 2000)
Yield Strength	0.11	Lognormal	(Ellingwood and Galambos 1982)
Ultimate Strength	0.04	Lognormal	(JCSS 2000)
Young's Modulus	0.03	Lognormal	(JCSS 2000)
Poisson's Ratio	0.03	Lognormal	(JCSS 2000)
Ultimate Strain	0.06	Lognormal	(JCSS 2000)
Geometry	0.05	Normal	(Sanjayan and Candy 2004)

A single variable will be considered herein; member strength. For the present analysis, a COV of 0.1 and a normal distribution are assumed. Similarly to Ellingwood and Galambos (1982), the COV is considered as a general COV which incorporates different aspects of the uncertainties, rather than just the material strength.

5.5 ANALYSIS METHOD

A Monte-Carlo simulation (MCS) will be used to investigate the degree to which uncertainties may affect structural robustness. In contrast with the conventional application of a MCS, the objective herein is not to determine the reliability or probability of failure of a structural system, but to establish the degree to which the structural capacity, which is pertinent to robustness, is sensitive to inherent variability. Figure 5-2 illustrates the difference between the two approaches; the conventional interpretation of reliability in terms of performance with respect to a limit state, and the relationship between robustness and the variability of structural performance.

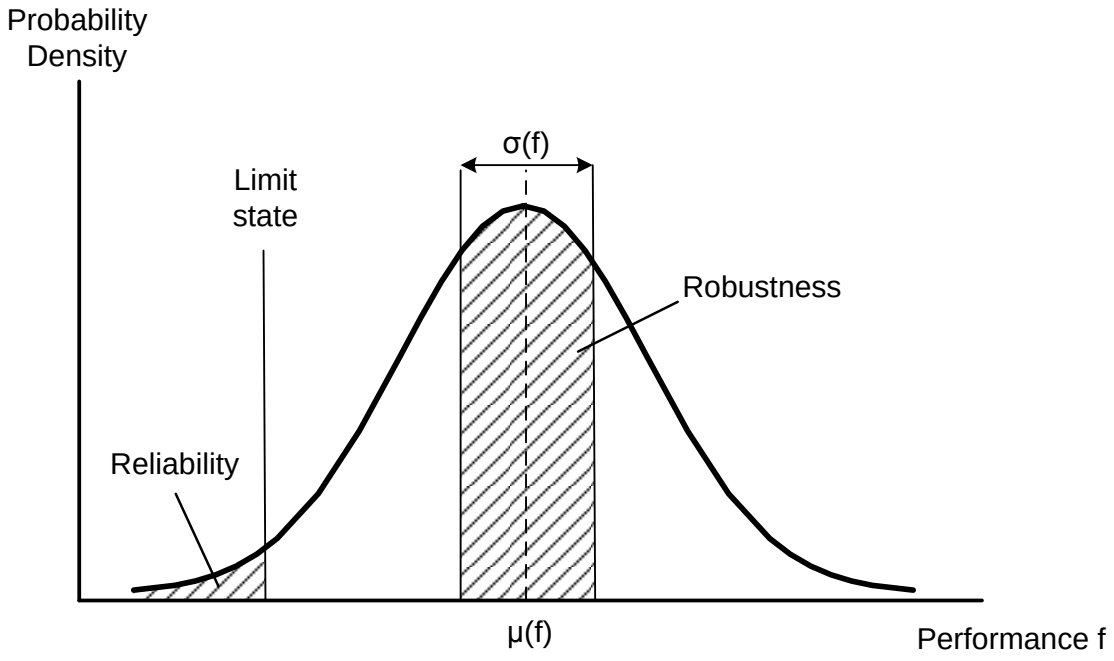

Figure 5-2: Difference between reliability and robustness (adapted from Doltsinis 2004)

The capacity of each structure will be considered with respect to the global ultimate strength and the ductility (and the plastic energy implied therein). Using both measures enables

different aspects of the performance sensitivity to member strength to be examined; the natural ultimate strength increase as a result of the increased member strength and also the more system-oriented effects caused by changes in the path to failure.

The assessment of robustness given variations in member strength requires a large number of simulations. Moreover, the modelling of sequences of member failure adds considerably to the computational demands and the difficulty of obtaining a convergent analysis solution. In light of these difficulties, it was determined that the definition of collapse as the failure of the first member is sufficient to investigate the importance of structural uncertainties in the quantification of robustness. One consequence of the restricted collapse definition is that the variation in ductility (or energy absorption) may be less than that observed if failure of several members is required for collapse. The definitions of the ultimate strength and ductility are illustrated in Figure 5-3. The ductility is defined as the global displacement at the failure of the first member.

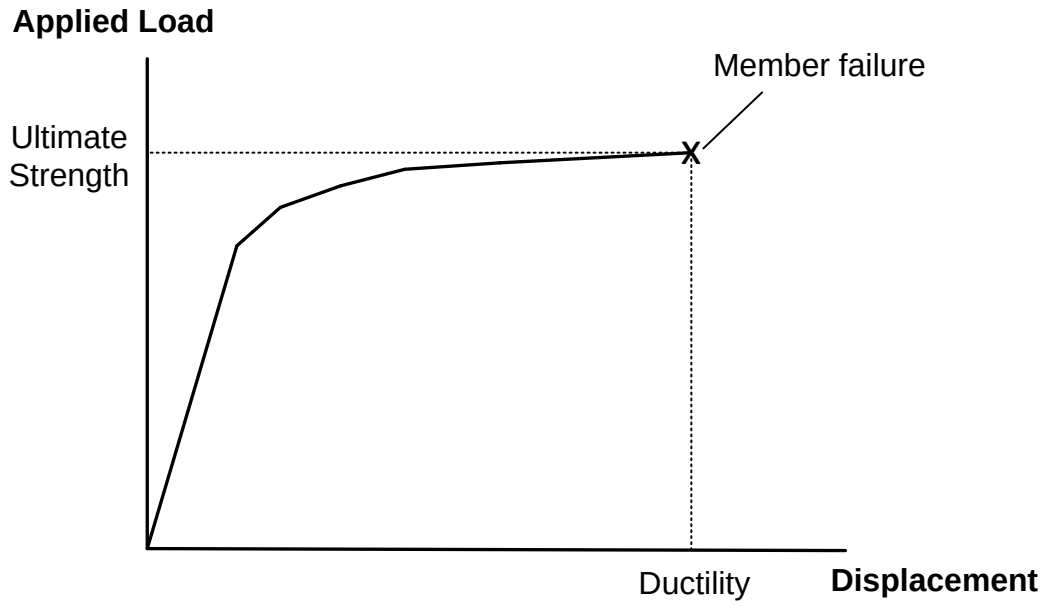

Figure 5-3: Definition of collapse

All members are steel. The material properties are the same as those specified in Section 3.2.1. It is assumed that the elastic and post-yield tangential modulus is the same for all simulations. Therefore, the yield strength and ultimate strength fluctuate by the same margin. Figure 5-4 illustrates the upper and lower strength bounds at +/- one standard deviation. However, varying degrees of uncertainty will be investigated.

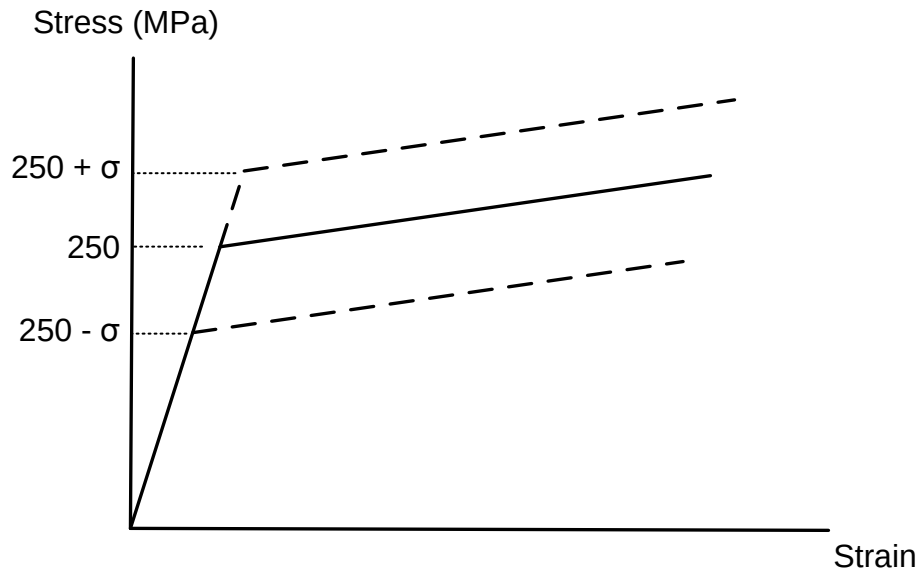

Figure 5-4: Strength variation

The coefficient of variation is used to indicate the sensitivity of a particular structural configuration to parameter variation. Therefore, the number of simulations was determined by observing the convergence of the coefficient of variation (COV) for the ultimate strength and the ductility of each configuration. This procedure was carried out using the full probability distribution. In the absence of any comparable figure from the literature, an error of 0.001 is used to assess the convergence of the COV. It was observed that 500 simulations were sufficient to satisfy this objective for all structural configurations. The convergence of both the strength and ductility for Configuration A is presented in Figure 5-5 and Figure 5-6.

The diagrams show that the convergence of COV for ductility required more simulations than the strength. A greater ductility variation was observed for all configurations; nevertheless 500 simulations were sufficient to achieve the convergence target in all cases.

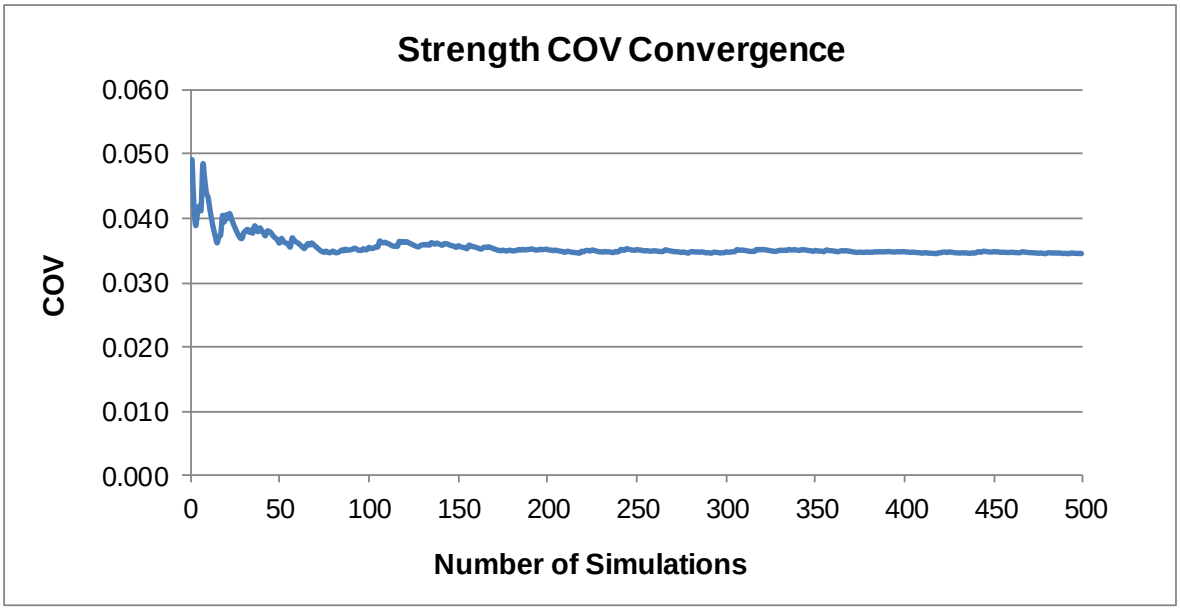

Figure 5-5: Strength COV convergence

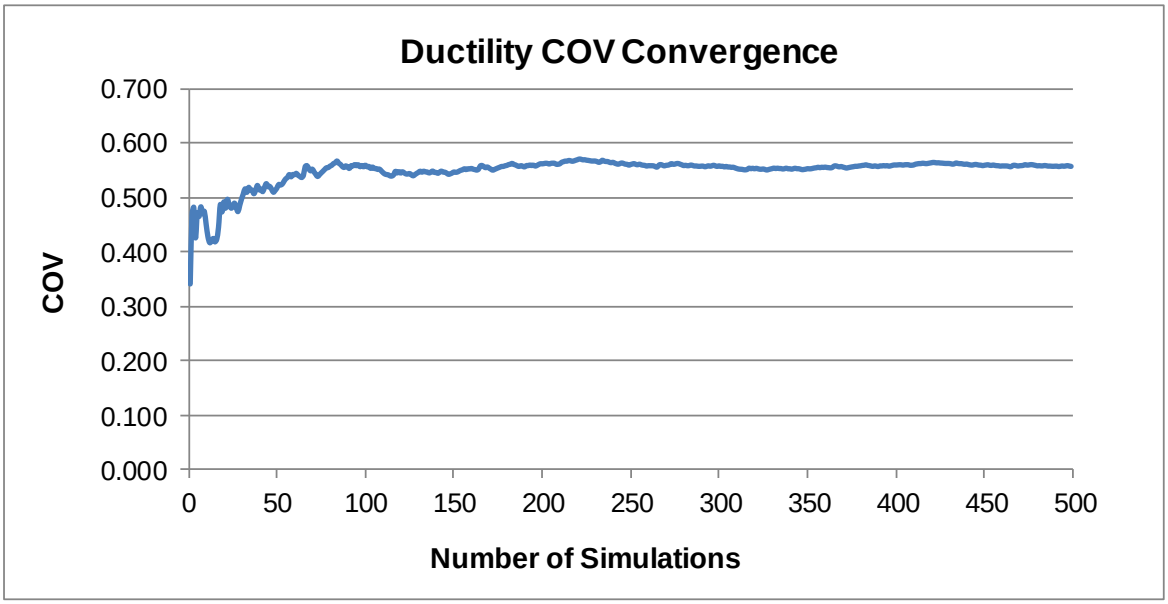

Figure 5-6: Ductility COV convergence

5.6 STRUCTURAL MODELS

As illustrated in Figure 5-7, each model has the same dimensions and topology. However, the areas of the members are different in each configuration. For Configuration A, the cross-section size of the members is optimised in order to minimise the volume of material. Therefore, most members have approximately the same axial stress in the intact structural state. For Configuration B, all members have the same cross-section area. Configurations C and D are mixed; some members have equivalent stress levels, however they are not fully optimised. Three equal concentrated loads are applied in each configuration. The load is incrementally increased until collapse occurs. The full details of each configuration are presented in Appendix B.

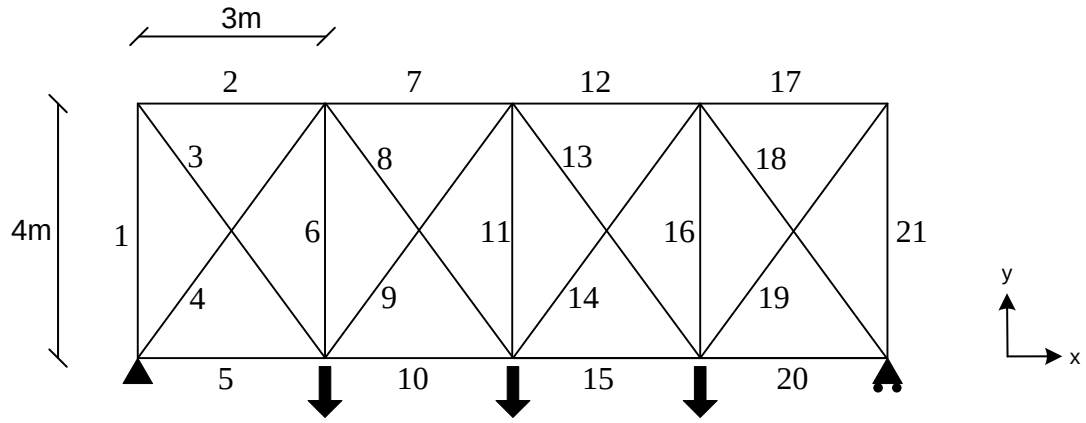

Figure 5-7: Model topology and dimensions

5.7 RESULTS FROM THE INTACT STRUCTURE AND DISCUSSION

5.7.1 Normal Distribution

Firstly, each structural configuration is analysed using the full distribution. 500 simulations are carried out for each configuration. Table 5-2 compares the ultimate strength results for each configuration. The results show that the degree of variation in ultimate strength is quite similar for each configuration. Configuration B has the highest COV with 0.05521, whereas Configuration D has the lowest COV with 0.04505.

Table 5-2: Comparison of the ultimate strength for structural configuration

Parameter	Structural Configuration			
	A	**B**	**C**	**D**
Maximum strength (kN)	3528.34	1364.46	3980.89	1452.46
Minimum strength (kN)	2361.49	947.46	2750.21	992.92
Mean (kN)	3147.98	1178.79	3492.43	1262.58
Standard deviation (kN)	167.43	65.09	182.26	68.92
COV	0.053	0.055	0.052	0.055

The variation in structural performance may also be illustrated using the load-displacement relationships for each simulation. Figure 5-8 to Figure 5-11 show the load-displacement relationship for all 500 simulations of each configuration. The diagrams highlight the degree of variation of the structural response for each structural configuration. The elastic stiffness is the same for each simulation as the only variable is the yield stress. However, it is evident that there is substantial variation in ultimate strength and ductility.

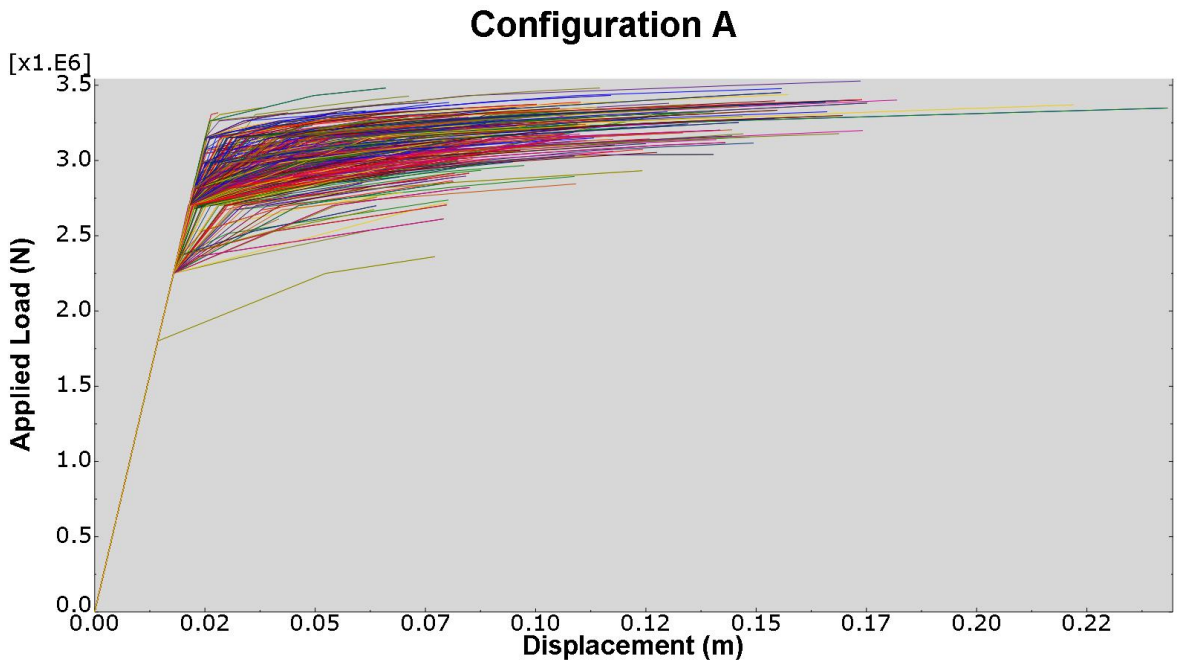

Figure 5-8: Load - displacement relationships for Configuration A (500 simulations)

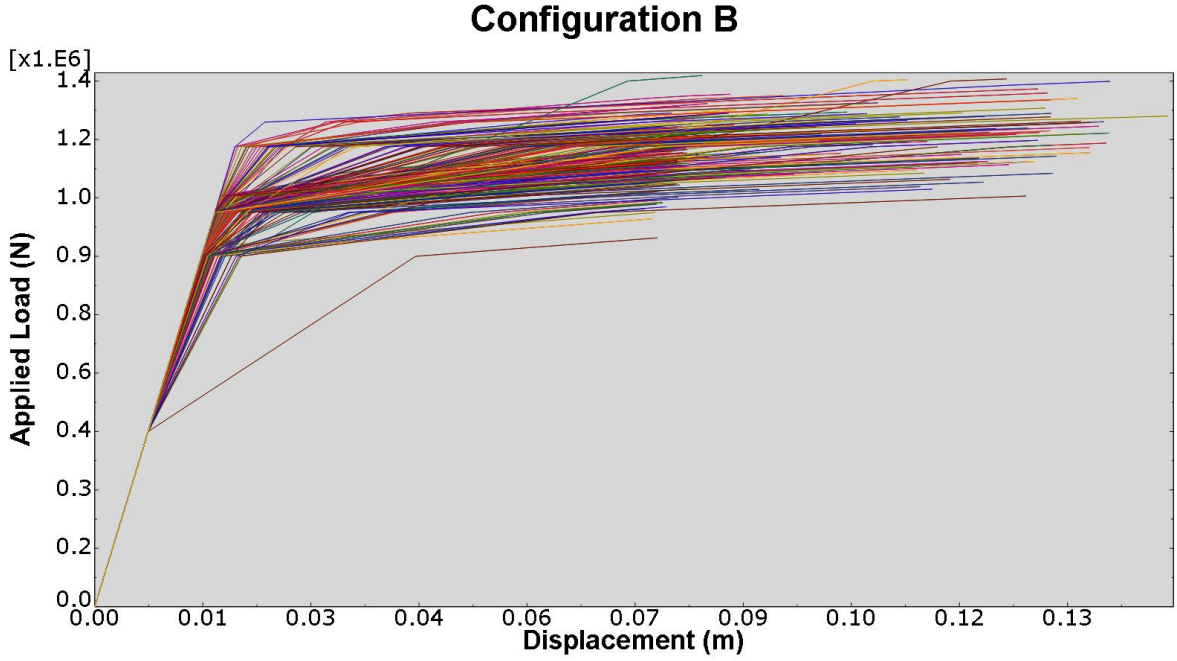

Figure 5-9: Load - displacement relationships for Configuration B (500 simulations)

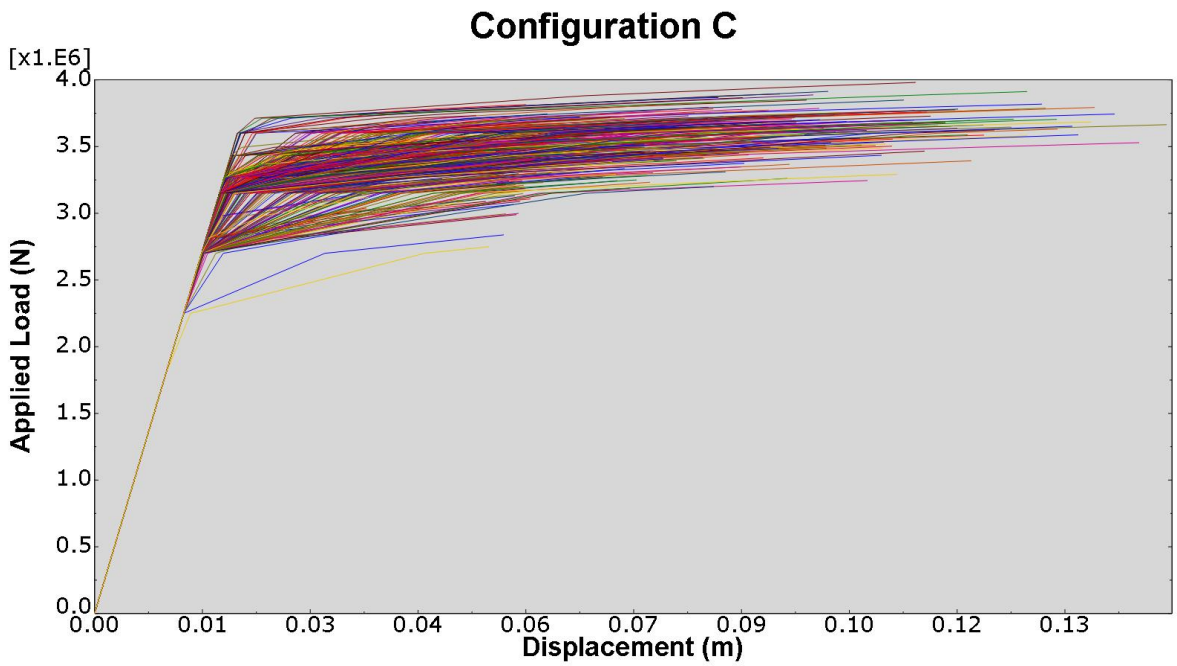

Figure 5-10: Load - displacement relationships for Configuration C (500 simulations)

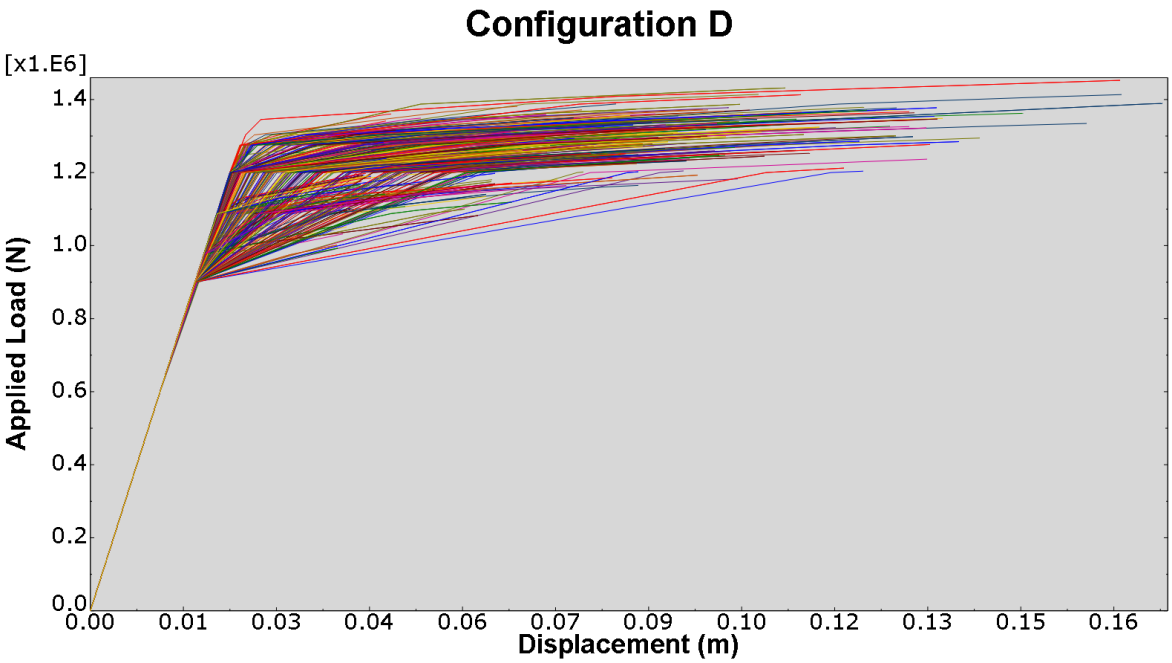

Figure 5-11: Load - displacement relationships for Configuration D (500 simulations)

Table 5-3 shows the results for the ductility of each configuration. The COVs for the ductility of each structure show much greater variation. Configuration A has the highest COV with 0.422, and Configuration B has the lowest COV with 0.249.

Table 5-3: Comparison of the ductility for each structural configuration

Parameter	Structural Configuration			
	A	B	C	D
Maximum ductility (m)	0.243	0.113	0.149	0.173
Minimum ductility (m)	0.023	0.043	0.037	0.040
Mean	0.088	0.068	0.073	0.080
Standard deviation	0.037	0.017	0.024	0.027
COV	0.422	0.249	0.327	0.335

Given that Configuration A is the optimised structure, it is expected that this configuration has the highest COV. This is due to the fact that, at each event in the failure propagation

process, there are many alternative events which are similarly probable. This can be illustrated by observing the stress in each member of the structure at first yield, as reported in Table 5-4. The structure is symmetrical. Therefore, the stress in Member 1 and 21 is the same and so, when Member 8 and Member 16 yield, there are 16 other members which are within 5 MPa of the yield stress. Consequently, the structure is sensitive to variations in member strength. Minor fluctuations in member strength are sufficient to cause deviations in the nominal failure path. Similarly, at later stages in the failure sequence, there are many alternative events.

Conversely, Configuration B is less sensitive to variations in member strength. Table 5-4 presents the stress in each member of Configuration B at first yield. Similarly to Configuration A, the structure is symmetrical. In this case, Member 7 and 12 yield, however the stress in the other members is much lower. Consequently, at least in the initial stages of the failure path, the path is relatively insensitive to member strength variations.

Configuration C is also symmetrical. Configuration C is relatively mixed in terms of optimisation. When yielding occurs in Members 6 and 16, there are 6 other members which are within 10 MPa of the yield stress.

Table 5-4: Stress in members of Configuration A at first yield

Member	Stress (MPa)		
	Configuration A	**Configuration B**	**Configuration C**
1, 21	-245.72	-122.41	-95.05
2, 17	-246.95	-91.81	-109.66
3, 19	246.46	153.01	238.95
4, 18	-247.24	-178.31	-90.90
5, 20	246.92	106.98	245.44
6, 16	244.53	74.36	250.00
7, 12	-247.61	-250.00	-145.96
8, 14	250.00	85.35	240.94
9, 13	-46.48	-25.09	-15.39
10, 15	246.03	213.85	243.15
11	74.36	40.14	47.75

Table 5-5 shows the stress in each member at first yield for Configuration D. The member sizing is not symmetrical for this configuration. As indicated by the stress values, the stress range is variable.

Table 5-5: Stress in members of Configuration D at first yield

Configuration D			
Member	**Stress (MPa)**	**Member**	**Stress (MPa)**
1	-145.53	12	-205.58
2	-161.70	13	-55.20
3	181.91	14	202.01
4	-250.00	15	186.90
5	97.50	16	191.76
6	75.27	17	-74.14
7	-165.14	18	-138.03
8	210.53	19	247.13
9	-115.96	20	212.02
10	208.43	21	-98.85
11	48.15		

The results in Table 5-3 highlight that ductility is particularly sensitive to variations in member strength. The primary reason for this sensitivity is the change in the failure path leading to collapse. At one extreme the failure path events may be localised and thus plasticity develops in relatively few members before collapse. This phenomenon is particularly relevant to pint-jointed trusses which naturally have a relatively low static indeterminacy. On the other hand, the failure path may be relatively more distributed, resulting in the development of plasticity in many members, and hence an increased energy absorption capacity. A deterministic analysis using nominal values cannot capture these potential differences in the structural behaviour.

This phenomenon is illustrated by examining some failure sequences. Table 5-6 shows two Configuration A failure sequences. Both simulations have similar ultimate strengths. However, the ductility for simulation 52 is much greater than the simulation 251. This can be

attributed to the distributed response of the structure in simulation 251, in which there are 9 yielded members at collapse. As a result, Simulation 52 has a much greater energy absorption capacity.

Table 5-6: Two Configuration A simulations

Simulation Number	Ultimate Strength (kN)	Ductility (m)	Number of Yielded Members
251	3137	0.025	9
52	3116	0.145	3

The plasticity distribution for each structure is illustrated in Figure 5-12 and Figure 5-13. In each diagram, the members which yield prior to structural failure are highlighted in red. Figure 5-12 shows the members which yield are concentrated in one area of the structure. In contrast, Figure 5-13 shows that development of plasticity in the structure is distributed throughout the structure, thereby enabling the structure to absorb more energy.

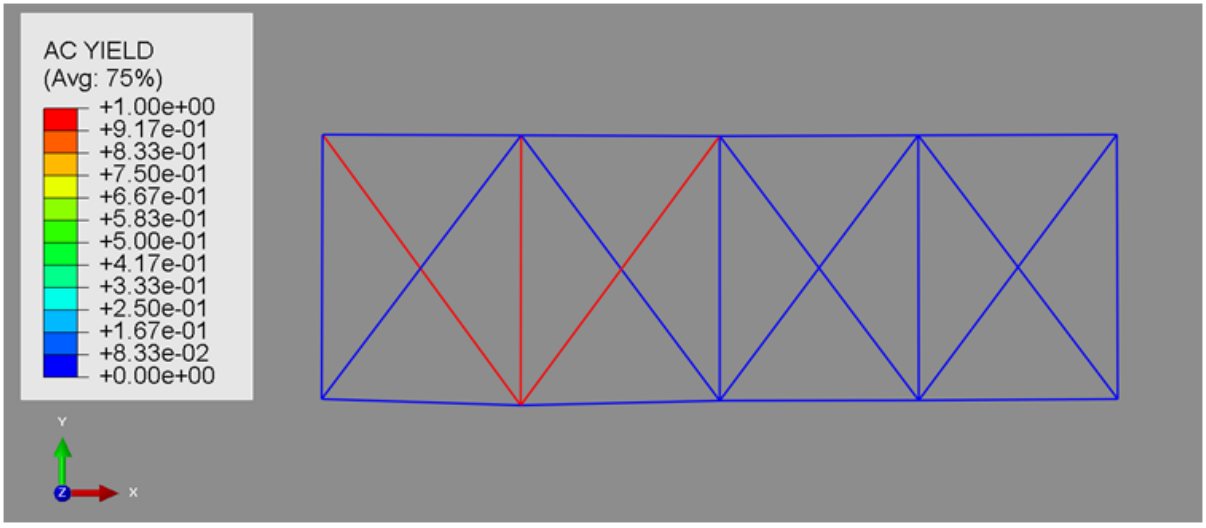

Figure 5-12: Configuration A - Simulation 251

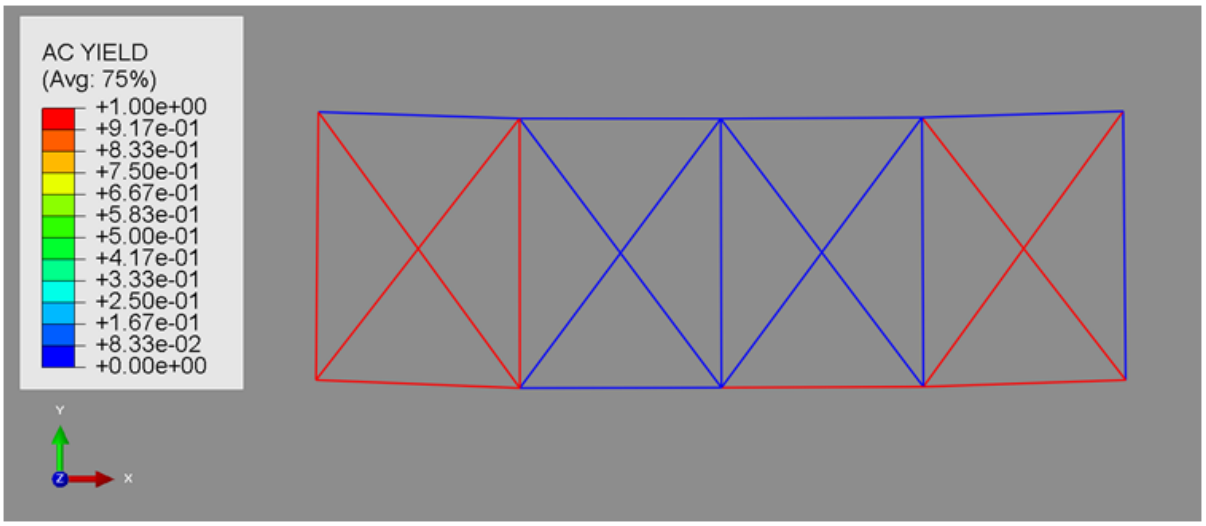

Figure 5-13: Configuration A - Simulation 52

A similar case is presented in Table 5-7 for configuration B. Simulation 32 and 36 have similar ultimate strength; however the ductility of simulation 36 is over two times greater.

Table 5-7: Two Configuration B simulations

Simulation Number	Ultimate Strength (kN)	Ductility (m)	Number of Yielded Members
32	1118	0.043	2
36	1142	0.090	4

The yielded members for each simulation are depicted in Figure 5-14 and Figure 5-15. The distribution of yielded members in the structure is similar; simulation 32 has two members and simulation 36 has 4 members. This highlights that relatively minor differences in the plasticity distribution and number of yielded members may result in significant differences in the overall energy absorption capacity of a structure.

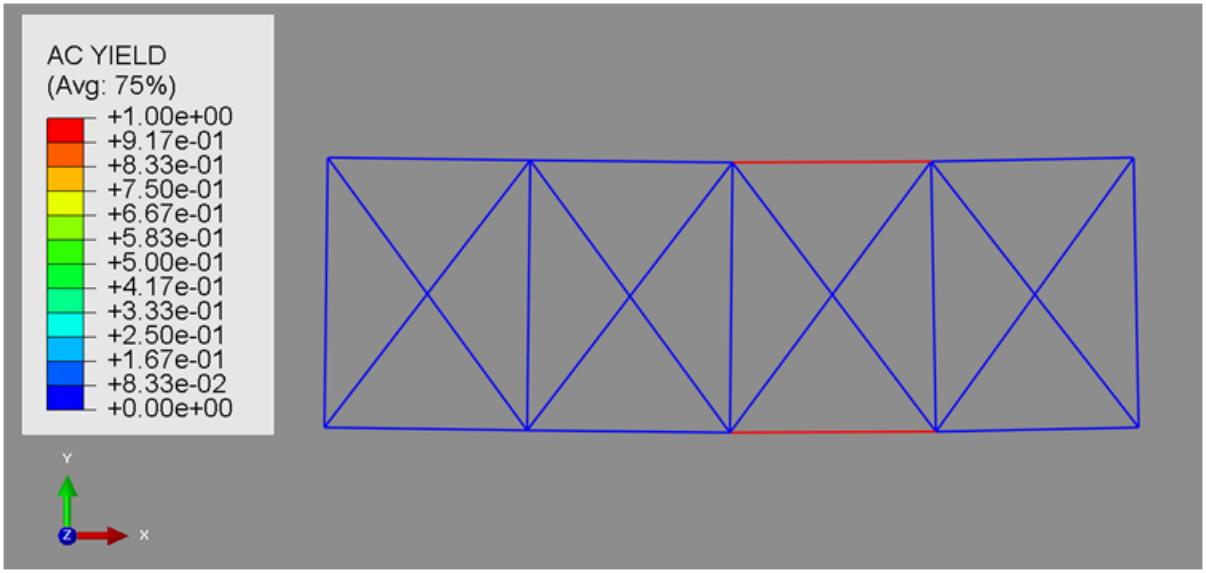

Figure 5-14: Configuration B - Simulation 32

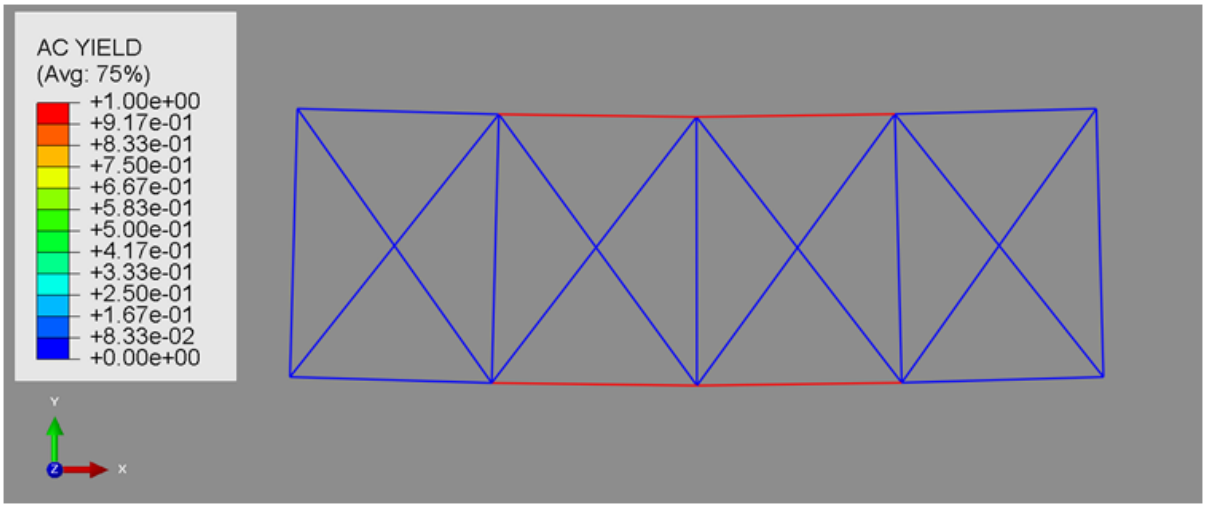

Figure 5-15: Configuration B - Simulation 36

5.7.2 Uniform Distribution

The previous examples have investigated the effect of variable member strength on the ultimate strength and ductility of a structure, using the full probability distribution. It is also desirable to investigate the sensitivity of the structural performance to minor variations in

member strength. The implication of investigating minor variations in member strength is that, each alternatively possible event will have an equivalent probability of occurrence. To this end, a uniform distribution with +/- 10 MPa is used for the subsequent analyses.

The results for the variation in ultimate strength are listed in Table 5-8. As expected, the coefficient of variation for the ultimate strength is significantly lower than the COV which was determined using the full normal distribution.

Table 5-8: Comparison of the ultimate strength for structural configuration

Parameter	Structural Configuration			
	A	**B**	**C**	**D**
Maximum strength (kN)	3628.63	1258.47	3903.24	1372.29
Minimum strength (kN)	3456.09	1186.18	3673.15	1266.23
% Difference	4.87	5.91	6.07	8.04
Mean (kN)	3549.79	1219.81	3766.40	1315.89
Standard deviation (kN)	23.86	15.50	39.43	25.42
COV	0.007	0.013	0.010	0.019

However, the ductility results in Table 5-9 indicate that despite the small variation in the ultimate strength of each member, there is substantial variation in the global ductility. The configuration with the highest COV is Configuration C, with a COV of 0.391. Given that a narrow uniform distribution is used rather than the normal distribution, the percentage difference between the highest and lowest is also informative. The largest difference, in Configuration C, is 118%.

Table 5-9: Comparison of the ultimate ductility for structural configuration

Parameter	Structural Configuration			
	A	B	C	D
Maximum ductility (m)	0.368	0.142	0.209	0.177
Minimum ductility (m)	0.126	0.093	0.084	0.046
% Difference	97.99	42.06	85.692	117.805
Mean (m)	0.259	0.127	0.153	0.067
Standard deviation (m)	0.039	0.010	0.024	0.026
COV	0.152	0.078	0.157	0.391

Figure 5-16 to Figure 5-19 present the load-displacement relationship for each structural configuration. The diagrams highlight that the variation in terms of ultimate strength is significantly less than the variation in ductility.

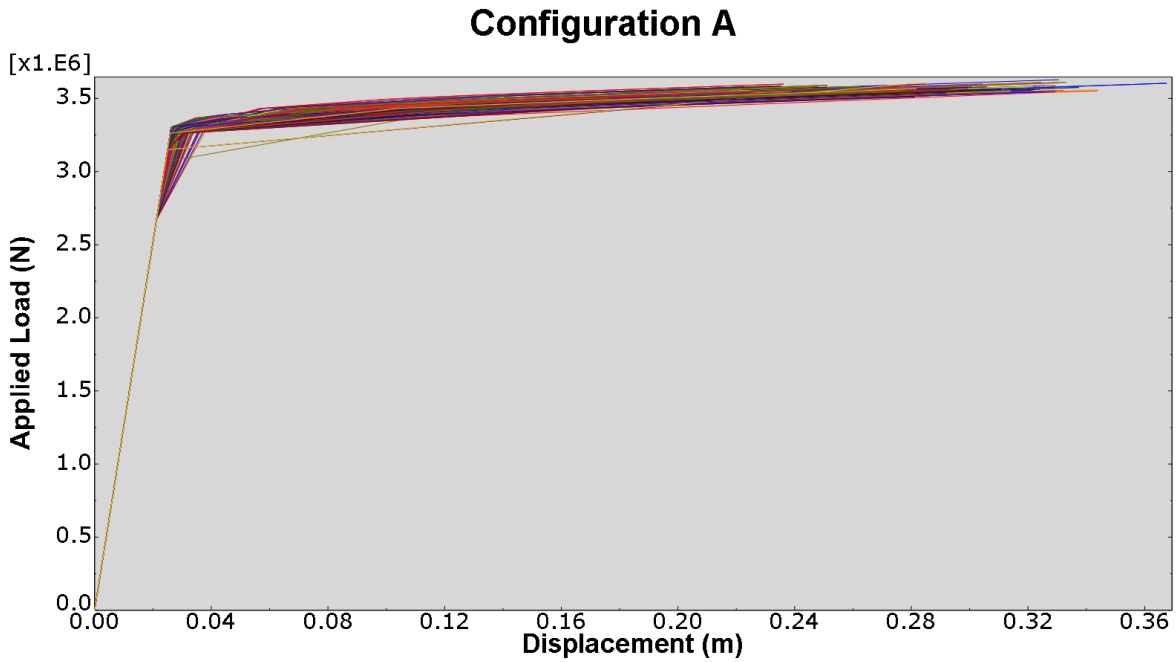

Figure 5-16: Load - displacement relationships for Configuration A

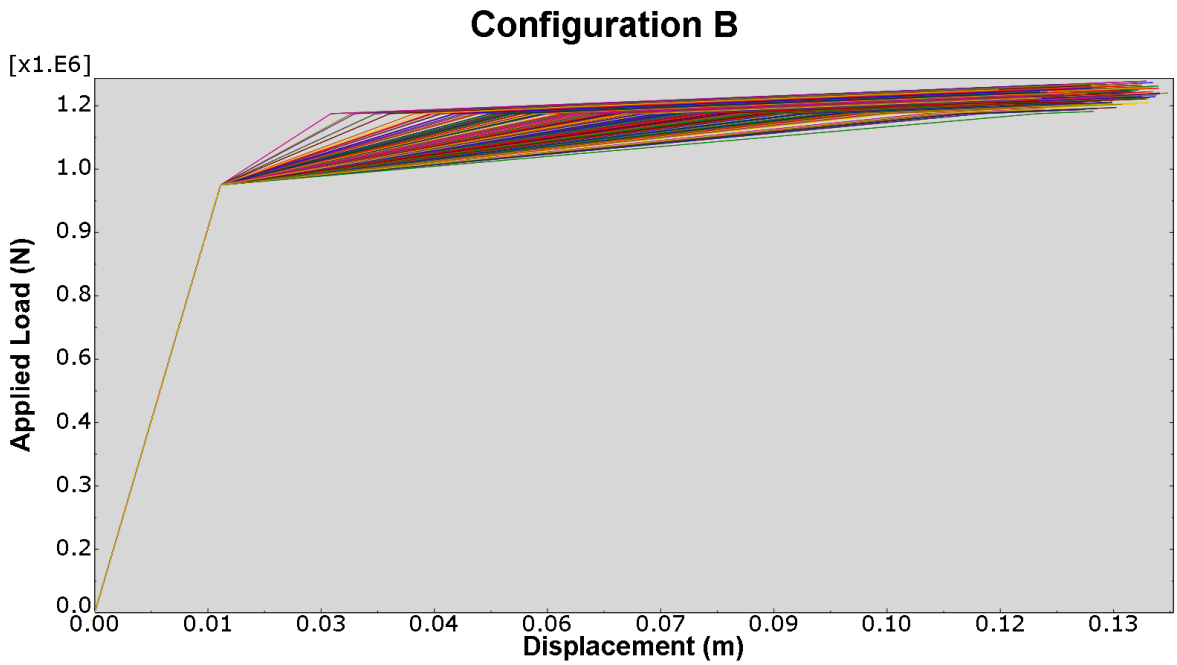

Figure 5-17: Load - displacement relationships for Configuration B

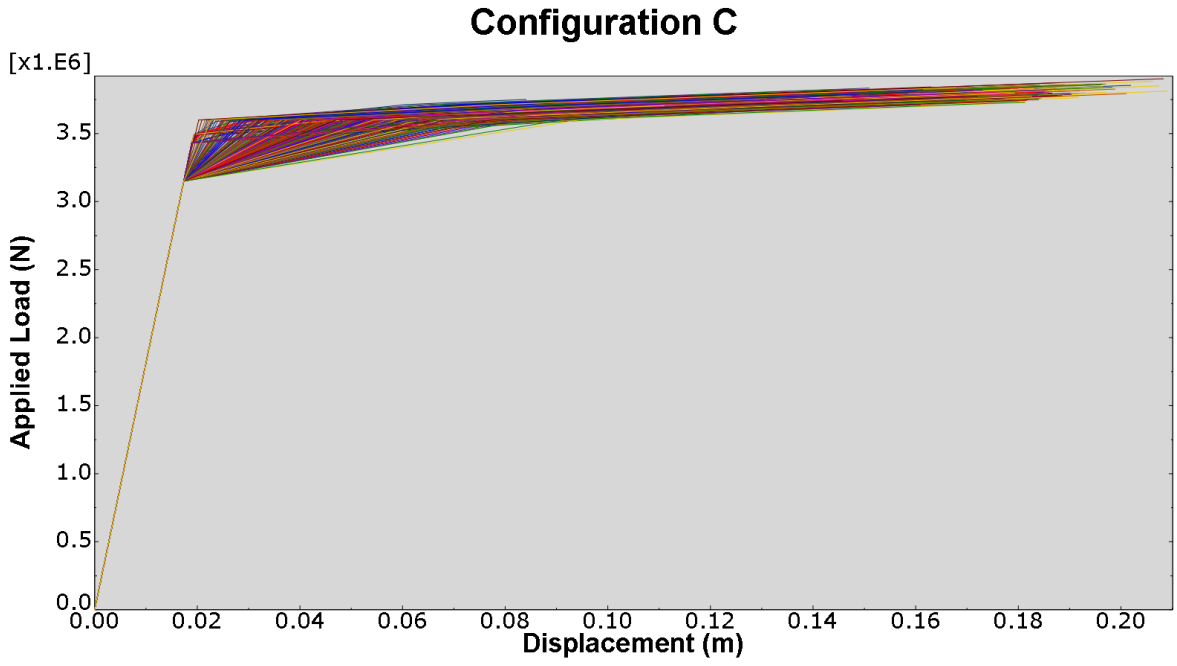

Figure 5-18: Load - displacement relationships for Configuration C

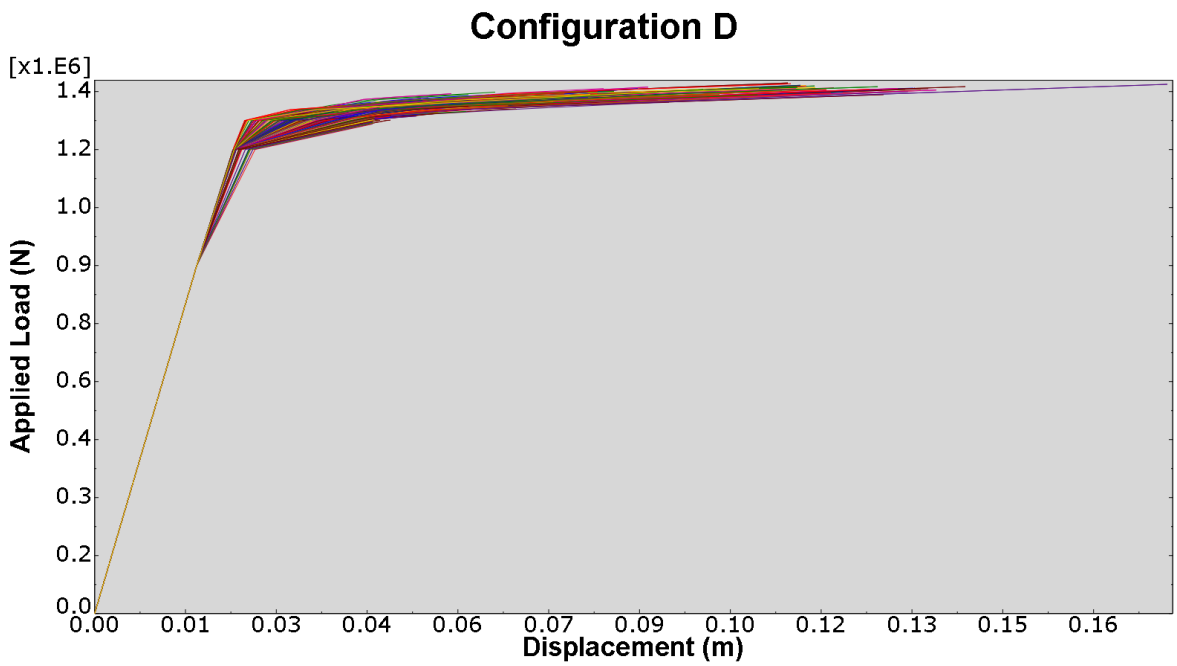

Figure 5-19: Load - displacement relationships for Configuration D

The configuration with the lowest variation in ductility is Configuration B (the structure in which all members have the same area). Given relatively large distribution in stress among the members of Configuration B, and the small degree of variation in the input parameters, it is expected that Configuration B exhibits relatively low sensitivity.

The configuration with the second lowest COV is Configuration A (the optimised structure). This differs to the original analysis in which Configuration A exhibited the largest sensitivity. It is apparent that if the variation of the input parameters is small, optimisation may actually decrease sensitivity. Significant changes in ductility arise when a failure sequence changes from one which is localised to distributed or vice versa. However, in the optimised structure, there are many members with approximately the same stress and almost all members yield prior to collapse. If the variation of the input parameters is small, the variation may not be sufficient to significantly alter the failure path. This is illustrated by observing the yielded members in the simulation with the lowest ductility (Simulation 205) and the simulation with

the highest ductility (Simulation 255). As illustrated in Figure 5-20, each simulation has the same distribution of yielded members at failure, although there are some minor differences in the sequential order of the yielded members.

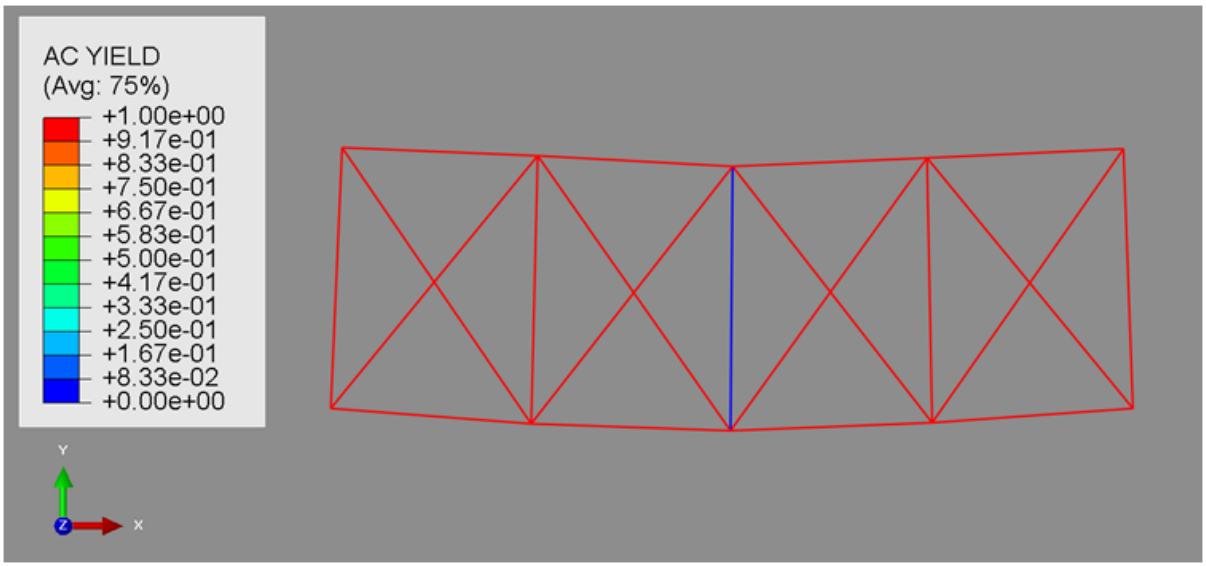

Figure 5-20: Configuration B (Simulation 205 and 255)

Configurations C and D exhibit a relatively high degree of sensitivity despite the small variation in member strength. Due to the configuration of these structures, they are sensitive to small variations in member strengths which can cause the failure path to deviate, resulting in either a localised failure path or one which is distributed.

Figure 5-21 shows the yielding distribution on simulation 213 of Configuration C. As indicated, there are many members involved in the failure process. Conversely, as illustrated in Figure 5-22, there are only 3 yielded members at failure in Simulation 204.

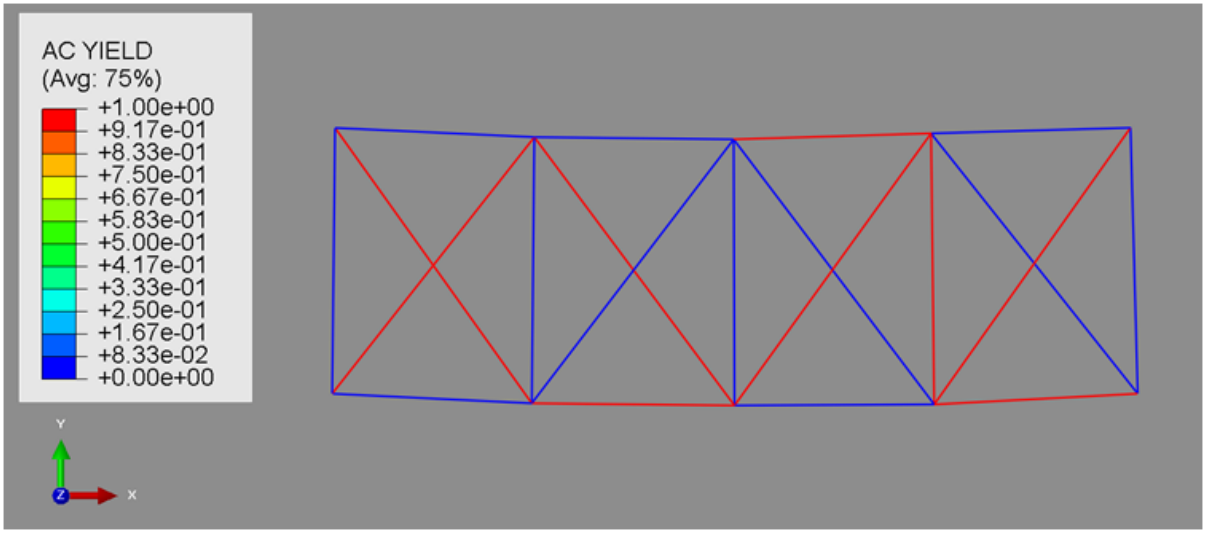

Figure 5-21: Configuration C (Simulation 213)

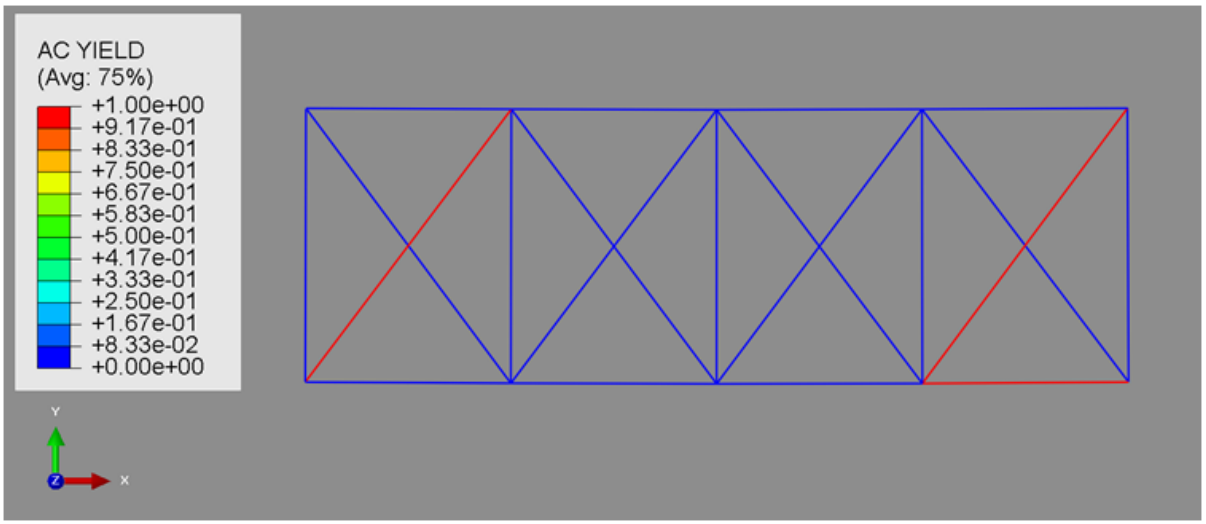

Figure 5-22: Configuration C (Simulation 204)

Table 5-10 summarises the simulations with the highest and lowest ductility for configuration C. Clearly, the ductility of the structure is sensitive to relatively small fluctuations in member strength. A similar observation may be made with respect to Configuration D.

Table 5-10: Two Configuration C simulations

Simulation Number	Ultimate Strength (kN)	Ductility (m)	Number of Yielded Members
204	1429.97	0.177	9
213	1319.19	0.046	3

The degree to which the system ductility is a function of the sequence of events leading to failure can be illustrated using a simple example. For each configuration the ductility is determined in three scenarios. Firstly, all members are assigned the lower bound member strength (240 MPa); secondly, all members are assigned the nominal member strength (250 MPa); and lastly, all members are assigned the maximum member strength (260 MPa). The results are presented in Table 5-11. The results show that increasing the strength of all members has negligible effect on the ductility. This is due to the fact that although increasing (or decreasing) the strengths of all members will change the ultimate strength of a structure; it will not significantly impact the ductility as the failure path will remain unchanged.

Table 5-11: Comparison of maximum and minimum ductility

	Ductility (m)			
Configuration	**A**	**B**	**C**	**D**
MCS Maximum Ductility	0.368	0.142	0.177	0.187
MCS Minimum Ductility	0.126	0.093	0.046	0.047
All members = 240 MPa	0.330	0.096	0.029	0.084
All members = 250 MPa	0.330	0.096	0.029	0.086
All members = 260 MPa	0.331	0.097	0.030	0.082

5.8 RESULTS FROM THE RESIDUAL STRUCTURE AND DISCUSSION

Section 5.7 has presented the case for the sensitivity of an intact structural state to variations in structural parameters. However, the variability in structural performance which might arise in a damaged structure is also of great importance; particularly in the case of damaged structures which exhibit increased sensitivity to uncertainties. The effect of member strength on the structural robustness will be investigated using Configuration C.

Chapter 4 presented four indices for a comprehensive quantification of robustness. In the context of member strength variations, the elastic stiffness does not change is therefore omitted from the following discussion. Changes in yield strength are a direct result of member strength variations, rather than any system change such as a deviation in the sequence of events leading to collapse. Therefore, for the sake of clarity, and consistency with Section 5.7, the yield strength is also omitted from the following discussion. Therefore, the robustness will be quantified using two indices; the residual strength index (Equation 5.1) and a ductility index (Equation 5.2) as presented in Section 4.2.

$$C_{u,f,i} = 1 - \frac{f_{u,i}}{f_{u,o}} \quad \textbf{5.1}$$

$$C_{u,d,i} = 1 - \frac{d_{u,i}}{d_{u,o}} \quad \textbf{5.2}$$

The structure is symmetrical. Therefore, only Members 1 to 11 are removed from the structure. The ultimate strength and ductility of each structural state are reported in Table 5-12. Figure 5-23 illustrates the load-displacement relationship for each residual structure. Evidently there is significant variation in the respective damaged states. Damage states 1 and 11 are the least critical. In contrast, damage states 7 and 10 exhibit a large reduction in ultimate strength.

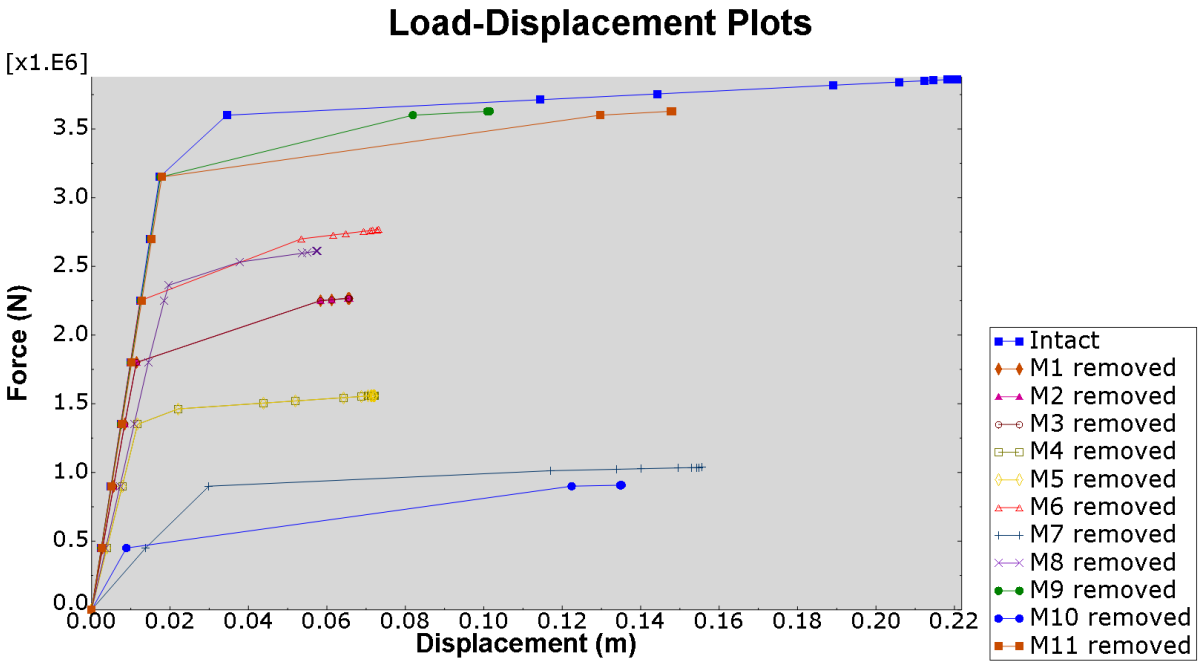

Figure 5-23: Load-displacement relationships for each residual structure

The load-displacement data is summarised in Table 5-12 in terms of the ultimate strength and ductility for each damage state.

Table 5-12: Ultimate strength and ductility of the intact structure and each residual state

Structural State	Ultimate Strength (kN)	Ductility (m)
Intact	3862.92	0.221
1	2268.65	0.066
2	2268.65	0.066
3	2268.65	0.066
4	1559.67	0.072
5	1559.67	0.072
6	2767.97	0.073
7	1036.88	0.156
8	2611.10	0.058
9	3629.15	0.102
10	907.29	0.135
11	3629.15	0.148

Table 5-13 presents the nominal indices for the ultimate strength and the ductility of each damaged state which are determined using Equation 5.1and 5.2.

Table 5-13: Ultimate strength and ductility indices

Structural State	Residual strength index	Ductility index
1	0.413	0.702
2	0.413	0.702
3	0.413	0.702
4	0.596	0.673
5	0.596	0.673
6	0.283	0.668
7	0.732	0.295
8	0.324	0.739
9	0.061	0.540
10	0.765	0.388
11	0.061	0.329

The next step is to investigate the effect of the member strength variability of each damaged state. Each member is removed from the structure and the residual state is analysed. Similarly to the intact state, a member strength variation of +/- 10 MPa is assumed. 500 simulations are carried out for each damage state.

The ultimate strength results are presented in Table 5-14. The results indicate that the degree of variation in ultimate strength is relatively consistent irrespective of which member is removed from the structure. The largest degree of variation in terms of the percentage difference between the maximum and minimum value, is damage state 9 with a percentage difference of 7.363%.

The COV of the intact structure is equal to 0.01 (see Table 5-8). The results in Table 5-14 show that the ultimate strength COV is greater than the intact structure for all damage states. This illustrates that the residual structures are more sensitive to uncertainties that the intact structure.

Table 5-14: Ultimate strength variation

Structural State	Minimum Strength (kN)	Maximum Strength (kN)	% Difference	COV
1	2189	2351	7.156	0.014
2	2198	2324	5.586	0.013
3	2189	2351	7.156	0.014
4	1504	1615	7.118	0.020
5	1502	1617	7.361	0.021
6	2670	2858	6.789	0.016
7	999	1075	7.355	0.022
8	2519	2683	6.297	0.016
9	3495	3762	7.363	0.019
10	874	940	7.307	0.021
11	3522	3728	5.685	0.014

In contrast, as indicated in Table 5-15, the variation in ductility is substantially different among the difference damage states. In terms of percentage difference, the damage state with the lowest variation is damage state 4, whereas the damage state with the highest variation is damage state 9. The COV for the intact structure is 0.157. In general the COV for the various damage states is substantially lower than the COV for the intact structure. This can be attributed to the fact that, in some cases, the initial damage causes the structural response to become more localised. Consequently the subsequent failure sequence is less susceptible to minor structural variations. On the other hand, the COV for damage state 9 is much higher than the intact structure, indicating that this damage state is particularly sensitive to member strength variation.

Table 5-15: Ductility variation

Structural State	Minimum Ductility (m)	Maximum Ductility (m)	% Difference	COV
1	0.070	0.043	47.978	0.099
2	0.070	0.040	53.949	0.104
3	0.070	0.043	47.978	0.099
4	0.073	0.072	1.356	0.004
5	0.073	0.072	1.428	0.004
6	0.074	0.073	1.545	0.005
7	0.158	0.153	3.464	0.010
8	0.067	0.057	16.238	0.024
9	0.187	0.078	82.060	0.238
10	0.136	0.133	2.337	0.003
11	0.189	0.137	32.041	0.078

The upper and lower strength and ductility bounds are used to determine indices for each damage state. For clarity, it is assumed that intact state is deterministic; the nominal intact ultimate strength and ductility values are used, as reported in Table 5-12. The ductility and strength indices are presented in Table 5-16. The results show that, particularly in the case of ductility, minor changes in parameter such as member strength may substantially change the quantification results. This is particularly evident for damage states 1, 2, 3 and 9.

Table 5-16: Residual strength indices

Structural State	Strength Indices		Ductility Indices	
	Minimum	Maximum	Minimum	Maximum
1	0.391	0.433	0.682	0.805
2	0.398	0.431	0.683	0.818
3	0.391	0.433	0.682	0.805
4	0.582	0.611	0.671	0.675
5	0.581	0.611	0.671	0.676
6	0.260	0.309	0.666	0.671
7	0.722	0.741	0.282	0.307
8	0.305	0.348	0.696	0.742
9	0.026	0.095	0.154	0.646
10	0.757	0.774	0.385	0.399
11	0.035	0.088	0.142	0.379

CONCLUSIONS

This chapter has illustrated the importance of structural uncertainties when quantifying the robustness of a structure. Two levels of uncertainty were investigated; a normal distribution and uniform distribution with +/- 10 MPa. The results show that variations in member strength may significantly affect the strength and in particular the ductility of a structure. The sensitivity of the ductility to structural uncertainties can be attributed to changes in the sequences of events leading to failure, which can substantially alter the global energy absorption capacity.

The impact of structural uncertainties is relevant to both the analysis of an intact structure and a post-damage residual structure. In some circumstances a residual structure may exhibit greater sensitivity to uncertainties when compared to the intact state. Such differences are

likely to be dependent on the particular damage event and also the structure. The degree of sensitivity is highly dependent on the structural configuration. This is primarily due to the fact the relative stress levels in the members of each configuration affects the number of members which develop plasticity prior to structural collapse.

A MCS may be used to investigate the effect of structural uncertainties on the quantification of robustness. In present study, 500 simulations were used for each analysis. The main disadvantage of this approach is the significant computational requirements. The computational demands are particularly onerous for robustness assessment in which many residual structural states must be simulated.

It should also be noted that for simplicity, without losing generality, the investigation on the variability of the overall structural behaviour in this chapter has been limited to the variation in the yield strength of individual members and the structural failure is defined in a simplified manner as the first member failure with a single failure strain criterion (2%). In a more comprehensive robustness analysis the entire failure process beyond the first failure of a member will generally be required, and furthermore the failure criterion of individual members itself would be a major source of uncertainty. With the consideration of these factors the demand on a full FE-based probabilistic simulation would be increased exponentially and becomes prohibitive considering also the numerical instability problem which could be involved in a computation into descending phase of the structure.

All the above reasons call upon the development of a simplified technique which would allow application in general practice and yet is capable of incorporating possible variabilities in the failure sequences. This is a topic which will be discussed in the next chapter.

6 AN INCREMENTAL ELASTIC ANALYSIS METHOD FOR STRUCTURAL REDUNDANCY EVALUATION

6.1 INTRODUCTION

Chapter 5 discussed the sensitivity of robustness measures to structural uncertainties using Monte Carlo simulations. Two robustness measures were considered; the residual strength factor and a ductility index. It was demonstrated that both strength and ductility are sensitive to variations in member strength. In particular the ductility of a structure is sensitive to relatively minor variations in member strength, such as +/- 10 MPa, which alter the sequences of events leading to collapse.

Structural robustness is typically evaluated using a direct FE analysis. In the simplest case, a linear elastic analysis may be used to analyse a structure. Although linear elastic analysis is attractive due its computational simplicity, it is not a useful method to analyse collapse sequences in a structure as key collapse resisting mechanisms such as the development of plasticity and force redistribution among members cannot be captured. It may however be relatively more useful in the case of simple structure, in which the nonlinear response may be intuitively predicted (Marjanishvili *et al.* 2006).

On the other hand, nonlinear FE analysis facilitates a complete analysis of collapse sequences in structures, and the possibility to quantify the capacity of a structure to survive a damage event through the development of alternative load paths. A notable feature of a deterministic nonlinear FE analysis approach is that it generates a unique failure sequence. If the intact structure or any particular damaged condition is pushed to collapse, the sequences of events

leading to failure will be unique. However, as illustrated in Chapter 4, structural uncertainties may lead to alternative sequences of events. At any given event in a failure sequence, branching paths, which represent alternative damage sequences, may exist.

As demonstrated in Chapter 5, the sensitivity of robustness to uncertainties can be investigated using Monte Carlo simulations. The primary disadvantage of this approach is the significant computation time required to analyse the intact structure and moreover the time required to simulate each residual structure. Additionally, an analysis of the full-load displacement relationship may encounter convergence difficulties in the case of member failure events.

An incremental elastic analysis (IEA) is proposed herein which facilitates a full non-linear structural analysis using a series of incremental elastic analyses. Using the IEA, the full load-displacement relationship may be determined, in addition to all parameters of interest such as the elastic stiffness, yield strength, ultimate strength, ductility and strain energy absorption. Additionally, by virtue of the incremental nature of the analysis, alternative events may be considered at each increment. Therefore, if there are a number of potential events, each event may be substituted into the analysis, thereby enabling an analysis of the new divergent failure paths. By considering the most critical and least critical events at each increment it is possible to efficiently identify the potential upper and lower ultimate strength and ductility bounds. This negates to the need to resort to a computationally expensive MCS for this purpose.

As a matter of fact, some sort of randomly generated structural properties will be needed to cover the above mentioned branching or alternative sequences for a general nonlinear FE approach, which also implies a need of a large number of analysis runs and hence high

computational cost. With the proposed incremental analysis method, the alternative sequences may be treated in a considerably simplified manner, albeit with similar outcome.

6.2 OUTLINE OF PROPOSED METHODOLOGY

The key features of typical FE nonlinear analysis and the proposed incremental elastic method are summarised below.

Features of nonlinear FEA:

- The complete force - defection relationship can be determined; including the elastic behaviour, subsequent plastic deformation and ultimate collapse
- Implicit static analysis can require significant computation time and suffer from convergence problems. Convergence problems arise in particular due to sudden changes in the structure such as the failure of a member
- Each analysis generates a unique failure sequence
- Each sequence is the natural failure sequence for the structural state being analysed

Proposed incremental analysis

- Failure sequences are the natural failure sequences for any given structural state
- For any particular structural state, several alternative sequences may be considered. Such sequences will have a similar probability of occurrence

- Methodology can be implemented using a series of incremental elastic analyses. This will have significant benefits in terms of computation time

- The method will not suffer from convergence problems which arise due to discontinuous events such as member failure

One of the key advantages of the proposed method is that the full load displacement relationship up to the point where the structural resistance has been completely exhausted may be determined using a series of incremental elastic analyses. Each increment in the procedure is projection of the structural behaviour from one point in the failure evolution, such as member yielding, to another point in the evolution such as member failure.

The structure can be analysed under any relevant loading combination such as dead load and live load, design load or normal service load. Each stage of the analysis uses the same loading conditions. A nominal service load, $\bar{F}$, is applied to the structure at each stage of the analysis. In the event that the structure has zero stiffness, a displacement controlled incremental analysis will be carried out.

The primary measures of interest are the member strain, member stress and the nodal displacement. The strain energy is also of interest, in particular from the point of view of using the analysis for a subsequent assessment of robustness. The strain energy may be tracked and continuously updated or determined using the final load-displacement relationship.

6.3 IEA METHODOLOGY AND DEVELOPMENT OF ANALYSIS PROCEDURE

6.3.1 General Method and Phase 1 Analysis: Identification of Yielding State

The incremental elastic analysis begins with a given initial (intact or altered) state of the structure under a nominal service load. The service load is applied to the structure and the stress, strain and nodal displacements are determined. These values are recorded. It is assumed that the initial structure remains linear elastic under the service load. Once the response of the structure under service load has been determined, the next step is to project the response to the first event in the failure path. The primary events in the failure path are member yielding and member failure, however other events such as unloading of a yielded member must be also considered.

Before the first event in the failure sequence, the structure remains linear elastic. Therefore, the stress, strain and nodal displacements will also increase linearly until an event such as member yielding or member failure occurs. For clarity, it is initially assumed that the first event in the sequence is the yielding of a member.

A scaling factor may be determined for each member in the structure. This is a factor by which each member may be scaled in order to project it to the first yield.

The scaling factor can be determined using member stress or member strain. If however, the material properties for a member are perfectly plastic, the strain must be used after yielding has taken place. Firstly the scaling factor is determined for each member:

$$\alpha_j^i = \frac{\sigma_{y,j}}{\sigma_j^i} \quad \text{or} \quad \alpha_j^i = \frac{\varepsilon_{y,j}}{\varepsilon_j^i} \tag{6.1}$$

where α_j^i is the scaling factor for member *j* of structural state *i*, σ_y is the yield stress for member *j*, σ_j^i is the stress in member *j*, $\varepsilon_{y,j}^i$ is the yield strain in member *j*, and ε_j^i is the strain in member *j*.

The member scaling factors can also be written more generally as follows;

$$\alpha_j^i = \frac{\sigma_{ne,j}^i}{\sigma_j^i} \quad \text{or} \quad \alpha_j^i = \frac{\varepsilon_{ne,j}^i}{\varepsilon_j^i}, \quad for\ j = 1, 2, ..., n \tag{6.2}$$

where the subscript *ne* refers to the next event in the failure evolution where event is defined as yielding, failure, member unloading and so on.

The scaling factor for each incremental stage in the analysis is simply the minimum member scaling factor:

$$\alpha^i = \min\left(\alpha_j^i\right), \quad for\ j = 1, 2, ..., n \tag{6.3}$$

α^i is denoted by superscript *i*, as the minimum scaling factor relates to the overall structural state, rather than a particular member.

The member stress, strain, nodal displacements, global applied load and so on are scaled using the minimum scaling factor, α^i. The stress in each member is scaled as follows:

$$\text{scaled member stress} = \sigma_j^i \times \alpha^i, \quad \text{for j=1,2,.....,n} \qquad \textbf{6.4}$$

For clarity, the initial structure will be denoted by the superscript *o*, and the first event is assumed to be member yielding. Therefore, in the case where the intact structure is being projected to first yield:

$$\sigma_j^{y,o} = \sigma_j^{\bar{F},o} \times \alpha^o \qquad \textbf{6.5}$$

where $\sigma_j^{y,o}$ is the stress in member *j* when first yielding occurs in the intact structure, $\sigma_j^{\bar{F},o}$ is the stress in member *j* of the intact structure under service load $\bar{F}$, and α^o is the scaling factor for the initial structure. The stress, member forces and so on are recorded for each member when first yielding of the initial structure occurs.

In addition to the stress, strain and nodal displacements, the global applied load is also scaled by the factor α^o:

$$F^{y,o} = \bar{F} \times \alpha^o \qquad \textbf{6.6}$$

$F^{y,o}$ is the global applied load at first yield in the initial structure and $\bar{F}$ is the service load. This is illustrated in Figure 6-1.

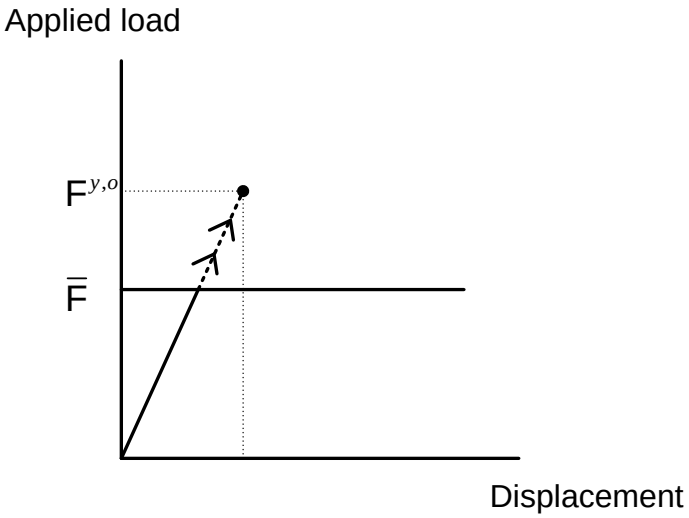

Figure 6-1: Scaled global structural response

A simple notional example is used to illustrate the scaling factor. A service load is applied to a structure. In the first example, the stress in each member is less than the yield stress (250 MPa). Therefore, in order to project to the first yielding, the member stresses are scaled up. The scaling factor, α_j, and the minimum scaling factor, α^o, are determined for each member.

Table 6-1: Scaling up the member forces

Member	Member stress under service load	Scaling procedure			Scaled stress values
	$\sigma_j^{\bar{F},o}$ **(MPa)**	α_j	α^o **= min(** α_j^o **)**	**Member Scaling**	$\sigma_j^{y,o}$ **(N/m^2)**
1	200	1.25	1.25	200 x 1.25	250
2	150	1.67		150 x 1.25	188
3	100	2.50		100 x 1.25	150

It is also possible that member stresses under service load may exceed the yield stress. In this case, the member forces will be scaled back to the point of first yielding. Similarly, the minimum scaling factor is used.

Table 6-2: Scaling down the member forces

Member	$\sigma_j^{\bar{F},o}$ **(MPa)**	α_j	α^o **= min(** α_j^o **)**	**Member Scaling**	$\sigma_j^{y,o}$ **(MPa)**
1	280	0.89	0.89	280 x 0.89	250
2	240	1.04		240 x 0.89	214
3	280	1.14		220 x 0.89	196

At each stage of the analysis, the total strain energy in the structure may also be tracked and recorded. This is equal to the area under the load displacement curve (Figure 6-2). The total strain energy under service load is:

$$\frac{1}{2} \times \bar{F} \times d^{o} \qquad \textbf{6.7}$$

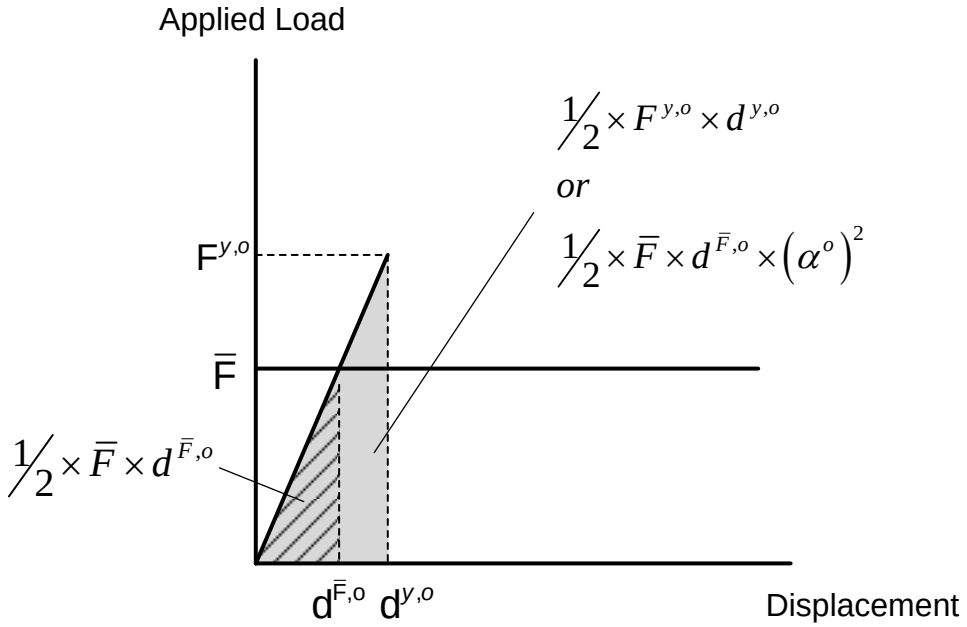

Figure 6-2: Strain energy

The total strain energy at first yield can be determined using the square of the scaling factor $(\alpha^{i})^{2}$, or simply using the global applied force at first member yield:

$$U^{y,o} = \frac{1}{2} \times \bar{F} \times d^{\bar{F},o} \times (\alpha^{o})^{2} \quad \text{or} \quad U^{y,o} = \frac{1}{2} \times F^{y,o} \times d^{y,o} \qquad \textbf{6.8}$$

where $U^{y,o}$ is the strain energy at first yielding of the intact structure, $d^{\bar{F},o}$ is the displacement under service load in the intact structure, $F^{y,o}$ is the global applied load at first yield of the intact structure and so on.

The key parameters which are recorded and then scaled are summarised below:

- Stress: $\sigma_{j}^{y,o} = \sigma_{j}^{\bar{F},o} \times \alpha^{o}$

- Strain: $\varepsilon_j^{y,o} = \varepsilon_j^{\bar{F},o} \times \alpha^o$

- Nodal Displacement: $\delta_n^{y,o} = \delta_n^{\bar{F},o} \times \alpha^o$

- Global Displacement: $d^{y,o} = d^{\bar{F},o} \times \alpha^0$

- Applied Load: $F^{y,o} = \bar{F} \times \alpha^o$

- Strain Energy: $U^{y,o} = U^{y,o} = 1/2 \times \bar{F} \times d^{\bar{F},o} \times \left(\alpha^o\right)^2$

At this point, all relevant aspects of the structural response at yielding of the first member have been determined. The next step is to perform an incremental analysis to determine the structural behaviour following yielding of the first member.

6.3.2 Post-yielding Phases until Member Failure

Different post yield material behaviour may be considered. The simplest case is that of a perfectly plastic material such as illustrated in Figure 6-3. For perfectly plastic material behaviour, a member has zero stiffness after yielding; however, it continues to contribute with its yielding capacity to the overall structural resistance until ultimate failure of the member occurs. The tangent stiffness of the structure following first yield is therefore equal to the stiffness of the structure when the member is completely removed. Therefore, the incremental analysis is implemented without the yielded member.

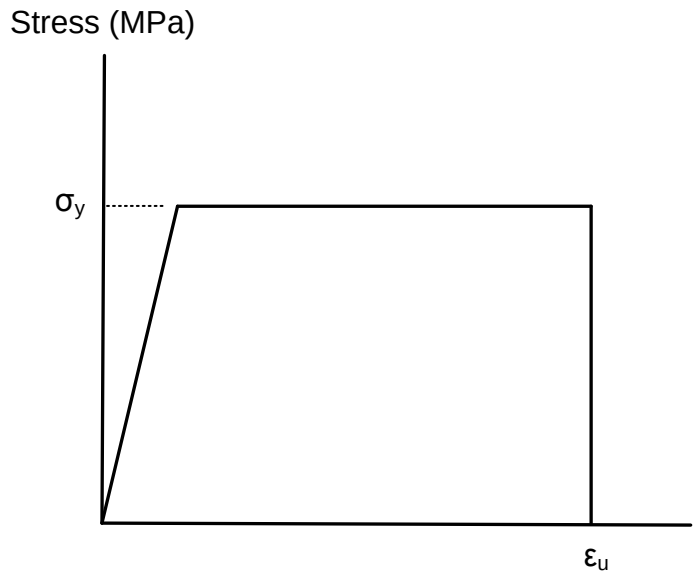

Figure 6-3: Perfectly plastic material behaviour

Alternatively, a member may have positive tangential stiffness (E_p), such as depicted in Figure 6-4. In this situation, the yielded member continues to contribute to the global stiffness of the structure. Therefore, rather than removing the member of the structure, for the purposes of the incremental analysis, the stiffness of the member is reduced to the tangential stiffness, E_p.

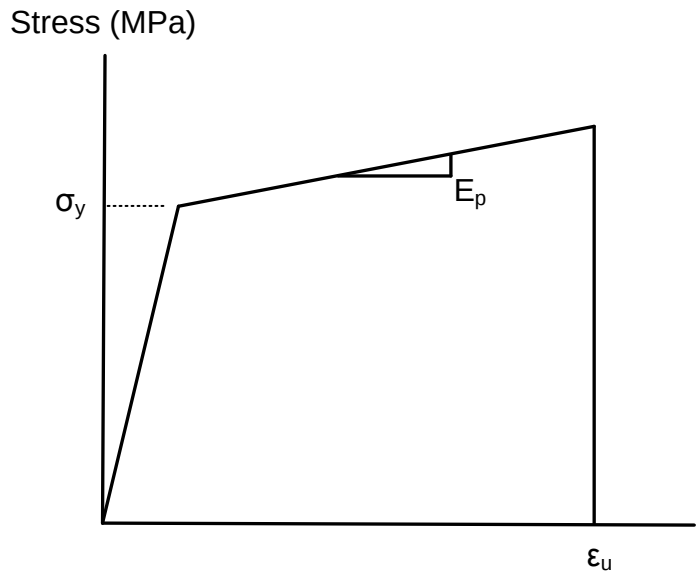

Figure 6-4: Positive post-yield stiffness

Given that the state of the structure at first yield is known, it is possible to determine the behaviour of the structure following first yield using an incremental elastic analysis. The general principle is illustrated below. The incremental analysis is carried out by removing the yielded member from the structure (or adjusting the stiffness) and analysing the residual state. The member forces, nodal displacements, and so on which are determined by the incremental analysis are recorded.

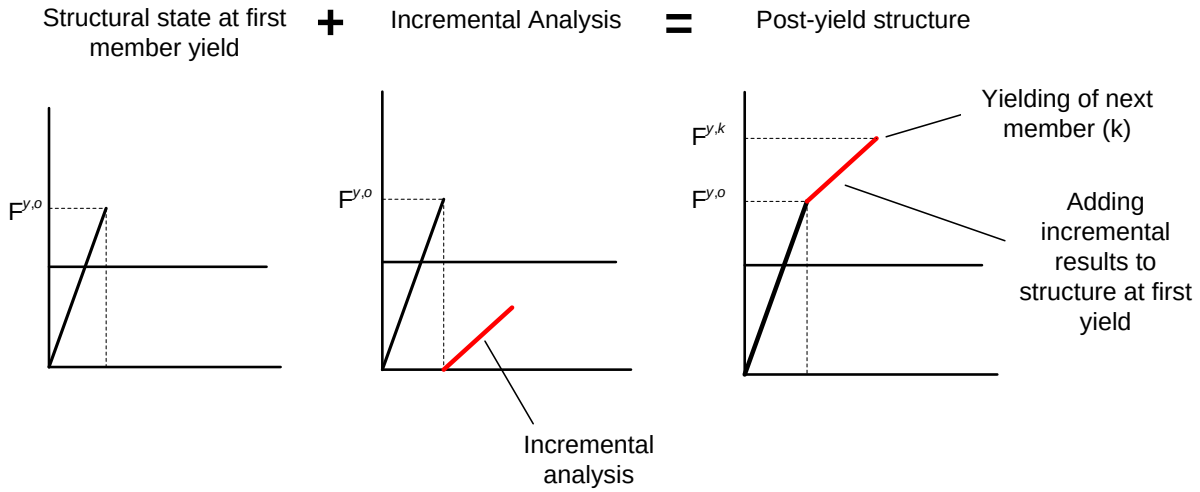

Figure 6-5: Addition of incremental behaviour

To implement the incremental analysis, the state of the *k-th* member is updated (removed or with reduced stiffness) and the service load, $\overline{F}$, is applied. As illustrated in Figure 6-6, the tangential stiffness of the structure following yielding of the first member is equal to the stiffness of the incremental structure with the updated member behaviour; $K^k = K^{\Delta k}$, where the superscript ΔK denotes the incremental structural state K.

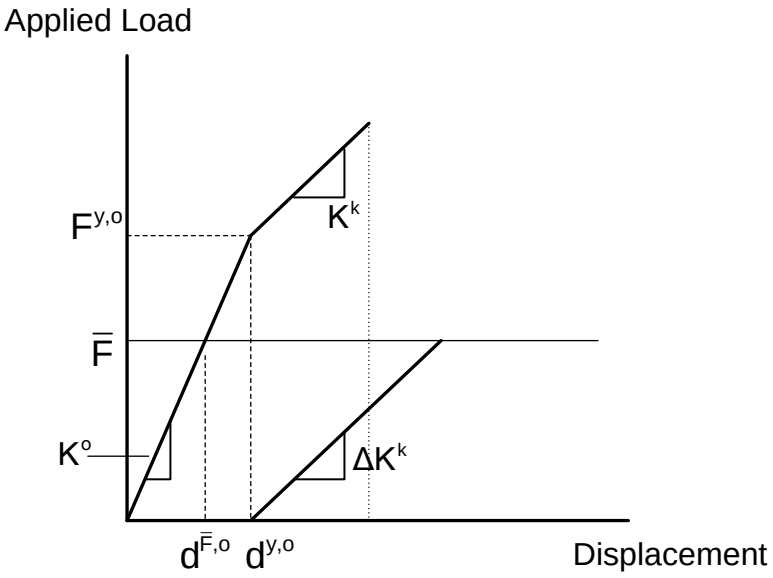

Figure 6-6: Tangential stiffness

The incremental analysis is carried out using an elastic analysis. This enables the member forces, displacements etc. to be determined under service load. The next step is to determine a new scaling factor which will project the structure to the next event. The scaling factor for the elastic members will be determined with respect to yielding, and the scaling factor for the yielded member will be determined with respect to member failure.

All parameters at the first yield of the initial structure, $\sigma_j^{y,o}$, have been recorded and are treated as a constant. As presented in Equation 6.9, in the case of the incremental analysis, the scaling factor will be applied to incremental parameters, e.g. $\sigma_j^{\Delta k}$. The equation for the elastic members is as follows:

$$\sigma_{y,j} = \sigma_j^{y,o} + \alpha_j^k \sigma_j^{\Delta k} \quad \textbf{6.9}$$

where $\sigma_{y,j}$ is the yield stress in member *j*, $\sigma_j^{y,o}$ is the stress in member *j* at the first yield of the intact structure, α_j^k is the member scaling factor for the incremental stress $\sigma_j^{\Delta k}$, following the removal of member *k*.

Thus the scaling factor for each member is as follows:

$$\alpha_j^k = \frac{\sigma_{y,j} - \sigma_j^{y,o}}{\sigma_j^{\Delta k}} \quad \textbf{6.10}$$

The general scaling factor for structural state *k* is simply the minimum scaling factor.

$$\alpha^k = \min\left(\frac{\sigma_{y,j} - \sigma_j^{y,o}}{\sigma_j^{\Delta k}} \right) \quad \textbf{6.11}$$

Similarly, the nodal displacements at yielding of the second member are determined by adding the scaled incremental displacements to the nodal displacements recorded at yielding of the first member.

$$\delta_n^{y,k} = \delta_n^{y,o} + \alpha^k \delta_n^{\Delta k} \quad \textbf{6.12}$$

If, given perfectly plastic material properties, member *k* is removed from the structure before conducting the incremental analysis, the incremental nodal displacements must be used to determine the incremental strain in member *k*.

Irrespective of whether the members are being scaled up or scaled down, each will be multiplied by the scaling factor α^k. If the members are being scaled up, $\alpha^k > 0$, and if the

members are scaled down, $\alpha^k < 0$. Figure 6-7 illustrates the case where member forces are scaled back to the point at which the second member yields.

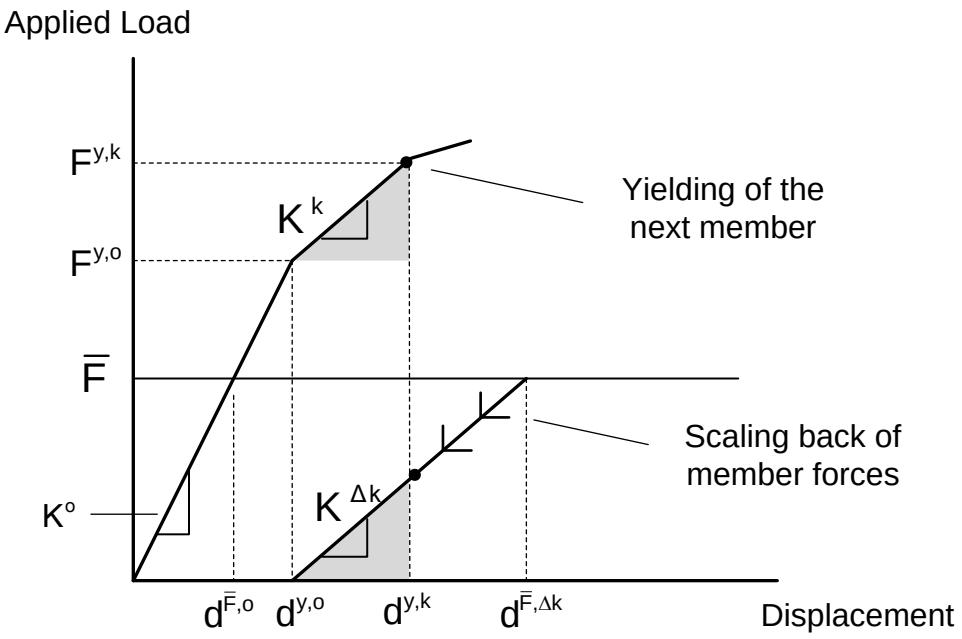

Figure 6-7: Second member yield

The updated strain energy may also be determined. The incremental strain is equal to the shaded area in Figure 6-7. Therefore, the total energy is equal to energy determined in the intact structure at yield plus the incremental energy plus the plastic strain energy identified by the hatched area (see Figure 6-8).

$$U^{y,k} = U^{y,o} + \tfrac{1}{2} \times (d^{\Delta k} - d^{y,o}) \times \bar{F} \times \left(\alpha^k\right)^2 + F^{y,o} \times \left(d^{y,k} - d^{y,o}\right) \qquad \textbf{6.13}$$

The total strain energy in the structure at second member yield is illustrated in Figure 6-8.

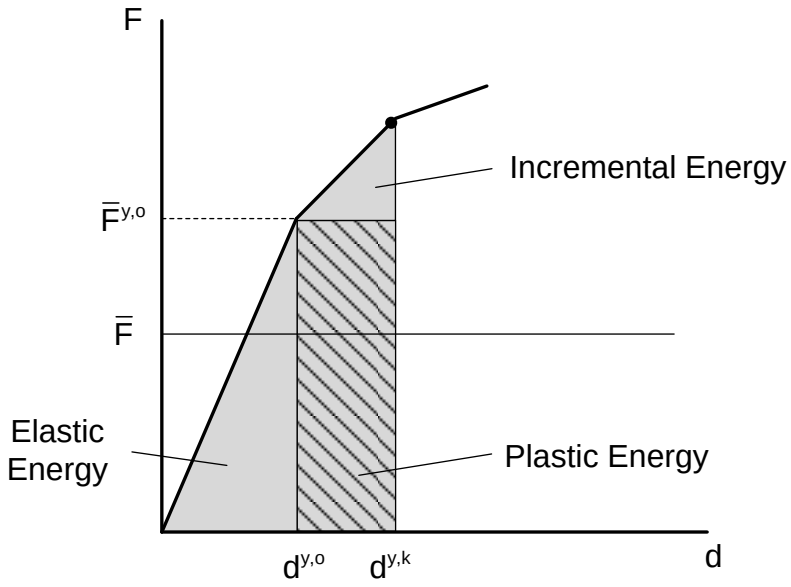

Figure 6-8: Strain energy

As outlined above, successive incremental analyses are used to determine each event in the failure path. As the structure becomes progressively more damaged it is possible that the structure may exhibit zero stiffness, such as illustrated below.

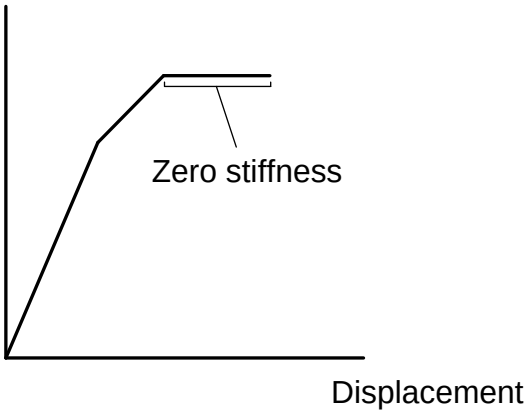

Figure 6-9: Loss of global stiffness

When the global stiffness is zero, the stress and strain will remain static in the elastic members, while the strain in the yielded members will increase. If for example, as illustrated below, members 3 and 5 have yielded, the structure will exhibit zero stiffness.

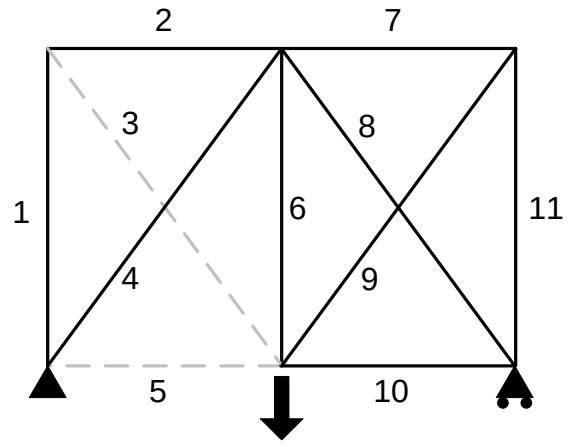

Figure 6-10: Truss with two failed members

An incremental displacement analysis is carried out with both members removed. This is implemented by applying some arbitrary global displacement. Next, a scaling factor is determined for the yielded members. It is only necessary to determine a scaling factor for the

yielded members as denominator of the scaling factor for the elastic members will be equal to zero. The scaling factor is determined as below. In the structure illustrated above, two members have yielded, so the structure has zero stiffness and the next event in the sequence will be the failure of member 3 or member 5. Consequently the scaling factor for members 3 and 5 is determined with respect to the ultimate strain.

$$\alpha^i = \min\left(\frac{\varepsilon_{u,j} - \varepsilon_j}{\varepsilon_j^{\Delta}}\right) \qquad \textbf{6.14}$$

where $\varepsilon_{u,j}$ is the ultimate strain for member *j*, ε_j is the previously recorded strain in member *j* and ε_j^{Δ} is the incremental strain in member *j*.

6.3.3 Member Failure Event

It is assumed that when a member reaches its ultimate strain it undergoes sudden and complete failure. The failure of a member has a number of important structural effects which must be determined; a drop in global resistance, a redistribution of forces in the remaining members of the structure and also a change of the nodal displacements. Two methods by which the state of the structure following the failure of a member may be determined are investigated.

6.3.3.1 Superposition of Failed Member Forces

One method of determining the state of a structure following the failure of a member is to use superposition of the forces present in the failed member prior to failure. The basic idea is similar to the superposition approach, used in URS (2006) and also Goto *et al.* (2011), to

determine dynamically amplified forces in a truss following member failure. The force present in a member at failure will be denoted by $P_{u,j}$, which represents the ultimate axial force present in member *j* in the case of a truss.

As illustrated in Figure 6-11, the structure after member failure (State C) can be determined by combining structural states A and B. This enables the member forces, structural resistance and the nodal displacements in State C to be calculated. The reduction in global resistance is equal to the vertical reaction force in State B.

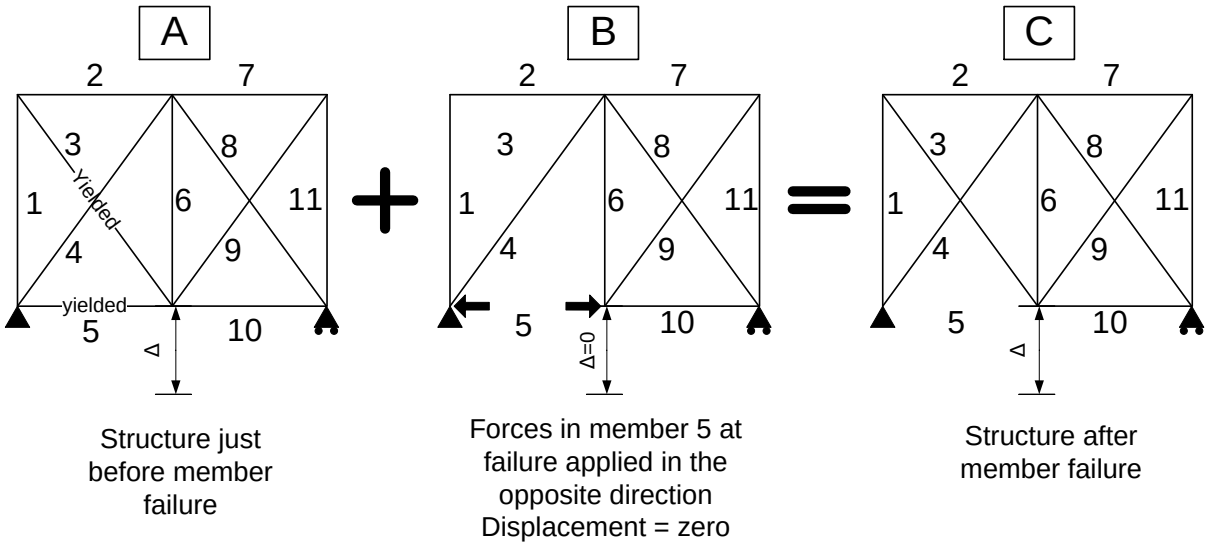

Figure 6-11: Superposition of failed member forces

Points A and C correspond to the example structure illustrated below. Two members yield prior to the member failure event. State A represents the structure just before member failure occurs. State C represents the structure following the failure of member 5. State B involves applying the forces which are present in Member 5 at failure (the yield force) in the opposite direction in order to determine the effect of the member failure in the remaining members of

the structure. Member 5 is in tension prior to failure and so the member forces are applied in the opposite direction. The global displacement at failure of member 5 is denoted by delta.

As shown in the Figure 6-12, the global displacement remains unchanged when member 5 fails. Therefore, as illustrated in Figure 6-11, when applying the failed member forces in the opposite direction, the vertical displacement is restrained. The resulting reaction force is equal to the drop in global resistance.

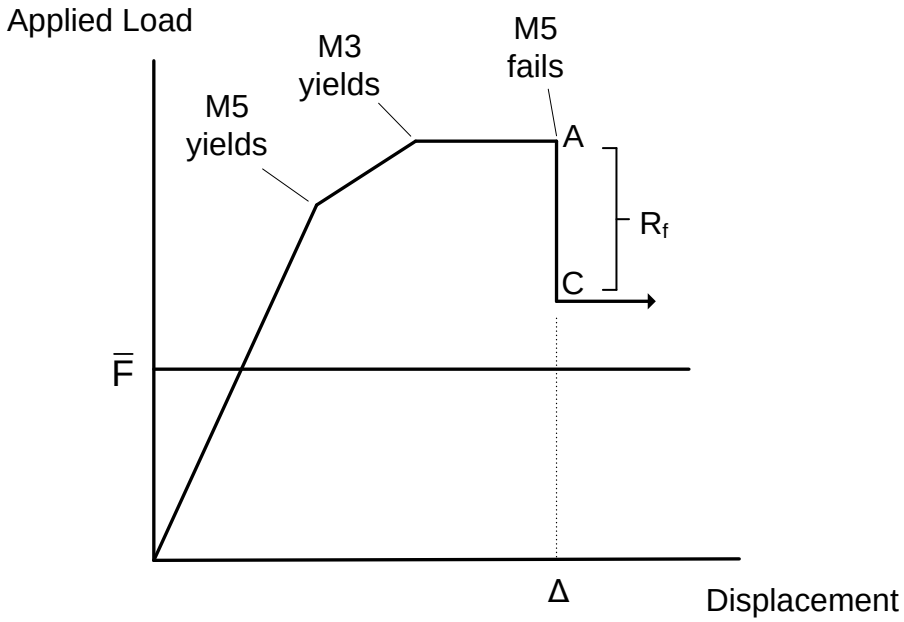

Figure 6-12: Reduction in resistance due to member failure

The first step is to determine how Member 3 is affected by the failure of Member 5. This is particularly important as Member 3 has yielded prior to member failure. Two situations are possible. The first is that failure of member 5 increases the strain in Member 3, which remains yielded. The second possibility is that failure of Member 5 causes Member 3 to unload.

In order to determine the behaviour of Member 3 following the failure of Member 5, an initial analysis is carried out without the member in place. The yield force of Member 5 is applied in the opposite direction and the nodal displacements are used to determine the strain in fictitious Member 3. If the strain indicates that the member remains fully stressed then the analysis is complete. However, if the strain indicates that the member unloads, the member is replaced in the structure and the analysis is implemented with the member in place. Therefore, either case can be easily accommodated.

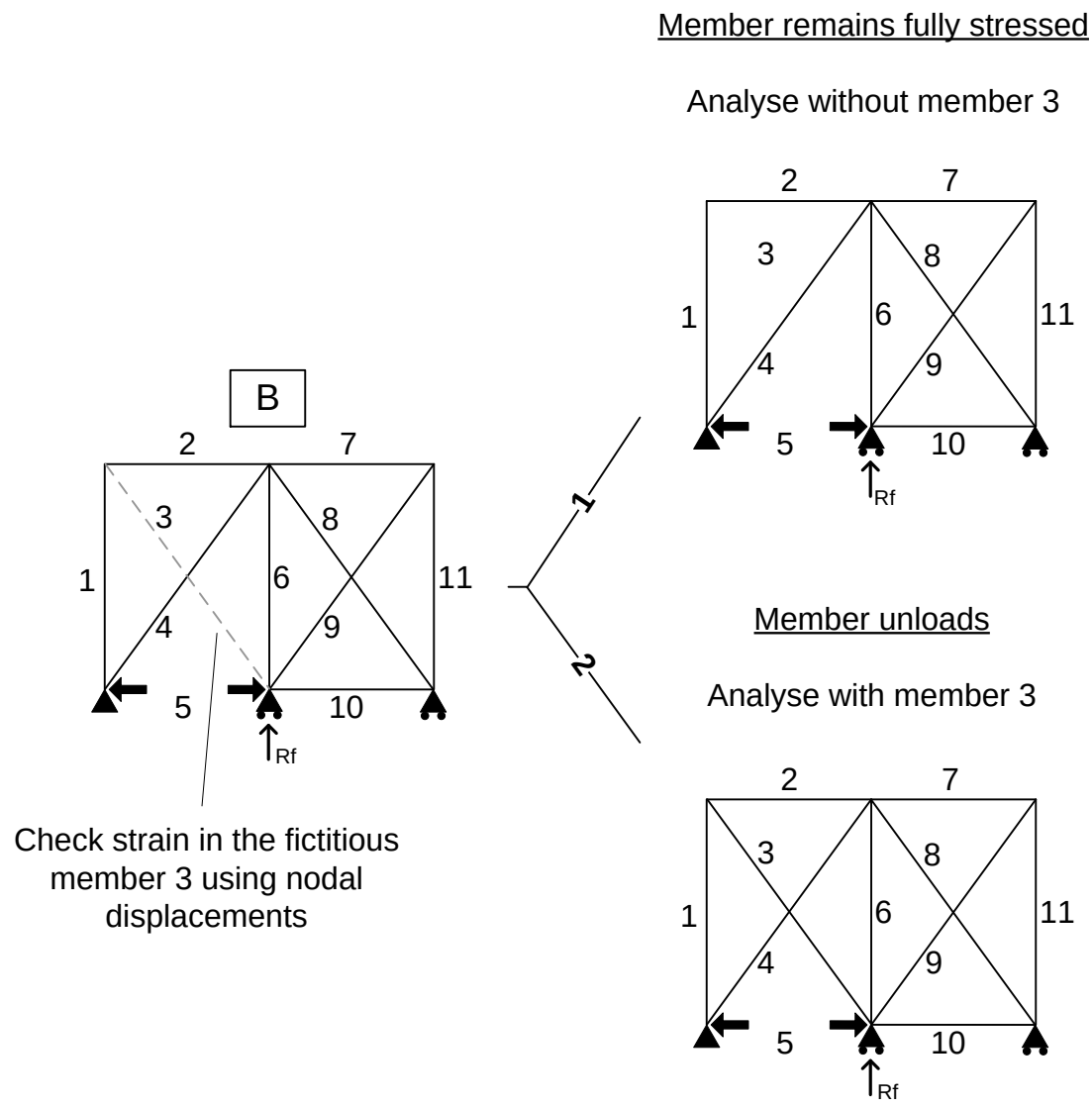

Figure 6-13: Treatment of an unloading member

Additional complications may arise during the superposition step such as when the failure of a member causes other members to yield or other members to fail. Therefore a scaling factor must also be determined for the superposition step. Similarly to the previous incremental analyses the scaling factor is determined with respect to the next event for each member.

$$\alpha^k = \min\left(\frac{\sigma_{y,j} - \sigma_j^{y,o}}{\sigma_j^{\Delta k}}\right) \text{ or, } \alpha^i = \min\left(\frac{\varepsilon_{u,j} - \varepsilon_j^{y,o}}{\varepsilon_j^{\Delta k}}\right)$$

There are two possible outcomes which can be identified using the scaling factor. The maximum value which the scaling factor may take is one, indicating that the superposition step does not cause any additional events:

- If $\alpha^{k} \geq 1$, this means that the full superposition force may be applied without causing additional events. Therefore, the scaling factor is set equal to one and superposition analysis is complete.

- If $\alpha^{k} < 1$, this means that before the full superposition force has been applied, another event has occurred. The structural parameters prior to the new event are recorded and additional steps must be taken into account for the new events.

If the new event is member yielding:

- The force applied at yield is: $P_{u,j} \times \alpha^{k}$. All stress, strain values etc. are recorded.

- The yielded member is removed from the structure.

- The remaining force is applied: $P_{u,j} \times (1-\alpha^{k})$.

- A new scaling factor ($\alpha^{k,2}$) is determined. If $\alpha^{k,2} \geq 1$, the step is complete

If a plastic member unloads, the required steps are the same; however, the unloading member will be replaced in the structure.

If the superposition force causes another member to fail, the procedure is similar:

- The force applied at member failure is: $P_{u,j} \times \alpha^{k}$. All stress, strain values etc. are recorded.

- The failed member, Member k, is removed from the structure.
- The remaining force in Member j, $P_{u,j} \times (1-\alpha^{k})$, and the force in Member k, $P_{u,k}$, are applied simultaneously.
- A new scaling factor is determined. If $\alpha^{k,2} \geq 1$, the step is complete.

The process is outlined in the flow charts which are presented in Section 6.4.

6.3.3.2 Reanalysis without the failed member

Another method to determining the state of the post member failure structure is to reanalyse the structure without the failed member. Similarly, this will enable the member forces, global resistance and nodal displacements to be determined following a member failure event. An alternative example structure is used to illustrate this.

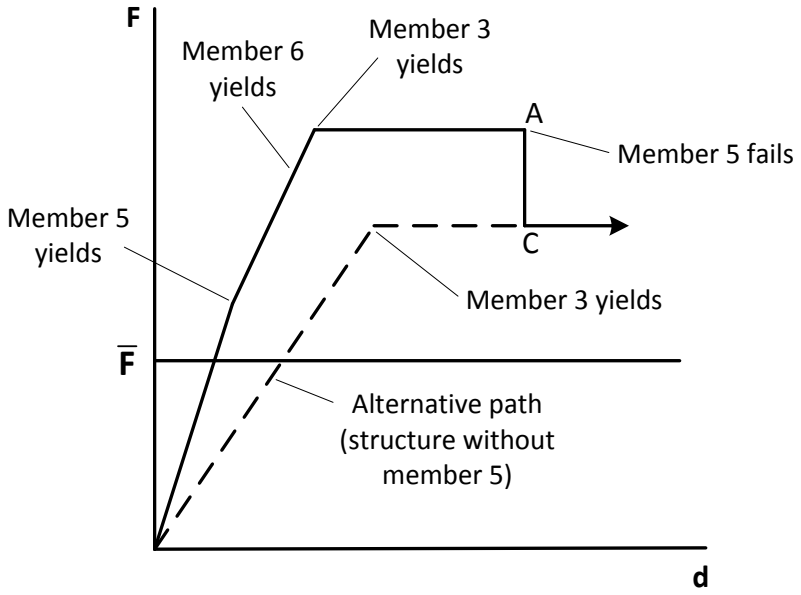

Figure 6-14: Structural reanalysis

An analysis of the residual structure following the removal of Member 5 has already been implemented as part of the initial incremental analysis. The sole difference with this analysis is that in this case the residual structure without Member 5 is projected until yield (in the original analysis the member forces for residual State 5 were added to the intact structure prior to projecting to the next yield event). When yielding of Member 3 occurs, the member is removed from the structure and an incremental displacement analysis is carried out. The displacement is increased until it is equal to the displacement in the original path at the point of member failure.

At this point, the internal member forces in the incremental analysis (dotted line) will be equal to the member forces in the real structure following the failure of Member 5. However, if any yielded member, such as Member 6 in the example above, experiences unloading following a member failure event, the member forces determined by the reanalysis will not agree with those observed in the true structure at Point C. This discrepancy will arise due to

the permanent deformation present in an unloaded member. As the alternative analysis begins with an initially unloaded structure, no permanent deformation will be included.

It is possible however, to tackle the issue of unloading members using this approach. Although the reanalysis does not directly determine the correct post failure member forces when unloading of a member occurs, additional steps may be taken to correct the procedure.

Prior to the failure of member the strain in all members is known. Therefore, the permanent deformation present in a member when it unloads is also known. Using this information it is possible to bridge the gap between the reanalysis without the failed member and the true path by using an incremental approach which incorporates the permanent deformation.

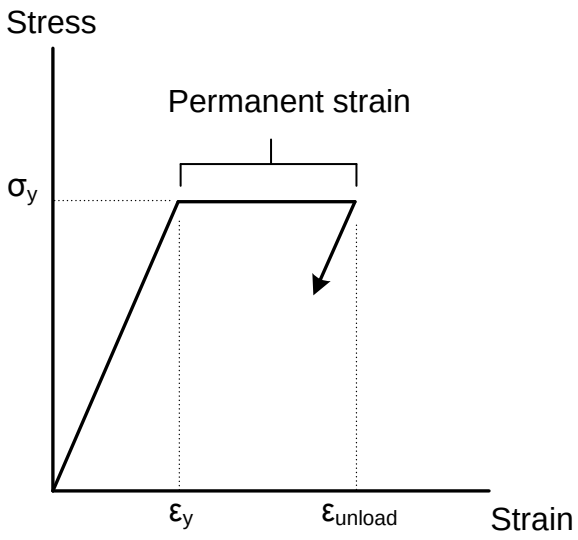

Figure 6-15: Member unloading

It is assumed that prior to the failure of Member 5, Members 5, 6 and 3 have yielded. Moreover the failure of Member 5 causes Member 6 to unload. When Member 6 unloads, it will retain the permanent deformation present at Point A.

The first stage is to analyse the structure without Member 5 and 6. The displacement is increased until the fictitious Member 6 attains a strain equal to the above strain at unloading. The second stage is to replace Member 6 in the structure and apply the service load. The service load is scaled such that the member stresses in Stage 1 plus the member stresses in Stage 2 bring the structure to first yield.

Figure 6-16 illustrates both stages. The goal is to include the effect of the permanent strain which is present in Member 6 following the member failure event, so that the reanalysis correctly determines the member stresses and strains. The first stage includes the permanent strain by removing Member 6 and increasing the displacement until the fictitious member reaches the permanent strain. Stage 2 proceeds with Member 6 in place. Combining the two stages is in effect equivalent to implementing an analysis in which the permanent strain present in Member 6 is included.

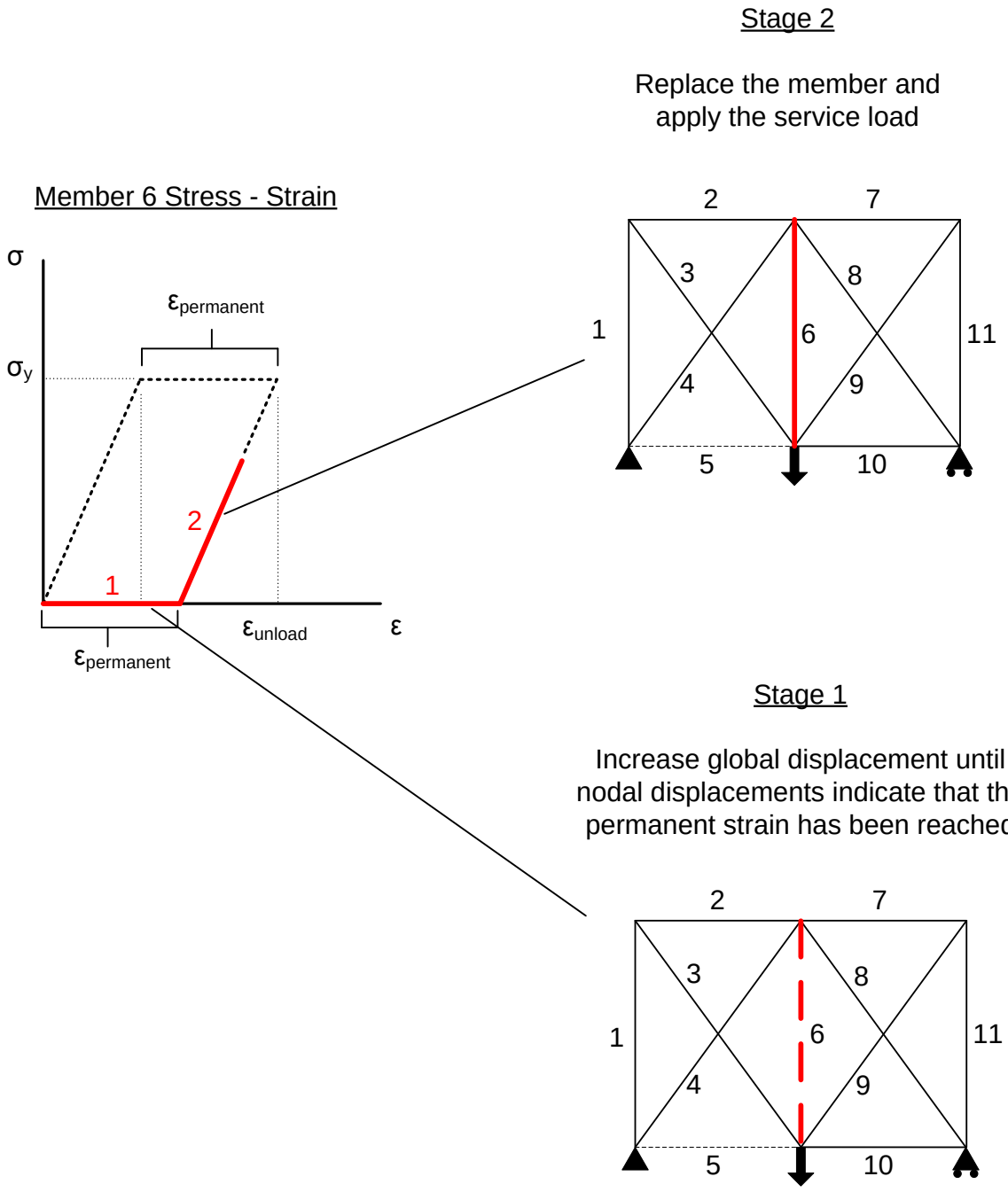

Figure 6-16: Two step incremental procedure

6.4 IEA ANALYSIS FLOW CHARTS

The above described procedure may be summarised in a flow charts as shown in Figure 6-17 to Figure 6-19. The flowcharts outline how the procedure can be automated using Matlab or even a spreadsheet in conjunction with an elastic structural analysis code. A sample excel based incremental elastic analysis step is presented in Appendix C. Figure 6-17 presents the general methodology flowcharts which describes the entire process from beginning to end. Figure 6-18 and Figure 6-19 outline the steps which are specific to member failure events.

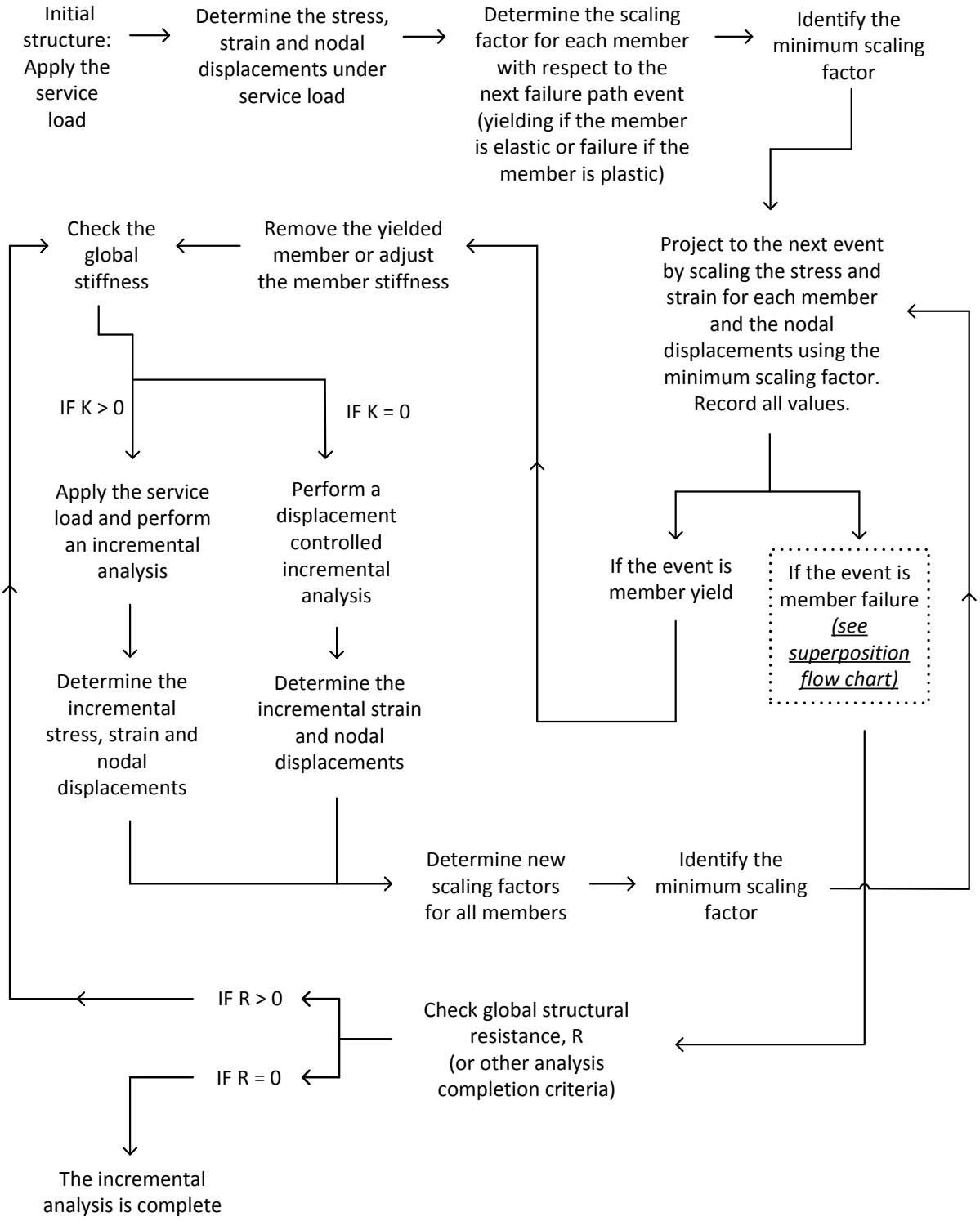

Figure 6-17: General IEA flowchart

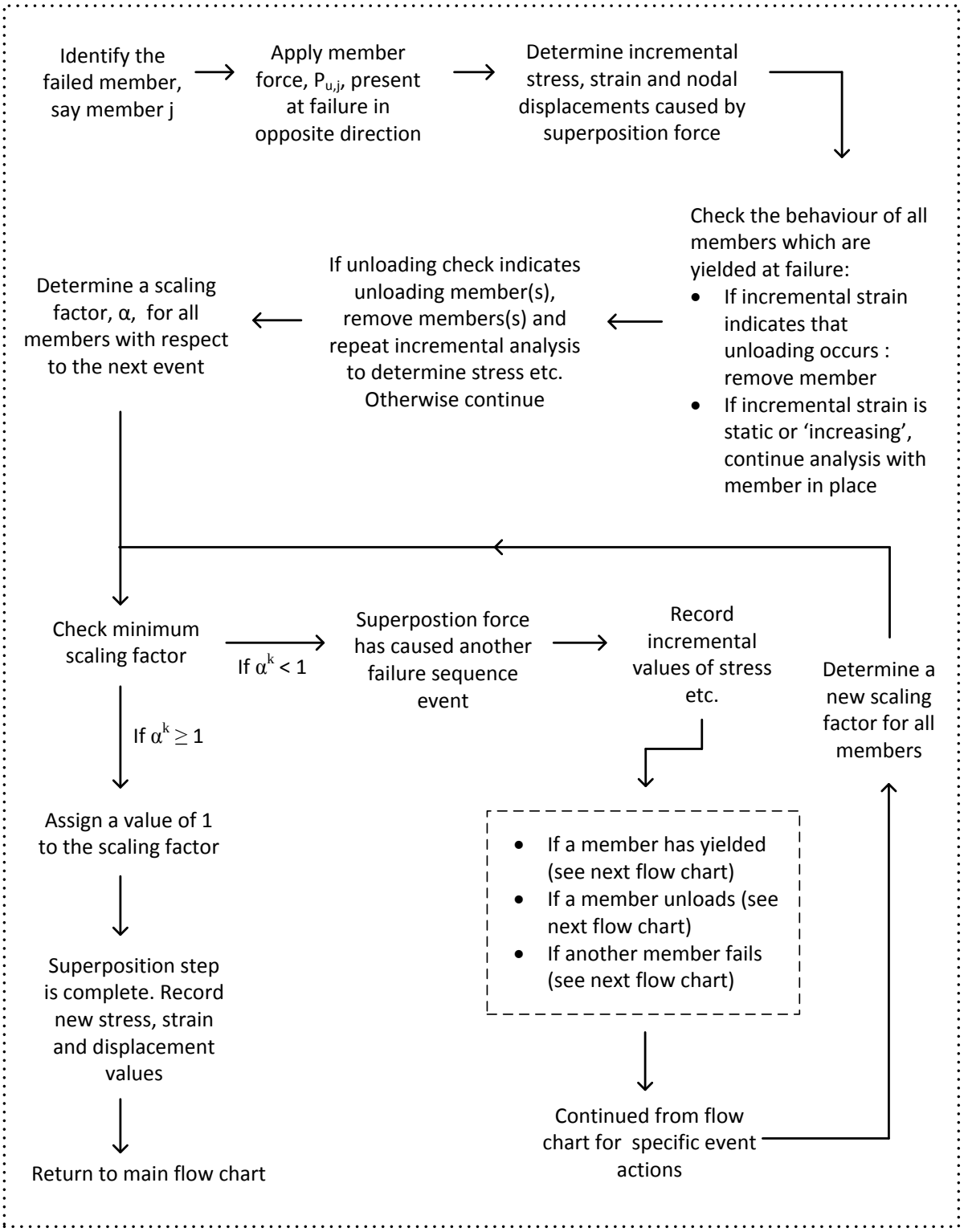

Figure 6-18: Superposition flowchart

Figure 7-2 presents the steps which are required to handle additional events which can be caused by a member failure event; yielding, unloading and the failure of another member.

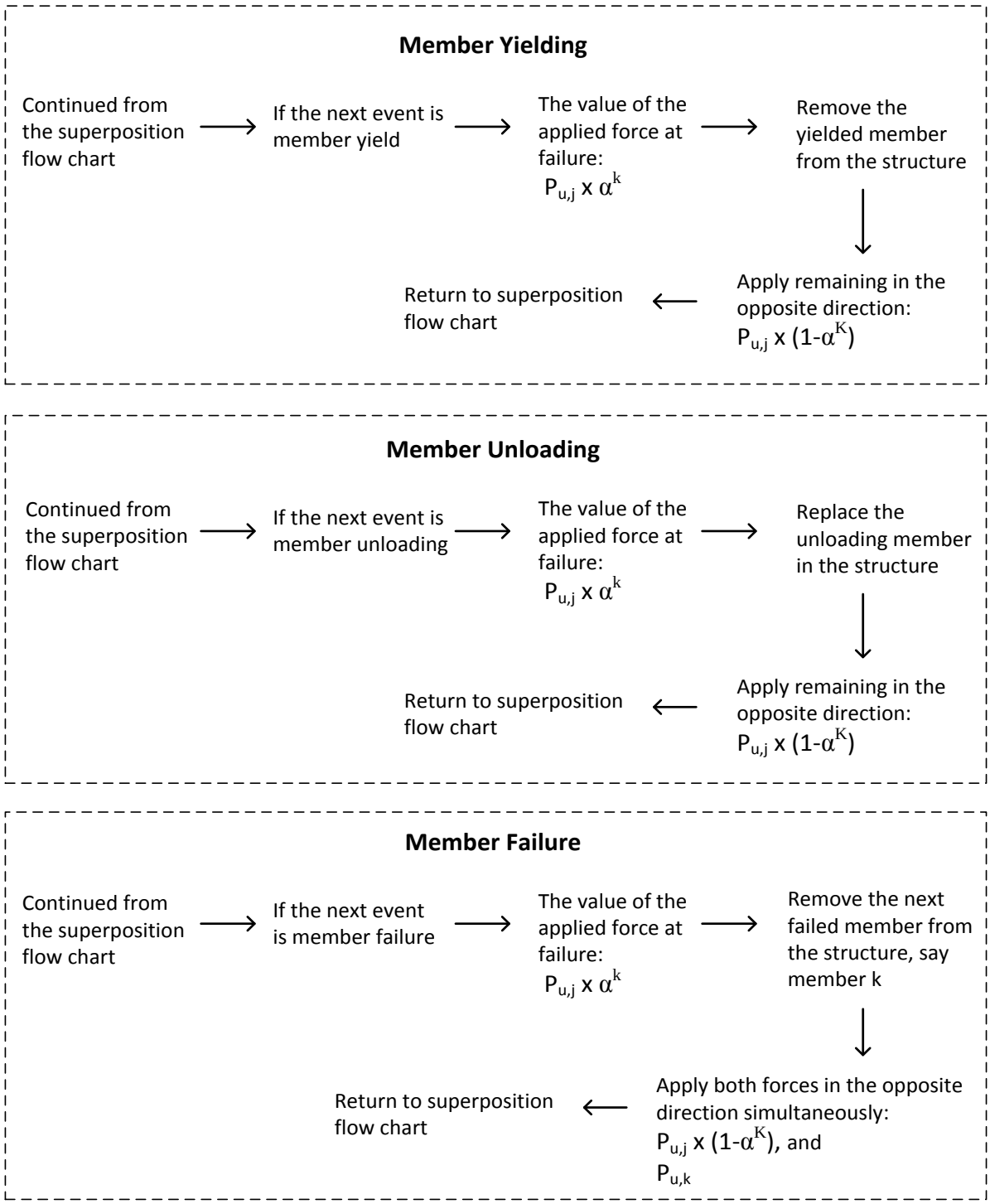

Figure 6-19: Superposition member behaviour flowcharts

7 IEA IMPLEMENTATION EXAMPLES AND APPLICATION TO ALTERNATIVE FAILURE PATHS ANALYSIS

7.1 INTRODUCTION

This chapter illustrates the proposed IEA method using six examples. The examples exhibit increasing complexity. The first example is an analysis of a truss with a single applied load and simple member behaviour; whereas Example 6 has three loading positions and complex member behaviour such as member failure and unloading of yielded members.

In addition to using the method to determine the load-displacement relationship for a structure, the application to an analysis of the alternative paths is also demonstrated. This application is discussed in detail in Section 7.10.

7.2 EXAMPLE 1 – SIMPLE MEMBER BEHAVIOUR

The incremental elastic method is demonstrated using the analysis of a two-dimensional truss structure. The truss is illustrated below. All joints are pins. Therefore, the members only transmit axial forces. Perfectly plastic material properties are assumed. Similarly to the material properties discussed in Section 3.2.1, a 2% strain limit is used. When the strain limit is reached, member unloading occurs and the member forces are redistributed to the rest of the structure.

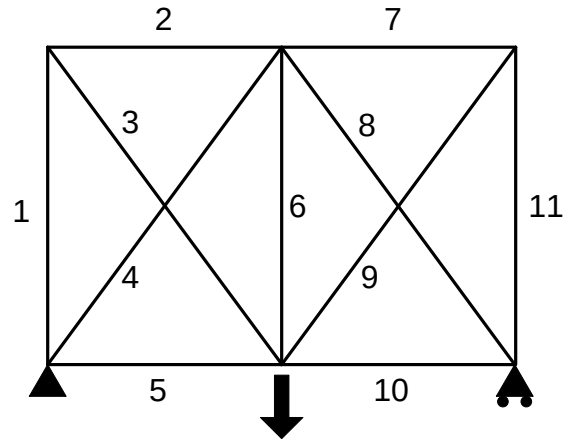

Figure 7-1: Two-dimensional truss

The structure is first analysed using a displacement controlled nonlinear finite element analysis. The material properties used are the same as those specified for the incremental analysis. In order to maintain agreement with the incremental analysis, a small displacement analysis with linear geometry is used. The global displacement is increased until total collapse occurs; the point at which the load carrying capacity of the structure is lost. The failure sequence leading to collapse of the structure is indicated in Figure 7-2.

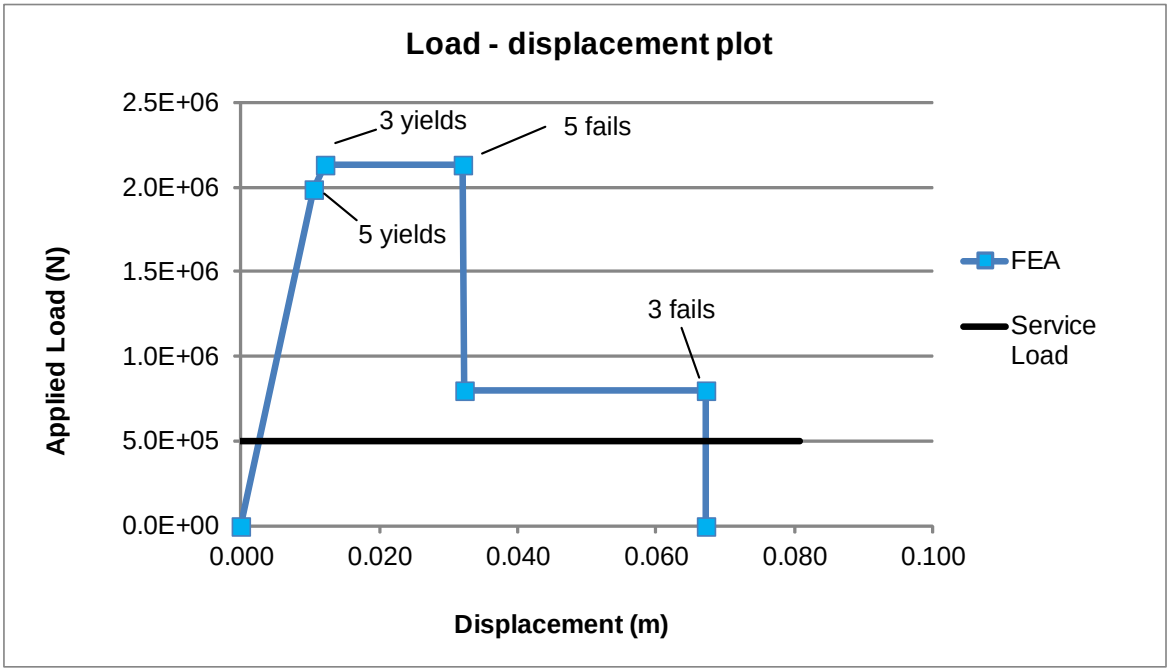

Figure 7-2: Finite element analysis

Firstly, Member 5 yields. This is followed by yielding of Member 3. After yielding of Member 3, the structure has zero stiffness and the displacement increases until the failure of Member 5 occurs. Failure of Member 5 results in a substantial drop in resistance. Following failure of Member 5 the displacement increases until the failure of Member 3 which causes complete collapse.

One of the goals of the incremental elastic analyses is to determine the entire load displacement path up to the collapse of the structure. Global resistance and displacement, as well as the internal member forces, will be calculated using the incremental analysis and compared with the nonlinear FE analysis to demonstrate their validity.

The IEA is implemented as outlined in Section 6.3 and the flowcharts presented in Section 6.4. Table 7-1 below shows the stress in each member of the structure under service load and the stress in each member which has been scaled by the scaling factor, α. First yield occurs in

Member 5, which is highlighted. The final column shows the percentage difference between the IEA and FEA results. Evidently there is excellent agreement between the two sets of results.

Table 7-1: Structure at first yield

Member	Stress (MPa)	α	min(α)	Scaled Stress (MPa)	% Difference
1	-41.37	6.04	3.99	-164.90	0.10
2	-31.03	8.06		-123.67	0.10
3	51.71	4.83		206.12	0.10
4	-41.81	5.98		-166.67	0.00
5	62.72	3.99		250.00	0.00
6	39.01	6.41		155.49	0.02
7	-39.44	6.34		-157.21	0.03
8	-36.21	6.90		-144.31	0.04
9	32.87	7.61		131.01	0.03
10	54.31	4.60		216.47	0.04
11	-52.59	4.75		-209.61	0.03

The structure at first yield is illustrated below with the corresponding global applied load and displacement. The strain energy, which is the area under the curve, is also determined.

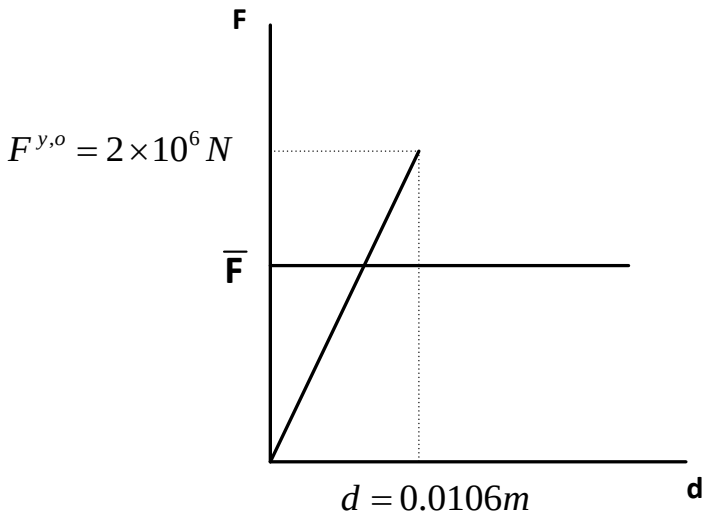

Figure 7-3: Scaled global applied load and displacement

The next step is to remove the yielded member, Member 5, from the structure in order to determine the incremental global force, displacement, and member forces. The incremental strain in Member 5 is determined using the incremental nodal displacements, and the scaling factor for Member 5 is determined using member strain with respect to the next event which is member failure.

Table 7-2 shows the stress in each member at yielding of the second member (Member 3) and also the results obtained using the nonlinear finite element analysis. The last column shows the percentage difference in member stress between the incremental analysis and the FE. As before, the results show good agreement. The other parameters such as nodal displacements show similar agreement.

Table 7-2: Comparison of IEA and FEA results

Member	Incremental Analysis		Nonlinear FEA		% Difference
	Stress (MPa)	Strain	Stress (MPa)	Strain	
1	-200.00	-0.0010	-200.00	-0.0010	-0.04
2	-150.00	-0.0008	-150.00	-0.0008	-0.03
3	250.00	0.0013	250.00	0.0013	0.00
4	-166.00	-0.0008	-167.00	-0.0008	-0.12
5	250.00	0.0013	250.00	0.0023	0.00
6	161.00	0.0008	161.00	0.0008	-0.10
7	-167.00	-0.0008	-167.00	-0.0008	-0.07
8	-155.00	-0.0008	-155.00	-0.0008	-0.08
9	139.00	0.0007	139.00	0.0007	-0.05
10	233.00	0.0012	233.00	0.0012	0.05
11	-223.00	-0.0011	-223.00	-0.0011	-0.09

Figure 7-4 shows the global applied load and displacement determined using the incremental analysis.

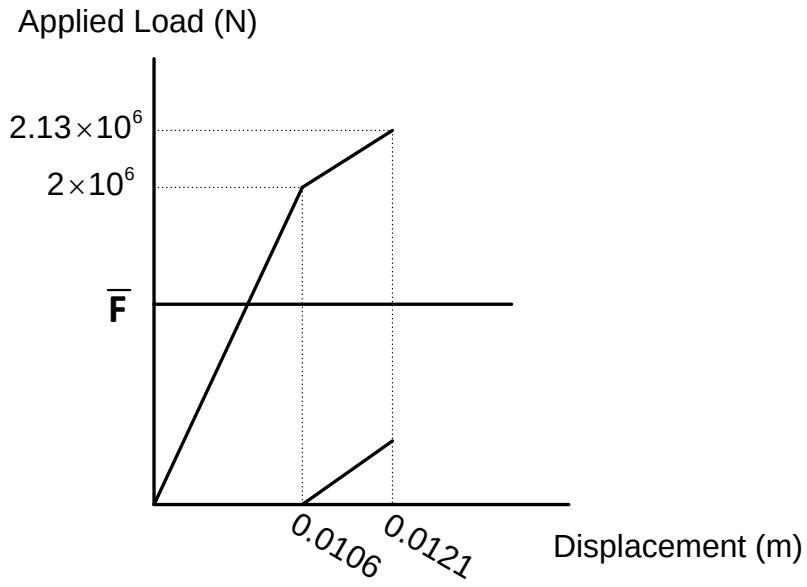

Figure 7-4: Load-displacement relationship at second yield

Following the yielding of the second member, the structure has zero stiffness. Therefore, although displacement will increase, the member forces in each member will remain constant. An incremental displacement analysis without both Members 5 and 3 is carried out in order to determine the state of the structure at A (see Figure 7-5). The ultimate strain is equal to 0.02. Therefore, in effect, the global displacement must be increased until the first member reaches its ultimate strain of 0.02. To achieve this, an arbitrary global displacement is applied and a scaling factor is determined which projects the structure to the first member failure event.

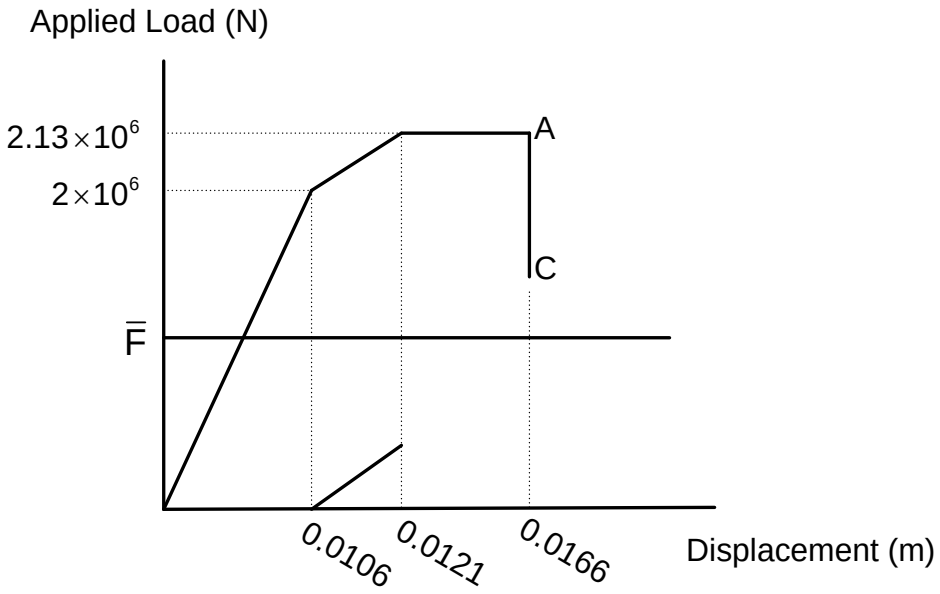

Figure 7-5: Load-displacement relationship at member failure

Following the displacement analysis, the structure is at state A which is indicated in Figure 7-5 above. The table below shows the incremental and FE values and the percentage difference in the stress values.

Table 7-3: Stress and strain at first member failure

Member	Incremental Analysis		Nonlinear FEA		% Difference
	Stress (MPa)	Strain	Stress (MPa)	Strain	
1	-200.00	-0.0010	-200.00	-0.0010	0.04
2	-150.00	-0.0007	-150.00	-0.0008	0.03
3	250.00	0.0076	250.00	0.0076	0.00
4	-167.00	-0.0008	-167.00	-0.0008	0.12
5	250.00	0.0200	250.00	0.0200	0.00
6	161.00	0.0008	161.00	0.0008	0.10
7	-167.00	-0.0008	-167.00	-0.0008	0.07
8	-155.00	-0.0008	-155.00	-0.0008	0.08
9	139.00	0.0007	139.00	0.0007	0.05
10	233.00	0.0012	233.00	0.0012	0.05
11	-223.00	-0.0011	-223.00	-0.0011	0.09

When a member fails the structural resistance drops until a new equilibrium is reached. As the resistance drops, the stress in the remaining members of the structure is redistributed. In order to continue the incremental analysis, the effect of the member failure must be determined. The redistribution, in terms of the change in member stress, is illustrated in Table 7-4 using the nonlinear FE analysis to compare member stress before and after the failure event; points A and C respectively in the diagram above. The results show that Members 6 to 11 experience a substantial drop in stress following member failure.

Table 7-4: Member stress before and after member failure event

FE Analysis		
Member	**Before Failure (A)**	**After Failure (C)**
	Stress (MPa)	**Stress (MPa)**
1	-200.00	-200.00
2	-150.00	-150.00
3	250.00	250.00
4	-167.00	0.00
5	250.00	0.00
6	161.00	31.10
7	-167.00	-56.60
8	-155.00	-62.30
9	139.00	47.20
10	233.00	93.40
11	-223.00	-75.50

7.2.1 Analysis of Member Failure Using Superposition

One method of determining the member forces following the failure event is to use superposition approach outlined in Section 6.3.3 and Figure 6-18. Firstly, it is determined that the failure of Member 5 does not cause any additional events ($\alpha^k \geq 1$). Therefore, the member forces in State A may be added to those in state B. Adding the member forces of States A and B is equivalent to cancelling the effect of Member 5 from the structure, thereby producing State C, which is the structure following member failure (see Figure 7-6 below).

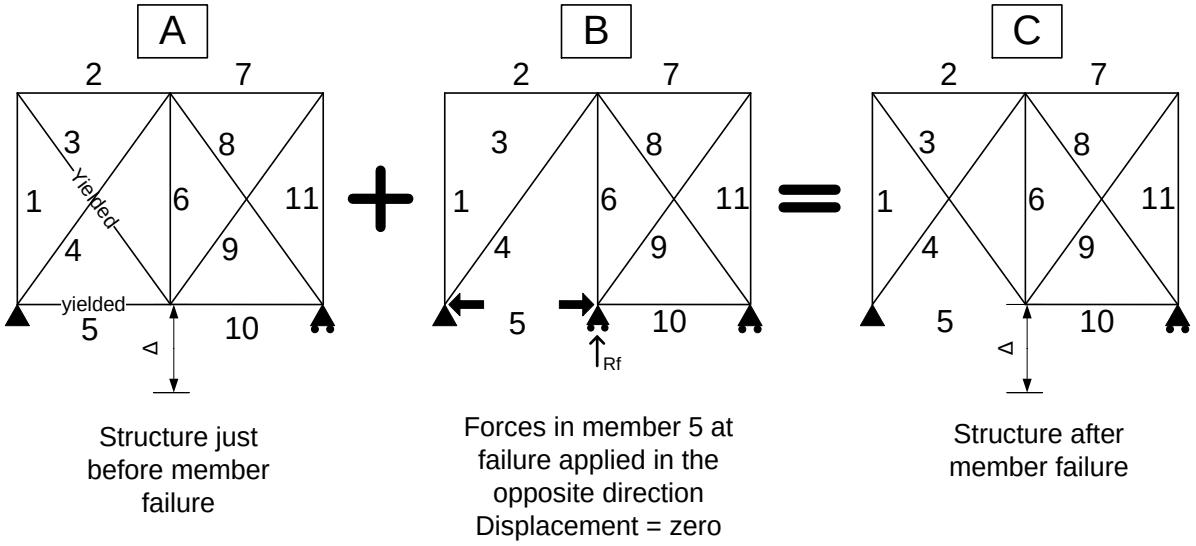

Figure 7-6: Superposition of Member 5 failure force

Figure 6-11 shows the member stresses determined in States A, B, C and also the member stresses determined using the nonlinear FE analysis for State C. The final column shows the percentage difference between the stress values at Point C determined using superposition and the FE analysis. Evidently the member stresses in State C agree with those determined using the FE analysis.

Table 7-5: Superposition step results

Member	State A	State B	State C	FEA – Member Stress after Failure (MPa)	Stress % Difference
	Stress (MPa)	Stress (MPa)	Stress (MPa)		
1	-200.00	0.00	-200.00	-200.00	0.000
2	-150.00	0.00	-150.00	-150.00	0.000
3	250.00	0.00	250.00	250.00	0.000
4	-167.00	-167.00	0.00	0.00	0.000
5	250.00	250.00	0.00	0.00	0.000
6	161.00	129.90	31.10	31.10	0.001
7	-167.00	-110.40	-56.60	-56.60	0.001
8	-155.00	-92.70	-62.30	-62.30	0.001
9	139.00	91.80	47.20	47.20	0.001
10	233.00	139.60	93.40	93.40	0.000
11	-223.00	-147.50	-75.50	-75.50	0.001

Once the state of the structure following member failure has been determined, the displacement analysis is continued. The incremental values for the displacement analysis, without Members 3 and 5, have already been determined. However, a new scaling factor is determined which projects Member 3 to its ultimate strain and, as illustrated in Figure 7-7, a new superposition step is implemented.

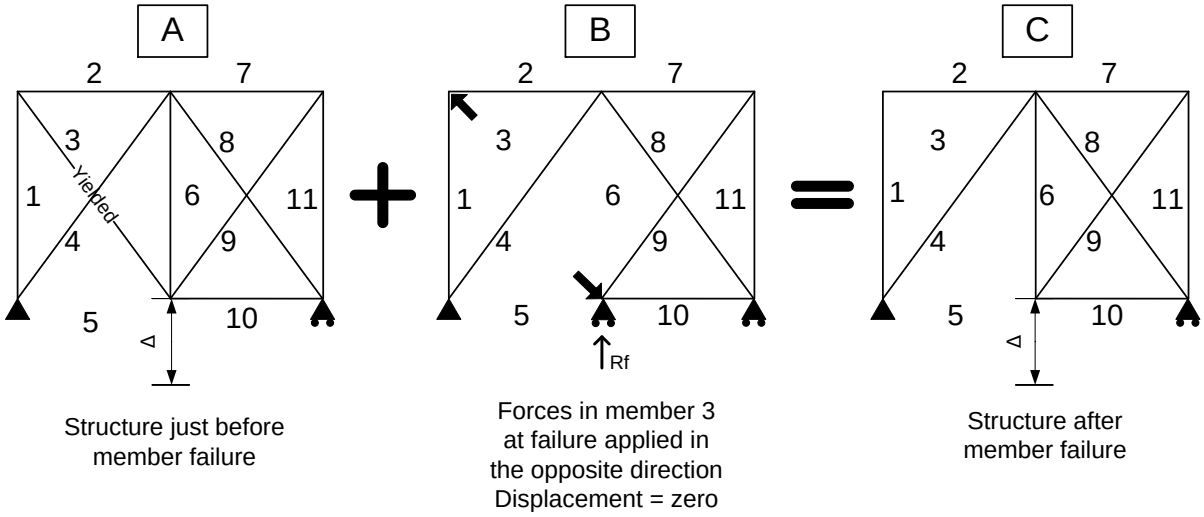

Figure 7-7: Superposition of Member 3 failure force

Table 7-6 presents the superposition results. When States A and B are added, it is observed that both member forces in the structure and the global resistance have decreased to approximately zero.

Table 7-6: Structural state after failure of the second member

Global Resistance (kN)	Stress (MPa)	Strain
33.3	0.00	0.0000
	0.00	0.0000
	0.00	0.0000
	333.33	0.0000
	0.00	0.0000
	443.39	0.0000
	-40.33	0.0000
	350.39	0.0000
	143.44	0.0000
	-40.33	0.0000
	-235.52	0.0000

Therefore, it is concluded that the structural resistance has been completely exhausted and the incremental analysis is complete. The full load displacement relationship has been determined and all values agree with those determined by the nonlinear FE analysis. The load-displacement relationship is illustrated in Figure 7-8.

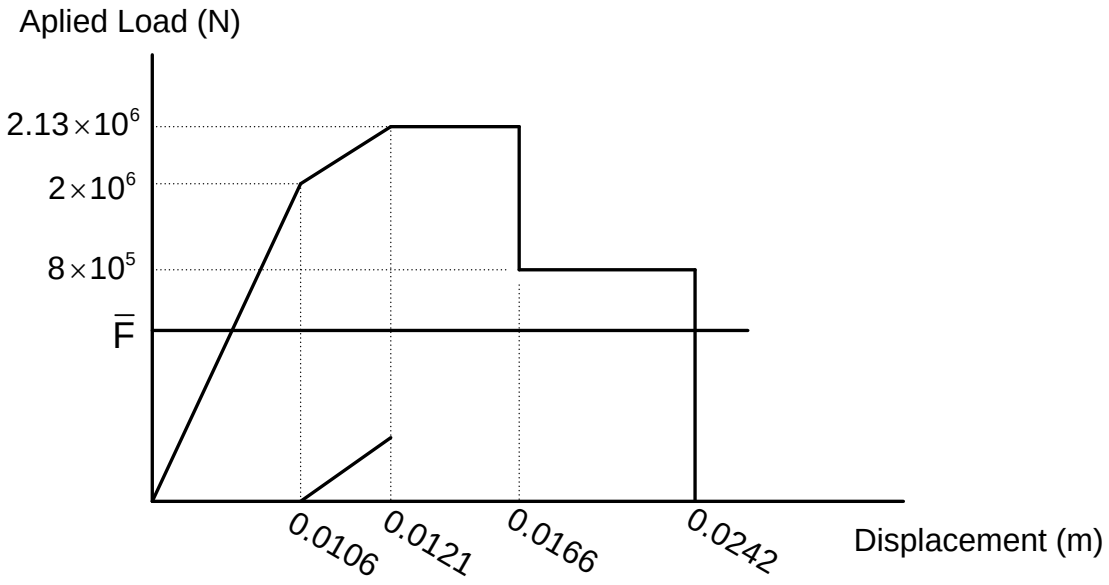

Figure 7-8: Full load-displacement relationship

7.2.2 Analysis of Member Failure Using a Reanalysis Without the Failed Member

The post member forces following member failure can also be determined using an incremental analysis. This is carried out by re-analysing the structure without the failed member. The service load is applied to the structure and the structure is projected to the first event which is the yielding of Member 3.

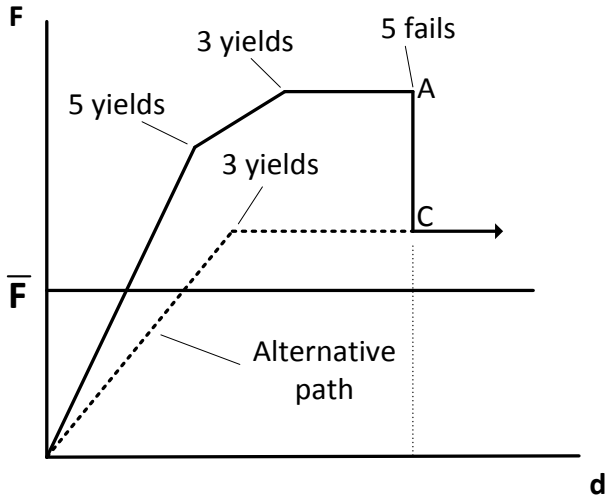

Figure 7-9: Incremental analysis without the failed member

When Member 3 yields, the resistance of the new path analysis is equal to the resistance at Point C in the original path. Following the yielding of Member 3, the stiffness of the new path is zero and a displacement controlled analysis is used to project the structure to Point C.

Table 7-7 shows the value of stress in each member at the yielding of Member 3 in the reanalysed structure. The results show that there is excellent agreement between the member stresses determined by the IEA and the nonlinear FE analysis following the failure of Member 5.

Table 7-7: Reanalysis results

Member	Incremental Analysis	Nonlinear FE analysis	% Difference
	Stress (MPa)	Stress (MPa)	
1	-200.00	-200.00	0.000
2	-150.00	-150.00	0.000
3	250.00	250.00	0.000
4	0.00	0.00	0.000
5	Failed Member		
6	31.10	31.10	0.002
7	-56.60	-56.60	0.001
8	-62.30	-62.30	0.001
9	47.20	47.20	0.001
10	93.40	93.40	0.001
11	-75.50	-75.50	0.001

Figure 7-10 shows the complete load displacement path determined by both the IEA and the nonlinear FE analysis. Clearly, the IEA results are consistent with those determined by the nonlinear FE analysis.

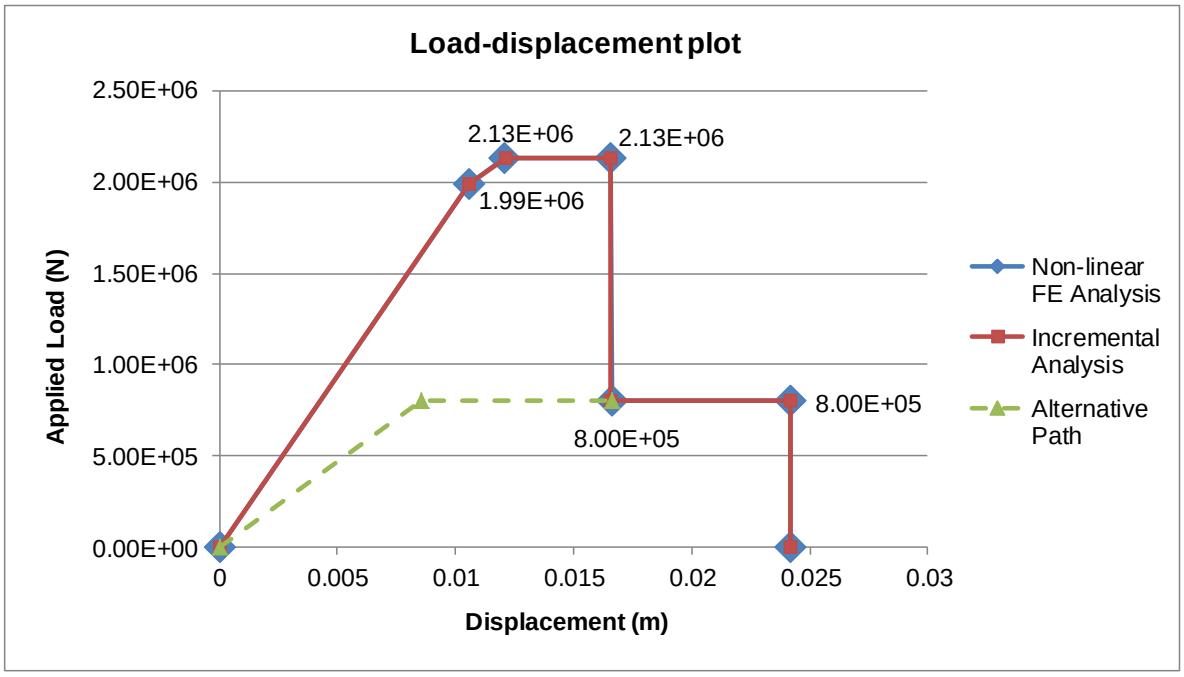

Figure 7-10: Load displacement relationship determined using each method

7.3 EXAMPLE 2 – UNLOADING OF A YIELDED MEMBER

This example will explore the problem posed by the unloading of a member which has already undergone permanent deformation. The basic structure (dimensions, boundary conditions and so on) are the same as in the previous example, however the cross-section areas have been modified to produce a different failure sequence. The load-displacement relationship and failure path events, which were determined using the FE analysis, are illustrated in Figure 7-11. Three members yield prior to the first member failure event; the failure of Member 5.

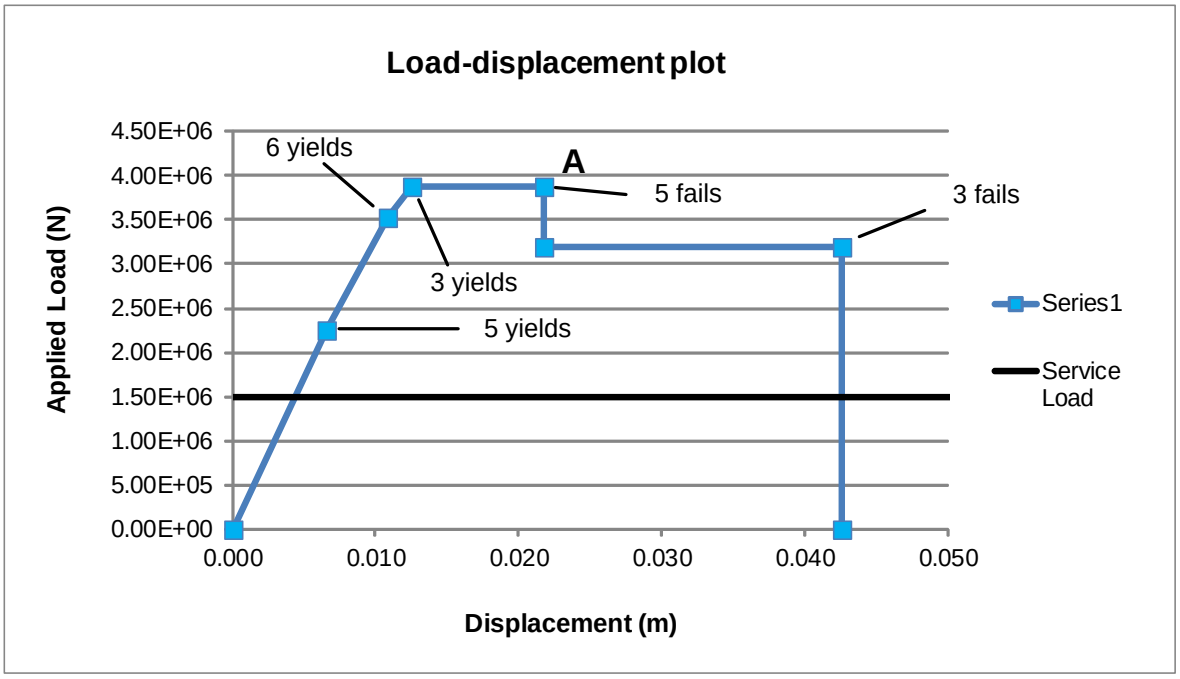

Figure 7-11: Collapse sequence events

Firstly, the IEA is used to determine the state of the structure up to the point of failure of Member 5 (point A on the diagram above). The next step is the identification of the post-failure structural state. This is demonstrated using each of the proposed methods.

7.3.1 Analysis of Member Failure Using Superposition

The superposition approach is use to determine the post failure structural parameters. The initial steps are illustrated in Figure 7-12. The analysis is initially carried out without Members 3 and 5. As outlined in relevant flowcharts (Figure 6-18 and Figure 6-19), it is observed that the failure of Member 5 causes Member 6 to unload. Therefore, Member 6 is replaced in the structure and the analysis is repeated by applying the yield force present in Member 5 at failure in the opposite direction. This is illustrated in Figure 7-13.

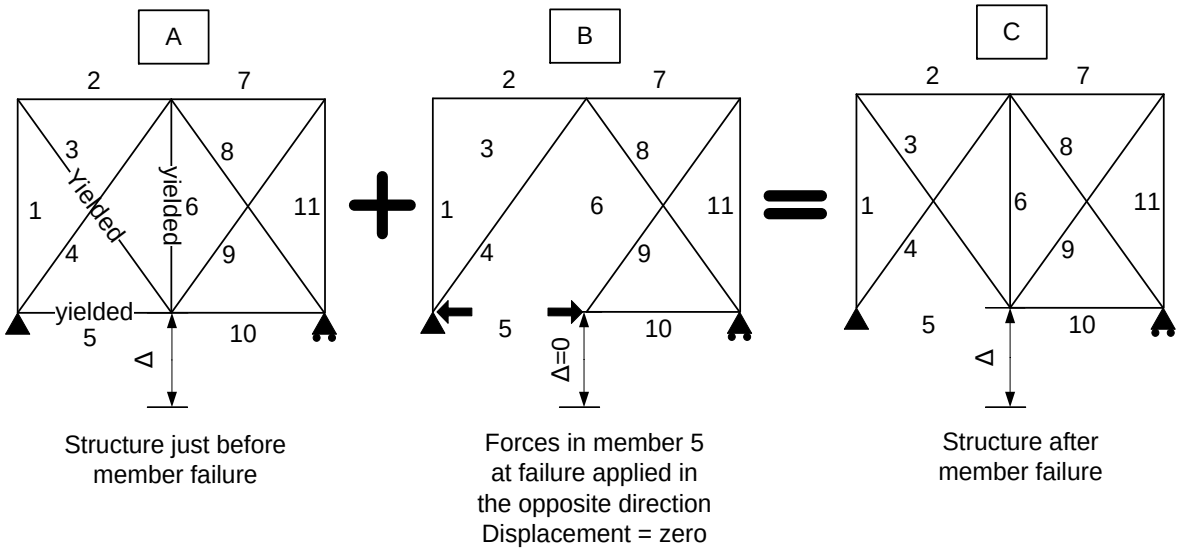

Figure 7-12: Superposition of Member 5 failure force (without Member 6)

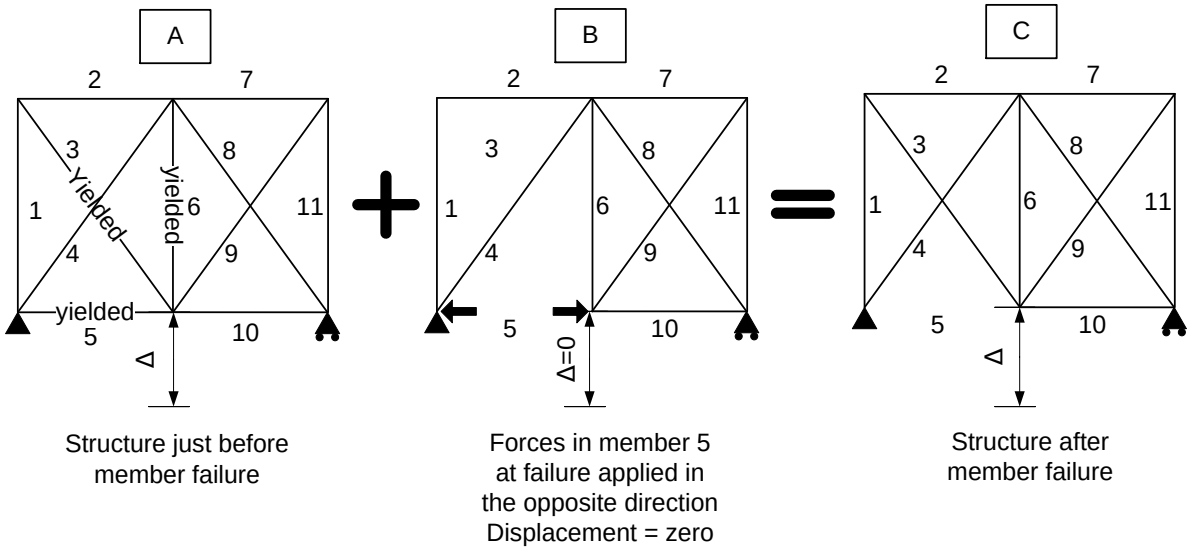

Figure 7-13: Superposition of Member 5 failure force (with Member 6)

The post failure IEA and FEA results are compared in Table 7-8. The results clearly show the effectiveness of the IEA approach.

Table 7-8: Comparison of superposition results and FEA

Member	State C		FE Analysis		Stress % Difference
	Stress (MPa)	Strain	Stress (MPa)	Strain	
1	-200.00	-0.0010	-200.00	-0.0010	0.000
2	-240.00	-0.0012	-240.00	-0.0012	0.000
3	250.00	0.0046	250.00	0.0046	0.000
4	0.00	0.0000	0.00	0.0000	0.000
5	0.00	0.0134	0.00	0.0134	0.000
6	160.00	0.0013	160.00	0.0013	0.000
7	-99.80	-0.0005	-99.80	-0.0005	0.000
8	-62.60	-0.0003	-62.60	-0.0003	0.000
9	166.00	0.0008	166.00	0.0008	0.000
10	120.00	0.0006	120.00	0.0006	0.000
11	-99.80	-0.0005	-99.80	-0.0005	0.000

7.3.2 Analysis of Member Failure Using a Reanalysis without the Failed Member

A reanalysis without the failed member is also used to determine the state of the structure after the member failure event. Firstly, the reanalysis in carried out without any additional steps to incorporate the permanent strain present in the unloaded member. This is illustrated in the table below by comparing the member stress after the failure of Member 5 determined with the FE analysis and the reanalysed structure. The results show a substantial discrepancy between the two sets of results for Members 6 to 12.

Table 7-9: Comparison of reanalysed structure and original FEA results

Member	New Path	Original Path	% Difference
	Stress (MPa)	Stress (MPa)	
1	-200.00	-200.00	0.00
2	-240.00	-240.00	0.00
3	250.00	250.00	0.00
4	0.00	0.00	0.00
5	0.00	0.00	0.00
6	180.00	160.00	11.45
7	-87.70	-99.80	12.98
8	-70.20	-62.60	11.45
9	146.00	166.00	12.98
10	135.00	120.00	11.45
11	-87.70	-99.80	12.98

The results show that the reanalysis does not directly determine the correct post failure member forces when unloading of a member occurs. As illustrated in Section 6.3.3.2, additional steps may be taken to correct the procedure by artificially incorporating the permanent strain in Member 6 in a two-step procedure.

The first stage is to analyse the structure without Member 5 and Member 6. The displacement is increased until the fictitious Member 6 attains a strain equal to the above permanent strain. The second stage is to replace Member 6 in the structure and apply the service load. The service load is scaled such that the member stresses in Stage 1 plus the member stresses in stage 2 bring the structure to first yield. Combining the two stages is in effect equivalent to implementing an analysis in which the permanent strain present in Member 6 is included.

Table 7-10 compares the stress and strain values obtained using the modified path and the original FE analysis after member failure (Point C on Figure 7-14 below). The results show

that the method proposed to incorporate the permanent strain present in the unloaded member is successful. The results show that by incorporating the permanent deformation in the new path, the stresses and member strains are in excellent agreement with those determined by the nonlinear FE analysis. However, while the correct outcome may be obtained by incorporating the permanent strain present in Member 6 using a two stage incremental approach, it is clear that reanalysing the structure without the failed member is more problematic than the superposition approach due principally to the fact that the new path begins from an initially unloaded structure.

Table 7-10: Comparison of the new path and the original FEA results

Member	New Path Analysis		Nonlinear FE Analysis		Stress % Difference
	Stress (MPa)	Strain	Stress (MPa)	Strain	
1	-200.00	-0.0010	-200.00	-0.0010	0.000
2	-240.00	-0.0012	-240.00	-0.0012	0.000
3	250.00	0.0046	250.00	0.0046	0.000
4	0.00	0.0000	0.00	0.0000	0.000
5	0.00	0.0134	0.00	0.0134	0.000
6	160.00	0.0013	160.00	0.0013	0.003
7	-99.80	-0.0005	-99.80	-0.0005	0.003
8	-62.60	-0.0003	-62.60	-0.0003	0.004
9	166.00	0.0008	166.00	0.0008	0.003
10	120.00	0.0006	120.00	0.0006	0.003
11	-99.80	-0.0005	-99.80	-0.0005	0.003

The load-displacement relationship, determined using each approach, is illustrated in Figure 7-14. As evidenced by the load-displacement relationship, each method exhibits good agreement with the FE analysis.

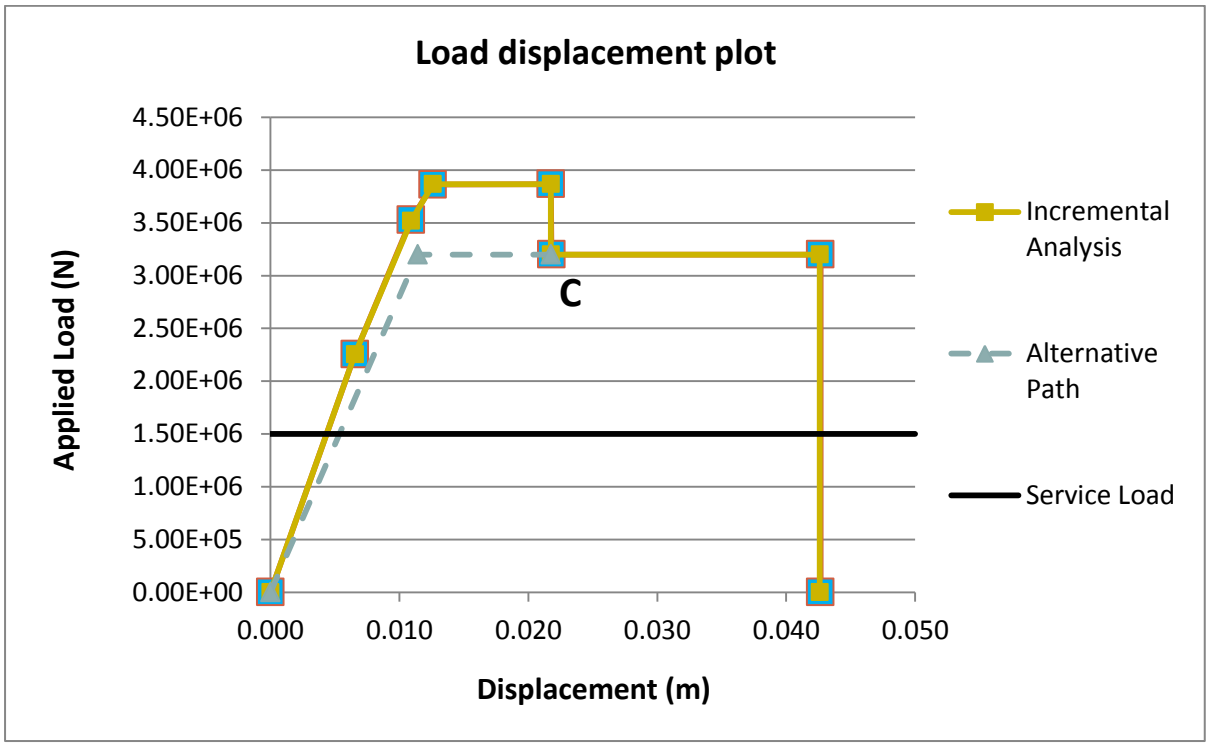

Figure 7-14: Load-displacement relationship determined using each method

7.4 EXAMPLE 3 – YIELDED MEMBERS WHICH CHANGE FROM COMPRESSION TO TENSION OR VICE VERSA

An additional complication may arise when unloading of a yielded member occurs. In Example 2, Member 6, which was in a plastic state, unloads during the analysis. However, although the member unloads, it remains in tension. It is also possible than an unloading member may change from tension to compression or vice versa.

The failure path for this example structure is illustrated Figure 7-15. Member 6 yields first, followed by Member 3 and Member 5. The failure of Member 3 causes Member 6 to unload and importantly to change from tension to compression.

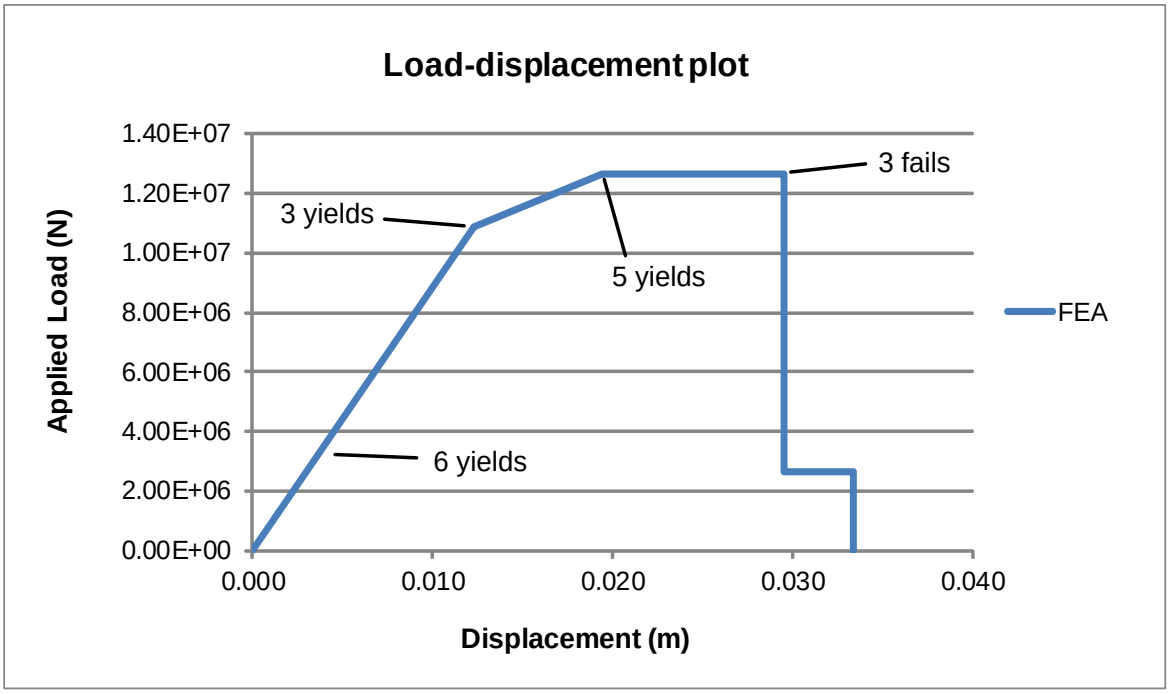

Figure 7-15: Failure sequence events

This behaviour poses a problem for the new path reanalysis demonstrated using the previous two examples. If a member changes from tension to compression (or vice versa), the strain present in the member after the failure event will be less than the permanent strain which is present in the member at unloading. If a two stage reanalysis without the failed member is used to try and incorporate the permanent strain present at unloading (see Figure 7-16), the unloaded member will remain unstressed, yielding incorrect results. Therefore, the two stage reanalysis cannot be used in this case.

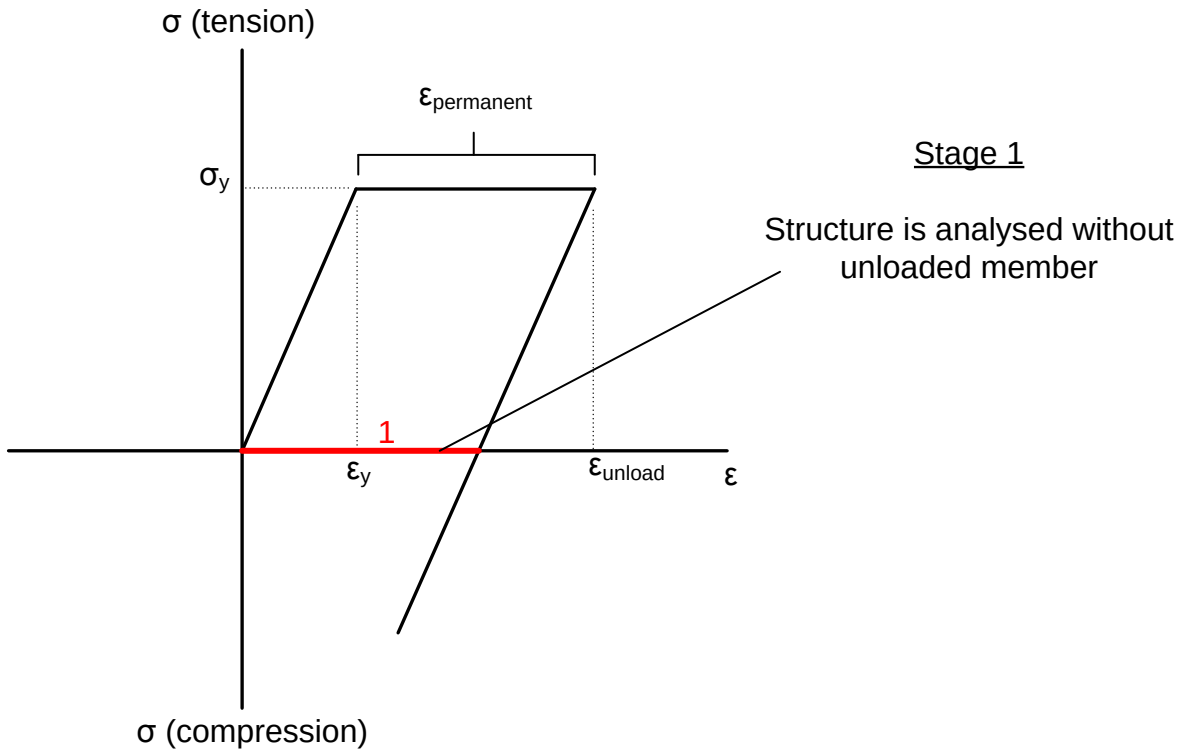

Figure 7-16: Step one of new path analysis

Rather than using the new path analysis, the superposition approach may be used effectively to determine the correct stress and strain values in all members after the failure of Member 5. The analysis is initially implemented without Member 6, which has yielded (Figure 7-17). However, the incremental strain indicates that Member 6 unloads. Therefore, it is replaced in the structure (Figure 7-18).

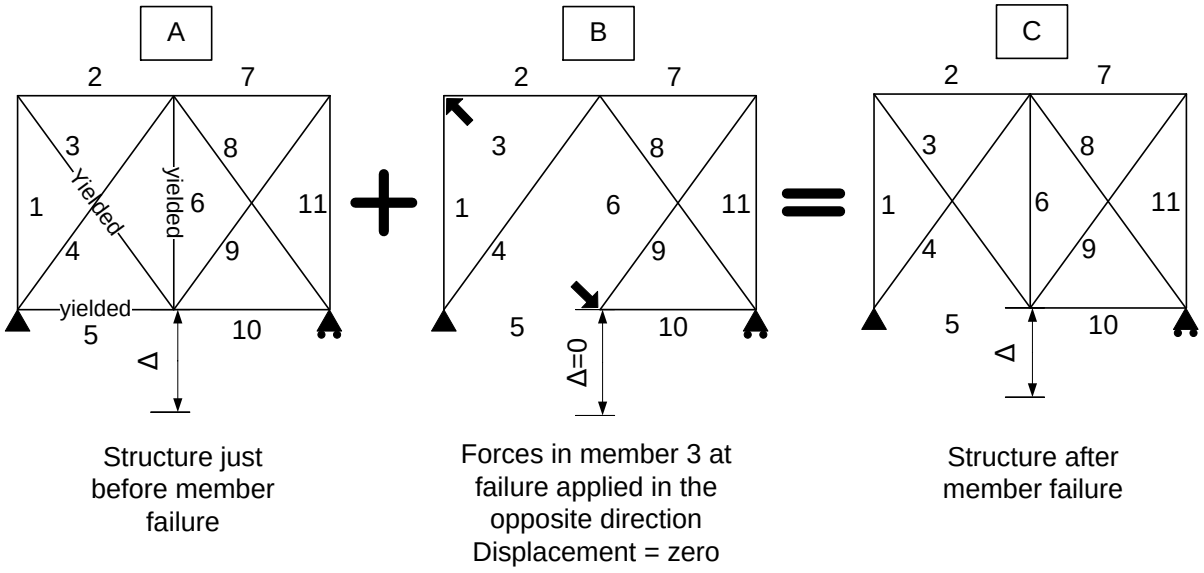

Figure 7-17: Incremental analysis without Member 6

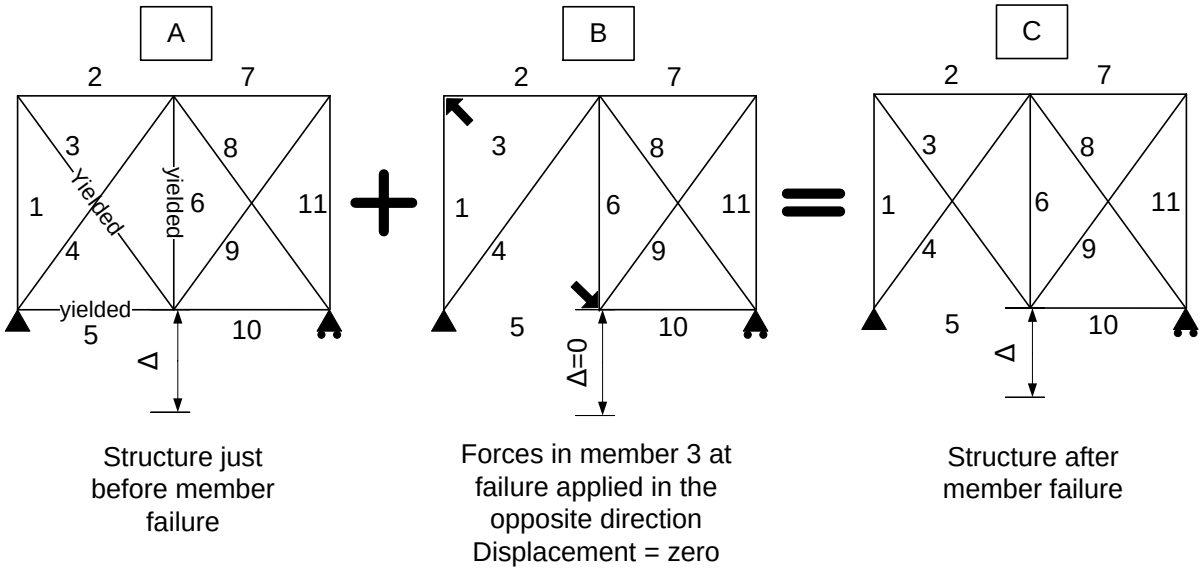

Figure 7-18: Incremental analysis with Member 6

The force at failure in Member 3 is applied in the opposite direction and States A and B are summed to determine State C. Table 7-11 compares the stress values obtained using the incremental analysis with superposition and the FE analysis. Clearly, the results agree.

Table 7-11: Comparison of superposition and FEA results

Member	State C (A+B)		FE Analysis	
	Stress (MPa)	Strain	Stress (MPa)	Strain
1	0.00	0.0000	0.00	0.0000
2	0.00	0.0000	0.00	0.0000
3	0.00	0.0086	0.00	0.0087
4	-104.00	-0.0005	-104.00	-0.0005
5	250.00	0.0178	250.00	0.0178
6	-159.00	0.0027	-159.00	0.0027
7	-68.30	-0.0003	-68.30	-0.0003
8	109.00	0.0006	109.00	0.0006
9	85.30	0.0004	85.30	0.0004
10	-210.00	-0.0011	-210.00	-0.0011
11	-78.00	-0.0004	-78.00	-0.0004

7.5 EXAMPLE 4 – FAILURE OF A MEMBER CAUSES ADDITIONAL MEMBERS TO YIELD

In the above examples each event in the failure sequences is distinct event. The scaling factor for the superposition analyses is greater than or equal to one ($\alpha^k \geq 1$). It is also possible that an event such as member failure will cause additional events such as the yielding or failure of other members in the structure ($\alpha^k < 1$). This example will illustrate how this behaviour may be handled using the superposition approach.

Similarly to the previous examples, the same structural configuration is used with some modifications to the section and material properties to elicit a different structural response. The load deflection path is illustrated in Figure 7-19. Member 5 and Member 10 yield before

the failure of member 5. The failure of Member 5 causes Member 10 to unload and Members 1 and 3 to yield. Prior to the failure of Member 5 the structure has positive stiffness, however after the failure of Member 5 the structure has zero stiffness due to the yielding of Members 1 and 3. Collapse occurs when Member 1 fails.

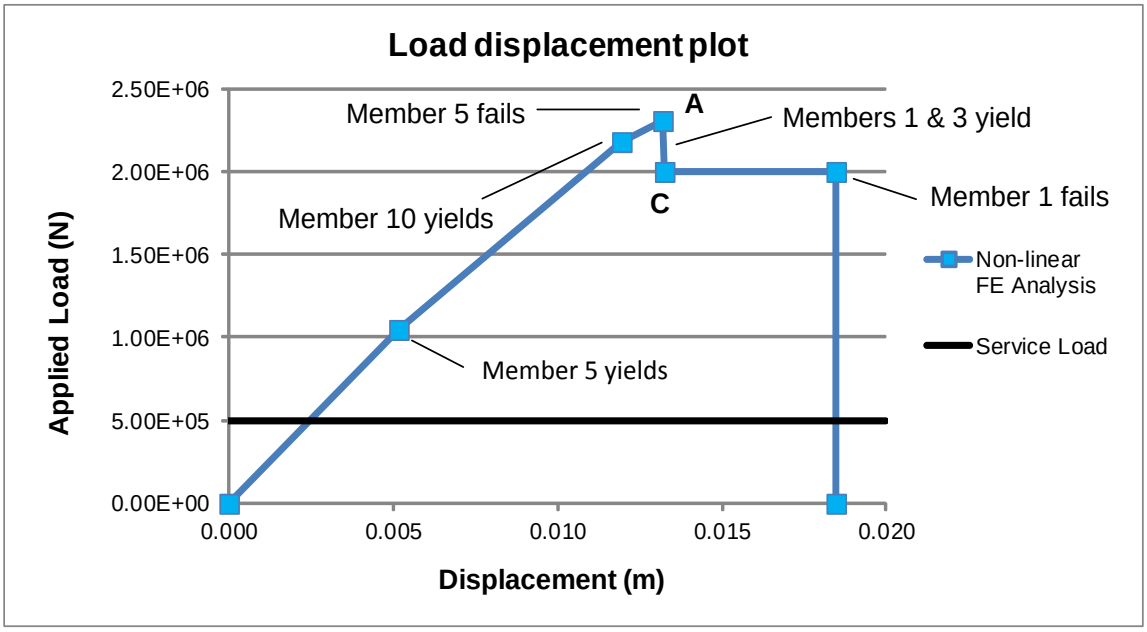

Figure 7-19: FEA load-displacement relationship

Incremental analyses are used to determine the full state of the structure prior to the failure of Member 5 (point A). Next, a superposition step is used to determine the state of the structure at Point C. The analysis indicates that Member 10 will unload. Therefore, Member 10 is replaced in the structure.

The force at failure in Member 5, $P_{u,5}$, is reapplied in the opposite direction. The analysis shows that at $0.167 \times P_{u,5}$, Members 1 and 3 yield. Therefore, Members 1 and 3 are removed from the structure. The analysis is continued by applying $0.833 \times P_{u,5}$. New scaling factors are

calculated for each member. The minimum scaling factor is greater than one, and so the step is complete. These steps are illustrated in Figure 7-20.

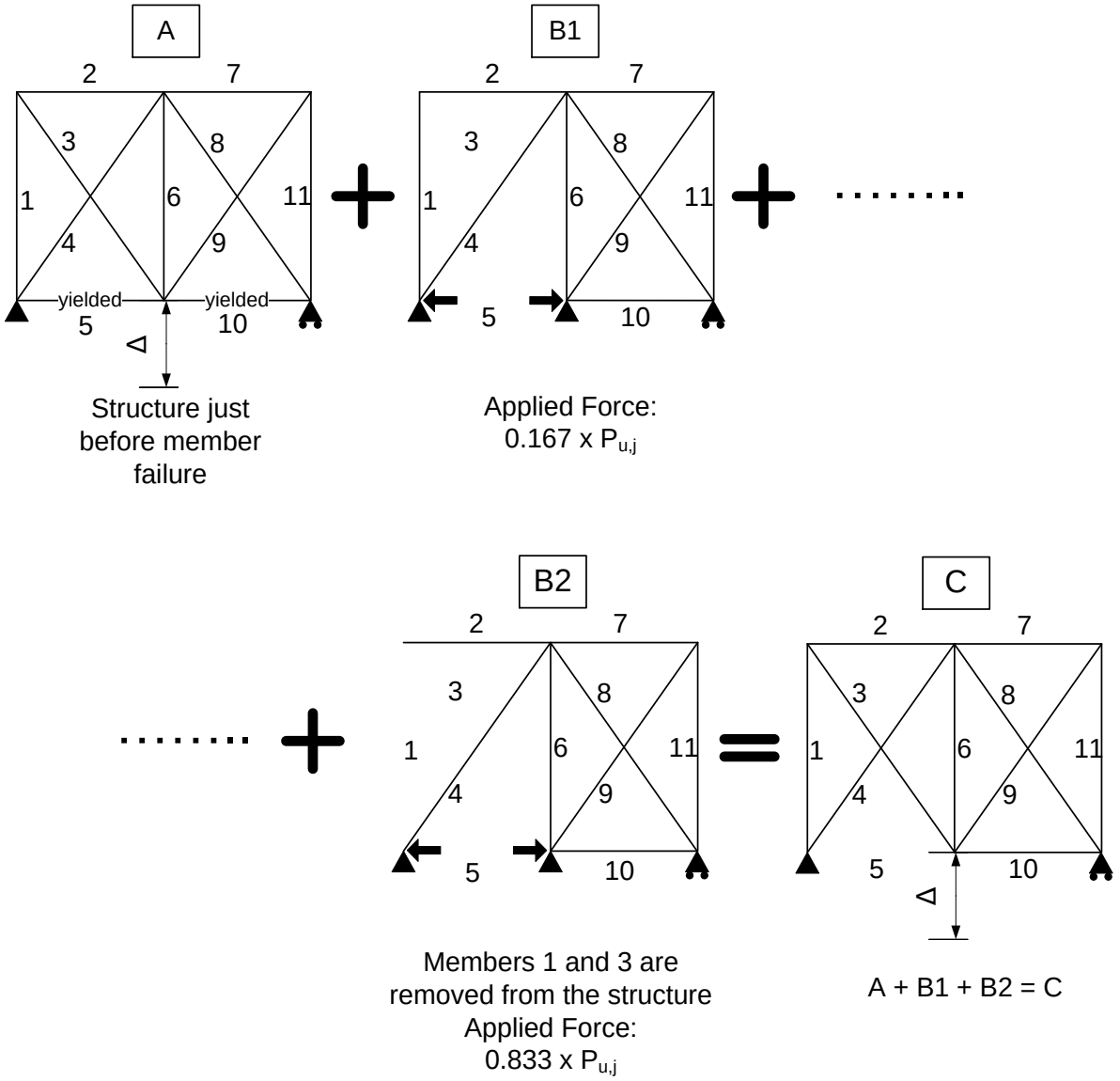

Figure 7-20: Superposition step

Once Stage B has been completed, the member forces, displacements and so on are added to State A to determine State C which is the structure after the member failure event. Table 7-12 presents the member stress and strain determined with the incremental superposition analysis

and the FE analysis. The rest of the analysis is continued, until collapse occurs, as demonstrated in the previous examples.

Table 7-12: Comparison of superposition and FE results

Member	Superposition Analysis		FE Analysis		Stress % Difference
	Stress (MPa)	Strain	Stress (MPa)	Strain	
1	-250.00	-0.0012	-250.00	-0.0016	0.000
2	-188.00	-0.0009	-188.00	-0.0009	0.000
3	250.00	0.0012	250.00	0.0013	0.000
4	0.00	-0.0001	0.00	0.0000	0.000
5	0.00	0.0051	0.00	0.0067	0.000
6	72.80	0.0005	72.60	0.0004	0.275
7	-157.00	-0.0009	-157.00	-0.0008	0.000
8	-146.00	-0.0008	-145.00	-0.0007	0.687
9	131.00	0.0007	131.00	0.0007	0.000
10	218.00	0.0019	218.00	0.0018	0.000
11	-209.00	-0.0012	-210.00	-0.0010	0.477

7.6 EXAMPLE 5 – FAILURE OF A MEMBER CAUSES ANOTHER MEMBER TO FAIL

This example illustrates the application of the proposed superposition method to the case in which the failure of one member causes another member to fail. Similarly to the previous examples, the material and section properties have been altered to produce a different failure sequence. The main events of this sequence are noted in Figure 7-21.

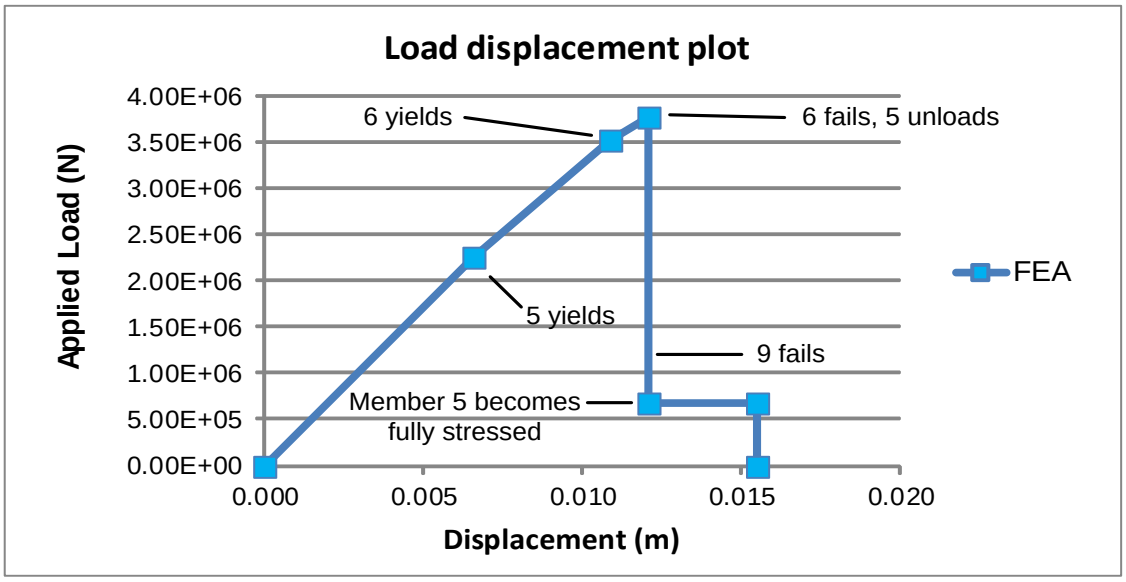

Figure 7-21: Load-displacement relationship

The incremental analysis until the failure of Member 6 is simple and proceeds as outlined in previous examples. As illustrated in Figure 7-22, the state of the structure following the failure of Member 6 is determined by applying the member force, $P_{u,6}$, present in Member 6 in the opposite direction. The initial analysis indicates that the failure of Member 6 will cause Member 5 to unload. Therefore, Member 5 is replaced in the structure (B1 in Figure 7-22).

The failure force of Member 6 is reapplied with Member 5 in place. A scaling factor is determined for each member in the structure. The minimum scaling factor is 0.876, indicating that a new event takes place, before the full force is applied. This event is the failure of Member 9. Therefore, Member 9 is removed from the structure (B2 in Figure 7-22).

The remaining portion of Member 6's failure force ($0.124 \times P_{u,6}$) and the failure force in Member 9, $P_{u,9}$, are applied simultaneously. A new scaling factor is now determined for all members. The minimum scaling is equal to 0.515, which indicates that another event takes

place; the yielding of Member 5. Therefore, Member 5 is removed from the structure (B3 in Figure 7-22).

After the removal of Member 5, the remaining portion of Member 6's failure force ($0.124 \times 0.485 = 0.06 \times P_{u,6}$) and Member 9's failure force ($0.485 \times P_{u,9}$) are applied. A new scaling factor is determined for all members. In this case the scaling factor is greater than one, indicating that the step is complete.

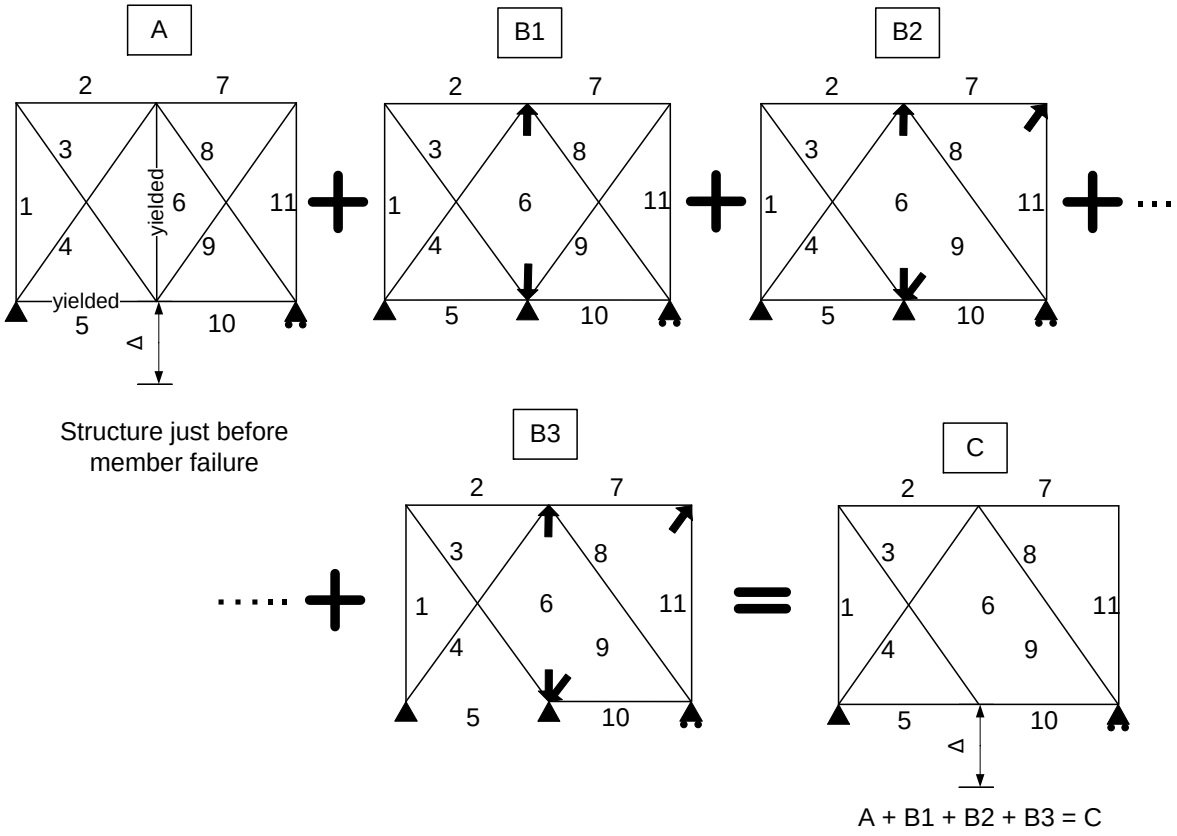

Figure 7-22: Superposition steps

Although the above failure sequence is somewhat complex, the process may be fully automated. Particular care needs to be taken with members such as Member 5 which undergo a number of different events. Figure 7-2 compares the IEA and FEA results and the

percentage stress difference. The results clearly demonstrate the viability of the IEA approach.

Table 7-13: Comparison of incremental analysis and FE results

Member	Incremental Analysis		FE Analysis		Stress % Difference
	Stress (MPa)	Strain	Stress (MPa)	Strain	
1	-83.30	-0.0004	-83.30	-0.0004	0.000
2	-100.00	-0.0005	-100.00	-0.0005	0.000
3	104.00	0.0005	104.00	0.0005	0.000
4	26.00	0.0001	26.00	0.0001	0.000
5	-250.00	-0.0044	-250.00	-0.0044	0.000
6	0.00	0.0000	0.00	0.0000	0.000
7	0.00	0.0000	0.00	0.0000	0.000
8	-26.00	-0.0001	-26.00	-0.0001	0.000
9	0.00	0.0029	0.00	0.0029	0.000
10	50.00	0.0003	50.00	0.0003	0.000
11	0.00	0.0000	0.00	0.0000	0.000

7.7 EXAMPLE 6 – THREE APPLIED LOADS

Each of the previous examples has been limited to a simple truss in order to facilitate a clear description of the structural behaviour and the steps involved in the incremental analysis. However, the proposed method is not limited to simple structures with one applied load. In order to further illustrate the method, Configuration C (Section 5.6) is analysed. Similarly to the material properties described in Section 3.2.1, a post yield tangential modulus of approximately 1 GPa is assumed. The structure is illustrated in Figure 7-23.

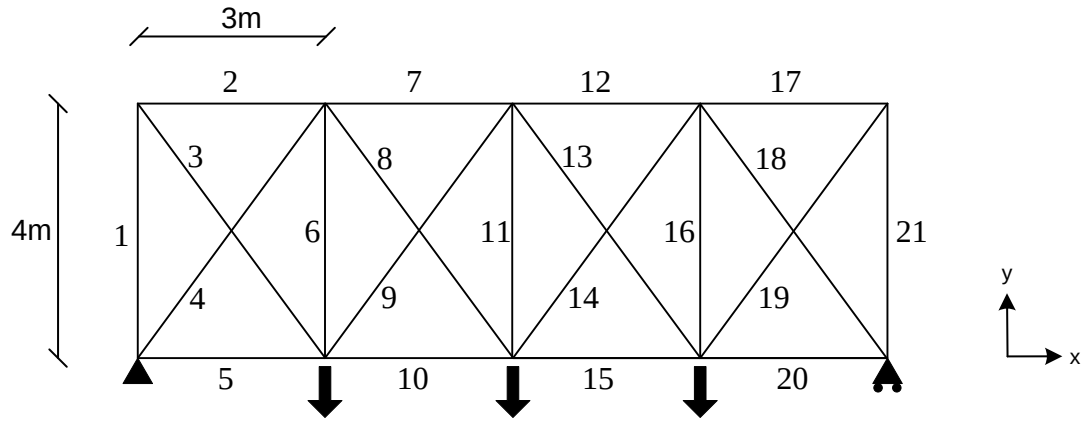

Figure 7-23: Truss model (Configuration C)

The IEA is carried out until the structure collapses. The events in the failure path are noted in Figure 7-24. Several members yield prior to the failure of the first member. The failure of Member 5 and 20 causes the failure of Member 3 and Member 19; after which the load carrying capacity of the structure is lost.

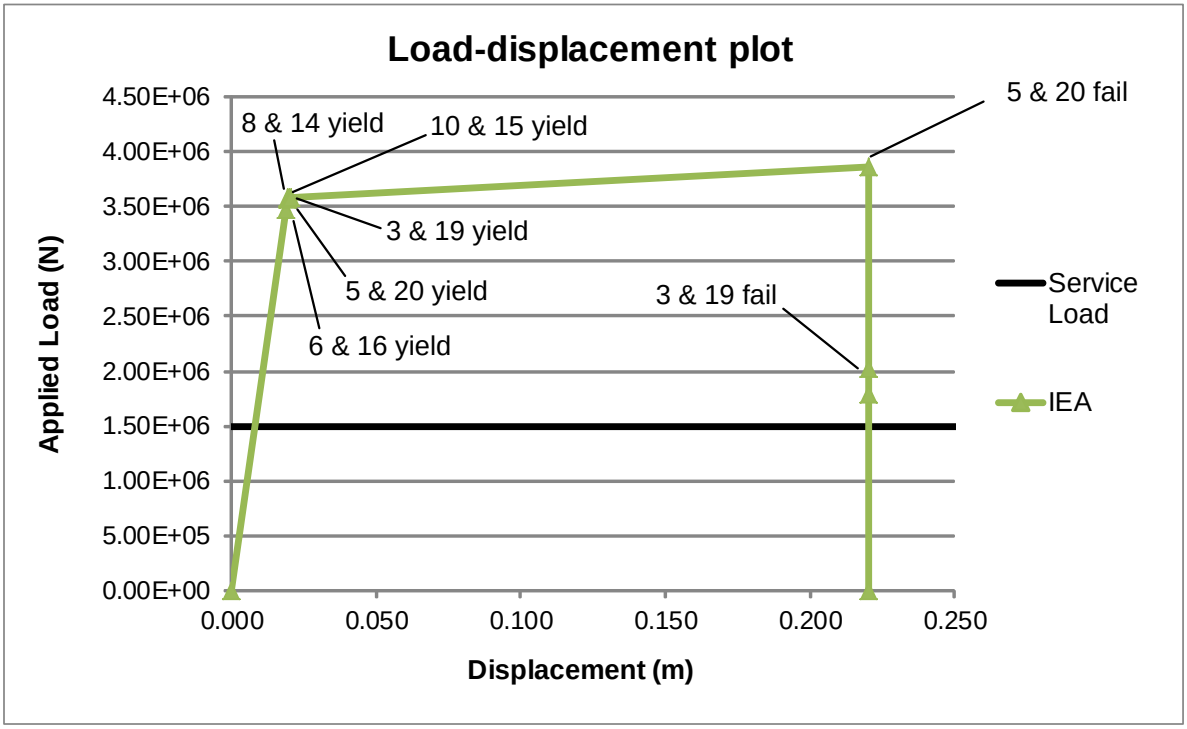

Figure 7-24: Failure path events

Figure 7-25 compares the load-displacement relationship determined with the IEA and FEA. Evidently, the results show excellent agreement.

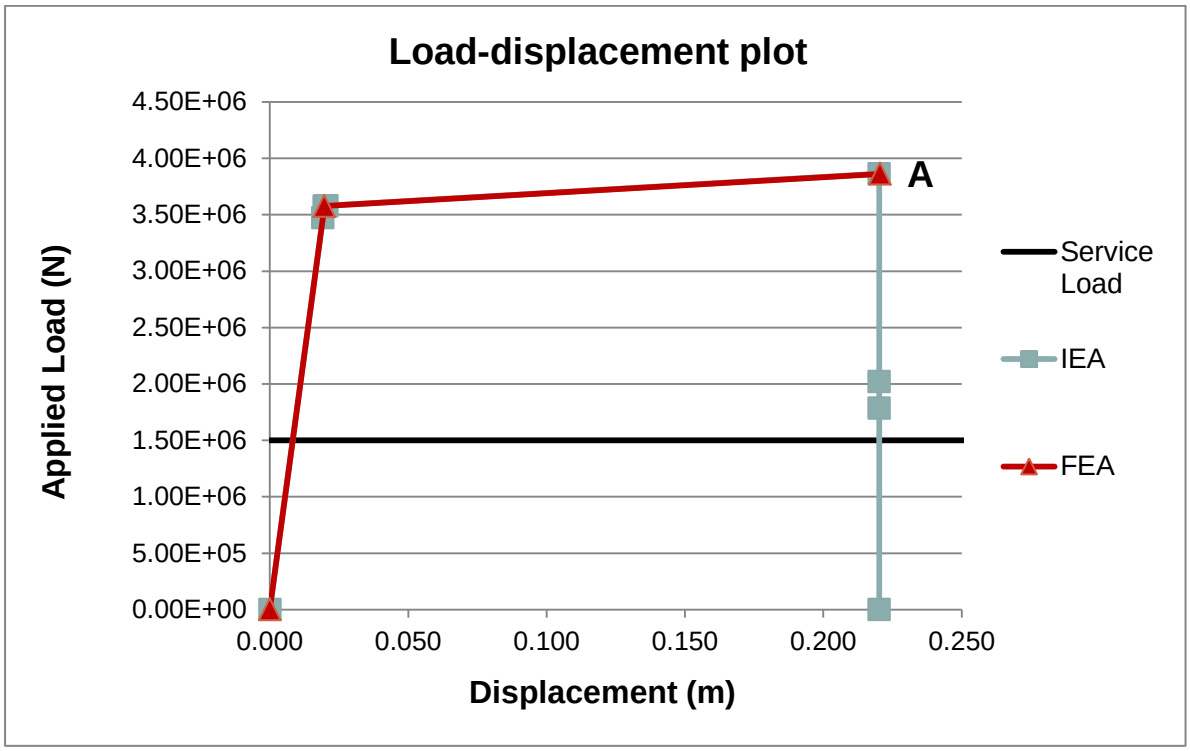

Figure 7-25: Load-displacement relationship for IEA and FEA

7.8 NONLINEAR GEOMETRY

The comparison of the incremental analysis output with the FE analysis shows excellent agreement and demonstrates the capacity of the incremental approach. In order to provide a consistent basis for comparison, the same properties and assumptions were used for each analysis. Therefore the FE analysis was conducted using nonlinear geometry.

However, it must be noted that due to the relatively large displacements which take place during a collapse analysis, p-delta effects will be observed. The diagram below shows the FE load-displacement relationship determined with and without nonlinear geometry. Evidently, the structure with nonlinear geometry exhibits some softening which is not present in the linear case. Although the effects of the nonlinear geometry are relatively minor in this case,

the absence of p-delta effects in the incremental analysis approach is one weakness which may result in behaviour which diverges from that of the real structural behaviour.

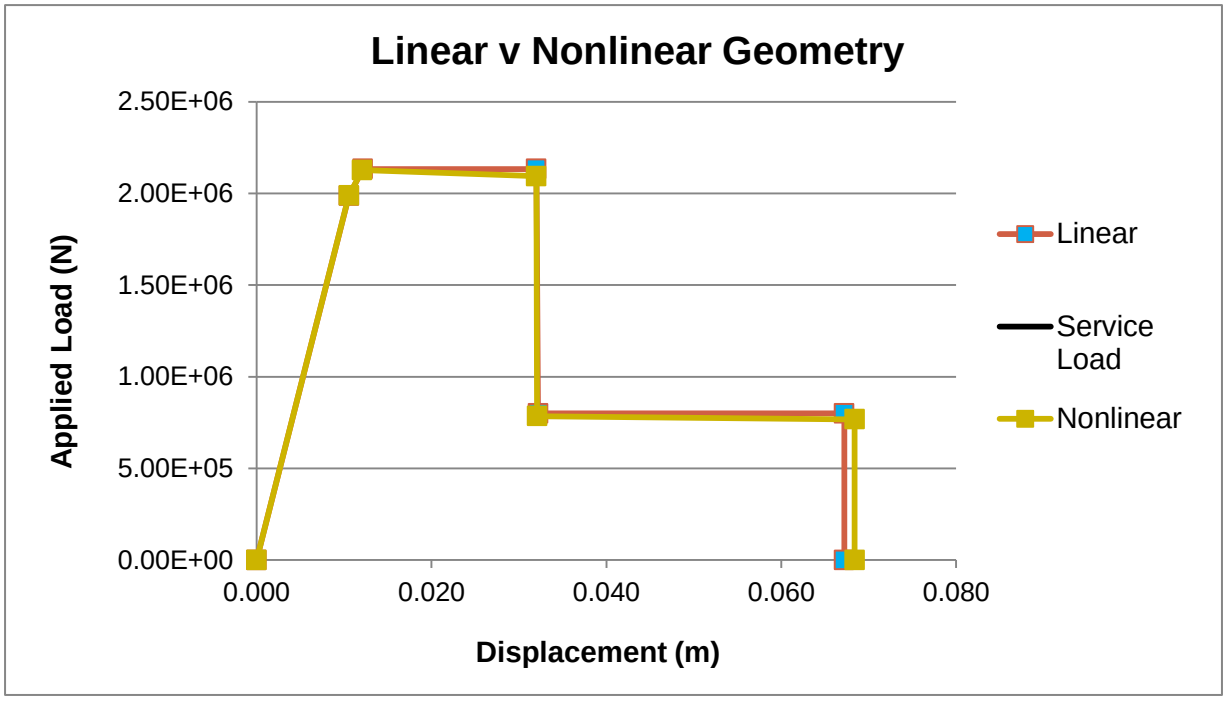

Figure 7-26: Comparison of linear and nonlinear geometry

7.9 APPLICATIONS TO OTHER STRUCTURES

The incremental elastic analysis has been illustrated using 2D pin-jointed trusses. The analysis of pin-jointed trusses is simplified by the uniform behaviour along the length of each member and in particular by the absence of bending stresses. However, other structures such as moment resisting frames may also be considered. In the case of moment resisting frames, the same principles may be applied; rather than removing a member from the structure or reducing its axial stiffness, the rotational resistance of members may be removed by changing a fixed joint to a pinned joint. Similarly, a series of incremental elastic analyses may be used to determine the overall capacity of a structure.

7.10 ALTERNATIVE FAILURE PATHS

One of the most useful advantages of the IEA is the capacity to investigate the alternative paths. Each stage involves an incremental analysis and a projection to the next event in the failure path, using the scaling factor, α. However, it is possible that given any particular event in the failure sequence such as yielding or failure of a member, there is another path which has a similar probability. This may occur if two members approach yielding or failure at the same time. When the member forces are scaled, Member j will be in its yield condition. However if another member in the structure, say Member k, then given the presence of normal structural variability, it is possible that Member k will yield before Member j. Each alternative event represents the start of new branching of the path leading to collapse.

As demonstrated in Chapter 5, minor variations in member strength may significantly affect the robustness of a structure. However, using a MCS to investigate the sensitivity of robustness is computationally expensive. Therefore, it is proposed to use the IEA as an efficient method to identify the upper and lower strength and ductility bounds. At each stage of the analysis, the most critical or least critical events will be identified. By identifying the most critical and least critical events at each stage, the upper and lower robustness bounds may be determined without exhaustive MCS.

7.10.1 Method

Similarly to Chapter 5, a member strength variation of +/- 10 MPa is assumed. A consequence of adopting such a small variation in member strength is that, at each stage, the alternative events have a similar probability of occurrence. Thus the total probability of each sequence is also similar.

The IEA is implemented as outlined in Section 6.3 and flowcharts in Section 6.4. Initially the structure is projected to the first event; generally member yielding. All members which as within 10 MPa of the yield stress (250 MPa) are identified as candidate members. For example, the stress each member of configuration D at first yielding is reported in Table 7-11. The candidate members are highlighted; member 4 and 19. The yield strength in each candidate member may be adjusted in the range of 240 MPa to 260 MPa. Both the selection of the next event and the magnitude of the member strength adjustment depend on whether the objective is to identify the most critical sequence or the least critical sequence.

Table 7-14: Member stress at first yielding (Configuration D)

Member	Stress (MPa)	Member	Stress (MPa)
1	-145.53	12	-205.58
2	-161.70	13	-55.20
3	181.92	14	202.01
4	-250.00	15	186.89
5	97.50	16	191.75
6	75.26	17	-74.14
7	-165.13	18	-138.03
8	210.52	19	247.13
9	-115.96	20	212.01
10	208.42	21	-98.85

In Chapter 5, it was observed that the degree to which a failure path is distributed throughout the structure or concentrated in small number of proximate members was an important factor in the ultimate strength, and particularly the ductility. This is reflected in the decision criteria for event selection and also member strength adjustment. A variety of criteria are used to guide the selection process:

- Total strain energy in the incremental structure (this is equivalent to the approach used by Smith (2003))
- The incremental strain energy in members which have already yielded
- The proximity of the candidate event to members which have already yielded
- The member failure events which have been identified by any previous analyses. For example, the nominal analysis may be used as a guide. If the plasticity is concentrated in one area of the structure it may be favourable divert the failure path other parts of the structure. Additionally, it may be necessary to explore more than one alternative path sequence. Therefore, the events of other sequences may also be used to guide the selection process.

7.10.2 Example

Configuration D of Chapter 5 is used to illustrate the approach. The nominal and MCS results are summarised in Table 7-15. The MCS results were obtained by assuming a member strength variation of +/- 10 MPa. 500 simulations were used.

Table 7-15: MCS results for Configuration D

	Strength (kN)	**Ductility (m)**
Maximum	1372.29	0.177
Minimum	1266.23	0.046
Nominal	1312.38	0.047

The maximum and minimum strength and ductility values serve as upper and lower bounds which may be used to determine upper and lower robustness bounds. The objective of the

incremental analysis is to efficiently determine these bounds without recourse to extensive MCS. Therefore the incremental analysis was used to analyse Configuration D.

Firstly, the most critical failure path is identified. The path is illustrated in Figure 7-27. The structure is projected to the first event in the path, which is the yielding of a member. There are two alternative events; the yielding of Member 4 or the yielding of Member 19. The total strain energy in the incremental analyses is determined following the yielding of each member (see Table 7-16). The results indicate that the yielding of Member 4 is more critical.

Table 7-16: Total incremental strain energy after each event

Residual structure	Total Strain Energy (Nm)
4	4256
19	3928

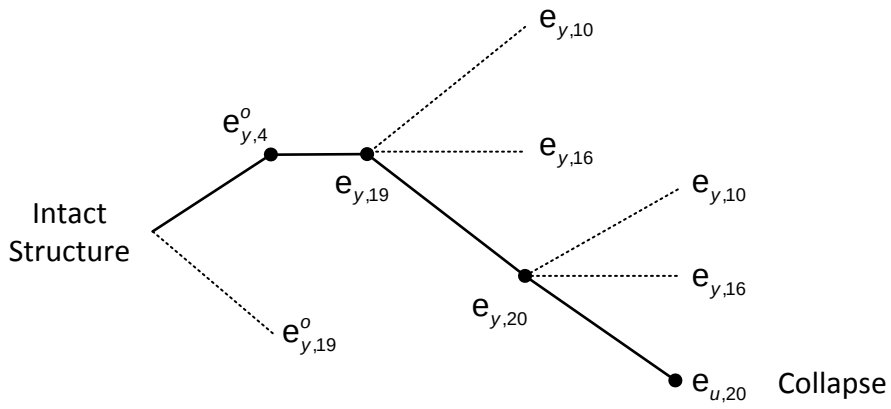

Figure 7-27: Most critical failure path

The yielding of Member 4 is identified as the most critical, as the total strain energy in the incremental analysis exceeds the total strain energy following the removal of Member 19.

The yield strength is initially unchanged, as the yielding of Member 4 is the first event in the nominal path. The structure is projected to the next event.

With respect to the second event, there is only one candidate, the yielding of Member 19. The yield strength of Member 19 is reduced to the minimum strength, given that Member 4 has yielded first. It is initially assumed that Member 4 yields first with a yield strength of 250 MPa. For this event to occur, the yield strength of Member 19 cannot be greater than 243 MPa. Thus the strength of member 19 is reduced to 248 MPa.

There are three candidates for the third event; the yielding of Member 10, 16 or 20. The total strain energy in each incremental analysis indicates that yielding of Member 20 is the most critical (see Table 7-17). Therefore, the yielding of Member 20 is selected as the most critical event and the member strength is reduced to the minimum bound of 240 MPa.

Table 7-17: Total incremental strain energy after each event

Residual structure	Total Strain Energy (Nm)
10	13336
16	8253
20	62917

There are also three candidates for the fourth event; the yielding of Member 10, the yielding of Member 16 and the failure of Member 20. Naturally, as the objective is to determine the most critical sequence, the failure of Member 20 is selected as the next event.

Table 7-18 compares the IEA alternative path results and the MCS results for the most critical scenario. Evidently the IEA results provide an excellent indicator of the lower bounds strength and ductility.

Table 7-18: Comparison of lower bound IEA and MCS results

	Strength (kN)	Ductility (m)
MCS	1266.23	0.0458
IEA	1275.80	0.0460
Nominal	1312.38	0.0470

An additional sequence is also considered. This path is illustrated in Figure 7-28. For this sequence, the first event is the yielding of Member 19, instead of Member 4. The yield stress is reduced to the minimum bound of 240 MPa. There is only one candidate for the second event; the yielding of Member 4. In this case the yield strength is increased to the maximum bound of 260 MPa, based on the observation that the most critical failure is primarily dependent of the development of plasticity in Member 19 and Member 20. Increasing the yield stress of Member 4 to 260 MPa allows greater plastic strain to develop in Member 19.

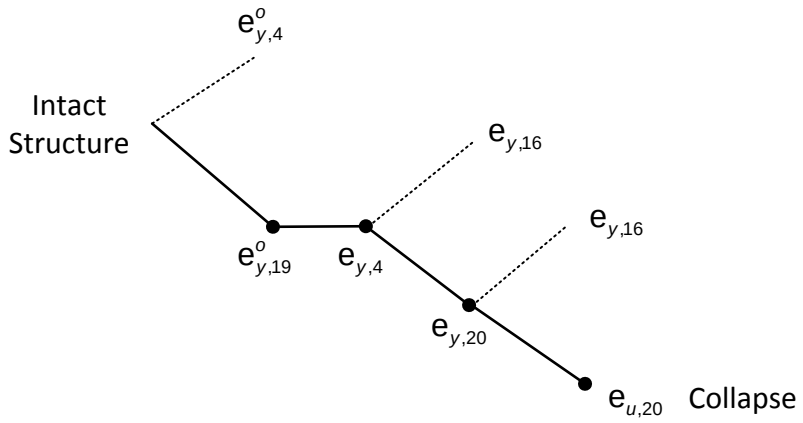

Figure 7-28: Failure path events

For the third event, there are two candidates; the yielding of Member 16 and 20. Member 20 is identified as the most critical event and the yield stress is reduced to the minimum bound

of 240 MPa. For the final event, there are two candidates; the yielding of Member 16 or the failure of Member 20. The failure of Member 20 is selected.

Table 7-19 compares the IEA and MCS results. The results demonstrate that the sequence identified by the IEA has a lower ultimate strength and lower ductility that the MCS. This demonstrates that the IEA may be used successfully used to determine the lower bound strength and ductility values.

Table 7-19: Comparison of lower bound IEA and MCS results

	Strength (kN)	**Ductility (m)**
MCS	1266.23	0.0458
IEA	1263.10	0.0456
Nominal	1312.38	0.0470

Next the least critical sequence is identified. This sequence is illustrated in Figure 7-29. The first is the yielding of Member 4. The general criteria used for selecting each event are the same as the criteria used for selecting the events in the most critical path. In contrast however, the guiding principle here is to ensure that the development of plasticity in the structure is distributed throughout the structure rather than concentrated in a few members.

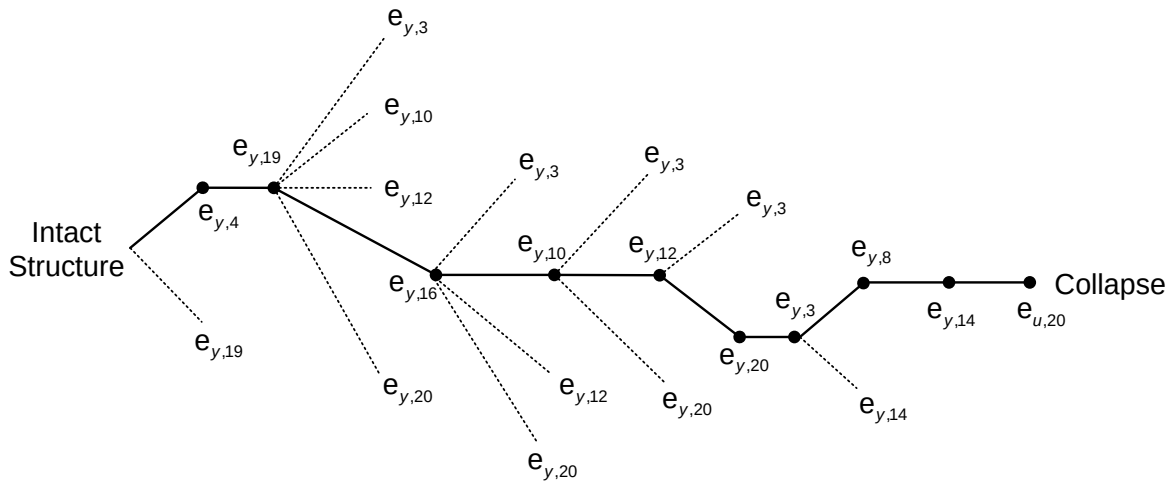

Figure 7-29: Least critical sequence

Member 4 is initially selected on the basis that the structure is susceptible to the concentration of damage in Member 19 and 20. Member 16 is selected on the basis of total strain energy in the incremental analyses. The strain energy in each incremental analysis are summarised in Table 7-20.

Table 7-20: Total strain energy in each incremental analysis

Yielded Member	10	12	16	20
Total Incremental Strain Energy (N/m)	13336	16864	8253	62917

The yielding of Member 10 is also selected on the basis total incremental strain energy. The results are summarised in Table 7-21.

Table 7-21: Total strain energy in each incremental analysis

Yielded Member	3	10	12	20
Total Incremental Strain Energy (N/m)	127558	17420	110972	65123

The next three events, the yielding of Member 12, 20, 3 and 8 are selected on the basis of the strain energy in members which are already yielded. At later stages in the failure path, as some member begin to accumulate significant amount of strain, it is more optimal to consider members which have already yielded, rather than the total strain energy in the structure. The path ends with the failure of Member 20.

The IEA alternative path analysis and the MCS results are presented in Table 7-22. The ultimate strength and ductility values, which were determined using the IEA, are marginally greater that the MCS results. This indicates that in addition to the lower bounds results, the upper bound results may be efficiently determined using the IEA.

Table 7-22: Comparison of upper bound IEA and MCS results

	Strength (kN)	**Ductility (m)**
MCS	1372.29	0.1772
IEA	1376.26	0.1783
Nominal	1312.38	0.0470

7.11 CONCLUSIONS

Chapter 5 illustrated the effect of the structural uncertainties on the quantification of structural robustness. Although, a MCS may be used to investigate the effect of structural uncertainties, the computational demands associated with simulating many residual structural

states is non-trivial. Added to the computation demands is the prevalence of convergence problems which are associated with collapse analyses.

Two approaches by which the structural state, following a member failure event, may be determined have been illustrated. Each method approaches the solution from a different perspective. A reanalysis without the failed member may be effective in many cases; however complications arise when permanent deformation is present in unloaded members. This is due to the fact that, by reanalysing the structure from an unloaded state, permanent deformation present in member is not directly considered. While steps may be taken to rectify problems associated with unloaded members, it is apparent that the primary weakness of this approach can be attributed to the analysis commencing from an unloaded structural state.

The superposition approach tackles the problem from a different starting point. With this approach, the starting point for the analysis is the structure just before member failure occurs. Therefore, the starting point represents the true state of the structure and importantly, any issues such as permanent strain in members are accounted for naturally. This simplifies the problem and also ensures that the solution is more transparent.

An elastic incremental analysis approach has been proposed for the generation of the global load-displacement skeleton curves, which provides comprehensive information for the evaluation of structural redundancy and robustness. Comparison of the IEA and FEA results for a number of different examples has demonstrated the efficacy of the IEA approach; given the assumption of geometric linearity, all relevant parameters such as the strength, ductility, energy absorption and so on may be accurately calculated.

Furthermore, the IEA may serve as an efficient method to investigate the effect of structural uncertainties on robustness. Similarly to the MCS analyses in Chapter 5, a uniform

distribution was assumed. Configuration C was used to illustrate the IEA alternative path approach. Using a variety of event selection criteria, it was demonstrated that the IEA approach can successfully and efficiently determine the upper and lower strength and ductility bounds. These bounds may be used to determine the relevant robustness indices. In terms of identifying the upper and lower robustness bounds, it has been demonstrated that the IEA approach can negate the need for computationally expensive MCS. The benefits of this significant increase in efficiency will be especially relevant to the analysis of many residual structural states.

8 CONCLUSIONS AND FURTHER WORK

8.1 INTRODUCTION

This thesis has investigated a number of key issues concerning the quantification of structural robustness. The original contributions to the research area are as follows:

- Chapter 2 provides an extensive review of the robustness assessment and related literature. This serves as a road map to the research area which helps to elucidate the diverse and multi-faceted research field. The key concepts and assessment methods are discussed.

- Chapter 3 critically assesses three alternative assessment methodologies; outlining the advantages and disadvantages of each. The provides a rigorous assessment of three methods which are both calculable and generally applicable; further helping to clarify the current state of the art in robustness assessment.

- Chapter 4 introduces a novel assessment framework in which four robustness performance indicators are combined to provide a comprehensive quantification of the structural deterioration caused by a localised damage event. Additionally, probabilistic index weights are proposed to account for the probability of occurrence of the initiating damage event.

- Chapter 6 and 7 introduce a novel incremental elastic analysis method. This method provides an efficient solution to the incorporation of structural uncertainties (the

importance of which are highlighted in Chapter 5) in robustness assessment by implementing a structural analysis in a series of incremental elastic steps.

8.2 CONCLUSIONS

From a qualitative point there is general agreement in the research literature regarding the basic definition of properties such as redundancy and robustness. However, as evidenced by the broad range of assessment methods discussed in Chapter 2, the qualitative consensus has not translated into generally accepted quantification approaches. Moreover, although robustness quantification has been approached from several different perspectives, many of the proposed methods are lacking some of the basic requirements of robustness measures which are described by Starossek and Haberland (2008); such as expressiveness, calculability and simplicity.

Three quantification approaches have been investigated in detail in Chapter 3; (i) a static stiffness-based vulnerability assessment, (ii) an energy-based vulnerability assessment and (iii) a redundancy analysis which incorporates three limit states. Each of these methods has respective advantages and disadvantages. A number of conclusions may be drawn from these methods:

- Static stiffness methods, due principally to the fact that they are load independent, yield results which are not consistent with conventional response-based analyses. Given the well-defined load and boundary conditions of most civil engineering structures, it is difficult to make the case for the application of such methods without the need to resort to a conventional response-based analysis.

- An important aspect of methods which analyse sequences of member failure events is that the sequences correspond with the expected or probable behaviour of the structure. If sequences are arbitrary with respect to the expected structural behaviour, the probability of occurrence and thus the importance to the robustness assessment of a structure is diminished.

- A common omission from quantification approaches is an explicit treatment of the distributed response to damage events. This aspect of robustness quantification is discussed further in the following paragraphs.

The most common approach to the assessment of system-oriented collapse resistance is to introduce a damage event and analyse the response of the residual structure. This response is normalised using the performance of the intact structural state. In such analyses, the focus is a quantitative assessment of the change in performance of a damaged structure with respect to its intact performance. Feng and Moses (1986), Frangopol and Curley (1987), Maes *et al.* (2006) and other authors have used the residual strength factor to quantify the structural redundancy. However, ultimate strength represents only one aspect of the structural change. The consequence of relying on one measure such as the ultimate strength is that other relevant aspects of the structural capacity are neglected; two residual structures with the same ultimate strength may have substantially different energy absorption capacities. Four measures may be used in order to fully quantify the post-damage reduction in capacity; the elastic stiffness, the ultimate strength, the yield strength and the ductility (which relates closely to energy). The novel method presented in this thesis (Chapter 4) facilitates a more comprehensive account of the structural deterioration, thus providing an improved platform for an assessment of the robustness.

Each residual structure corresponds to a single damage event. Quantifying the robustness of a structure necessarily involves the analysis of many residual structural states. Naturally, the analysis of multiple residual structures results in a spectrum of residual capacities. The reliance on a single measure, such as the most critical value, may mask underlying differences in the capacity of a structure to withstand a localised damage event; thus providing a poor platform for a comparative robustness rating.

In addition to the distribution, the probability of occurrence of the initial event is an important consideration from a broader risk-oriented perspective. The inclusion of the probability of occurrence facilitates a more holistic quantitative outcome which ensures, for example, that very low probability events do not have an undue contribution to the overall robustness rating.

Each of these issues, the distribution and the probability of occurrence, may be effectively addressed using a weighted mean system index, in which the index weights are defined as the probability of occurrence of the initial damage event. This is an effective means of ensuring that the final index reflects the overall robustness of a structure and additionally its vulnerability to initiating damage events.

The thesis then (in Chapter 5) investigated the importance of the sequence of events which lead to the collapse of a structure. It has been demonstrated that structural uncertainties, such as variations in member strength, can affect (in many cases significantly) the strength and ductility, and thus the robustness of a structure. Relatively minor variations, such as +/- 10 MPa, may have substantial effects. It was found that ductility was particularly sensitive to member strength variations due to changes in the sequence of events leading to failure; minor member strength changes are sufficient to change the degree to which the development of

plasticity is distributed (or localised) in a structure. The inclusion of structural uncertainties in the quantification of robustness can be achieved using Monte Carlo simulations. However, such simulations are computationally demanding and susceptible to numerical instabilities during collapse analyses. These difficulties present significant challenges to the analysis of multiple residual structures during the quantification of robustness.

The incremental elastic analysis method has been developed (in Chapter 6 and 7) to address the difficulties associated with full scale Monte Carlo simulations for large numbers of residual structures. By virtue of the incremental nature, the most critical or least critical events may be considered at each stage. Additionally, as the method comprises a series of elastic analyses, the computational demands are minimal and the method enables an identification of the upper and lower robustness bounds much more efficiently than a Monte Carlo simulation. Furthermore, it has been demonstrated that the IEA output accords well with Monte Carlo output.

8.3 LIMITATIONS

The probabilistic weighting which is proposed in Chapter 4 is based on the strength reserve of a member. This definition limits the scope to initiating events which are related to the stress level such as overloading or fatigue. It cannot account for other potential unforeseen exposures such as collision or explosion.

The investigation of alternative failure paths in Chapter 5 defined collapse as the failure of the first member. This definition was chosen to streamline the Monte Carlo simulations by reducing the computation time and eliminating the susceptibility to numerical instabilities. The variation in structural response due to the member strength uncertainties was naturally

reduced by limiting the analyses to a single member failure event. However, the failure of one member was deemed sufficient to illustrate the effect of variations in member strength and the changes in the path to failure.

The incremental elastic analysis, presented in Chapter 6 was illustrated using analyses of pin-jointed trusses. The application to other structures is not investigated in this thesis. However, an extension to the moment resisting frames is briefly considered in Section 7.9. Another limitation of the incremental elastic analysis is the fact that it cannot account for large displacement effects. This means that the incremental method will exhibit some divergence with a nonlinear FE analysis, particularly at the stage of the response approaching collapse. It should be mentioned, however, that the incremental analysis is primarily meant to provide a simple and yet effective means for the generation of the structural capacity parameters for the purpose of the robustness assessment. For detailed analysis of the structural behaviour at advanced nonlinear stages, a full nonlinear FE analysis is still indispensable.

8.4 FUTURE WORK

A weighting factor is proposed in Section 4.2.1, as a means to adjust the combination of the indices. If the weight for each index is equal, then each indicator will have an equal contribution to overall combined system index. If any particular measure deemed more important, the weights may be adjusted so that the greater importance is reflected in the combined index. This aspect of the methodology may be explored further in order to clarify the optimal combination of the indices in different structural settings.

The analysis of alternative failure paths demonstrates the importance of the sequences of events leading to the collapse of a structure. Future work may investigate how such

information may be incorporated into the design stage by tuning the structural configurations so that favourable sequences of events are more probable.

It has been noted that the results determined using the proposed incremental elastic analysis diverge with the nonlinear FE analysis when nonlinear geometry is considered. Further investigation regarding how the IEA results can be improved may be merited. In keeping with the relative simplicity and efficiency of the IEA, it may be possible to bridge the gap using a simple amplification factor. Additional research would be required to determine a suitable value for such an amplification factor.

The application of the incremental elastic analysis has been demonstrated using different configurations of two dimensional pin-jointed trusses. The method can be extended to other structures such as rigid-jointed trusses or moment resisting frames. It is envisaged that, while some modifications will be necessary to account for the more complex member behaviour, the basic concept of the IEA can be maintained.

The failure of members in the IEA is treated using the superposition of the force present in the failed members in order to determine the post-failure structural state. The superposition step presents the possibility to incorporate dynamic effects by amplifying the failed member forces using a dynamic amplification factor. The usefulness of this approach in the present analyses has not yet been sufficiently investigated, however is represents an interesting extension.

The underlying concept of the proposed IEA is an incremental analysis which has the capacity to select the most critical event at each stage in the analysis. It is not intended or conceivable that the IEA can replace a traditional nonlinear FE analysis. However, the process of identifying the most critical sequences may be incorporated within a conventional

FE environment. This could conceivably be implemented by stopping a simulation at each event, introducing the necessary model modifications and restarting the analysis. This approach would alleviate many of the complexities which arise during the IEA such as complicated member unloading and issues such as nonlinear geometry. While bypassing some of the inherent complexities associated with the IEA, this approach could potentially retain substantial advantages in efficiency when compared with a conventional Monte Carlo simulation.

REFERENCES

AASHTO, (2002). *Standard Specifications for Highway Bridges*. 17th ed. Washington DC: American Association of State Highway and Transportation Officials (AASHTO).

Agarwal, J., Blockley, D., and Woodman, N., (2001). Vulnerability of 3-dimensional trusses. *Structural Safety*, 23 (3), 203–220.

Agarwal, J., Blockley, D., and Woodman, N., (2003). Vulnerability of structural systems. *Structural Safety*, 25 (3), 263–286.

Alexander, S., (2004). New approach to disproportionate collapse. *The Structural Engineer*, 82 (December), 14–18.

Arup, (2011). *Review of international research on structural robustness and disproportionate collapse*. London: Department for Communities and Local Government.

ASCE 7-05, (2005). *Minimum design loads for buildings and other structures*. Reston, VA: American Society of Civil Engineers (ASCE).

Augusti, G., Borri, C., and Niemann, H.-J., (2001). Is Aeolian risk as significant as other environmental risks? *Reliability Engineering & System Safety*, 74 (3), 227–237.

Baker, J., Schubert, M., and Faber, M., (2008). On the assessment of robustness. *Structural Safety*, 30 (3), 253–267.

Beeby, A.W., (1999). Safety of structures , and a new approach to robustness. *Structural Engineer*, 77 (4), 16–21.

Bertero, R.D. and Bertero, V. V., (1999). Redundancy in Earthquake-Resistant Design. *Journal of Structural Engineering*, 125 (1), 81–88.

Biondini, F. and Restelli, S., (2008). Damage propagation and structural robustness. *In*: *Proceedings of the International Symposium on Life-Cycle Civil Engineering*. 131–136.

Brown, C.B., Elms, D.G., and Melchers, R.E., (2008). Assessing and achieving structural safety. *Structures & Buildings*, 161 (4), 219–230.

BS 5950-1:2000, (2008). Structural use of steelwork in building - Part 1: Code of practice for design - Rolled and welded sections. British Standards Institution (BSI).

Choi, S.-K., Grandhi, R. V., and Canfiel, R.A., (2007). *Reliability-based structural design*. Journal of the Structural Division. Springer London.

Connor, R., Dexter, R., and Mahmoud, H., (2005). *NCHRP Synthesis 354: Inspection and Management of Bridges with Fracture-Critical Details*. Transportation Research Board, National. Washington, D.C.

Deco, A. and Frangopol, D., (2011). Risk assessment of highway bridges under multiple hazards. *Journal of Risk Research*, 14 (9), 1057–1089.

Dijkstra, E.W., (1959). A note on two problems in connexion with graphs. *Numerische Mathematik*, 1 (1), 269–271.

Doltsinis, I., (2004). Robust design of structures using optimization methods. *Computer Methods in Applied Mechanics and Engineering*, 193 (23-26), 2221–2237.

Dusenberry, D., Juneja, G., and Gumpertz, S., (2002). *Review of existing guidelines and provisions related to progressive collapse*. Workshop on Prevention of Progressive Collapse.

Dusenberry, D.O. and Hamburger, R.O., (2006). Practical Means for Energy-Based Analyses of Disproportionate Collapse Potential. *Journal of Performance of Constructed Facilities*, 20 (4), 336–348.

Dwight, J., (1975). Use of Perry Formula to Represent the New European Strut-Curves. *IABSE Reports of the Working Commissions*, 23, 399–411.

Ellingwood, B. and Galambos, T. V., (1982). Probability-based criteria for structural design. *Structural Safety*, 1 (1), 15–26.

Ellingwood, B. and Leyendecker, E., (1978). Approaches for design against progressive collapse. *Journal of the Structural Division*, 104 (3), 413–423.

Ellingwood, B.R. and Dusenberry, D.O., (2005a). Building Design for Abnormal Loads and Progressive Collapse. *Computer-Aided Civil and Infrastructure Engineering*, 20 (3), 194–205.

Ellingwood, B.R. and Dusenberry, D.O., (2005b). Building design for abnormal loads and progressive collapse. *Computer-Aided Civil and Infrastructure Engineering*, 20 (3), 194–205.

Elms, D.G., (2004). Structural safety–issues and progress. *Progress in Structural Engineering and Materials*, 6 (2), 116–126.

EN 1991-1-7:2006, (2010). Eurocode 1 - Actions on structures - Part 1-7: General actions - Accidental actions. Comité Européen de Normalisation (CEN).

EN 1993-1-1:2005, (2010). Eurocode 3: Design of steel structures - Part 1-1: General rules and rules for buildings. Comité Européen de Normalisation (CEN).

England, J. and Agarwal, J., (2008). Recent developments in robustness and relation with risk. *Proceedings of the ICE - Structures and Buildings*, 161 (4), 183–188.

Fang, Z.-X. and Li, H.-Q., (2009). Robustness of engineering structures and its role in risk mitigation. *Civil Engineering and Environmental Systems*, 26 (3), 223–230.

Feng, Y.S. and Moses, F., (1986). Optimum design, redundancy and reliability of structural systems. *Computers & Structures*, 24 (2), 239–251.

Frangopol, D., Kawatani, M., and Kim, C., (2008). *Reliability and Optimization of Structural Systems: Assessment, Design, and Life-Cycle Performance*.

Frangopol, D.D.M. and Nakib, R., (1991). Redundancy in highway bridges. *Engineering Journal*, 28 (1), 45–50.

Frangopol, D.M. and Curley, J.P., (1987). Effects of Damage and Redundancy on Structural Reliability. *Journal of Structural Engineering*, 113 (7), 1533–1549.

Frangopol, D.M., Iizuka, M., and Yoshida, K., (1992). Redundancy Measures for Design and Evaluation of Structural Systems. *Journal of Offshore Mechanics and Arctic Engineering*, 114 (4), 285.

Frangopol, D.M. and Klisinski, M., (1989). Weight-strength-redundancy interaction in optimum design of three-dimensional brittle-ductile trusses. *Computers & Structures*, 31 (5), 775–787.

Ghosn, M. and Moses, F., (1998). *NCHRP Report 406: Redundancy In Highway Bridge Superstructures*. onlinepubs.trb.org. Washington, D.C.: Transportation Research Board.

Ghosn, M., Moses, F., and Frangopol, D.M., (2010). Redundancy and robustness of highway bridge superstructures and substructures. *Structure and Infrastructure Engineering*, 6 (1-2), 257–278.

Goto, Y., Kawanishi, N., and Honda, I., (2011). Dynamic Stress Amplification Caused by Sudden Failure of Tension Members in Steel Truss Bridges. *Journal of Structural Engineering*, 137 (8), 850–861.

GSA, (2003). *Progressive collapse analysis and design guidelines for new federal office buildings and major modernization projects*. The U.S. General Services Administration (GSA).

Hendawi, S. and Frangopol, D.M., (1994). System reliability and redundancy in structural design and evaluation. *Structural Safety*, 16 (1-2), 47–71.

Husain, M. and Tsopelas, P., (2004). Measures of Structural Redundancy in Reinforced Concrete Buildings. I: Redundancy Indices. *Journal of Structural Engineering*, 130 (11), 1651–1658.

Husain, M., Tsopelas, P., and Asce, A.M., (2004). Measures of Structural Redundancy in Reinforced Concrete Buildings . I : Redundancy Indices, (November), 1651–1658.

IStructE, (2010). *Practical guide to structural robustness and disproportionate collapse in buildings*. London: Institution of Structural Engineers International HQ, 11 Upper Belgrave Street, London SW1X 8BH.

Izzuddin, B. a., (2010). Robustness by design - Simplified progressive collapse assessment of building structures. *Stahlbau*, 79 (8), 556–564.

Janssens, V. and Dwyer, D.W.O., (2001). Disproportinate Collapse in Building Sructures. *In*: *Joint Symposium on Bridge and Infrastructure Research in Ireland (BRI 10) and Concrete Research in Ireland (CRI 10)*. 1–8.

JCSS, (2000). *Probabilistic Model Code - Part 3*. JCSS. Joint Committee on Structural Safety (JCSS).

JCSS, (2001). *Probabilistic Model Code - Part 1*. Structural Safety. Joint Committee on Structural Safety (JCSS).

JCSS, (2008). *Risk Assessment in Engineering*. Joint Committee on Structural Safety.

Kim, T. and Kim, J., (2009). Investigation of progressive collapse-resisting capability of steel moment frames using push-down analysis. *Journal of Performance of Constructed Facilities*, 23 (5), 327–335.

Kirkegaard, P. and Sørensen, J., (2009). System reliability of timber structures–ductility and redundancy. *Joint workshop of COST*, 165–173.

Knoll, F. and Vogel, T., (2009). *Design for robustness*. System. IABSE.

Kuhlmann, U., Rölle, L., and Pereira, M., (2009). *Steel structures*. Ljubljana.

Lind, N., (1995). A measure of vulnerability and damage tolerance. *Reliability Engineering & System Safety*, 48 (1), 1–6.

Lu, Z., Yu, Y., Woodman, N.J., and Blockley, D.I., (1999). A theory of structural vulnerability. *Structural Engineer*, 77 (18), 17–24.

Maes, M.A., Fritzsons, K.E., and Glowienka, S., (2006). Structural Robustness in the Light of Risk and Consequence Analysis. *Structural Engineering International*, 16 (2), 101–107.

Marjanishvili, S., PE, M., Agnew, E., others, Ph, D., and Asce, M., (2006). Comparison of various procedures for progressive collapse analysis. *Journal of Performance of Constructed Facilities*, 20 (November), 365.

Naess, a., Leira, B.J., and Batsevych, O., (2009). System reliability analysis by enhanced Monte Carlo simulation. *Structural Safety*, 31 (5), 349–355.

Nafday, A.M., (2008). System Safety Performance Metrics for Skeletal Structures. *Journal of Structural Engineering*, 134 (3), 499–504.

Nowak, A. and Collins, K., (2012). *Reliability of structures*.

Paik, J. and Thayamballi, A., (2003). *Ultimate Limit State Design of Steel Plated Structures*. 1st ed. West Sussex: John Wiley & Sons, Inc.

Park, S., Choi, S., Sikorsky, C., and Stubbs, N., (2004). Efficient method for calculation of system reliability of a complex structure. *International Journal of Solids and Structures*, 41 (18-19), 5035–5050.

Pinto, J.T., Blockley, D.I., and Woodman, N.J., (2002). The risk of vulnerable failure. *Structural Safety*, 24, 107–122.

Sanjayan, J. and Candy, C., (2004). Reliability Analysis to Verify the Currently used Partial Safety Factors in Bridge Design : A Case Study using Baandee Lakes Bridge No . 1049. *In*: *Fifth AusRoads Bridge Engineering Conference, Hobart*.

Schafer, B. and Bajpai, P., (2005). Stability degradation and redundancy in damaged structures. *Engineering Structures*, 27 (11), 1642–1651.

Sebastian, W., (2004). Collapse considerations and electrical analogies for statically indeterminate structures. *Journal of Structural Engineering*, (October), 1445–1453.

Slotine, J. and Li, W., (1991). *Applied nonlinear control*. Englewood Cliffs (NJ): Prentice Hall.

Smith, J.W., (2003a). Energy approach to assessing corrosion damaged structures. *Proceedings of the Institution of Civil Engineers. Structures and buildings*, 156 (2), 121–130.

Smith, J.W., (2003b). The vulnerability of structures to unpredictable damage events. *of XL2003 response of structures to extreme loading.*

Starossek, U., (2007). Typology of progressive collapse. *Engineering Structures*, 29 (9), 2302–2307.

Starossek, U. and Haberland, M., (2008). Measures of Structural Robustness — Requirements and Applications. *In*: *Structures Congress 2008*. Reston, VA: American Society of Civil Engineers, 1–10.

Starossek, U. and Haberland, M., (2009). Evaluating Measures of Structural Robustness. *In*: *Structures Congress 2009*. Reston, VA: American Society of Civil Engineers, 1–8.

Starossek, U. and Haberland, M., (2011). Approaches to measures of structural robustness. *Structure and Infrastructure Engineering*, 7 (7-8), 625–631.

Starossek, U. and Haberland, M., (2012). Robustness of structures. *International Journal of Lifecycle Performance Engineering*, 1 (1), 3.

Szyniszewski, S. and Krauthammer, T., (2012). Energy flow in progressive collapse of steel framed buildings. *Engineering Structures*, 42, 142–153.

The Building Regulations, (1970). *The Building (Fifth Amendment) Regulations*. (S.I. 1970/109).

The Building Regulations, (1985). Approved Document A: Structure. A3 - Disproportionate Collapse. Her Majesty's Stationery Office (HMSO).

Thoft-Christensen, P. and Murotsu, Y., (1986). *Application of Structural Systems Reliability Theory*. Berlin, Heidelberg: Springer Berlin Heidelberg.

UFC 4-023-03, (2005). *Design of Buildings to Resist Progressive Collapse*. Department of Defence (DOD).

UFC 4-023-03, (2009). *Design of Building to Resist Progressive Collapse*. Department of Defence (DOD).

URS, (2006). *URS Corporation Fatigue Evaluation and Redundancy Analysis Draft Report for Bridge #9340*. Analysis. Minneapolis.

Wisniewski, D., Casas, J.R., and Ghosn, M., (2006). Load Capacity Evaluation of Existing Railway Bridges based on Robustness Quantification. *Structural Engineering International*, 16 (2), 161–166.

Yuansheng, F., (1988). The theory of structural redundancy and its effect on structural design. *Computers & Structures*, 28 (1), 15–24.

Appendix A

Table A1: Hasofer Lind-Rackwitz Fiessler iterative calculation

Iteration	1	2	3	4	5	6
fpP	9.34E-07	1.26E-07	7.40E-09	2.01E-09	1.79E-09	1.82E-09
FpP	0.5703	0.9558	0.9975	0.9993	0.9994	0.9994
μp	1.69E+06	1.36E+06	6.28E+05	2.51E+05	2.17E+05	2.22E+05
σp	4.21E+05	7.42E+05	1.06E+06	1.19E+06	1.20E+06	1.20E+06
g(.)	7.74E+05	3.17E+05	8.79E+04	-3.23E+03	-4.08E+03	-1.84E+03
dg/dA	2.50E+08	2.17E+08	2.26E+08	2.32E+08	2.34E+08	2.34E+08
dg/dS	5.00E-03	4.87E-03	4.91E-03	4.93E-03	4.94E-03	4.94E-03
dg/dP	-0.615	-0.615	-0.615	-0.615	-0.615	-0.615
β	2.584	3.183	3.302	3.297	3.291	3.289
αA	-0.209	-0.114	-0.084	-0.078	-0.078	-0.078
αS	-0.459	-0.280	-0.201	-0.182	-0.180	-0.180
αP	0.864	0.953	0.976	0.980	0.981	0.981
A(k)	4.87E-03	4.91E-03	4.93E-03	4.94E-03	4.94E-03	4.94E-03
S(k)	2.17E+08	2.26E+08	2.32E+08	2.34E+08	2.34E+08	2.34E+08
P(k)	2.62E+06	3.61E+06	4.06E+06	4.10E+06	4.09E+06	4.09E+06
μA(k)	-0.539	-0.361	-0.277	-0.256	-0.255	-0.255
μS(k)	-1.186	-0.890	-0.664	-0.599	-0.593	-0.593
μP(k)	2.232	3.035	3.222	3.232	3.228	3.225
ε		0.232	0.037	0.002	0.002	0.001

Appendix B

Table B1: Member cross-section areas for each structural configuration

Member	A	B	C	D
1	0.0027	0.0020	0.0073	0.0020
2	0.0020	0.0020	0.0047	0.0014
3	0.0033	0.0020	0.0036	0.0020
4	0.0052	0.0020	0.0144	0.0013
5	0.0031	0.0020	0.0032	0.0020
6	0.0019	0.0020	0.0020	0.0020
7	0.0068	0.0020	0.0117	0.0030
8	0.0028	0.0020	0.0028	0.0007
9	0.0001	0.0020	0.0032	0.0008
10	0.0051	0.0020	0.0055	0.0023
11	0.0001	0.0020	0.0017	0.0020
12	0.0068	0.0020	0.0117	0.0026
13	0.0001	0.0020	0.0032	0.0005
14	0.0028	0.0020	0.0028	0.0010
15	0.0051	0.0020	0.0055	0.0023
16	0.0019	0.0020	0.0020	0.0010
17	0.0020	0.0020	0.0047	0.0020
18	0.0052	0.0020	0.0144	0.0032
19	0.0033	0.0020	0.0036	0.0010
20	0.0031	0.0020	0.0032	0.0013
21	0.0027	0.0020	0.0073	0.0020

Appendix C

Table C1: Sample incremental elastic analysis step

Member	State	Previous stress	Previous strain	Incremental stress	Incremental strain	Yield strain	Ultimate strain
1	elastic	-2.00E+08	-0.001	-1.06E+08	-0.00053	0.00125	0.02
2	elastic	-2.40E+08	-0.0012	-1.28E+08	-0.00064	0.00125	0.02
3	yielded	2.50E+08	0.00125	1.33E+08	0.02494	0.00125	0.02
4	elastic	1.48E+07	0.00007	7.90E+06	0.00004	0.00125	0.02
5	elastic	-3.58E+07	-0.00018	-7.59E+07	-0.00038	0.00125	0.02
6	Failed					0.00125	0.02
7	elastic	-1.52E+08	-0.00076	-8.11E+07	-0.00041	0.00125	0.02
8	elastic	-1.50E+07	-0.00007	-7.90E+06	-0.00004	0.00125	0.02
9	yielded	2.54E+08	0.00202	1.35E+08	0.02535	0.00125	0.02
10	elastic	2.87E+07	0.00014	1.52E+07	7.59E-05	0.00125	0.02
11	elastic	-1.52E+08	-0.00076	-8.11E+07	-4.06E-04	0.00125	0.02

Table C2: Sample incremental elastic analysis step continued

Next Event	α	Scaled Load	Scaled Stress	Scaled Strain	Updated State	Action	Member
-0.00125	0.470	2.94E+06	-2.08E+08	-0.0010			
-0.00125	0.078		-2.50E+08	-0.0013	Yielded	Adjust	2
0.02000	0.752		2.60E+08	0.0032			
0.00125	29.761		1.54E+07	0.0001			
-0.00125	2.823		-4.17E+07	-0.0002			
Failed	Failed						
-0.00125	1.203		-1.59E+08	-0.0008			
-0.00125	29.734		-1.56E+07	-0.0001			
0.02000	0.710		2.65E+08	0.0040			
0.00125	14.579		2.99E+07	0.0001			
-0.00125	1.203		-1.59E+08	-0.0008			